Mooring system design, related to Pioneering Spirit

Improvement of a mooring system to secure a barge alongside Pioneering Spirit in offshore conditions, including an evaluation of the dynamic mooring loads

A. Sinke 4715233

Master of Science Thesis

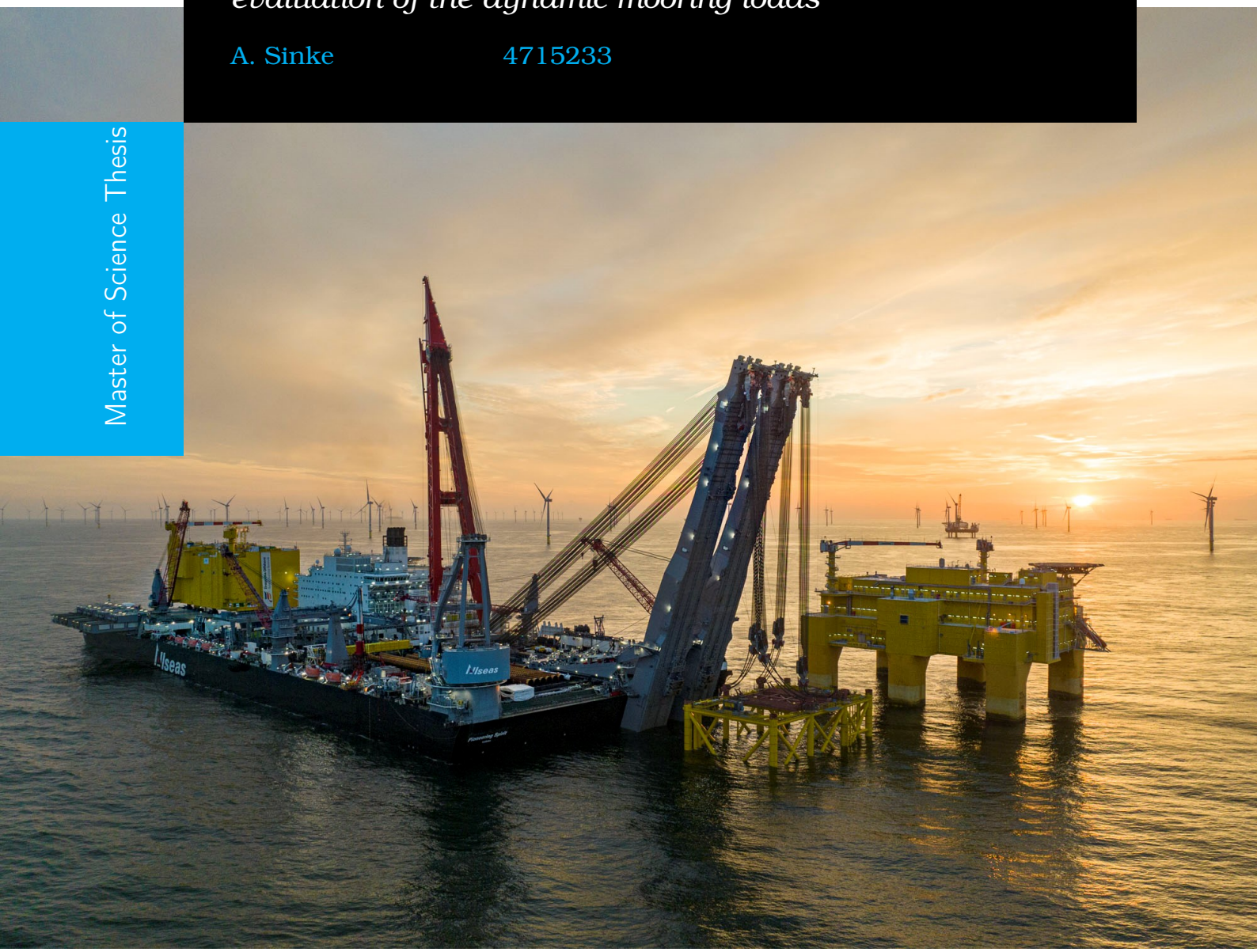

TU Delft Delft University of Technology

Allseas

Offshore and Dredging Engineering

October 19, 2022

MASTER OF SCIENCE THESIS

Mooring system design, related to Pioneering Spirit

Improvement of a mooring system to secure a barge alongside Pioneering Spirit in offshore conditions, including an evaluation of the dynamic loads

Written by

A. Sinke 4715233

Master of Science

Faculty of Mechanical, Maritime and Materials Engineering
Technische Universiteit Delft.

To be defended publicly on Wednesday October 26, 2022

Under supervision of

Dr. J.O. Colomés Gené (TU Delft)
Dr. Ing. S. Schreier (TU Delft)
Ir. D. Marón Blanco
Dr. Ir. N.J. Mallon

October 19, 2022

TU Delft Delft University of Technology

Abstract

Continuous development in the wind turbine industry leads to increasing size of wind turbines. Allseas investigates the possibility to enter the offshore wind turbine installation industry with the large sized multi-purpose vessel, *Pioneering Spirit*.
For Allseas' preliminary wind turbine installation design, wind turbines are assembled offshore, requiring wind turbine components to be brought from shore to *Pioneering Spirit* by means of a cargo barge. This operation requires a proper mooring procedure of which the mooring system is an essential part. Moreover, the workability of the wind turbine installation operation is expected to be limited by the mooring system. The mooring system secures the barge alongside *Pioneering Spirit* where it has to stay for multiple days.

In this research a pre-defined vessel orientation is analysed where the barge stern is extended 40m in longitudinal direction from *Pioneering Spirit* stern, to increase the barge area reachable by the unloading crane. This barge position is challenging due to limited shielding from *Pioneering Spirit*, leading to excessive environmental loads acting on the barge. Due to the barge extension, properly connecting the mooring system to Pioneering Spirit is a challenge.
The above leads to the main objective of this thesis: improve the mooring system to secure a barge alongside *Pioneering Spirit*, including an evaluation of the dynamic mooring loads.

The main mooring system design requirements are that the Safe Working load and motion limits are not exceeded. Evaluation of dynamic loads starts with a multi-body diffraction analysis with hydrodynamic matrices and other hydrodynamic properties as output. This data is imported in a time domain model which enables capturing non-linearities, e.g. the mooring system and wind and current loads.
Validation and verification steps are required to assure realistic outcome and understanding limitations of the numerical models.

Before new mooring systems are introduced, a base case mooring system is defined and modelled in the time domain. Finding the limiting sea state for which the Safe Working Load limit is reached enables to compute the workability for the reference location defined. Two reference locations are considered: a wind sea area and swell sea area.Wind and current speed is assumed to be constant over time and independent of elevation. Workability is defined as the percentage of time the mooring system is able to operate.

Evaluating the base case mooring system shows a performance of 67% workability for wind areas and 16 % for swell areas. Next to the base case, four mooring improvement concepts are evaluated from which the Moormaster system shows most promising results. This system consists of three main components: 'fixed structure - hydraulic cylinder - vacuum pad' that connects the barge to *Pioneering Spirit*. This system is modelled as a link with constant stiffness and damping properties within its operational limitations.

The Moormaster system, shows perspective to improve the workability for both wind and swell seas. Besides workability, the Moormaster system improves the entire mooring procedure by quick connection and safe disconnection upon exceeding operational limits.

Preface

Passion for technology is a clear characteristic of me and my beloved family. My passion for Offshore started during a guided tour on *Pioneering Spirit*, currently worlds' largest construction vessel, when I was still in high school. Therefore, finishing my Masters degree in Offshore and Dredging Engineering at Delft University of Technology, involving *Pioneering Spirit*, makes me proud.

I would never have reached this point without the help of all the people involved in the courses during my bachelors and Masters, a special thanks to my TU supervisor Oriol Colomes Genè for being always available for help.

My sincere gratitude goes out to my colleagues in Allseas Engineering that are involved in the passed 9 months.
A special thanks goes to Marijn Dijk for his supervision and making it possible to spend two weeks on *Pioneering Spirit*. As a result, I want to thank the crew on board *Pioneering Spirit* for their contribution to the results of this thesis.

Thanks to Daniel Marón Blanco for his supervision. Thanks to Niels Mallon for sharing part of his great understanding of dynamics. I want to give thanks to the entire Naval Architecture department within Allseas, for the answers to my questions, all the coffee's and chilled beers at Friday afternoon.

Finally, I am grateful to my ever compassionate family for their support during my entire time at TU Delft. A very special thanks to my brother Marius, growing up together, working at the same company, working at the same vessel at the same time, that's a story not many people can tell which I am very proud of. Thanks for your help especially during writing of the report.

Delft - October 19, 2022

Abraham Sinke

Guide to the reader

This thesis presents the methodology and results of improving a mooring system for mooring a barge alongside *Pioneering Spirit* in offshore conditions, related to wind turbine installation.
Each step contributes to the step-by step thesis approach as will be represented in chapter 3.

The content is subdivided in the following chapters.

Chapter 1 introduces the reader to this thesis subject and provides the thesis objective.

Chapter 2 gives background information on the thesis subject.

Chapter 3 explains the stepwise approach followed in this thesis.

Chapter 4 describes the mooring system involving design requirements and criteria. The base case mooring system is defined.

Chapter 5 explains the diffraction analysis and modelling in the frequency domain.

Chapter 6 describes modelling in the time domain.

Chapter 7 presents new mooring system concepts.

Chapter 8 shows the results found in this thesis.

Chapter 9 discusses the methodology applied and results found, including recommendations for future research.

Chapter 10 gives a summary and final conclusion of this research.

Information considered as less relevant is included in the appendices and will be referred to throughout the report.

Table of Contents

List of Figures

List of Tables

Glossary

CoB	Center of Buoyancy
CoG	Center of Gravity
DoF	Degree of Freedom
DP	Dynamic Positioning
EoM	Equation of Motion
Hs	Significant wave height
HSE	Health, safety and environment
ILID	Internal LID in the numerical model
JLS	Jacket Lift System
JONSWAP	Joint North Sea Wave Project
MBL	Maximum breaking load
MCA	Multiple Criteria Analysis
MPM	Most Probable Maximum
Multi-body	Configuration with *Iron Lady* alongside *Pioneering Spirit*
RAO	Response Amplitude Operator
Sensitivity analysis	Systematically adjust variables and analyse how it affects the results
SWL	Safe Working Load
Three hours maximum	Maximum value that occurs in a three hour lasting sea state.
Tp	Peak period
Validation	Model check with experimental results
VCG	Vertical Center of Gravity
Verification	Model check with analytical results and literature
VLID	Damping LID between vessels in the numerical model
Workability	Annual percentage of time that operational limits are not exceeded given the environmental conditions.

1 Introduction

1.1 Energy transition and offshore wind market development

Nowadays, the world is in the middle of an energy transition, replacing fossil fuels with low carbon energy sources. While foreseeing the increasing demand for energy, energy production from wind got attention around the globe.
Lately the Dutch government announced plans to double the capacity of offshore wind energy production in the North Sea, [1]. Harvesting wind energy at offshore locations is promising by multiple reasons. Many other countries around the globe, with a coastline, are investing in offshore wind.
Continuous development in the wind turbine industry leads to increasing size of wind turbines. Upcoming wind turbine designs are of such size that they reach or exceed the limits of conventional heavy lift vessels.
Allseas, having the large sized multi-purpose vessel, *Pioneering Spirit*, in its fleet, investigates the possibility to enter the offshore wind turbine installation industry. A preliminary design for how to install an offshore wind turbine using *Pioneering Spirit* is discussed in chapter 2.

1.2 Thesis motivation

As part of a wind turbine installation, wind turbine components have to be delivered to *Pioneering Spirit*, using a cargo barge. To unload the cargo barge, it has to be brought to and connected alongside *Pioneering Spirit*. The connection, securing the barge alongside Pioneering Spirit, is referred to as a mooring system. Barge mooring is considered to determine the workability in the wind turbine installation process.
In order to increase the workability and reduce the waiting for weather time, Allseas is looking to improve the existing mooring procedure and mooring system. The mooring procedure entails a broader scope, ranging from a barge leaving the harbour up to barge disconnecting from *Pioneering Spirit* after it is successfully unloaded.
The aim of the thesis is to deliver a proper design for the mooring system, satisfying the design requirements. Moreover, improve the mooring arrangement such that the workability increases compared to the current existing mooring arrangement.

1.3 Literature research

This Master Thesis started with a literature research into the work that has already been done is this field. The main topics that are addressed are listed below

- Hydrodynamics, related to single floating bodies.
- Floating multi-body hydrodynamic interaction.
- Modelling methods and numerical software that is available to solve a multi-body hydrodynamic problem. Including numerical challenges.

- Mooring systems and procedures, including current state-of-the-art methods.
- Multiple Criteria Analysis for evaluating the mooring procedure.
- Workability to comparing mooring system concepts.

Theory that is required to understand choices and findings of this Thesis will be included throughout the report or in the appendix. Besides, Appendix A includes a reflection on the literature report explaining what theory has been used and what not.
For the enthusiastic reader that is interested in this topic, the literature report can always be requested as the writer is happy to share the report, [2].

Floating bodies are excited by wave forces. With contributions from first and second order effects. First order forces has contributions from incoming, diffracted and radiated waves. Radiation and diffraction effects are also known as wave shielding. Second order wave drift forces consist of a steady contribution and from sum and difference frequencies. Wind and current loads mainly depend on the relative velocity, subjected area and the drag coefficient [3].

A hydrodynamic numerical model, that solves the equations of motion, can be build both in frequency or time domain. Building such a model starts with a diffraction analysis to determine the hydrodynamic system matrices and other hydrodynamic properties. Diffraction software applies potential theory which assumes the fluid around the floating structure to be incompressible, inviscid and irrotational. Disregarding viscosity underestimates damping and is known for some frequencies to overestimate the wave height in a gap between two floating vessels, [4]. Additionally, a numerical effect is 'irregular frequencies' which correspond to fictitious eigenmodes of the internal flow of a floating body which can lead to spikes in the hydrodynamic data, they only occur in numerical software and do not have a physical meaning, [5]. This hydrodynamic data can be imported in a frequency domain or time domain model. To capture non-linear effects, e.g. a non-linear mooring system, requires a time domain model, [6].

A mooring system is required to secure a barge alongside a large vessel in offshore conditions. Such a mooring system usually consist of mooring lines and fenders, their properties and orientation determines the mooring system properties. By adjusting these properties, the relative vessel motions and loads in the mooring system can be regulated [7].
A state-of-the-art mooring system is developed by Cavotec Moormaster ® which restricts relative vessel motions by means of a vacuum pad with a hydraulic cylinder attached that has certain stiffness and damping properties [8].

1.4 Gaps in literature

While doing research the following three gaps have been identified in literature and will be discussed in this research.

1. Challenging mooring arrangement.
    - **Gap.** The mooring system has to secure the barge alongside for multiple days. Therefore, high workability is required.
    - **Gap.** The barge is extending from *Pioneering Spirit* stern causing in low shielding (and non-symmetric loading along the barge), therefore excessive environmental loading results in excessive mooring loads.
    - **Gap.** The mooring arrangement design is restricted due to the barge extending from *Pioneering Spirit* stern.
    - **Solution.** Understanding the mooring system behavior and advising on improving the mooring system by design and implementation of new mooring system concepts.

2. Implementing a state of the art mooring system, Cavotec Moormaster®, in the time domain model. See section 7.6.
    - **Gap.** No method to model the complex Moormaster system is shared in literature.
    - **Gap.** No detailed system properties are available for this system and its limitations are only partly available.
    - **Gap.** This system is not applied in offshore conditions before.
    - **Solution.** Simplify the complex Moormaster system by modelling it as multiple links with non-linear stiffness and damping properties.
    - **Solution.** Define stiffness and damping properties and provide directions on optimizing the Moormaster system performance/settings.
3. Validation and verification of numerical results, included in section 5.5 and 6.5.
    - **Gap.** No data is available to judge the outcome and acceptability of the results from the numerical model. For example, what fender damping coefficient is realistic or whether assuming maximum mooring line loads to be Rayleigh distributed is allowed.
    - **Solution.** Validate and verify with: literature, based on industry/Allseas experience and verify with analytical results. If no satisfactory outcome is acquired, a sensitivity analysis is performed or directions are given to do so in order to understand its effect on the results of this research.
      For example, validation is relevant for numerical effects in a multi-body diffraction analysis.

1.5 Thesis objective

Mooring a barge to the *Pioneering spirit* to deliver components requires a safe and effective operation. The main purpose of the mooring system is to secure the barge to the Pioneering spirit and to minimize the relative motions between the two floating objects. A more effective mooring system is defined as a mooring system that has more resistance against forces that are causing relative motions.

The main focus of this thesis will be on optimizing the design of the mooring system. The design and optimization is covered in the following research question.

'How can the mooring system to secure a barge alongside Pioneering Spirit in offshore conditions be improved?'

The main research questions is subdivided in four sub questions.
To be able to analyse a mooring system, the whole operation should be clear in order to define design requirements. This leads to the first sub question being

'How is the mooring system enclosed in the larger scope of an offshore mooring procedure and what mooring system design considerations are applicable, related to wind turbine installation?'

To evaluate dynamic loads in the mooring system, a multi-body hydrodynamic model should be build in the time domain, including a mooring system. Model validation and verification is required to assure finding realistic results and understanding limitations of the model. Captured in the second sub question being.

'What methodology is required to build a validated and verified multi-body hydrodynamic model, including a mooring system?'

One of the mooring systems incorporates the state-of-the-art Cavotec Moormaster system, therefore the third question is.

'How can the Cavotec Moormaster system realistically be modelled and implemented in the time domain model?'

The multi-body hydrodynamic model will be used to evaluate dynamic loads in the base case and the improved mooring system concepts, leading to the fourth and final sub question.

'What methodology enables evaluating the mooring system concepts performance?'


Allseas
Pioneering Spirit

2 Background information

2.1 Allseas' preliminary design of offshore wind turbine installation.

At the moment of writing, the procedure for wind turbine installation is still in concept phase within Allseas' innovation department. Therefore, the most promising concept is used for reference throughout this thesis.
In this concept, wind turbines are assembled offshore. Wind turbine parts have to be transported from shore to *Pioneering Spirit*. This is done by a barge, manoeuvred with tugs. A mooring system will secure the barge to *Pioneering Spirit*. The crane that is located at port side stern of *Pioneering Spirit* is used for unloading the barge. Therefore, the barge is moored alongside port side stern of *Pioneering Spirit* to be within the crane reach. One barge is expected to bring eight disassembled wind turbines at a time. Due to the limited free deck space available on *Pioneering Spirit*, the barge is expected to be moored alongside for approximately eight days. After fully unloading the barge it is transported back to shore, again manoeuvred with tugs. At the moment of disconnecting the empty barge, another fully loaded barge will be present to enable continuous operation. Additionally, the mooring system workability is expected to limit the workability of the entire wind turbine installation procedure. That feeds the urge to increase the workability of the mooring system.

Figure 2.1 represents the cargo barge bringing the wind turbine parts to *Pioneering Spirit* on the left hand side, on the right hand side Allseas' preliminary design for assembling wind turbines offshore is visualized.

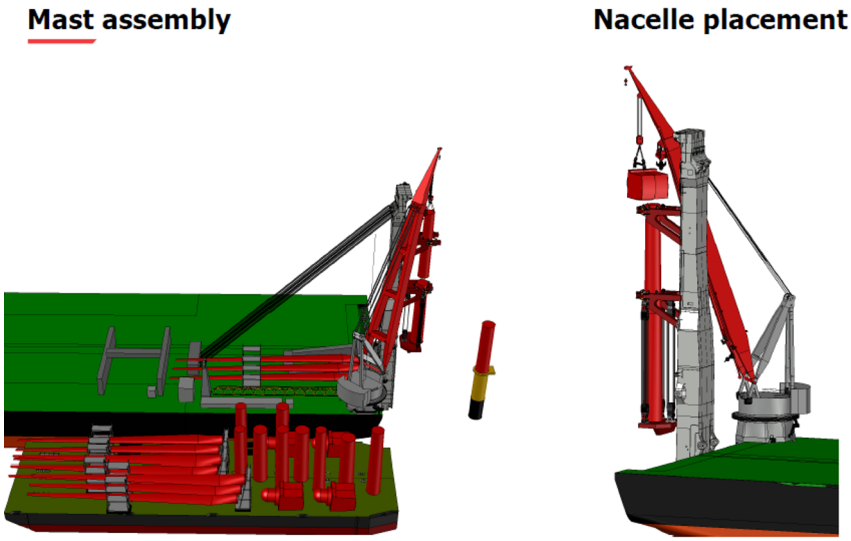

Figure 2.1: Offshore wind turbine assembly, Allseas' preliminary design

2.2 Vessels involved

The most important vessel involved in this wind turbine installation operation is *Pioneering Spirit*. Besides, different barges and tugboats are involved.

2.2.1 Pioneering Spirit

Pioneering Spirit is known as the pride and glory of Allseas, represented on the front page of this report, will be the core of the wind turbine installation process. *Pioneering Spirit* is a so called multi-purpose vessel which can be used for deep water pipe lay, topside and jacket installation but also decommissioning and in the future possibly wind turbine installation.
Especially the aft part of *Pioneering Spirit* will be used during wind turbine installation, mainly due to the location of the 5000 Tons crane and the wind turbine assembly and installation equipment, as can be seen in Figure 2.2.

At the aft of *Pioneering Spirit*, two beams with a length of 170 m are installed, initially designed to lift jackets. These beams, later referred to as Jacket Lift System (JLS) beams, can be tilted up to 110 °. Wind turbines will be installed with use of the JLS beams.
Pioneering Spirit consist of a Dynamic Position (DP) system to keep position. More specifically, the DP system is of class DP-III which refers to redundancy. The DP system is capable of keeping position, even in case that one of the four engine rooms is lost due to fire or flooding. Furthermore, the DP system has sufficient capacity to hold position when a loaded barge is moored against *Pioneering Spirit*.
Table 2.1 lists the length breadth and draft of *Pioneering Spirit*. Due to the large ballast capacity, the operational draft can be varied between 12 and 27 m.

Figure 2.2: Vessel orientation during wind turbine installation, top view. Blue circle: pre-installed foundation. Red cross: crane. Grey blocks (2x): JLS beams and the dashed line a mooring line.

2.2.2 Iron Lady

The rectangular shaped barge, *Iron Lady*, will be the main barge used in the process of wind turbine installation. The reason for that is *Iron Lady* being the largest barge in the Allseas fleet. The draught, trim and heel of *Iron Lady* can be adjusted by changing ballast conditions. *Iron Lady* will be used as reference barge throughout this thesis, its dimensions are captured in Table 2.1.

2.2.3 Tug(s)

The Allseas fleet currently contains no tugs. Therefore, local tugs are used to transport the barge from shore to the *Pioneering Spirit*. The main requirement for the tug is the force it can exert on the barge, also known as 'bollard pull'.

2.3 Equipment involved

2.3.1 Pioneering Spirit Cranes

The 5000 Tons crane that is located at port side stern of *Pioneering Spirit* will be used for unloading the wind turbine components. Besides, there is a 'small' crane, with a 600 ton capacity, that might be used for low weight wind turbine components.
Each crane has its load curve that relates the capacity with its reach. Crane load curves and Exact data on operational limits cannot be given as it is confidential information.

2.3.2 Towing system

The towing system entails towing lines, winches and connection points. Towing lines are used to connect the tug(s) to the barge when pulling during transport.

2.3.3 Crew on board the vessels

Besides the mooring equipment, the experienced crew on board of the vessels that need to be connected is of outmost importance. The crew required to install the mooring system as it is designed. The crew responsible for the mooring system are the mates together with the riggers.
The crew on *Pioneering Spirit* mainly operate the winches while the crew on *Iron Lady* attach the mooring lines to the bollards.

2.4 Reference wind turbine

For this research, A 14+ MW wind turbine will be used as reference to determine the size of the wind turbine components. Each wind turbine is assumed to be split up in one nacelle, three blades and one tower, the blades will be stored in a so-called blade racks. The weights as given below include 10 % weight contingency. The blade racks, consisting of three blades above each other, are expected to have a height of approximately 30 m and a total weight of 186 Tons. The Nacelle + transport frame is expected to be cube shaped with a height of 18.5 m and a weight of 801 tons. The turbine tower, in one piece, is assumed to have a height of 111 m with a weight of 793 Tons, [9].
These numbers show that the weights are relatively low. The sizes however are huge.

2.5 Broader scope, the mooring procedure

The mooring procedure entails a broader scope, ranging from a barge leaving the harbour up to barge disconnecting from *Pioneering Spirit* after it is successfully unloaded. The mooring procedure can be split up in four steps, transit, approach, secured alongside and finally after fully unloading the barge is unmoored. The performance of the mooring procedure heavily depends on the experience and know-how of the crew involved. The mooring system involves the third step of the mooring procedure, when the barge is secured to *Pioneering Spirit*.
The two most important design requirements of the mooring procedure is safely bringing wind turbine components from shore to *Pioneering Spirit* and ensuring the barge to be fully unloaded with the designated crane.
Satisfying the requirement of fully unloading the barge is challenging due to the combination of a large sized barge, loaded with large and heavy wind turbine components.
Several options to optimize the barge area that can be reached by crane are available. For the research question stated in this thesis, the barge stern extends 40m in longitudinal direction from *Pioneering Spirit* stern, shown in Figure 2.5b.

Heading control is preferred to obtain maximum shielding and thus reduce relative vessel motion resulting in minimum mooring loads. However, installing a wind turbine onto the pre-installed foundation requires a pre-defined heading. During the wind turbine assembling process, the heading can be set based on weather forecasts. Therefore, sufficient heading control can be assumed such that the floating bodies are subjected to environmental loads for three main directions that will be defined in section 2.7.

The mooring system is part of the mooring procedure, therefore the entire mooring procedure in analysed in Appendix B, including a more elaborated discussion of the topics addressed in this section. Starting with a stepwise approach to improve and evaluate the mooring procedure. This approach begins with stating the design requirements and criteria, performing a risk assessment, describing the base case mooring procedure and a concept for improvement. Finally the methodology to evaluate

whether the mooring procedure is improved is explained and applied to the base case and improved concept.

2.6 Mooring in general

Mooring, securing a vessel to a fixed or floating connection point, has been done for centuries. When human mankind built the first boat, they had a way to moor it. From that moment onward, until the last decades, mooring has been done with using ropes, let it be made out of different materials. However, currently new mooring techniques are being developed. For example, the Moormaster design which uses 'vacuum pads' for securing a floating object [10], more on this to come in this report.

For mooring systems, the distinction can be made between mooring to a fixed location, for example anchoring or mooring to a quayside and mooring to a moving object, for example another vessel. The latter mooring operation is referred to as side-to-side mooring.
The focus in this thesis will be on a side-to-side mooring system. The main purpose of a side-to-side mooring system is to prevent the moored vessel for drifting away and to reduce relative motions. That requires for some degrees of freedom to be restricted by a mooring system.
To restrict relative vessel motions, a mooring system should be able to withstand the loads caused by the most adverse environmental conditions that occur. These environmental conditions depend on the location and the duration that the mooring system is installed.

Figure 2.3 shows a typical mooring configuration at a tanker terminal, it represents the naming of different mooring lines. In general, the breast lines take mainly transverse loads, the spring lines take most of the longitudinal loads.

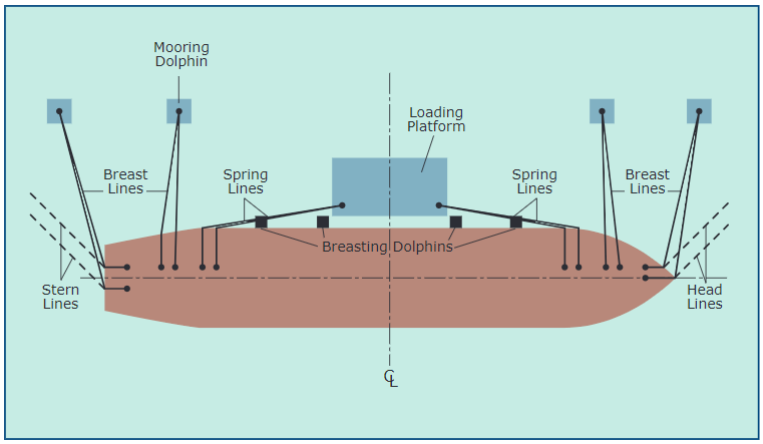

Figure 2.3: Typical Mooring pattern
source: Oil Companies International Marine Forum [7]

Having a mooring system consisting of mooring lines, the material properties and line dimensions play a major role in the mooring system properties. Next to mooring lines, the the most important parts in a mooring configuration are: fenders, winches, bollards and fairleads. [11].

2.7 Sign convention

The standard sign convention for vessels will be used throughout this thesis, represented in Figure 2.4. Each free floating body in water has six degrees of freedom. Translations x, y, z are called surge, sway and heave respectively. Rotations ϕ, θ, ψ are called roll, pitch and yaw respectively.

Two vessel moored to each other can be seen as a system consisting of 2 bodies, both with six degrees of freedom.
In this thesis there will be referred to vessel motions, this includes position, velocity and acceleration. Most often only the position will be shown.
Figure 2.5 includes a top view and view from aft of the multi-body system. Relevant dimensions are denoted including the corresponding symbols. Table 2.1 represents the project specific dimensions, that are relevant for this thesis.

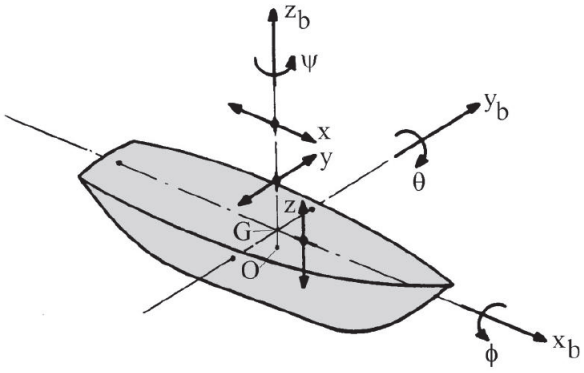

Figure 2.4: Definition of ship motion in six degrees of freedom
source: Offshore Hydromechanics [3]

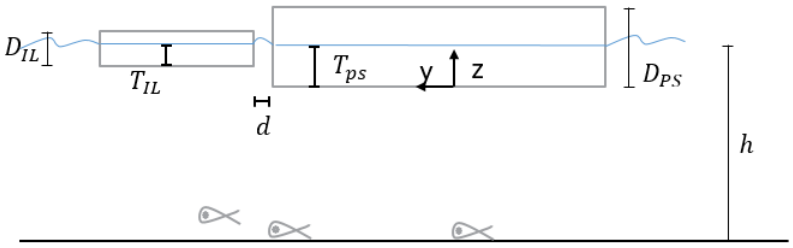

(a) Multi-body view from aft

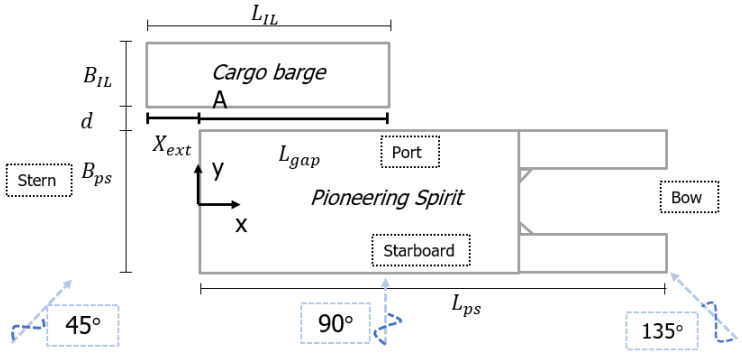

(b) Multi-body view from top. Including beam and quartering incoming wave directions

Figure 2.5: Multi-body top view and view from aft. Including relevant dimensions and corresponding symbols. 'A' denotes the location for computing relative vessel motions later in the report.

Table 2.1: Research specific dimensions

	Variable	Symbol & unit	Value
Pioneering Spirit	Length overall	L_{ps} [m]	382
	Breadth overall	B_{ps} [m]	124
	Operational draft	T_{ps} [m]	17
Iron Lady	Length overall	L_{IL} [m]	200
	Breadth overall	B_{IL} [m]	57
	Depth at side	D_{IL} [m]	13
	Draft	T_{IL} [m]	6
Gap between *Pioneering Spirit* & *Iron Lady*	Gap width	d [m]	3.6
	Gap length	L_{gap} [m]	160
	Longitudinal extension	X_{est} [m]	40
General	Water depth	h [m]	30

2.8 Reference location

Two reference locations are used in this thesis. The first location is located in the Southern North Sea. For this reference location a large amount of data is available ranging from bathymetry to metocean data. This data can be used to compare the base case and the improved mooring system in the end. Some site specific information:

- Water depth ranging from 18- 27 m.
- Minimal spacing between turbines four times turbine diameter. Resulting in a spacing of approximately 800 m. [12]
- 10 year return period significant wave height and wind speed is 6.1 m and 33 knots, respectively. Based on 42 years data from [13].
- 50 year return period current is expected to be 1.0 m/s [12].

The second reference location used in this thesis is located in the Bay of Biscay, which is known for its rough environment, mainly due to long period swell waves. Enabling the possibility to compare to areas with different wave conditions: wind waves and swell waves.

3 Thesis approach

The aim for this thesis is to improve the workability of the mooring system connecting *Iron Lady* and *Pioneering Spirit*.
Next to that, touch upon improving the mooring procedure in a thought provoking way.

These goals can be reached by going step by step through the stepwise approach, after a detailed literature research has been done into the relevant literature.

3.1 Step wise approach

The approach can be summarized in a 15 step plan.
Approach to improve the mooring system:

1. Define the mooring system requirements for barge mooring, as part of the wind turbine installation process.
2. Define the base case mooring system configuration.
3. Define the environmental conditions based at the reference location for wind turbine installation, including wind waves and current.
4. Define loading conditions for the cargo barge, *Iron lady*, to transport wind turbine components. Define loading conditions for *Pioneering Spirit* to assemble and install wind turbines.
5. Build the single body (barge only) and the multi-body (*Pioneering Spirit* and *Iron Lady*) model in the diffraction analysis software, Ansys Aqwa.
6. Validate and verify the diffraction analysis and perform a single and multi-body sensitivity analysis.
7. Acquire results from the multi-body diffraction analysis. Including the hydrodynamic matrices, displacement and load RAOs.
8. Build the single body and multi-body model in the time domain software, Orcaflex, and import results from the diffraction analysis.
9. Validate and verify the time domain model and perform a single and multi-body sensitivity analysis.
10. Build the base case mooring system in the time domain model, in Orcalfex.
11. Come up with concepts for improving the mooring system.
12. Build the concepts for improving the mooring system in the time domain model, in Orcaflex.
13. Find the limiting sea state for each mooring system, for environmental conditions coming from 135°.
14. Post process results, determine the corresponding workability.
15. Conclude and discuss whether the workability of the improved mooring system concepts is improved, compared to the base case.

Figure 3.1 represents the stepwise approach to improve the mooring system in a flow chart.

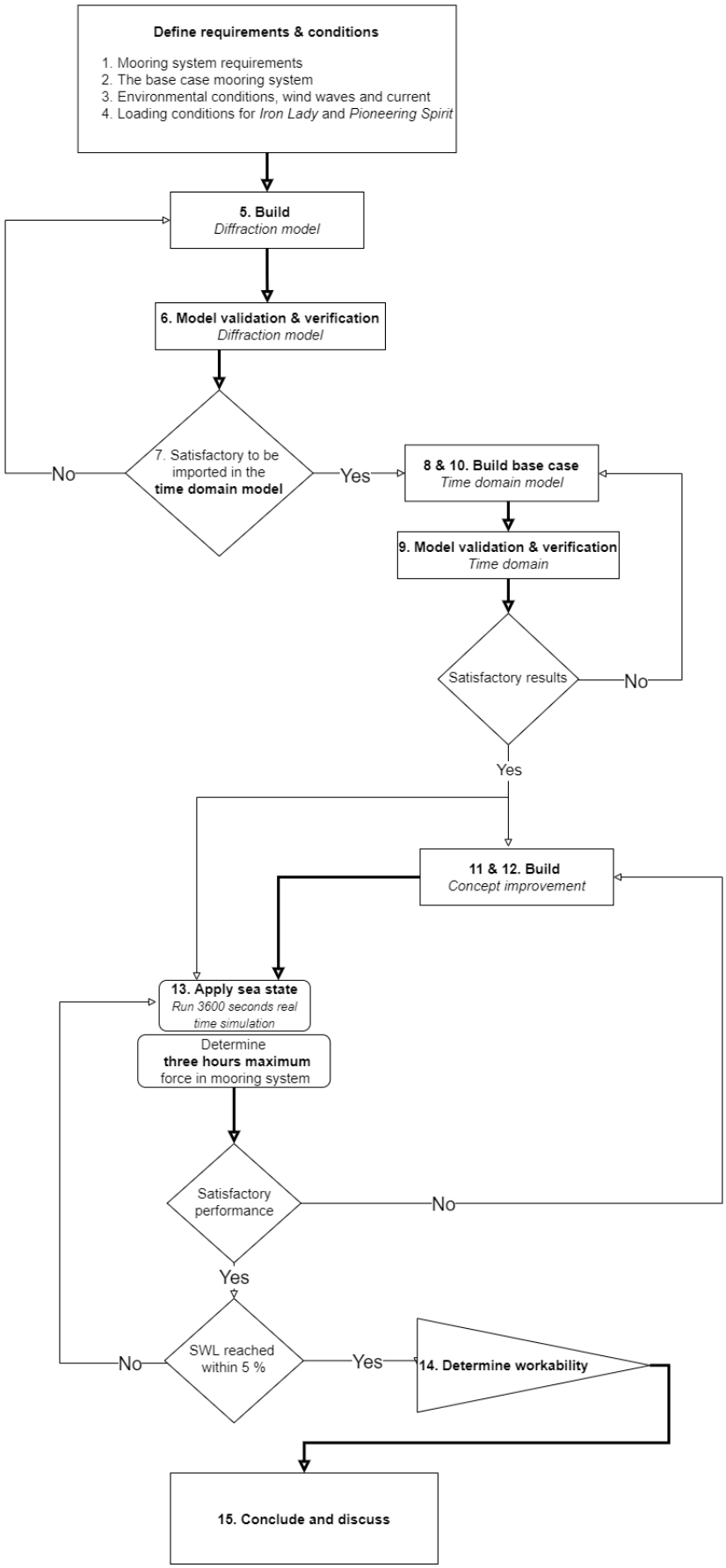

Figure 3.1: Flow diagram showing the thesis approach to improve the mooring system.

3.2 Assumptions

This research includes building a numerical model that describes reality based on analytical relations. Since these analytical relations are based on assumptions, the results of this research will be too.
Most important assumptions are listed and justified below, others will be explained in the sections where they are implemented.

1. The surface elevation is assumed to be Gaussian distributed, the wave amplitudes are assumed to be Rayleigh distributed.
2. Waves are expected to have small amplitude compared to wave length. Resulting in small sloped waves.
3. Ship motions can be represented as the sum of the harmonic and linear response to a distribution of random regular waves with different frequencies represented by the wave spectral energy.
4. Environmental conditions are not affected by bathymetry, assuming a flat seabed.
5. Current and wind velocity is assumed to be constant over time and independent of elevation above the seabed and the free surface respectively.
6. Environmental loading is assumed to be co-linear and wind, waves and current to be aligned.
7. Both vessels have zero forward speed.
8. *Pioneering Spirit* has sufficient DP capability to keep position when a barge is moored to it.
9. The axial stiffness of the mooring lines is assumed to be constant.
10. Both vessels are rigid bodies so no deformation will be present.

Assumption 1 to 4 comprises that linear waves are applied, represented by a pre-defined a wave spectrum. Considering the water depth at the reference location, intermediate water depth conditions are present. The linear wave assumptions would better fit deep water conditions since the limited water depth can affect the wave profile which means that more non-linear wave types need to be considered. The amount of non-linearity can be indicated by the Ursell number and the effect of (non-)linear wave patterns can be considered in follow-up research.
The assumption for constant wind and current velocity over height is rather conservative, because in reality the wind and current velocity will be lower close to the boundaries (sea surface and seabed). More detail can be added by applying wind spectrum (e.g. Froya spectrum) and apply a current velocity profile as described by R. Stewart *et al.*, [14].
In reality, depending on the reference location, co-linear environmental loads is not likely to occur and therefore a conservative assumption.
Zero vessel speed is a valid assumption when the mooring system is connected. Transit between pre-installed wind turbine foundations will either be supported by tugs or happen at very slow speed, in the order of 1 or 2 knots.
Pioneering Spirit has DP capabilities to keep a small offset, when having a barge moored alongside while having 500 Ton bottom tension in pipelay mode. Therefore, in this research *Pioneering Spirit* is assumed to follow first order motions only. Exact DP capability values are confidential but a close-to-zero offset is realistic.
Constant Young's modulus of the mooring lines is realistic when operating in the material elastic region only. Since the mooring lines in this research are relatively long and they are not new but used before, the cross-sectional area can be assumed to be constant provided that the Safe Working Load is not exceeded. Making the assumption of constant axial stiffness realistic.
Assuming the vessel deflection in transverse direction to be zero is realistic considering the high stiffness compared to the external forces in transversal direction. Long waves, in the order of the body length, can cause sagging and hogging resulting in vertical vessel deflection. However, throughout this research it will come clear that mooring line loads do not restrict vertical motions and therefore the assumption of rigid bodies is not expected to affect the results of this research.

4 Mooring system

The side-to-side mooring system connects two vessels that are alongside. By this connection the relative vessel motions are restricted. As described in chapter 2, the mooring system consists of multiple components, each bringing in its own design requirements. The main requirement is that the Safe Working Load of the mooring system is exceeded. The main criteria is that the workability of the mooring system is maximized.
The mooring system will be subjected to three incoming directions, bow-quartering, beam and stern-quartering, respectively 45, 90 and 135°.
This section starts with the purpose of the mooring system. After which the different mooring system components are discussed. Then the base case mooring system will be explained. This base case mooring system will be used for comparison of the mooring system improved concepts. The design requirements and criteria will be given. Finally the method on how the mooring system concepts will be compared is explained.
This chapter includes step 1 and 2 of improving the mooring system, as explained in section 3.1.

4.1 Purpose of the mooring system

The main purpose of a side to side mooring system is to restrict relative vessel motions. More specifically restrict the drift motions and limit the vessel offset.
The position of the vessel consists of a mean and a time varying part. The time varying part consist of first order and low frequency motions. These low frequency motions are sometimes referred to as second order because they are mainly induced by the second order wave drift force. The mean part is referred to as the offset.
The first order motions in general cannot be restricted because of the large mass and inertia of the vessels involved in this thesis.
The low frequency second order body motions can be restricted by the mooring system.
The difference between the first and second order motions is well represented in Figure 4.1.
Considering the forces in the mooring system, for simplicity looking at the static problem. The following conditions should hold.

$$\sum F_x = 0 \sum F_y \quad = 0 \sum M_z = 0 \tag{4.1}$$

When environmental conditions are added. The mooring system has to counteract these forces to make sure equation 4.1 is satisfied. These simple relations should be kept in mind when designing a mooring system.
For an ordinary mooring system, consisting of mooring lines and fenders, the stiffness and elongation/-compression determines the force in the lines or fenders. Due to the yaw angle, the elongation depends on the location line or fender is attached to.

Regarding the influence of the mooring system properties, the motion frequency for a non-restricted Degree of Freedom (DoF) will be equal to the incoming wave frequency, the amplitude however will differ. For a restricted DoF, the mooring system properties cause the vessel to respond with a different

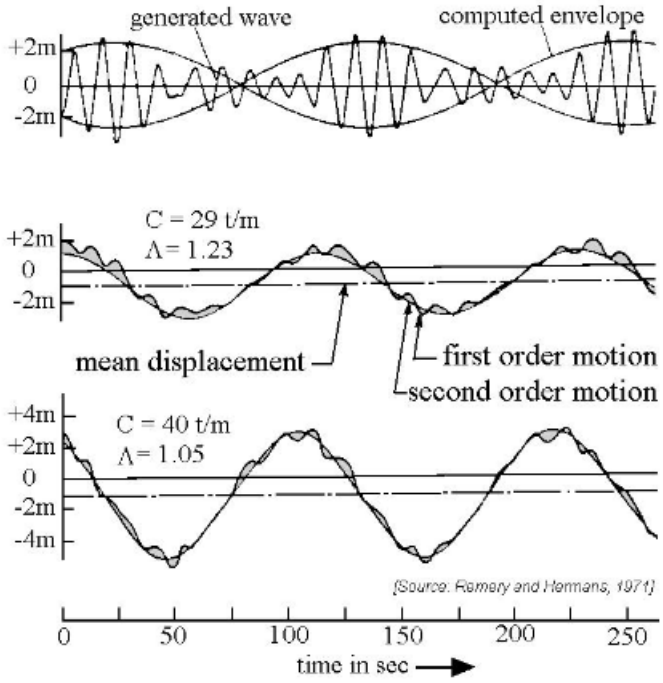

Figure 4.1: Low-frequency surge motion of a barge
source: Offshore Hydromechanics [3]

frequency. Each DoF of the floating body has its natural frequency, which is important since exciting the system with frequencies in the vicinity of this natural frequency and sufficient amplitude might lead to resonance.
The natural frequency depends on the mooring system properties, stiffness, damping, mass and added mass of the restricted body.

4.2 Equipment involved in the mooring system

The mooring system includes a number of key components that together determine the mooring system properties. The equipment involved determines most of the mooring system requirements. The mooring system components of the conventional way of mooring, the mooring lines, fenders and connection points will be discussed in this section. Next to the mooring equipment, also the crew that is required to operate the mooring system will be mentioned.

4.2.1 Mooring lines

A mooring line can be modelled as a spring, where stiffness and elongation determines the load. These loads result from restricting relative vessel motions. The mooring line properties depend on the mooring line material and the design of the mooring line, for example how the individual strains are oriented.
Considering the static situation, it can be stated that a small allowable offset requires a stiff mooring arrangement $F = k \cdot x$ with x being the mooring system displacement and k the mooring system stiffness. Besides stiffness, the mooring line can be described with a total force contribution form damping. Since limited research is found by the author on mooring line damping, a sensitivity analysis is performed and described in section E.0.4.2. Mooring line tension is learned to be limited sensitive to the mooring line damping, therefore the mooring line is modelled with zero damping.

The mooring line length for this thesis consist partly of steel wire and stretchers, these stretchers are made out of polypropylene. Steel wire can be considered as stiff while the stretchers can be considered as soft. Steel wire is stored on the winch and stretchers can be manually connected to the steel wire.
For offshore mooring systems, a typical stretcher length is 20 % of the total line length. Therefore, also in this thesis, each mooring line has a length ratio of 20 % stretcher and 80% steel wire. In reality, the length percentage of wire and stretchers cannot be adjusted easily because the stretcher will have a pre-defined length.

4.2.1.1 Mooring line stiffness

The mooring system stiffness is determined by the stiffness of the individual components. Regarding the mooring lines, the axial stiffness (stiffness per unit length) is determined by the Young's modulus, E, and the cross-sectional area, A. In order to be able to model the mooring line as a linear spring, the axial stiffness is assumed to be constant with line extension. The axial stiffness at 10 % line extension is used as axial stiffness over the entire range of extension. In reality the axial stiffness will not be constant, as both the Young's modulus and cross sectional area will change upon extension.
The Young's modulus dependence on line extension, strain, can be learned from the stress strain curves represented in Figure 4.2. The cross sectional dependence on line extension, depends on the orientation of individual line strains.
With assuming the axial stiffness to be constant, this research assumes the mooring lines to operate in the elastic region, constant E, and therefore not taking into account non-linear material properties.
Assuming the line cross-sectional area to be constant neglects reorientation and deformation of individual strains depending on tensile stress.

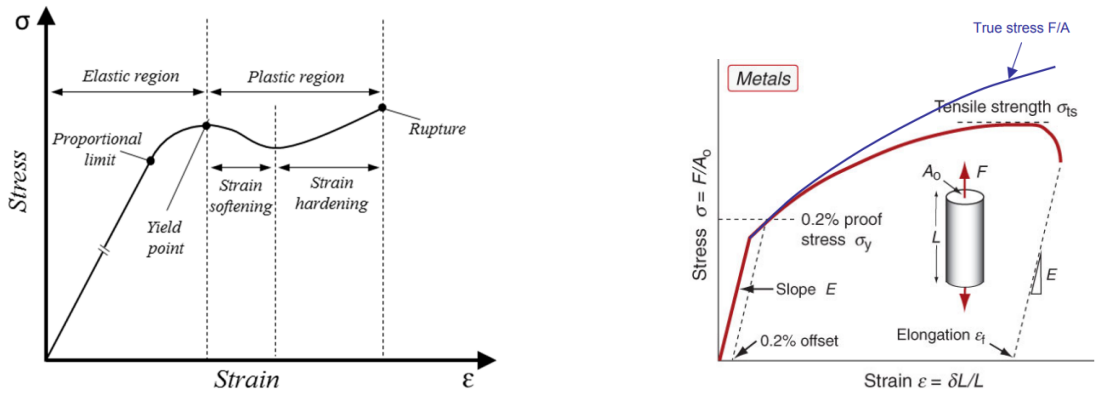

(a) Polymer optical fibre *source: Journal of Marine science and engineering* [15]

(b) Metal *source: Materials engineering, science, processing and design* [16]

Figure 4.2: Typical stress-strain curves for an optical fiber and metal

The mooring line stiffness, with unit kN/m, depends on the axial stiffness and the line length according to the following equation.

$$k = \frac{EA}{l_0} \tag{4.2}$$

With EA the axial stiffness in kN and l_0 the initial line length in m. The mooring line generally consists of two sections. One section made of steel wire and the other part a stretcher, connected to each other. These two sections can be modelled as serial springs as they both take the same force but will have different elongation, depending on their properties.
The axial stiffness, EA, for the steel wires, on the drum on *Pioneering Spirit* and the polypropylene stretchers available are respectively $90.75E3$ kN and $11.08E3$ kN, [17]. To limit complexity of the problem, only

the common used mooring line materials and diameters are involved in this research.

$$EA_{tot} = \frac{f_{tot}}{(\frac{f_{wire}}{EA_{wire}} + \frac{f_{str}}{EA_{str}})} \tag{4.3}$$

f_{wire} and f_{str} are defined as the ratio's of wire and stretcher length respectively, a ratio for the steel wire of 0.97 means that 97 % of the mooring line consists of steel wire. Equation 4.3 enables to calculate the corresponding axial stiffness of both the stretcher and steel wire considering it as a single line. The derivation of this formula can be found in section E.0.3.2. Substituting $f_{str} = 0.03$ and $f_{wire} = 0.97$ results in a combined axial stiffness of $EA_{tot} = 75E3$ kN. The intention was to use a value of 20 % stretcher length, a typical mooring line material ratio which can be used in industry. However, due to incorrect methodology applied to compute the combined axial stiffness, the axial stiffness corresponds with 3% stretcher length, this will be discussed in section 9.3.4.

For a mooring system, the system stiffness in a certain DoF is determined by multiple components. These components can be modelled as parallel springs. Therefore the total system stiffness is related via equation 4.4. In the time domain model, the equivalent stiffness also depends on the mooring line catenary shape.

$$k_{x,system} = \sum k_{x,components} \tag{4.4}$$

4.2.1.2 Stretcher purpose

Regarding the stretchers, these do have three main purposes. First, to reduce the mooring line stiffness. The mooring wire on the winch cannot easily be adjusted, therefore the mooring wire properties are optimized by connected another mooring line to the mooring wire. The length ratio between these lines determine the total mooring line stiffness which enables the engineer to optimize the stiffness. A stiff mooring system will generally result in higher loads and lower offset.
Second, the Safe Working Load for the entire mooring line depends on the weakest link. The stretcher is usually designed to be the weakest link as it can easily be replaced. Therefore the stretcher is connected to the mooring wire on one side and to the bollard on the other side, as this part goes through the fairleads where usually most of the wear and tear happens. Wear and tear is disregarded for now.
Lastly, the stretcher is usually more ductile and therefore improves the ability to store energy in the mooring line which is important upon high impacts.

4.2.2 Fenders

The main purpose of a fender is to prevent for collision between both vessels. Additionally, to absorb energy upon impact during berthing.
Fenders can be described by a stiffness and damping curve. The specifications of the fenders that are available on *Pioneering Spirit* are applied in the modelling part of this thesis. The dimensions of these, Yokohama 3.3x6.5 pneumatic, fenders are given in table 4.1 referring to the symbols stated in Figure 4.3.

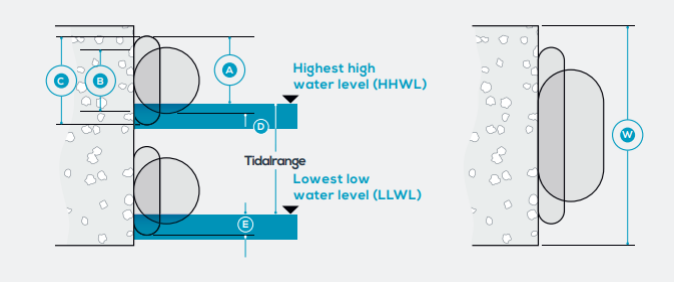

Figure 4.3: Fender dimensions definition, *source: Trelleborg Marine systems* [18]

Table 4.1: Fender installation dimensions of the Yokohama 3.3 x 6.5 pneumatic fenders. Dimensions are given in [m]

Size	A	B	C	D	E	W
3.300 x 6.50	3.38	3.14	4.46	0.50	1.08	8.50

The total mass of a single fender is 5370 kg. The uncompressed net pressure in the fender is 0.8 bar. The Yokohama pneumatic fender supplier, Trelleborg, provides fender displacement and corresponding reaction force data, research into pneumatic fender behavior by Park *et al.* shows that the stiffness curve shape can be estimated by a third order polynomial, [18] [19]. The stiffness curve applied in the numerical model, including data points, is represented in Figure 4.4.

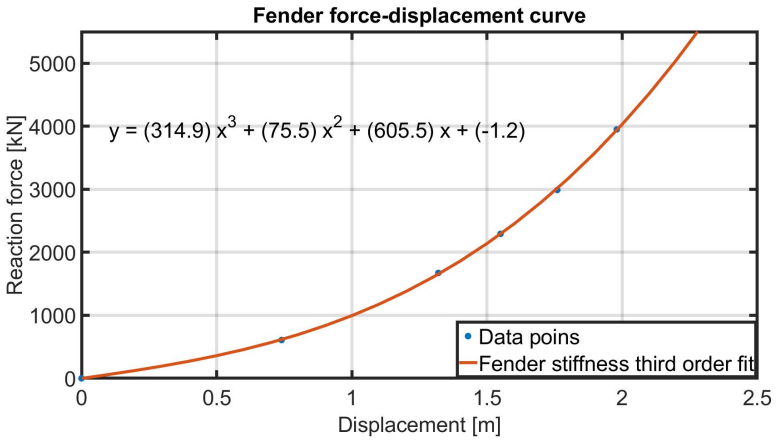

Figure 4.4: Force vs displacement curve of Yokohama 3.3x6.5 P80 pneumatic fender representing the stiffness.
source: Trelleborg Marine systems [18]

The non-linearity in the fender force-displacement curve is related to non-linear material properties of the fender material under pressure.
Research regarding the fender damping properties is found to be limited described in literature. A small damping term is considered in this research, including a sensitivity analysis, as will be explained in section 6.4.2. This damping term represents energy dissipation for example due to deformation.

4.2.3 Connection points

The mooring line connection points at *Pioneering Spirit* and *Iron Lady* consists of bollards, fairleads and winches, Figure 4.5 shows examples of these. Bollards are structures to attach the end of a mooring line to, as can be found on quaysides. Fairleads guide the mooring line from the winch overboard the vessel to the other vessel.
The winches are used to adjust the mooring line length and with that applying pre-tension, the unused mooring line length can be stored on the winch drum.
Mooring winches are usually driven by an electric engine and consist of a winch brake that prevents the mooring line from unwinding. This brake is applied whenever the pre-tension is set, so this winch does not apply constant tension but constant line length. The winch brake includes a safety system that whenever the maximum allowable tension is exceeded, the brake will be released and the mooring line can slip through the winch.
Iron Lady consists of bollards and fairleads, while *Pioneering Spirit* also consists of winches, located close to the fairleads. That means that the mooring line comes from *Pioneering Spirit* and will be attached to *Iron Lady*. The locations of fairleads and bollards on both vessels are shown in Figure 4.6.

(a) Winch *Courtesy: WÄRTSILÄ* (b) Fairlead at *Pioneering Spirit* (c) Bollard *Courtesy: Straatman BV*

Figure 4.5: Typical winch, fairlead and bollard

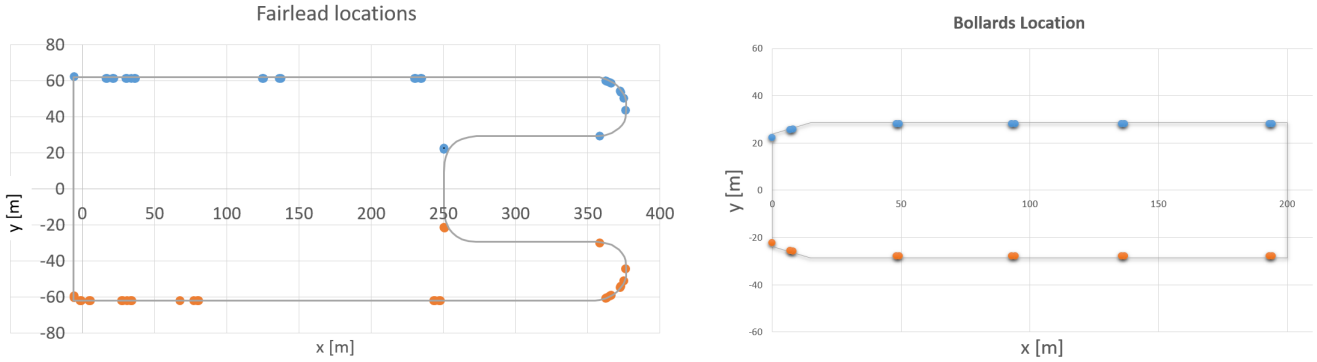

(a) Fairlead locations on *Pioneering Spirit* (b) Bollard locations on *Iron Lady*

Figure 4.6: Currently existing mooring equipment on *Pioneering Spirit* and *IL*

In this research, the connections are assumed to have sufficient structural capacity and the original connection point locations are incorporated as much as possible.

4.3 Mooring system design requirements

Each concept has to satisfy the design requirements. Design criteria however, are defined as 'would like to have'.
The main mooring system requirement is to restrict the vessel motions while keeping forces within design limits [20]. A more elaborated list of design requirements is given below. These requirements should be satisfied for every valid mooring concept.

1. Maximum mooring load in the mooring system does not exceed the Safe Working Load (SWL).
2. Relative surge and sway motion amplitude should not exceed 1.0m around the offset, based on industry experience. No limit on the offset is stated, except that for the improvement concepts the offset should be in the same order or smaller than for the base case mooring system.
3. Crane operational limits should be satisfied. More specifically, relative heave motion at the crane tip with respect to the deck of the barge may not exceed the crane operational limits.
4. Safety requirements should be met, for example the mooring system should be redundant.
5. The mooring lines should have a minimum pre-tension of 50 kN each, to have an initial stiffness in the system and to prevent for lines coming slack.
6. Regarding barge unloading, the barge needs to be 40m extended in longitudinal direction.

4.3.1 Mooring system Safe Working Load

The SWL is defined as the maximum load that is allowed to occur in the the mooring system. The SWL depends on the Maximum Breaking Load (MBL) and the applied Safety Factor (SF) via $SWL = \frac{MBL}{SF}$. The safety factor depends on the accuracy of the analysis method applied. In case multiple components are connected in series, the 'weakest-link' principle applies which means that the component with the lowest SWL is governing the maximum allowable load.
The MBL for winches, barge bollards and mooring lines on the winches are respectively 77, 135 and 169 Ton, [21]. The safety factor is equal to 1.67 [-] for a dynamic analysis, as given in Table C.1, [22]. Resulting in a mooring line SWL is equal to 46.2 Ton or 453 kN.
While the mooring system is installed between the cargo barge and *Pioneering Spirit*, the SWL of the mooring system may not be exceeded.

4.3.2 Relative motions

The relative motion is defined as the motion at the tip of the crane that will be used for unloading the wind turbine components, relative to deck of the barge at the exact same x and y locations. The x and y location will be chosen outside the Center of Gravity of the barge, to also take into the roll and pitch motions when determining the relative heave motion. This location is denoted as location 'A', as represented in Figure 2.5b.

The relative motions together with the mooring system properties determine the forces that will occur in the mooring system. The purpose of this research is to increase the workability by making sure the SWL of the mooring system is not exceeded. Besides, the relative motion have to be considered at the maximum workable sea state, based on the SWL limit. Section 4.6 provides limits for the relative motions that should be satisfied for each mooring system concept.

4.3.3 Crane operational limits

Crane operational limits are defined as the boundaries at which the crane can operate. These operational limits are given in terms of relative velocity at the crane-tip and wind speed. Crane operational limits are considered outside the scope of this thesis.

4.3.4 Offset in surge and sway direction

The stiffness of the mooring system, together with the mean environmental load that is applied, determines the mean position of the barge with respect to *Pioneering Spirit* and is defined as offset.
The offset is preferred to be small to keep the barge close to the vessel to make sure the barge cannot build up speed and bump into the fenders. This would result in peak loads in the fenders. Next to that, the offset is preferred to be limited to maximize the area on the barge that can be reached by the crane. Limiting the offset adds requirements to the system stiffness.
Furthermore, the offset in sway direction is important regarding safety. For the wind turbine installation procedure, the stern of *Pioneering Spirit* will be close to the foundation of the wind turbine to install. Therefore the offset in sway, and therefore also yaw, is preferred to be limited to make sure the barge will not collide with the wind turbine foundation.
No limit on the offset is stated, except that for the improvement concepts the offset should be in the same order or smaller than for the base case mooring system.

4.3.5 Safety

Safety has number one priority at all times. With safety to personnel the highest weight. No dangerous situations are allowed to occur. Risks should be limited by reducing severity, probability or adding mitigation's and pre-cautions.
According to DNV, at least the following three mooring system conditions should be checked for all incoming wave directions, [22]. First for normal conditions. Second, for a single line failure. Third, thruster assistance failure. So in the case when a thruster is involved in the mooring configuration, for example when a vessel is on DP, the system should be checked in case one thruster fails.

The second and third case refers to redundancy of the mooring system, which is a required that is related to safety. Meaning that the barge should still be kept in position in case of a single line or thruster failure. The redundancy check will not be part of this thesis scope.
Other than the risk assessment, as described in appendix B, safety will not be further adressed in this work.

4.3.6 Pre-tension

Pre-tension is a rather theoretical concept. Because in the numerical models, pre-tension is defined as the tension in the mooring lines when no external forces are applied. This mooring line tension comes from initial compression of the fenders.
The purpose of pre-tension is to reduce the catenary shape of the mooring lines, besides it also make sure there is stiffness in the mooring system at all times. Additionally, pre-tension is applied to prevent for snap loads to occur in the system due to unloaded lines. As these snap loads can lead to excessive dynamic loads in the mooring system.

In reality pre-tension cannot be applied as in the numerical model, because there are always external forces present. The funny fact, that I learned during my time offshore, is that the mooring winches, available on *Pioneering Spirit*, cannot read the tension that is applied by the winch but only the percentage of the maximum torque that the winch applies. The mooring line tension corresponding with that torque depends on the radius of the winch drum and with that on the mooring line length that is stored on the drum. Therefore, the amount of pre-tension or initial tension that is applied on the mooring lines is only based on experience of the crew.
With use of a sensitivity analysis, it is found that pre-tension in the numerical model is not affecting the results of this research, as described in section I.1.

4.3.7 Barge longitudinal extension

One requirement for the mooring procedure is that all wind turbine components need to be unloaded, as explained in section B.4.2. To satisfy that requirement for a barge with a length of 200m, for example *Iron Lady*, the stern of the barge needs to be extended in longitudinal direction by at least 40m.

4.4 Design criteria

1. High mooring system workability is preferred to maximize time to operate. This will be further discussed in section 4.7.
2. The mooring system is preferred to be suitable to multiple barge sizes.
3. The fenders are preferred to be compressed at all times to prevent the barge from re-hitting the fenders.

4.4.1 Multiple barge sizes

To have a continuous operation, the mooring system should be applicable to multiple barge sizes because it will not always be a similar sized barge that brings the wind turbine components.
Iron lady is expected to be the largest barge so crane reach will not be a problem. However, use of bollards, fairleads and winches should be applicable to a smaller barge size.

4.4.2 Limited fender re-hitting

Because the wind and current forces are assumed to be large constant forces, coming from a 45, 90 or 135 ° angle, compressing the fenders will be rather unique.
For these directions, it cannot be realised that the fenders are compressed at all times, this would lead to excessive mooring line forces.
Whenever the fender is not compressed, the vessel can build up speed and bump into the fenders which can lead to excessive forces in the fender. Next to that, it can lead to a shock on both vessels the latter however can be neglected due to the large sized vessels that are involved in this thesis.
Nevertheless, the maximum speed at which the barge encounters the fender should be considered.

4.5 Base case mooring system

Mooring systems are designed according to offshore experience that satisfies the classification codes, e.g. DNVGL-ST-N001 [22]. Important considerations when designing the mooring arrangement are the governing environmental loading maximum magnitude and incoming direction and also the allowable relative motions. Moreover, equations 4.1 should be satisfied at each time step. Preferably with each line taking approximately the same load since the heaviest loaded line determines the performance of the mooring system.

Mooring system improvement requires a base case system that will be installed if no improvement can be realised with this research. This base case system uses the mooring equipment, and its location, as currently available on *Pioneering Spirit*, as shown in Figure 4.6.

Figure 4.7 Represents an example mooring system that is used within Allseas for an earlier project. However, for that project, the barge stern was not extending from *Pioneering Spirit*. Extending the barge requires a mooring line at the barge stern that is oriented in sway direction, in order to restrict both sway and yaw motions. No winches are available at stern of *Pioneering Spirit* yet, therefore the additional line that is required an additional (dashed) line is drawn in Figure4.7.

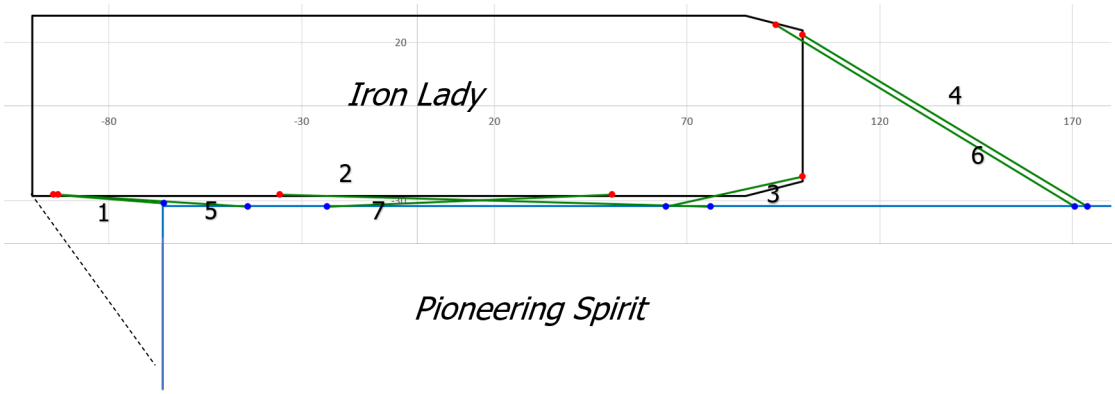

Figure 4.7: Example mooring system. Mooring lines like the dashed line are required to make this mooring system realistic and feasible.

For the base case system to be feasible, mooring lines in the orientation of the dashed lines are required. This brings to the mooring configuration as shown in Figure 4.8 where two winches are located at the stern of *Pioneering Spirit*, line 1 and 8. Placing winches at *Pioneering Spirit* stern is argued to be a realistic design choice and can be realised on board, according to engineers and crew within Allseas.
Additionally, the orientation of the other lines are changed to be optimized for environmental loading conditions coming from 135°, this will be considered as the governing direction for this thesis to have maximum shielding. The mooring system that will be used as base case for this thesis, Figure 4.8, is confirmed to be feasible within the Naval Architecture department of Allseas.

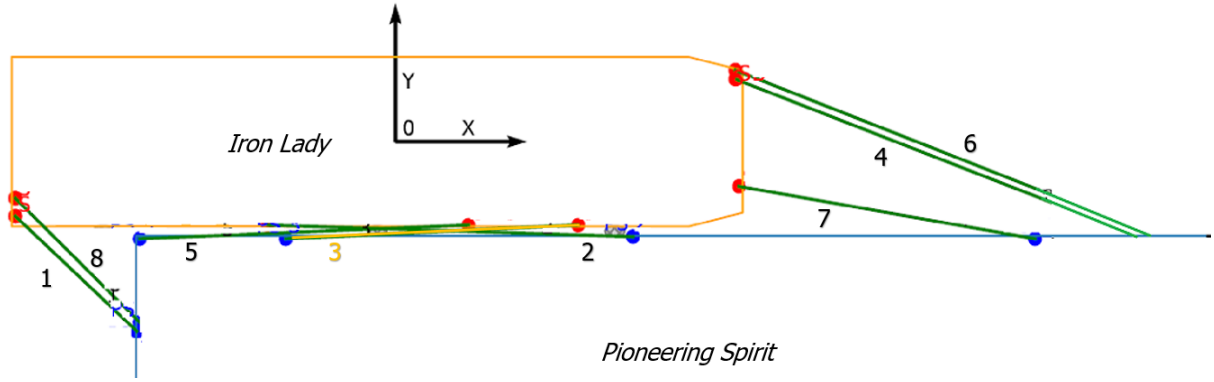

Figure 4.8: Mooring system for barge extending form *Pioneering Spirit* stern, using two additional winches at *Pioneering Spirit* stern

The above mooring configuration will be used as base case for comparing with other mooring improvement ideas. The base case consists of 8 mooring lines and 3 fenders. With each line a SWL of 453 kN. The three fenders are separated over the length of the gap between the vessels. The number of mooring lines and fenders will be kept constant for all the mooring improvement concepts.
The mooring system improvement concepts will be discussed in chapter 7.

4.5.1 Challenges in the base case mooring system, room for improvements

From discussions with Allseas personnel both in the office and on *Pioneering Spirit* a few challenges for the base case mooring system became clear. These shortcomings are listed below and will be considered when discussing the mooring system improvements in chapter 7.

- The workability of the base case mooring system is limited and is preferred to be improved.
- *Pioneering Spirit* has a large variable draft, resulting in a vertical distance between winch and bollard on the barge up to 17m. This can lead to steep mooring lines that require high mooring line forces to exert considerable forces on the barge in the horizontal plane.
- Another practical comment is the many lines that come together at *Pioneering Spirit*. This has to do with the fact that the mooring lines are steep but also that the winches are located close together. Because of all these lines coming together it is difficult for the winch operator to see which lines need to be tensioned. This could lead to unsafe mooring operations.
- The crane reach that is used for barge unloading is limited. Therefore the barge has to be extended from *Pioneering Spirit* stern. This barge extension leads to excessive environmental loads acting on the barge due to reduced shielding. A sensitivity analysis is performed and described in section 7.1, to address the effect of barge extension on environmental and mooring loads acting on the barge.

4.6 Comparing mooring systems with relative motions

Following the mooring system design requirements, the relative surge and sway motion should have an amplitude smaller than 1.0m around the offset. This relative motion should be checked for the sea state that is workable in terms of SWL.

4.7 Comparing mooring systems with workability

Multiple mooring systems will be presented throughout this research. The first system, the base case, is already discussed. To ultimately conclude which mooring system fits the mooring system criteria best, all designs should independently be compared.
Each mooring system concept has to satisfy the design requirements, but can be scored on the design criteria. The main design criteria in the scope of this research is optimizing the workability. Workability is defined as the percentage of time where the operation can be executed based on location specific hindcast data, [23].
The workability depends on the environmental conditions, wind, waves and current. To simplify the problem, the wind and current speed will be set constant. Resulting in a fixed workability for wind and current. For waves, the sea state will be varied to find the limiting sea state, from that the workability is computed.
This method assumes wind, waves and current to be co-linear and have its maximum at the same time and will therefore provide conservative results regarding workability.
The method applied to compute the workability will be explained in the remainder of this chapter.

4.7.1 Post-processing data to compute the workability

The mooring system is modelled in the time domain, as will be extensively discussed in the coming chapter. Analysing the outcome of the time domain, resulting in the three hours maximum value of relative motions and mooring loads is used to compute the workability. Three hours maximum is defined as the maximum value that is reached in a three hour lasting sea state.

Computing the typical three hours maximum value, based on data from a frequency domain model or based on a time series, requires the maxima in the data to follow a Rayleigh distribution. Frequency domain modelling applied in this research consist of using the motion RAOs from the diffraction analysis and computing the relative vessel motions. Figure 4.9 represents a typical Rayleigh distribution.

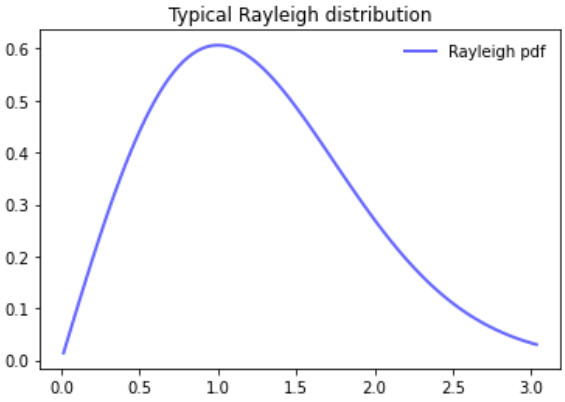

Figure 4.9: Typical Rayleigh distribution

Whenever a Gaussian distributed, narrow banded, linear wave surface is applied, in other words, a Gaussian distributed wave spectrum with a not too wide frequency range. The extreme wave elevation can be assumed to be Rayleigh distributed, this assumption is known to be valid and rather conservative for linear waves, [3]. The relative vessel motions depends on the incoming wave train, more specifically on the incoming wave height. Next, the force in the mooring system depends on the relative vessel motion. Following this theory, the maximum relative vessel motion and the maximum force in the mooring system are assumed to be Rayleigh distributed. With that, assuming a linear relation between wave elevation and vessel motions and mooring loads. The accuracy and validity of assuming the maximum relative motions and mooring line force to follow a Rayleigh distribution is treated in the time domain validation and verification, can be found in section 6.5.

The three hours maxima enables to compute data related to time, based on frequency domain data. The methodology applied to compute the three hours maximum based on frequency domain and time domain data will be shown in the remainder of this section.
For the frequency domain calculations an example calculation will be shown for computing the three hours maximum sway motion.
The sway RAOs is acquired from the diffraction analysis. From the applied wave spectral density and the sway RAO, the spectral response in sway direction can be determined by applying equation 5.7 which provides the energy in the system depending on the frequency.

$$S_r(\omega) = \left| \frac{r_a}{\zeta_a}(\omega) \right|^2 \cdot S_\zeta(\omega) \mid \tag{4.5}$$

Integrating the response spectra over frequency gives the zeroth order spectral moment, represented in equation 5.8. With this information, the three hours maximum sway motion can be found by substituting the zeroth order spectral moment and N, being the number of waves passing by, in equation 4.7. Assuming a wave spectrum with a not too wide frequency range is used means that approximately 1000 waves are passing in three hours. This excludes the need to compute the exact number of waves that are passing with $N = \frac{T}{T_z}$ where T is 10800 seconds (3 hours) in this case and T_2 the mean zero crossing wave period, [3].

$$m_{n\zeta} = \int_0^\infty \omega^n \cdot S_\zeta(\omega) \cdot d\omega \tag{4.6}$$

$$\text{Three hours max single amplitude} = \sqrt{2 \cdot m_0 \cdot ln(N)} \tag{4.7}$$

Computing the three hours maximum value from time domain simulations is similar but more time consuming. This method reduces the required computation time because the maximum force in the mooring system can be determined without running a three hour real time simulation.
As an example, the method to compute three hours maximum mooring line force will be explained in this section.
Assuming the maxima of the cycles to follow a known contribution, e.g. Rayleigh or Weibull allows to

statistically compute the maximum value occurring in a three hour sea state. What distribution will be applied and why will be explained in section 6.5.3.

From the mooring line load time history output, the standard deviation, σ, can be computed and imported in equation 4.8 to determine the zeroth order spectral moment. Equation 4.9 can be applied to compute the mean period, of crossing the mean mooring line load, T_z. m_2 is the second order spectral moment, and the N number of cycles in the simulation time, T. Finally, equation 4.11 enables to compute the three hours maximum force. Consisting of a static and dynamic part. The dynamic part depends on the simulation time via number of line load oscillations, denoted as N.

$$m_0 = \sigma_{zeta}^2 \tag{4.8}$$

$$T_z = 2 \cdot \pi \cdot \sqrt{\frac{m_0}{m_2}} \tag{4.9}$$

$$N = \frac{T}{T_z} \tag{4.10}$$

$$F_{max} = F_{static} + F_{max,dyn} = \mu + \sigma \cdot \sqrt{2 \cdot ln(N)} \tag{4.11}$$

The advantage of this method is that the maximum mooring line load, occurring in a three hour lasting sea state, can be computed from a shorter real time simulation length, together with the term 'ln(N)' and extrapolating 'N' by assuming the zero up-crossing period to be constant over time. This requires that the variable maxima, in this case mooring line load, to be Rayleigh distributed as explained in the beginning of this section.
Three hours maxima is a typical value, used in industry, to know the system performance. Having the three hours maximum enables to compute the workability of the mooring system for a reference location, as will be explained in the next section.

4.7.2 Metocean data

The two locations, that are explained in section 2.8, will be used for reference to determine the workability. The metocean data includes all environmental conditions, waves, wind and current. Each of these can be described with workability, defined as the percentage of time, annually, that these conditions are not exceeded. To make a conservative estimate of the total workability, these individual workabilities have to be multiplied.

Figure 4.10 shows the wave scatter plot for the reference location in the Southern North Sea. Each colored cell entry represents the percentage of annual occurrence. The workability can be determined by running simulations for all Hs and Tp combinations and summing up the entries of the scatter diagram for which the Safe Working Load of the mooring system is not exceeded. However, this is very time consuming therefore the computing the workability is simplified.
This simplified method assumes that a Tp of 7 seconds and Hs = 2.5 m results in lower forces and lower relative motions in the mooring system compared to Tp = 8 seconds and Hs = 2.5 m.
This results in that the workability can be estimated by running only a limited number of sea state. More specifically, sea states with two different peak periods will be checked in combination with varying significant wave height to find the sea state for which the Safe working load is reached.
The grey square in Figure 4.10 gives an example of entries that have to be summed to check the workability for a Tp value of 8 s and Hs of 2.5 m.

The assumption for lower mooring loads for lower sea state is expected to be valid for peak periods moving away from the vessels and mooring system natural periods. However, in case the lower periods are closer towards the system natural period, more excessive motions are expected to occur resulting in

higher mooring loads.
It is recommended to justify this assumption by running all combinations of Hs and Tp and determine for which sea state the SWL is exceeded, this justification is excluded from this research and subject of future research.

Tp [s] -->		0	1	2	3	4	5	6	7	8	9	10	11	12	13	14	15	16	17	18	19		
Hs [m]		1	2	3	4	5	6	7	8	9	10	11	12	13	14	15	16	17	18	19	20	Total	Accum
0	0.5	-	0.15	2.55	2.77	2.17	1.11	0.88	0.72	1.08	0.89	0.72	0.46	0.40	0.43	0.38	0.28	0.26	0.11	0.06	0.04	15.5	15.5
0.5	1	-	-	0.36	6.39	8.15	4.87	3.35	2.35	1.73	1.49	1.39	0.84	0.52	0.32	0.24	0.20	0.17	0.15	0.10	0.04	32.7	48.1
1	1.5	-	-	-	0.24	4.60	8.88	3.11	2.17	1.40	0.81	0.71	0.66	0.48	0.23	0.16	0.06	0.03	0.01	0.01	0.01	23.6	71.7
1.5	2	-	-	-	-	0.18	3.88	5.22	1.43	0.78	0.42	0.16	0.14	0.09	0.09	0.09	0.02	0.02	0.00	0.00	-	12.5	84.2
2	2.5	-	-	-	-	-	0.22	4.29	1.78	0.60	0.21	0.05	0.03	0.02	0.01	0.01	0.01	0.00	-	-	-	7.2	91.5
2.5	3	-	-	-	-	-	-	0.81	2.59	0.57	0.14	0.01	-	0.00	0.00	-	-	-	-	-	-	4.1	95.6
3	3.5	-	-	-	-	-	-	0.01	1.41	0.66	0.23	0.02	-	-	-	-	-	-	-	-	-	2.3	97.9
3.5	4	-	-	-	-	-	-	-	0.23	0.72	0.18	0.04	0.00	-	-	-	-	-	-	-	-	1.2	99.1
4	4.5	-	-	-	-	-	-	-	0.01	0.31	0.11	0.04	0.01	0.00	-	-	-	-	-	-	-	0.5	99.6
4.5	5	-	-	-	-	-	-	-	-	0.06	0.07	0.07	0.01	0.00	-	-	-	-	-	-	-	0.2	99.8
5	5.5	-	-	-	-	-	-	-	-	0.01	0.03	0.04	0.01	0.00	-	-	-	-	-	-	-	0.1	99.8
5.5	6	-	-	-	-	-	-	-	-	-	0.01	0.01	0.01	0.00	0.00	-	-	-	-	-	-	0.0	99.9
6	6.5	-	-	-	-	-	-	-	-	-	-	0.00	0.00	0.00	-	-	-	-	-	-	-	0.0	99.9
6.5	7	-	-	-	-	-	-	-	-	-	-	-	-	-	-	-	-	-	-	-	-	0.0	99.9
7	7.5	-	-	-	-	-	-	-	-	-	-	-	-	-	-	-	-	-	-	-	-	0.0	99.9
7.5	8	-	-	-	-	-	-	-	-	-	-	-	-	-	-	-	-	-	-	-	-	0.0	99.9
8	8.5	-	-	-	-	-	-	-	-	-	-	-	-	-	-	-	-	-	-	-	-	0.0	99.9
8.5	9	-	-	-	-	-	-	-	-	-	-	-	-	-	-	-	-	-	-	-	-	0.0	99.9
9	9.5	-	-	-	-	-	-	-	-	-	-	-	-	-	-	-	-	-	-	-	-	0.0	99.9
9.5	10	-	-	-	-	-	-	-	-	-	-	-	-	-	-	-	-	-	-	-	-	0.0	99.9
10	10.5	-	-	-	-	-	-	-	-	-	-	-	-	-	-	-	-	-	-	-	-	0.0	99.9
10.5	11	-	-	-	-	-	-	-	-	-	-	-	-	-	-	-	-	-	-	-	-	0.0	99.9
11	11.5	-	-	-	-	-	-	-	-	-	-	-	-	-	-	-	-	-	-	-	-	0.0	99.9
11.5	12	-	-	-	-	-	-	-	-	-	-	-	-	-	-	-	-	-	-	-	-	0.0	99.9
Total		0.0	0.2	2.9	9.4	15.1	19.0	17.7	12.7	7.9	4.6	3.3	2.2	1.5	1.1	0.9	0.6	0.5	0.3	0.2	0.1		
Accum		0.0	0.2	3.1	12.5	27.6	46.5	64.2	76.9	84.8	89.4	92.6	94.8	96.3	97.4	98.3	98.9	99.3	99.6	99.8	99.9		

Figure 4.10: Annual wave scatter diagram of the reference location in the Southern North Sea, based on 37 years of hindcast data.

The wave probability scatter diagram provides discrete data with a step size in significant wave height of 0.5m. The limiting sea state for the different mooring system concepts will be rounded to one decimal point. Therefore, interpolation between the wave probability data points is required. Based on industry experience, linear interpolation will be applied.
Additionally, because the limiting sea state is rounded to one decimal point, the mooring line load is not exactly equal to the SWL for the limiting sea state but within a range of approximately 5 %. Resulting in a small error in the probability calculation, in the order of permille.

An example to calculate the workability for Tp is 8 seconds and Hs is 1.3 m is computed with equation 4.12. With W the workability in %, P the probability in %, equation 4.13 represents how the total probability of the sea state being equal or lower than Hs = 1.0m and Tp = 8 seconds can be computed from the wave probability scatter diagram.

$$W_{Hs=1.3m,Tp=8s} = P_{Hs=1.0m,Tp=8s} + 0.3 \cdot \frac{P_{Hs=1.5m,Tp=8s} - P_{Hs=1.0m,Tp=8s}}{0.5} \tag{4.12}$$

With

$$\begin{aligned} P_{Hs=1.0m,Tp=8s} =& P_{Hs=0.5m,Tp=8s} + P_{Hs=1.0m,Tp=8s} \\ =& \sum (0.15 + 2.55 + 2.77 + 1.11 + 0.88 + 0.72) + \\ & \sum (0.36 + 6.39 + 8.15 + 4.87 + 3.35 + 2.35) = 33.7\% \end{aligned} \tag{4.13}$$

Figure G.1 includes the wave scatter diagram for the reference location in the Bay of Biscay, this Figure can be found in Appendix G.

Same as for waves, also for wind and current a probability scatter diagram exists, depending on the reference location. Figure 4.11 shows the annual wind scatter diagram for the reference location. The colored data represents the percentage of occurrence per year. Summing all values to the left of the grey bar gives a value of 92.5 % meaning that 92.5 % of the annual time, the wind speed will be lower than 25 knots. This workability is assumed to be sufficient, as for larger wind speeds, also the sea state

is expected to exceed the operational limits. Therefore a constant wind speed of 25 knots is taken into account. The wind speed is assumed to be constant over height.
The analyses were based on wind data for the period of January 1979 untill January 2016. The temporal resolution of the modelled wind speed data is 1 hour, the values are considered representative of an average window of 2 hours.

U10m_2h [m/s]		0	2	4	6	8	10	12	14	16	18	20	22	24	26	28	30		
		2	4	6	8	10	12	14	16	18	20	22	24	26	28	30	32		
U10m_1h [kts]		0.0	4.0	8.0	12.0	16.0	19.9	23.9	27.9	31.9	35.9	39.9	43.9	47.9	51.9	55.8	59.8		
Hs [m]		4.0	8.0	12.0	16.0	19.9	23.9	27.9	31.9	35.9	39.9	43.9	47.9	51.9	55.8	59.8	63.8	Total	Accum
0	0.5	2.10	6.38	5.81	1.15	0.05	-	-	-	-	-	-	-	-	-	-	-	15.5	15.5
0.5	1	1.57	5.59	11.28	11.13	2.93	0.23	0.01	0.00	-	-	-	-	-	-	-	-	32.7	48.2
1	1.5	0.36	1.41	3.32	7.69	8.22	2.29	0.28	0.02	-	-	-	-	-	-	-	-	23.6	71.8
1.5	2	0.07	0.19	0.62	1.92	3.87	4.47	1.23	0.13	0.02	0.00	-	-	-	-	-	-	12.5	84.3
2	2.5	0.00	0.01	0.07	0.45	1.12	2.44	2.54	0.52	0.05	0.00	-	-	-	-	-	-	7.2	91.6
2.5	3	-	-	0.00	0.06	0.33	0.68	1.44	1.37	0.22	0.02	0.00	0.00	-	-	-	-	4.1	95.7
3	3.5	-	-	-	0.00	0.08	0.28	0.36	0.84	0.66	0.10	0.01	-	-	-	-	-	2.3	98.0
3.5	4	-	-	-	0.00	0.01	0.07	0.14	0.21	0.40	0.30	0.05	0.00	0.00	-	-	-	1.2	99.2
4	4.5	-	-	-	-	-	0.01	0.05	0.09	0.07	0.15	0.09	0.02	-	-	-	-	0.5	99.7
4.5	5	-	-	-	-	-	-	0.03	0.04	0.04	0.03	0.03	0.03	0.00	-	-	-	0.2	99.9
5	5.5	-	-	-	-	-	-	0.00	0.01	0.03	0.02	0.01	0.01	0.01	0.00	-	-	0.1	100.0
5.5	6	-	-	-	-	-	-	-	0.00	0.01	0.00	0.01	0.00	0.00	0.00	-	-	0.0	100.0
6	6.5	-	-	-	-	-	-	-	-	0.00	0.00	0.00	0.00	-	-	-	-	0.0	100.0
6.5	7	-	-	-	-	-	-	-	-	-	-	-	-	-	-	-	-	0.0	100.0
7	7.5	-	-	-	-	-	-	-	-	-	-	-	-	-	-	-	-	0.0	100.0
7.5	8	-	-	-	-	-	-	-	-	-	-	-	-	-	-	-	-	0.0	100.0

Figure 4.11: Annual wind scatter diagram of reference location in the Southern North Sea, based on 37 years of hindcast data.

Similar as for wind, a current scatter plot exists. Especially for the Southern North Sea location the current can well be estimated, due to the tidal difference.
In this research, the current will be assumed to be constant over time and constant over height. A current velocity of 0.9 m/s will be applied, 99 % of time annually the current velocity will be equal to or lower than this value. Therefore it can be stated that the workability, when considering current load only, is 99 %.
Since wind and current loads are taken to be constant with a workability over 90 %, the workability from sea state is expected to be governing for the mooring system and can be computed based on wave probability scatter diagrams for the reference locations.

Since wind and current corresponding with a high workability is considered and is kept constant for all mooring systems, the focus in this research is on comparing workability regarding sea state. Usually for high wind speeds, also the sea state is excessive.
The source for the Southern North Sea metocean data is *www.metoceanview.com*, [13]. This data is received from four different datasets 'North Sea Wave', 'MSL WW3 Global ST4', 'CFSR' and 'CFSR2'. The metocean data for the Bay of Biscay is received from Allseas internal.

5 Diffraction analysis and frequency domain modelling

5.1 Introduction to the diffraction analysis

To build up complexity in the modelling phase step by step, a quasi-static model is build to perform a sensitivity analysis on various variables, e.g. mooring line stiffness, before performing the diffraction analysis and start modelling in the frequency domain. The static model and results from the sensitivity analysis are described in Appendix C. Results from the static model will be used as validation step for the time domain solution, described in section E.0.3.1.

The diffraction analysis can be performed both in frequency and time domain. For this research, the diffraction analysis is performed in frequency domain methods because it is most common and therefore broader described in literature, additionally it requires less computation time. The output from the diffraction analysis is used as input for the frequency and time domain modelling. This chapter describes both the diffraction analysis and the modelling in frequency domain, the next chapter describes modelling in the time domain.

The behaviour of a floating structure, the hydrodynamic data and the equations of the motion, can be solved by applying potential flow theory. The potential flow software Ansys Aqwa solves the equations of motion in the for different frequencies, providing the motion response for each specific frequency and wave direction.
Fluid flow is best described by the Navier Stokes equations, however solving these equations numerically requires comprehensive Computational Fluid Dynamics Solvers. Simplifying fluid flow with applying potential theory, where the fluid is treated as ideal non-viscous, incompressible and irrotational, enables to reduce computation effort.
With the assumptions of potential theory and the boundary conditions that needs to be satisfied, the fluid potential can be determined at every location in the fluid, for each frequency and incoming wave direction.
Numerical software based on potential theory can be applied to perform the diffraction analysis in order to determine the hydrodynamic matrices and the first and second order wave forces that are acting on a floating body. With this data, the equations of motion can be solved, providing the motion RAOs (displacement, velocity and acceleration) as output.
The hydrodynamic matrices will have dimensions NxN with N being the total number of DoF in the system, 12 for a mulit-body system consisting of two bodies.
The equation of motion for a multi-body in the frequency domain can be written as:

$$\sum_{i=1}^{12} \left\{ -\omega^2 \left(m_{ki} + a_{ki}(\omega) \right) - i\omega b_{ki}(\omega) + c_{ki} \right\} \cdot X_i(\omega) = F_k(\omega) \quad \text{for k} = 1, \ldots 12 \tag{5.1}$$

The added mass, damping and external force depends on frequency and are found for various incoming wave directions. The diffraction analysis is performed for frequencies in the range of [0.1,1.3] rad/s with a step size of 0.05 rad/s.

Linear interpolation in between these data points will be applied in the time domain model. In terms of extrapolating, for lower frequencies the data point with the lowest frequency is used. For frequencies above the highest frequency data point, zero response at infinite frequency is assumed, because non-zero response at infinite frequency is not realistic. For larger frequencies, interpolation between the highest frequency data point and infinity is performed by assuming the data to decay with a third order function [24]. The lowest analysed frequency is chosen based on the fact that the wave spectral density is very low for these frequencies, as can be seen in Figure 6.2a.
The highest analysed frequency comes from the requirement regarding the mesh size, that the shortest wave length should be at least 7 times the mesh size, as described in section 5.5.4. The mesh size for *Pioneering Spirit* is equal to 4.5m. Figure C.2 shows that for frequencies of 1.3 rad/s, and higher, the wave spectral density is not yet zero, which could cause an inaccuracy because of extrapolating hydrodynamic data for higher frequencies. A minor inaccuracy is expected because the spectral density is already tending to zero and the RAOs are close to zero for these frequencies, as can be seen in Figure 5.5 for *Iron Lady* and the same can be found from the RAOs of *Pioneering Spirit*.

In future research this could be solved by applying a smaller mesh sizes for *Pioneering Spirit* enabling solving the diffraction analysis for larger frequencies and with that capturing larger fraction of the frequency range corresponding with non-zero wave spectral density. An optimum should be found between computation time and accuracy by means of a mesh convergence test.
The frequency step size affects computation time and accuracy when linear interpolation is used for frequencies in between data points, the value 0.05 rad/s is based on industrial experience. A sensitivity analysis could be performed to find the optimum step size for future research.
Incoming waves in the range of [-180,180]° with a step size of 15° is considered. This full 360 ° range is required as the multi-body model is not symmetric. The step size is applied to have data available at the governing incoming directions analysed in this research, 45, 90 and 135 °, providing the option to analyse other relevant wave directions. Furthermore, in case the effect of wave spreading needs to be analysed, a small direction step is preferred as linear interpolation is used between incoming wave directions.

- m_{ki} is the size [12, 12] structural mass/inertia matrix.
- $a_{ki}(\omega)$ is the size [12, 12, ω] added mass/inertia matrix. Varying with incoming wave direction.
- $b_{ki}(\omega)$ is the size [12, 12, ω] potential damping matrix. varying with incoming wave direction.
- $c_{ki}$is the size [12, 12] stiffness matrix.
- $F_k(\omega)$is the size [12, ω] complex force vector for each DoF. Varying with incoming wave direction.
- $X_i(\omega)$ is the size [12, ω] body motion vector for each DoF. Varying with incoming wave direction.
- i and k the mode of the motion.

The following topics will be dressed in this chapter: diffraction analysis modelling procedure, model preparation, validation and verification, model limitations, results and closing off with conclusion and reflection.
Procedure and preparation explain what steps are required to be able to perform the diffraction analysis and the simulations in frequency domain. Validation and verification together with model limitations investigates the consequence of decisions that are made in building the model and discusses the accuracy of the outcome. The results and conclusion can be taken to the next step in the methodology.

Considering the extraordinary shape of *Pioneering Spirit*, the focus will be on understanding the the hydrodynamic behaviour of the cargo barge. First as a single body and afterwards as part of the multi-body model, including both *Pioneering Spirit* and the cargo barge, *Iron Lady*.

5.2 Diffraction analysis procedure

The diffraction analysis procedure is visualized in Figure 5.1. The barge loading conditions and the vessel orientation, as shown in Figure 2.5b, are required input for building the model to perform the diffraction analysis in the frequency domain. In case validation and verification provides satisfactory results, the results from the diffraction analysis can be imported in the time domain model, why modelling in the frequency domain is not applicable will be explained in section 5.6. This chapter explains steps 4 to 8 from the thesis approach as represented in section 3.1.

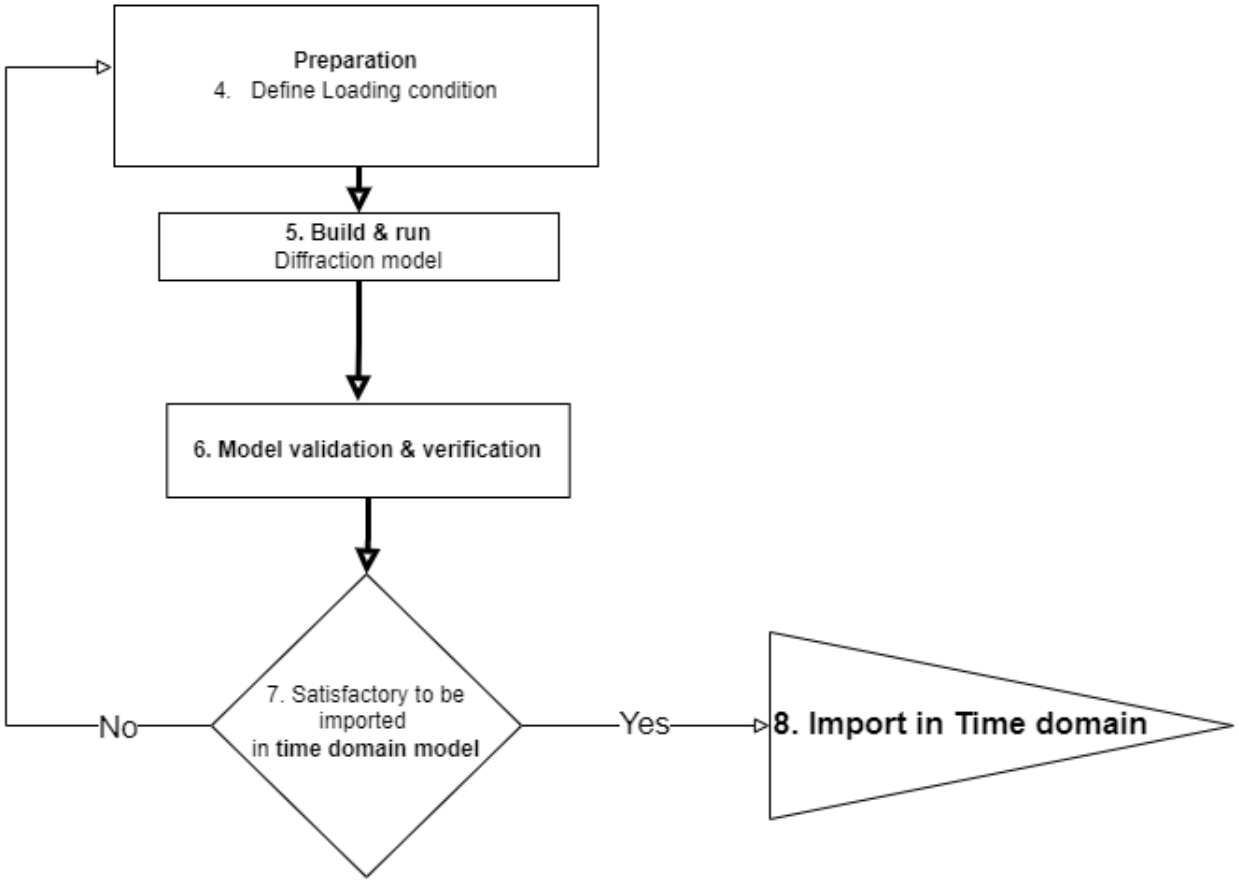

Figure 5.1: Diffraction analysis modelling procedure.

5.3 Diffraction analysis preparation

The dimensions and the body shape are pre-set as described in sections 2.2 and 2.7, only the loading condition will be described in this section.
The loading condition depends on how the vessel is loaded. This includes contributions for example from the deck loading, the vessel empty weight and ballast conditions.
Topics that will be touched upon in determining the loading condition are:

- Center of Gravity (CoG). Both separate for each weight contribution and the combined CoG.
- Mass radii of gyration.
- Area moment of inertia.
- Ballast conditions.
- Static draft, trim and heel

For *Iron Lady* the loading condition is specified for transport of eight, 14+ MW, wind turbines. Resulting in a deck weight of approximately 14,000 Ton.
For *Iron Lady* the trim and heel is set to be zero, meaning that the longitudinal and transverse center of gravity are located at the same vertical as the Center of Buoyancy (CoB). The draft of *Iron Lady* is set to be 6m, which is the minimum draft required for transport over sea. For stability aspects the Vertical Center of Gravity (VCG) is an important parameter as it heavily affects the inertia term of the roll and pitch motion and the roll and pitch restoring term.
Considering the wind turbine components that are loaded on the deck, the ballast conditions and the empty barge conditions (including fuel and general equipment) the combined VCG can be determined. Ballast and fuel tanks that are filled between 0 % and 100 % do have a free surface for which a free surface correction has to be taken into account, expressed in a virtual shift of the VCG.
The free surface correction for small heel angles, meaning $\frac{1}{2}\tan^2\phi$ small relative to 1, depends on the density of the fluid in the tank, ρ', the area moment of inertia of the tank free surface, i. This reduction of metacentric height, GZ, can be determined with the following equation. Which sums the free surface correction for multiple tanks, [3]. This equation is known to give accurate results up to heel angles of 10 ° , these heel angles will not occur in this research, [25]. Besides, the reduction of metacentric height is only a small fraction of the total metacentric height, in the order of 1 % for zero heel. For larger heel angles, the metacentric height reduction is expected to increase more rapidly because the shifted distance of the fluid CoG increases in transverse direction. The virtual shift of the VCG can be computed with:

$$\overline{GG''} = \frac{\sum\{\rho' i\}}{\rho\nabla} \cdot \left(1 + \frac{1}{2}\tan^2\phi\right) \tag{5.2}$$

The individual components of the VCG and the combined VCG is included in Table 5.1. The combined VCG can be calculated by substituting the VCG and mass of each component,j.

$$VCG = \frac{\sum(VCG_j \cdot M_j)}{\sum(M_j)} \tag{5.3}$$

Table 5.1: VCG individual contributions, for 8 wind turbines each with 3 blades. VCG defined from keel line. Free surface correction of tanks is included.

Object	VCG [m]	Mass [Ton]
Empty barge	7.12	2.43E+04
Water ballast	6.28	2.97E+04
Fuel	2.97	44.06
Other tanks	3.92	7.50
Blade racks	24.70	1.49E+03
Towers	68.50	6.34E+03
Nacelles	21.30	5.86E+03

Table 5.1 shows the VCG and mass of the individual components of the loading condition. Input for the wind turbine components is described in section 2.4. The VCG of the barge without deck loading is located at 6.65 m above the keel line, this makes sense because the barge draught is equal to 13 m. The VCG of the deck loading is located 41.6m above the deck. This results in a combined VCG at 13.2 m above the barge keel line. This data, together with assuming the combined CoG to be located at the vertical of the CoB, can be used to compute the moments of inertia in section D.0.1.

For *Pioneering Spirit*, an already existing loading condition is used because computing the hydrostatic data is more difficult for this vessel and less relevant for this research. In this pre-defined loading condition *Pioneering Spirit* is at a draft of 17 m with initially zero heel and trim, CoG at the same vertical as CoB. The center of gravity located 19.47 m above the keel line. This draft of *Pioneering Spirit*

corresponds with shallow water conditions because wind parks with bottom founded foundations are commonly in relatively shallow water.

5.4 Diffraction analysis model build

The numerical model will be build in the radiation and diffraction solver software 'Ansys Aqwa'. Figure 5.2 shows the approach that is applied to build the diffraction model, as part of the procedure, represented in Figure 5.1. Afterwards, each step of the model build is briefly explained.

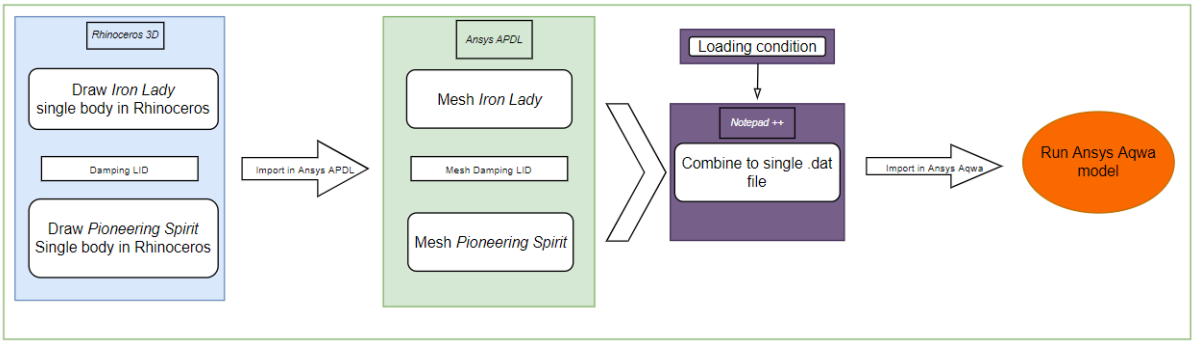

Figure 5.2: Method to build the diffraction model

Since the diffraction calculation applies a panel method based computation, creating the hydrodynamic multi-body model starts with the Computer-Aided Design software 'Rhinoceros'.

- Both vessels are independently drawn in Rhinoceros. From Rhinoceros the body shape is exported as an IGES file.
- This IGES file is imported in Ansys APDL, this software package can be used to mesh the body shape. From Ansys APDL a .dat file is exported which includes the nodes and panel specifications.
- In case of a multi-body model, the different .dat files will be converted to a single .dat file. Additionally, the hydrostatic data, computed from the loading condition, such as mass matrix and the location of the CoG is imported.
- This .dat file can be used as input for Ansys Aqwa by which the diffraction analysis is performed. Resulting in the hydrodynamic data, load and displacement RAOs and the QTF matrices of the multi-body model, this data is stored in a .LIS file.
- This data can be put in a Graphical Supervisor, Aqwa GS, and can be used to plot the pressure contours and the wave contours around the structure. Furthermore, the .LIS file can be used to calculate the (relative) motions at a certain location on the body with use of a frequency domain model.

No mooring system is included in the diffraction analysis, this will be added in the time domain model to properly account for non-linearities. Therefore, no wind and current forces can be included as these contribute to the mean forces acting on the floating body. Besides, wind and current forces are non-linear because they scale with relative velocity squared.
The wind and current force for the body at zero speed are calculated in section E.0.1.3, being in the order of 100 kN and depend on the incoming direction.
Regarding waves, a defined wave spectrum with Hs and Tp and peakedness factor will be applied. Detailed explanation about this wave spectrum and its effect on the results will follow when explaining the time domain model, 6.3.2.1.

5.5 Validation and verification of the diffraction analysis

The purpose of a numerical model is to describe reality with use of analytical equations. Before using the output of the numerical model, it has to be properly checked. In general, there are two types of checks to judge whether the numerical model correctly describes reality. Validation using model scale tests and verification that compares results with an analytical model or with literature.
For this thesis, no model tests have been performed to validate the numerical model. However, the work of H. Radfer, includes the validation of the diffraction analysis of both *Iron Lady* and *Pioneering Spirit*, [26]. This work will be used for reference.
Verification checks have been performed with analytical results. In addition, sanity checks and sensitivity analyses have been performed, with use of literature, all to assure the output is acceptable.

The most relevant validation and verification steps are listed and described below. Additionally, Appendix D includes results from a sensitivity analysis on the diffraction analysis and the frequency domain model, e.g. what is the effect of the Vertical Center of Gravity on the first order relative vessel motions. Besides, the hydrostatic data is analytically computed to verify whether the units in the diffraction analysis software.

- Compare RAOs with typical barge shape RAOs in literature.
- Is additional roll damping required to account for viscosity?
- Numerical effects in the diffraction analysis. Gap resonance and irregular frequencies.
- Mesh size convergence.
- Sea state RAOs.

5.5.1 Typical barge shape RAOs

The cargo barge in this research is not the first barge that has been analysed, therefore it is interesting to compare the RAOs of *Iron Lady* with the RAOs of a typical barge shape, as described in literature.
5.3 shows the barge shape from literature, both *Iron Lady* and this barge, has a rectangular shape and vertical walls. Both barges are in shallow water conditions.
Figure 5.4 shows the RAOs in all 6 DoF. Comparing these figures to the RAOs of *Iron Lady*, in Figure 5.5, shows similar shapes. This Figure is included in the Appendix and contains elaborated explanation on the RAOs shape. Obviously, the peaks in the RAO are located at different frequencies, as the resonance frequency of both barges differs.
These results point out that the diffraction analysis applies an acceptable method leading to the correct RAO shapes. However, it cannot yet be stated whether the amplitude of is correct as well.

Figure 5.3: Snapshot of the barge shape used for comparing RAOs of *Iron Lady*
source: Motion responses of a moored barge in shallow water. [27]

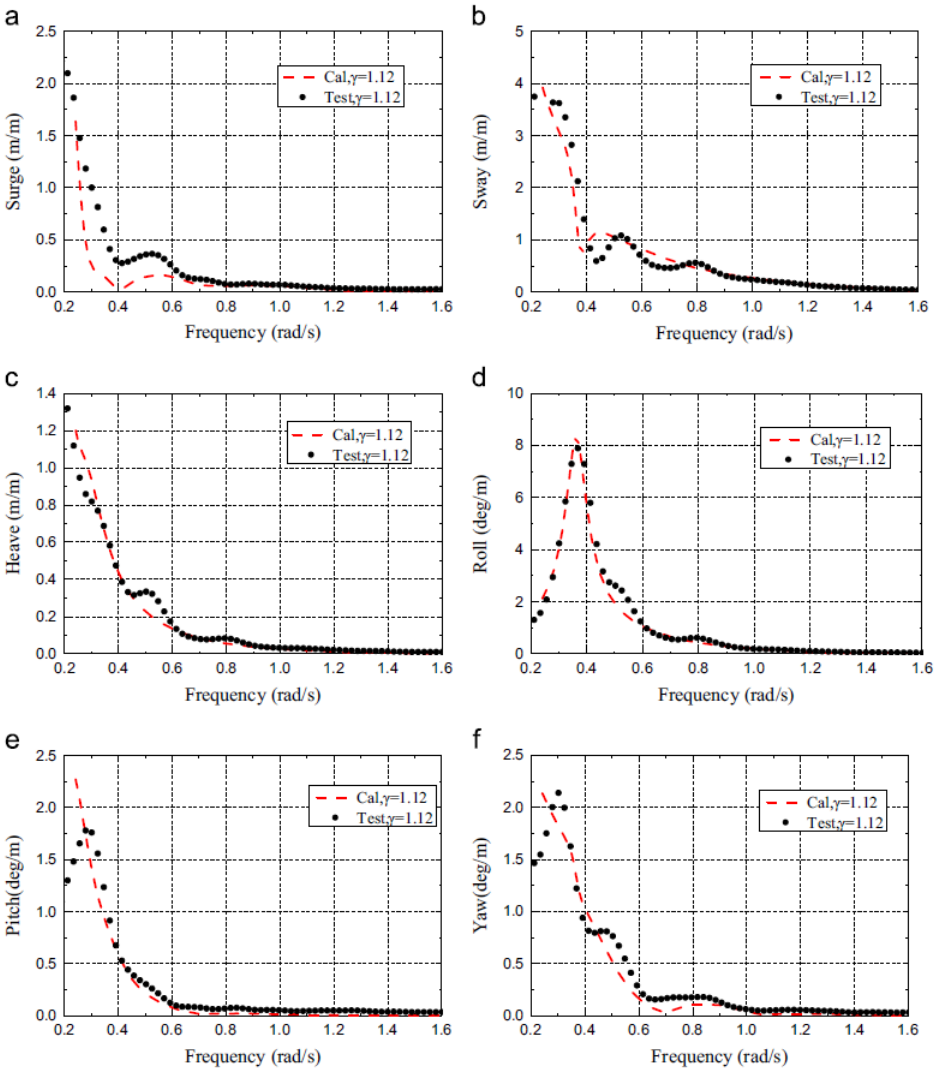

Figure 5.4: Typical barge shape RAOs, with (a) surge,(b) sway,(c) heave,(d) roll,(e) pitch,and (f) yaw. Only the black dots are of interest, as it represents test results.
source: Motion responses of a moored barge in shallow water. [27]

Figure 5.5 represents the RAOs of *Iron Lady*, these are briefly discussed below.

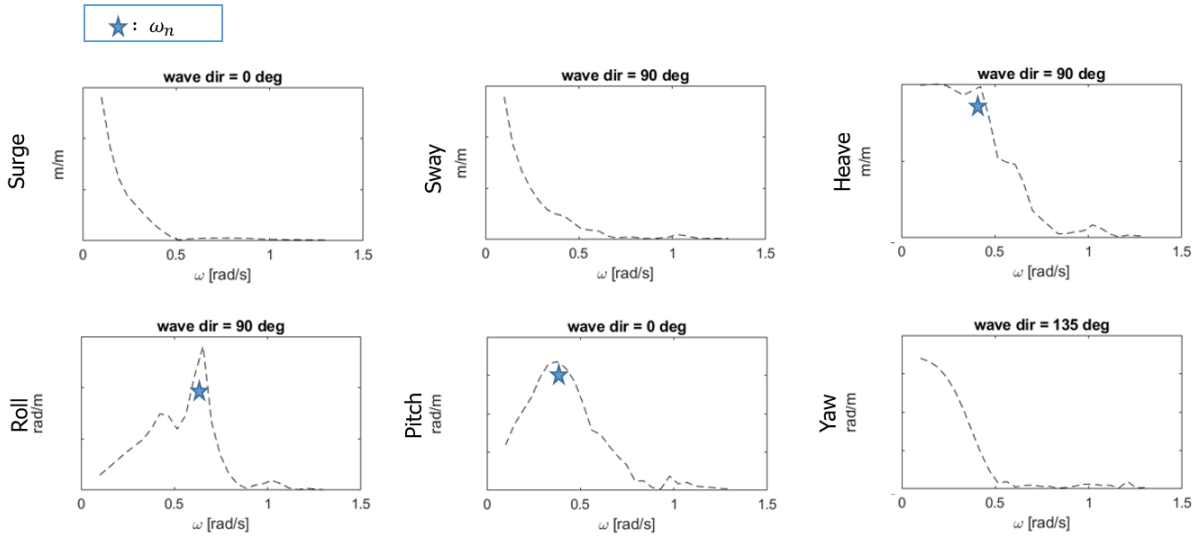

Figure 5.5: RAOs for all 6 DoF of *Iron Lady* as part of the multi-body model, including *Pioneering Spirit* and *Iron Lady*. RAOs are given for beam, stern or bow quartering waves. The blue star denoting natural frequencies, for heave roll and pitch respectively 0.47, 0.64 and 0.44 rad/s. Values on the y-axis cannot be shown due to confidentiality.

The barge is not restricted for surge, sway and yaw motions. Therefore no resonance peak is visible in these RAOs.
For low frequency waves, the heave motion follows the wave elevation, which means an RAO close to 1. The heave resonance frequency can be found close to 0.5 rad/s, corresponding with the computed natural frequencies as listed in table F.5.
For low frequencies, no roll and pitch motion occurs. The small peak in the roll RAO, at approximately 0.45 rad/s, is expected to be caused by the interaction between *Pioneering Spirit* and *Iron Lady* because in the roll RAO for *Iron Lady* as a single body, this peak does not occur but only the highest peak.
Due to symmetry no yaw motion occurs for stern or bow waves. Therefore the yaw RAO is represented for bow-quartering waves.

5.5.2 Additional viscous damping

For floating structures there are two types of damping, potential and viscous damping. Potential damping includes for example energy dissipation due to wave generation of a body moving through a fluid. Viscous damping includes for example skin friction and the formation of vortices.

Diffraction solvers, based on potential flow theory, do not take viscosity into account and therefore neglect viscous damping. To understand the effect of viscous damping on the vessel motions. Model free-decay tests can be performed in a basin. The damping ratio from the model tests can be compared with the numerical results, showing the contribution of viscous damping.
Especially for the large structures involved in this thesis, only viscous roll damping has to be considered. For other DoF the contribution of viscous damping is negligible, as it has only a very small contribution compared to potential damping.

Free-decay model tests have been performed by the Maritime Research Institute Netherlands (MARIN) for *Pioneering Spirit* [28]. Comparing results from this free-decay model tests to free-decay tests in the

numerical model in Ansys Aqwa correspond well when no additional viscous damping is added, [26]. These values are reasonably close to conclude that viscous damping can be neglected for *Pioneering Spirit*. This corresponds with literature that additional viscous damping only has to be added for slender structures, as *Pioneering Spirit* is not a slender structure, [3].

Compared to *Pioneering Spirit*, *Iron Lady* is a more slender structure where the contribution of viscous roll damping might be considerable compared to potential damping. The results of the work of H. Radfar and also S. Bitounis, who did free-decay model tests for the roll motion of *Iron Lady*, show that results from the model test and Ansys Aqwa converge, [26]. This means that viscous damping can be neglected for *Iron Lady* as well. Especially when analyzing the case of the body having zero velocity.

5.5.3 Numerical effects in the diffraction analysis

The diffraction analysis of floating bodies in close proximity is known to be prone to the numerical effect of gap resonance and irregular frequencies. Several methods to remove or reduce these numerical effects are provided in literature, the VLID and ILID will be applied in this research [2]. This section includes explanation of the cause of these numerical effects, how they effects can be removed/reduced and how they are affecting the results in this research.

Mutli-body interaction is clearly visualized in Figure 5.6 where the hydrodynamic data regarding the heave motion of *Iron Lady* is shown for the case the single body case and the multi-body case, in the orientation represented in Figure 2.5b.

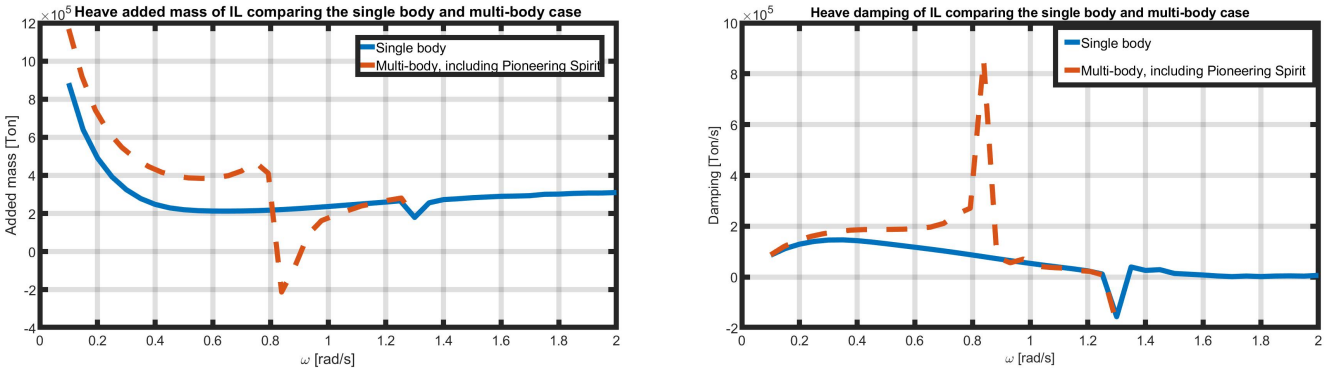

(a) Heave added mass

(b) Heave damping

Figure 5.6: Heave added mass (left plot) and damping (right plot) of *Iron Lady* at the CoG, comparing Iron Lady single body (blue line) and the multi-body case when *Pioneering Spirit* is interacting (red dashed line). The transverse vessel spacing between both vessels is 3.6m.

The irregularities in the multi-body data are related to the gap resonance effect, the sudden troughs in the single body data correspond are caused by irregular frequencies, the corresponding explanation will follow in this and the subsequent section. The shape around 0.8 rad/s is related to the gap resonance frequency. The small trough at 1.3 rad/s can be recognized in both the multi-body and single body added mass curve and are related to the numerical effect of irregular frequencies.
Increased added mass and damping for the multi-body case is not clear but are expected to be caused by the fact that water particles are more restricted to follow the vessel heave motions.

5.5.3.1 Gap resonance and damping lid (VLID)

The numerical effect of gap resonance is caused by the fact that diffraction solvers are based on potential flow theory, meaning that the flow is assumed to be incompressible, irrotational and non-viscous. Gap resonance refers to resonance of the wave in the gap between floating bodies, leading to unrealistically

high wave heights. This effect is mainly caused by disregarding viscosity which causes these waves to dampen out in reality. To assure realistic surface elevation in the gap, commonly a 'damping lid' is applied reaching over the area in the gap. This damping lid (VLID) adds a damping factor to the water surface as an additional boundary condition and with that suppressing the wave elevation, [29]. The VLID typically has a damping value between 0 and 0.2 where 0 will give no effect and 0.2 will result in heavy damping of the surface elevation.

Figure 5.7 gives a graphical visualization of the effect of the VLID. Figure 5.7a shows that in case no VLID is applied, the wave height exceeds the freeboard of the cargo barge. Figure 5.7b presents the case when a VLID is included.

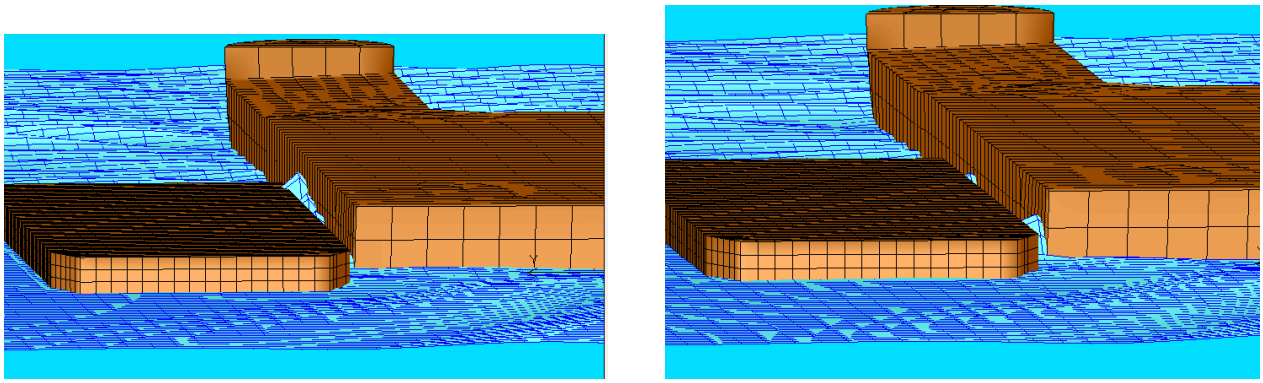

(a) No VLID

(b) VLID with damping factor of 0.05 (base case)

Figure 5.7: Visualization of the wave amplitude in the gap between *Pioneering Spirit* and *Iron Lady* for waves coming from 135°. For a frequency of 1.20 rad/s and incoming wave height of 2.5 m.

Before analysing the effect of the damping LID on the hydrodynamic parameters, first the frequency corresponding with the gap resonance effect by applying the method as derived by Chen *et al.* in their paper about effects of gap resonance, [4]. Equation 5.4 represents the relation between frequency, ω and gap parameters with g the gravitational acceleration, S the transverse spacing, body breadth B, body draft T and water depth h. Table 5.2 provides the corresponding input for the configuration of this thesis.

$$\omega = \sqrt{\frac{g}{\frac{S \cdot B}{h-T} + T}} \tag{5.4}$$

Table 5.2: Input dimensions for gap resonance frequency

Variable	Symbol & unit	Value
Water depth	h [m]	30
Body breadth	B [m]	57
Draft	T [m]	6
Transverse spacing	S [m]	-

Substituting variables corresponding with the vessel orientation in this research, shown in table 5.2, gives that a gap width of respectively 3.6, 6.9 and 15 m results in resonance frequencies as stated in table 5.3. Next to that, the resonance frequencies determined by using the relation found by Chen *et al.* are represented in table 5.3 as well as the percentile difference and the absolute difference. The numerical results are read from the peaks in Figure D.2a, included in the appendix.
Figure 5.8 represents the effect of the damping LID on the added mass and damping in sway direction for a gap width of 3.6m. It can be seen that the VLID suppresses the peak at and around the resonance frequency for sway motions. Similar results are seen for roll motions as can be seen in Figure D.1 in

Table 5.3: Gap resonance frequency from Ansys Aqwa data and analytical relations

Transverse spacing [m]	Resonance frequency numerical model [rad/s]	Resonance frequency Analytical method [rad/s]	Percentile difference [%]	Absolute difference [rad/s]
3.60	0.83	0.82	1.64	0.01
6.90	0.75	0.66	12.70	0.08
15.00	0.61	0.49	25.03	0.12

appendix D . Results for applying a damping factor of 1.0 are considered unrealistic as it removes the surface elevation entirely.

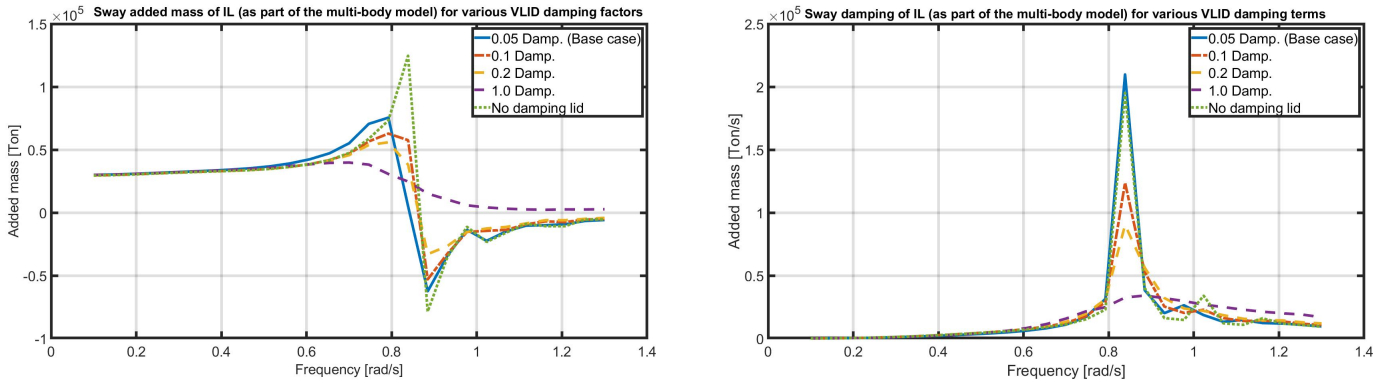

(a) Sway added mass

(b) Sway damping

Figure 5.8: Sway added mass (left) and damping (right) of Iron Lady at the CoG, for various VLID damping factors

Regarding the objective in this research to evaluate mooring loads, the effect of gap resonance on the vessel motions needs to be considered. Because these first order vessel motions contribute to the mooring loads. Since the diffraction analysis computes the first order motions, the effect of the VLID damping factor on the vessel motions will be analysed by considering the RAOs, as shown in Figures 5.9 and 5.10. These RAOs show that the gap resonance effect does not have a considerable effect on the first order motions. The reason for that is the gap width being rather small compared to the vessel sizes in this research. Related to this vessel size, the vessels have large mass and inertia, therefore only very high forces are required to affect the first order motions. Figures 5.9 and 5.10 also represents the effect of a so-called 'ILID' on the RAOs. This will be explained further in the subsequent section.
Figure 5.9 shows the RAOs for waves coming from a 135° angle. It can be concluded that the VLID do not influence the first order motions of Iron Lady as part of the multi-body model. Similar results are seen for different incoming wave directions and DoFs.

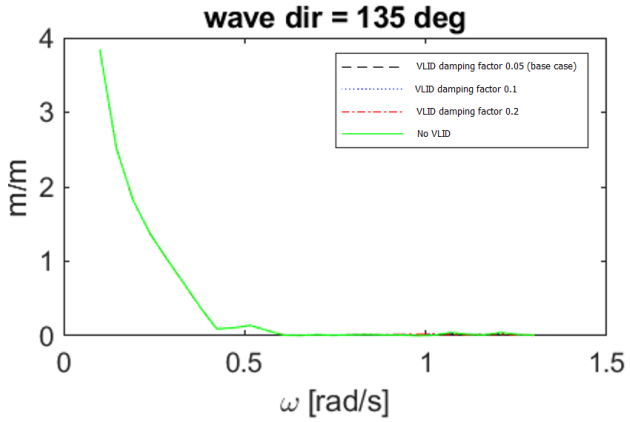

(a) Sway RAO for different VLID damping parameters

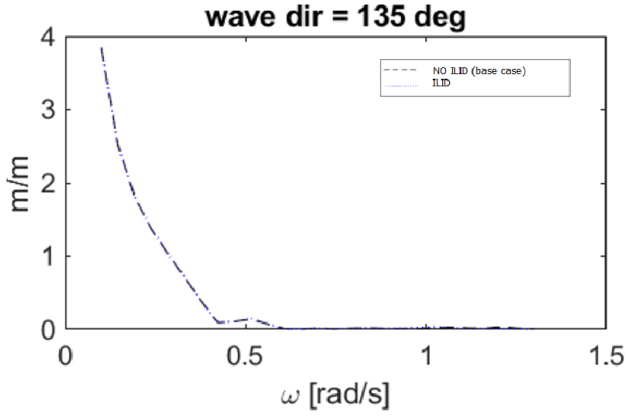

(b) Sway RAO for in- and excluding ILID.

Figure 5.9: Sway RAOs of Iron Lady at the CoG representing the effect of VLID (left) and ILID (right), as part of a multi-body model, for waves coming from 135°.

Most of the energy in the wave spectrum will be in the range of 0.5 and 1.0 rad/s, as can be seen in Figure 6.2a. As the sway RAO is already close to zero for these frequencies, it would be interesting to look at the pitch RAO which has its peak in this frequency range. These pitch RAOs, showing the effect of the VLID and ILID are shown in Figure 5.10.

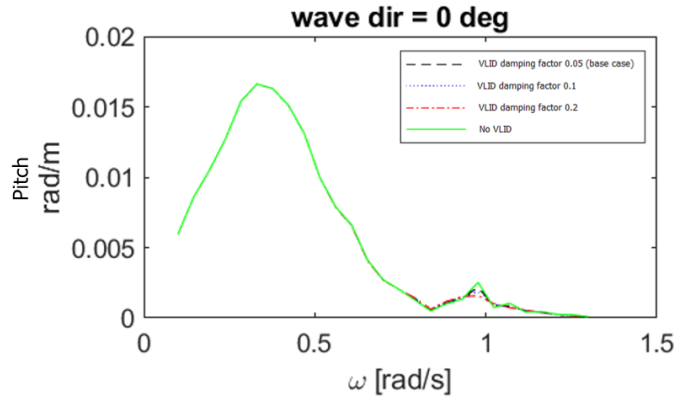

(a) Pitch RAO for different VLID damping parameters

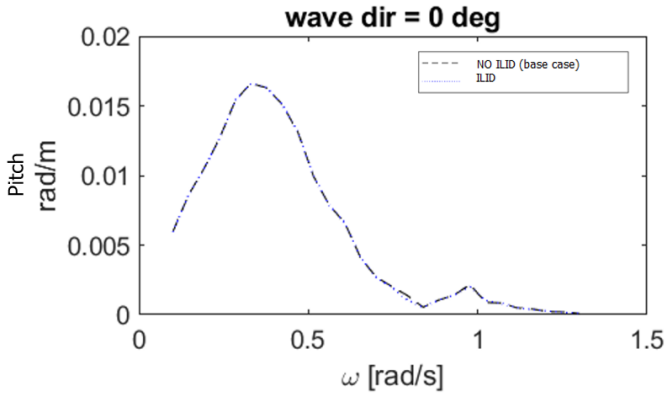

(b) Pitch RAO for in- and excluding ILID.

Figure 5.10: Pitch RAOs of Iron Lady at the CoG representing the effect of VLID (left) and ILID (right), as part of a multi-body model, for stern waves

Figure 5.10 shows the pitch RAOs for stern waves for including the ILID and different VLID damping terms. It can be seen that the pitch RAO is slightly sensitive to the damping term around a frequency of 1 rad/s. However, this minor effect is not expected to affect the workablity results of this research. Because, pitch motion results in vertical motions which are not affecting the mooring loads since the mooring lines are rather long.
Besides first order motions, it is interesting to analyse the relation between the damping term and the second order forces acting on the barge to assure that the VLID is having any effect and because these second order forces contribute to the low frequency barge motion and ultimately contribute to the mooring loads. Due to limited time, this is considered subject to further research.

Equation 5.4, involves a relation between gap width and the resonance frequency, more specifically the wave length. The effect of gap resonance is expected to reduce by increasing gap width because the vessel interaction will reduce. Additionally this equations shows that increasing the gap width should reduce the resonance frequency. This is proven to be correct in Figure D.2 representing the heave added mass and damping for various gap widths.

Concluding. A VLID will be included in this research to account for the gap resonance effect. However, based on the RAOs presented, it is challenging to argue what factor should be added. Analytical relations are derived in literature to estimate the designated VLID damping factor, as explained in D.0.1.2, future research is required to understand whether this method is applicable to this research.
Therefore, based on Allseas experience and model tests that are performed by H. Radfar, a damping factor of 0.05 will be applied in this research, [26]. This damping factor will not affect the results of this research via the first order motions because the mooring system does not restrict first order motions. The affect of the damping lid on the mooring loads requires further investigation by plotting the QTF for different VLID damping factors and running time domain simulations for different VLID damping terms.
The mesh size of the VLID is set equal to the mesh size of *Iron Lady*, 2.5m, to have similar accuracy.

5.5.3.2 Irregular frequencies and Internal lid (ILID)

Determining the source strength for each panel in the diffraction analysis entails computing the determinant of a matrix, [5]. For some frequencies this determinant happens to be zero. Resulting in an infinite source strength, resulting in spikes in the hydrodynamic matrices. These frequencies are known as irregular frequencies. The occurrence of Irregular frequencies has to do with the fact that the potential flow software models the floating body as having an internal free surface. These irregular frequencies can be accounted for by adding an Internal LID (ILID) to both *Pioneering Spirit* and *Iron Lady*, this ILID removes the elevation of the internal free surface.

First, it is important to know the frequency at which these irregular frequencies occur. These can be estimated by applying the method as explained by H. Radfar, [26].

$$\omega_{irr} = \sqrt{\gamma \cdot g \cdot coth(\gamma \cdot T)} \tag{5.5}$$

with g the gravitational acceleration, and T the draft, γ is a factor depending on the internal modes of the body, n and m, with respect to the body length and breadth, L and B in m.

$$\gamma = (\frac{\pi \cdot n}{B})^2 + (\frac{\pi \cdot m}{L})^2 \tag{5.6}$$

The input for equations 5.6 and 5.5 and the result it provides is listed in table 5.4.

Table 5.4: Irregular frequencies input and results

Variable	Symbol & unit	*Pioneering Spirit*	*Iron Lady*
Draft	T [m]	17	6
Breadth	B [m]	124	57
Length	L [m]	382	200
Internal mode	n [-]	1	1
Internal mode	m [-]	1	1
Result			
Irregular frequency	[rad/s]	0.76	1.28

Comparing the analytical results from Table 5.4 with the heave added mass and damping, as shown in Figure 5.6, it can be seen that for *Iron Lady* the irregular frequency corresponds with the trough in the heave added mass and damping data. Besides, the large peak in 5.6a at 0.76 rad/s is expected to be

related to the irregular frequency of *Pioneering Spirit* affecting the motion of *Iron Lady*.

To remove the effect of irregular frequencies, the ILID can be applied. As a result, the irregularities in the hydrodynamic data are removed, as shown in Figure 5.11. It can be concluded that the hydrodynamic data for *Iron Lady* as a single body, regarding sway motion, shows only a minor influence from irregular frequencies. More specifically it only affects the high frequency terms which are not relevant for the large structures that are involved in this thesis, as can be seen in the RAOs in Figure 5.9b.
Pioneering Spirit however, is more affected by these irregular frequencies as shown in the hydrodynamic data in sway direction of *Pioneering Spirit*, shown in Figure 5.12. It can be seen that due to the ILID, the peak at the frequency corresponding with the irregular frequency as derived and shown in Table 5.4, is affected but not entirely removed. Based on Allseas experience, it is expected that other numerical effects contribute to the behavior at this specific frequency. Possibly wave resonance in between the bows of *Pioneering Spirit*. More in depth research is required to understand this behavior. For this research however, mainly the effect on the vessel motions is important. Therefore, the effect of irregular frequencies and the ILID on the RAOs is shown in Figures 5.9b and 5.10b. Where similar as for the gap resonance effect, the ILID has only a minor effect on the first order motions.

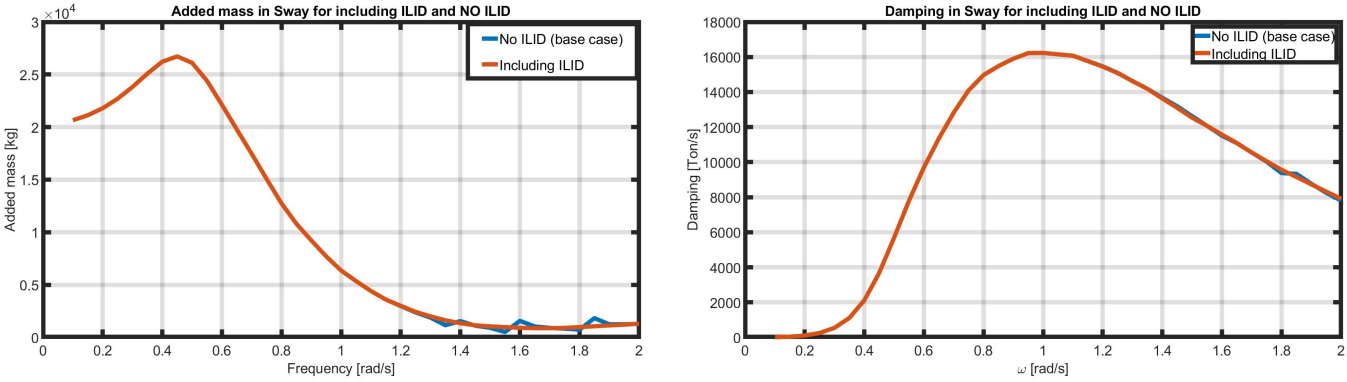

(a) Sway added mass (b) Sway damping

Figure 5.11: Sway Added mass (left) and damping (right) of *Iron Lady* at the CoG, as single body, for including an ILID and the base case without ILID.

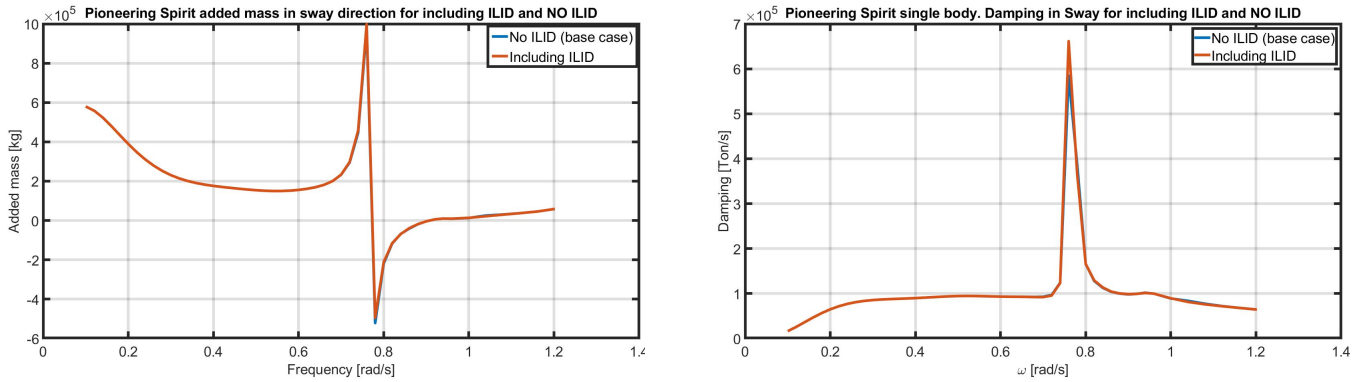

(a) Sway added mass (b) Sway damping

Figure 5.12: Sway added mass (left) and damping (right) of *Pioneering Spirit* at the CoG, as a single body model, for including an ILID and the base case without ILID.

In view of computation time and the effect on the first order motions, the ILID is disregarded in the

diffraction analysis. Because, including the ILID drastically increases the computation and its effect is seen to be negligible and will therefore not affect the workability results.

5.5.4 Mesh size convergence

The software used to perform the diffraction analysis applies the so-called panel method.
This means that each structure has to be subdivided in panels. While setting the panel size, the consideration should be made between accuracy and computation time. Reducing the panel size will increase the accuracy but also the computation time to run the model.
The panel size should be within limitations set by the numerical software, as explained in the literature report, section 5.6 [2]. The most important requirements are: max panel size should not exceed 1/7 of the smallest wave length, and the element centres (the panel sources) should be at least one element equivalent (facet radius) apart, [30]. Therefore, the panel size determines the maximum wave frequency that can be analysed.

For *Pioneering Spirit* an already existing diffraction model is used, with a mesh size equal to 4.5m. The validation of this model has been the Master Thesis work of H. Radfar, [26]. Who validated the numerical model of *Pioneering Spirit* in Ansys Aqwa with experimental results.
The mesh size of both bodies in the multi-body model should be in the same order. Because having one fine mesh and one coarse mesh does not increase the overall accuracy, however the fine mesh does increases the computation time.

The largest possible mesh size of *Iron Lady*, to stay within the before mentioned limitations, is found to be 2.5 m.
To understand the accuracy of this mesh, the diffraction analysis is performed for a finer and a very fine mesh of 1.4m and 0.75m respectively. The results of this research depend on the vessel motions and hydrodynamic forces. Additionally, forces and motions in the horizontal plane are most important as these need to be restricted by the mooring system. Therefore, the relation between mesh size and both first order motions (RAOs) and first order forces are represented in Figure 5.13.

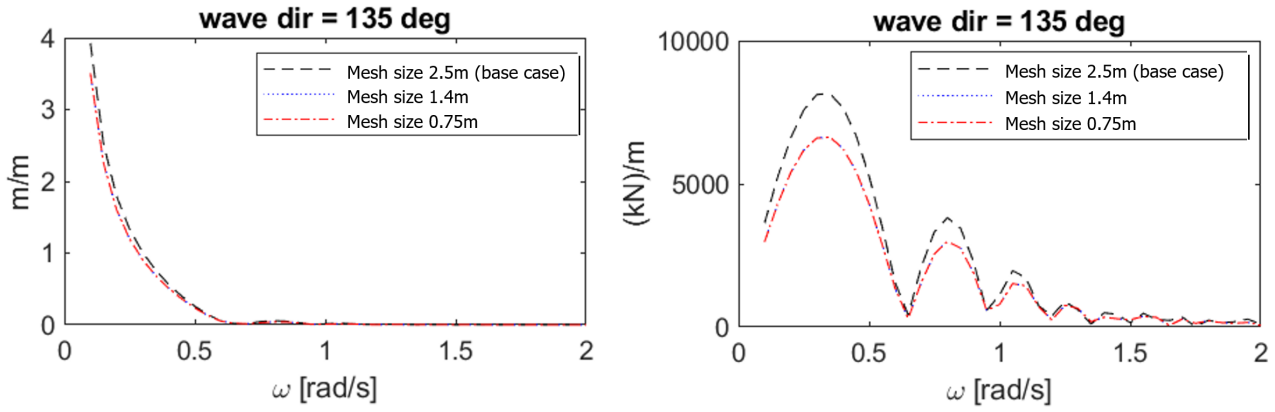

(a) Sway motion RAO.

(b) Sway first order forces (Froude-Krilov and diffraction).

Figure 5.13: Sway RAO (left) and first order force (right) of *Iron Lady* at the CoG, Comparing coarse, medium and fine mesh of 2.5m, 1.4m and 0.75m respectively.

Figure 5.13a represents the sway motion RAO for different mesh sizes when analysing *Iron Lady* as a single body. It can be seen that the results converge with a very small discrepancy in the order of 1%. Similar results are found for other DoF and incoming wave directions.
Figure 5.13b represents the first order force contribution from the Froude-Krilov and diffraction force in

sway direction, acting on *Iron Lady*, for different mesh sizes. A discrepancy of the order of 20 % is found for the first order force. For 1.4m however, the mesh size is converged as the curve aligns with the 0.75m mesh size. Similar ratio's were found for the second order forces, these results are not represented in this report.

This discrepancy of first order force will affect the mooring loads in this research. However, as can be concluded from Figure 7.4a, the mooring system is not affecting motions due to first order wave excitation forces. Therefore the mooring loads will have equal effect on each mooring system concept. Since this research compares the mooring system concepts, the results from the comparison and with that the results of this research are expected not to be affected. Further research is required to confirm this hypothesis.

Fortunately, finer mesh results in lower motions and forces which means that the results in this research are conservative.

5.5.5 Sea state RAOs

The diffraction potential software 'Ansys Aqwa' calculates the fluid potential around the structure. This potential can be expressed and visualized as the wave amplitude pattern around the structure, showing the shielding around a floating structure. This shielding pattern can be judged with engineering intuition on whether the results are acceptable.
To visualize shielding, sea state RAOs and shielded wave spectra can be plotted for field points at the water surface around the floating structure.
The sea state RAOs describes the ratio between surface elevation due to the undisturbed incoming wave and the sea surface elevation at the defined location location.
Shielding effects, including radiation and diffraction effects, are included when calculating the sea state RAO. Figure 5.14 represent the locations at which the shielding RAO is calculated. The y-coordinate of these locations corresponds with the transverse center of the barge for the base case vessel orientation as shown in Figure 2.5b. To determine the shielding RAOs, *Pioneering Spirit* is analysed as a single body.

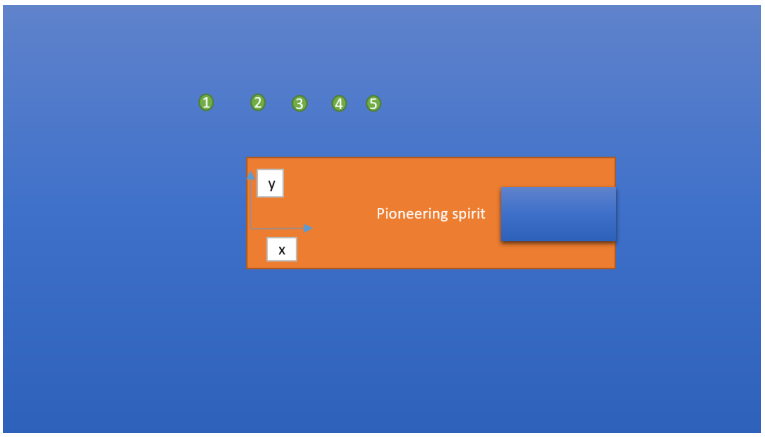

Figure 5.14: Field points around *Pioneering Spirit* for which the sea state RAO is computed.

The shielding ratio depends on the incoming wave direction. Figure 5.15a represents the shielding RAO for various incoming wave directions, it can be seen that an incoming wave direction of 135 ° provides maximum shielding. Besides, it can be seen that shielding occurs only for the higher frequencies, for low frequencies the waves pass underneath *Pioneering Spirit* which means that the wave height is not disturbed. The shielding RAO curve shows an irregular shape, probably due to the relatively large step size.
Furthermore, it is interesting that the RAO for 180 and 90 ° at some point exceeds a value of 1.0 which

means that the wave amplitude is amplified. This can be related to the roll natural frequency of *Pioneering Spirit*, equal to 0.43 rad/s. At this natural frequency excessive roll motion occur which could contribute to increased amplitude of the radiating waves.
Figure 5.15b shows the shielded wave spectra, for the various incoming wave directions. The shielded wave spectrum shows the energy distribution of the wave spectrum at that specific location.
The shielded wave spectrum can be computed from the shielding RAO and the incoming undisturbed wave spectrum, by means of equation 5.7.

$$S_{shielded}(\omega) = \left| \frac{\zeta_{sh}}{\zeta_a}(\omega) \right| \cdot S_\zeta(\omega) \mid \tag{5.7}$$

With ζ_{sh} the shielded wave amplitude and ζ_a the undisturbed incoming wave amplitude and $\frac{\zeta_{sh}}{\zeta_a}(\omega)$ the sea state RAO or amplification factor.

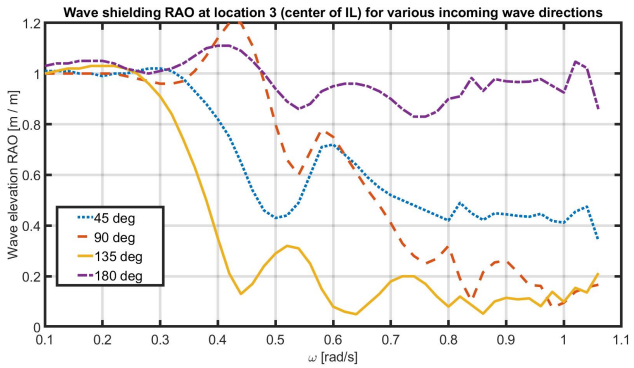

(a) Sea state RAO

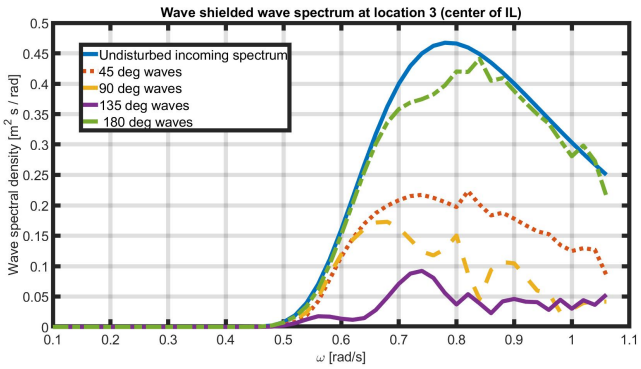

(b) Wave spectra, including undisturbed Pierson-Moskowitz wave spectrum with Hs = 2.5m and Tp = 8s.

Figure 5.15: Sea state RAO (left) and wave spectra (right) at location 3, denoted in Figure 5.14, Corresponding with the center of *Iron Lady*.

For this shielded wave spectrum, the zeroth order spectral moment can be calculated by integrating the shielded wave spectrum from frequency 0 to ∞, captured in equation 5.8.

$$m_{n\zeta} = \int_0^\infty \omega^n \cdot S_\zeta(\omega) \cdot d\omega \tag{5.8}$$

From this zeroth order spectral moment, the significant wave height can be computed with equation 5.9. Dividing this shielded significant wave height with the significant wave height of the undisturbed wave train gives the shielding factor, represented in equation 5.10. As a result, the shielding factors that are computed with the described method are captured in table 5.5.

$$H_{s,shielded} = 4 \cdot \sqrt{m_0} \tag{5.9}$$

$$\text{Shielding factor} = \frac{H_{s,shielded}}{H_{s,undisturbed}} \tag{5.10}$$

Table 5.5: Shielding factor at different locations for different incoming wave directions. For a Pierson-Moskowitz spectrum with Tp = 8s.

Location	Coordinate			Shielding factor per wave direction [°]			
	x	y	z	45	90	135	180
1	-40	94.1	0	0.98	0.94	0.42	0.92
3	60	94.1	0	0.69	0.54	0.35	0.96
5	160	94.1	0	0.47	0.45	0.41	1.02

From the above results it can be learned that heading control is closely related to the wave pattern *Iron Lady* will be exposed to. Therefore, optimum heading to provide maximum shielding is preferred to reduce relative motions and with that mooring loads. Especially for wind seas with high frequency waves. Minor shielding is seen for the lower wave frequencies, therefore optimum heading control will be less relevant for swell ares.
Figure 5.16 visualizes the amount of shielding when waves coming from 135°. It can be seen that for high frequencies, *Pioneering Spirit* provides more shielding than for the lower frequencies. The result includes the incoming wave, radiated and the diffracted wave.

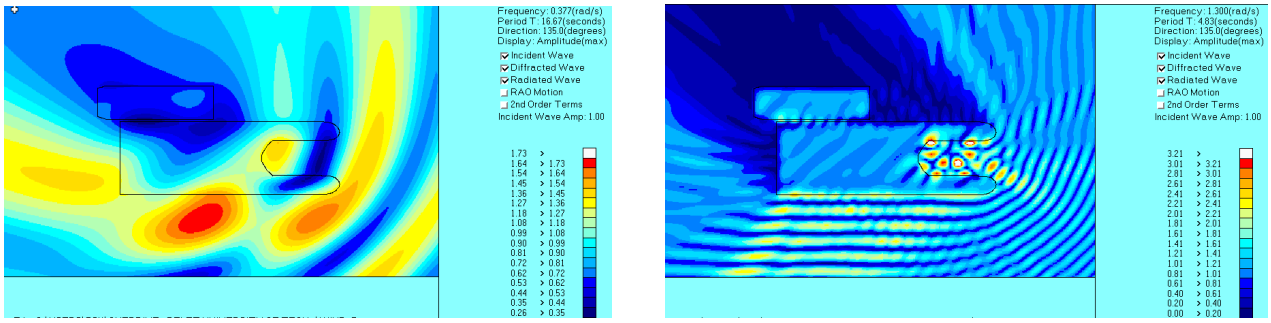

(a) Low frequency (0.38 rad/s).

(b) High frequency (1.30 rad/s).

Figure 5.16: Visualization of wave amplitude shielding from *Pioneering Spirit* for waves coming from 135°, at low frequency (left) and high frequency (right). Beware of the difference in color scaling between Figure 5.16a and 5.16b.

It is interesting to see the shielding pattern for waves coming from 45° and how waves interact at the corner between *Pioneering Spirit* and *Iron Lady* stern. These results are captured in Figure D.4 in appendix D.

5.6 Frequency domain model limitations

Where the the quasi-static solution, as described in appendix C, only includes the mooring system forces and the equilibrium vessel positions, the diffraction analysis in the frequency domain provides the motion and force RAOs at the CoG of the bodies that are involved for every requested incoming wave frequency and direction. With this data, the first order forces and relative motions can be computed in the frequency domain. However, a mooring system and wind and current loads cannot be well described in the frequency domain due to non-linearities.

Non-linearity in the mooring system is recognized when imagining excitation in sway motion. Translation in positive sway direction results in different reaction forces in the mooring system compared to moving in negative y-direction. For the first case, fenders disconnect the fender reaction force reduces to zero upon disconnection and the mooring line force increases. For the second case, motion in negative y-direction, fenders are more compressed, following its non-linear force-displacement curve and

mooring lines become slack, increasing the catenary shape.
Overall, this leads to a non-linear force-displacement curve for sway motion, as represented with the non-linear curve in Figure 5.17b. Non-linearity can also be recognized in the force-displacement curve in surge direction, can be seen in Figure 5.17a.
Non-linearities in the mooring system mainly originate from material and geometric effects. Material is related to the mooring system properties, geometric is related to the change in shape of the fenders and mooring lines over time [6].
Regarding the material, the fenders are modelled as links with a stiffness curve following a third order polynomial function and a damping curve with saturating reaction force upon exceeding the expected maximum velocity that occurs.
the mooring lines are modelled as linear springs with constant axial stiffness and without a limit on the maximum force and therefore bringing no non-linearities, in reality however the axial stiffness will be non-linear as described in section 4.2.1.
Same as for the fender damping curve, some mooring systems are modelled with saturating stiffness and damping curves, represented in section 4.3.
Variable mooring line tension over time leads to slack and taut lines. Slack lines having a non-linear catenary shape while taut lines have more linear shape, depending on the tension applied. Since the mooring line shape cannot be described as a harmonic motion, time domain modelling is required, [31].

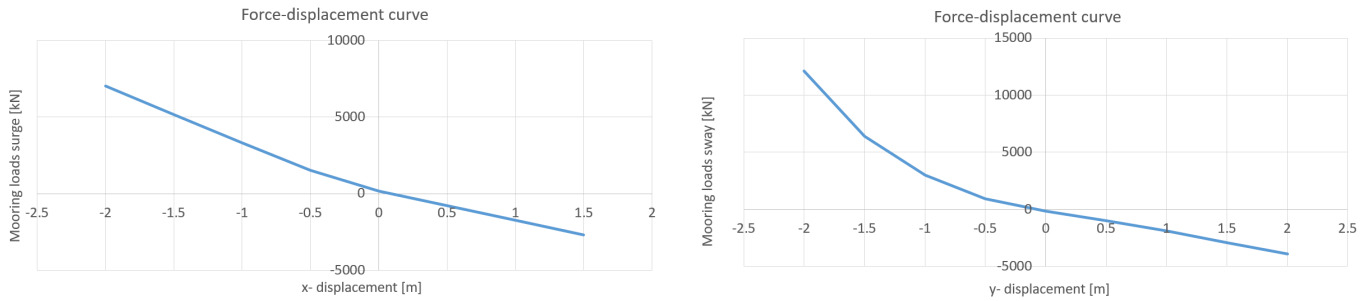

(a) Force-displacement for surge motion

(b) Force-displacement for sway motion

Figure 5.17: Force-displacement curve representing the relation between barge connection and displacement for surge (left) and sway (right) motion. Representing non-linearity in the mooring system.

Besides non-linearity in the mooring system, wind and current forces are non-linear because of their quadratic relation with the fluid flow relative to the floating body. To account for these non-linearities, time domain modelling is required and will be the next step in the methodology.

5.7 Diffraction analysis outcome and purpose

In the diffraction analysis the frequency dependent added mass and damping are computed, Snap shots of this data is listed in appendix F section F.1.1. Furthermore, from the fluid potential, the pressure distribution over the floating body is determined, varying with frequency and incoming wave direction. These first order wave loads are captured in the so-called wave load RAO. In the same format, the motion RAOs including displacement, velocity and acceleration are provided. This hydrodynamic data is acquired from Ansys Aqwa and is input for the time domain simulation software 'Orcaflex', as will be discussed in the next chapter.

5.8 Conclusion and reflection

The purpose of the diffraction analysis is to find the hydrodynamic matrices, displacement and load RAOs and the Quadratic Transfer Functions. This is required as input for the time domain model.
For *Iron Lady* the procedure for building the diffraction analysis model is performed. For *Pioneering Spirit* an already existing diffraction model input, including loading condition, together with the *Iron Lady* model is converged to a multi-body model for which the diffraction analysis is performed to find the corresponding frequency dependent hydrodynamic data.
Several validation and verification steps are performed, showing satisfactory results.
Due to non-linearities that come with properly modelling a mooring system, the mooring system securing *Iron Lady* to *Pioneering Spirit* is excluded from the diffraction analysis and also from the frequency domain modelling and will be included in the time domain. Further inaccuracies in the results from the diffraction analysis will be discussed in chapter 9.

Before going to the time domain model and as a summary from the validation and verification steps, the 'base case' parameters that are applied in the diffraction analysis to determine the results required for the time domain model are listed in Table 5.6, general dimensions as listed in 2.1 are incorporated.

Table 5.6: Specification of base case model parameters.*The VCG is defined from the keel line of *Iron Lady*

Variable	Symbol & unit	Value
Additional viscous roll damping for *Iron Lady*	$b_{\phi\phi}$ [-]	0.0
Off-diagonal inertia terms included for *Iron Lady*	$I_{i,j}$ [-]	No
Vertical center of gravity for *Iron Lady**	VCG [m]	12.1
Damping factor of VLID	b_{VLID} [-]	0.05
Internal lid included for *Pioneering Spirit* and *Iron Lady*	$ILID$ [-]	No

To account for viscosity, that is initially disregarded in potential flow software, an additional damping term can be included for the roll motion. As pointed out in section 5.5.2, no additional roll damping needs to be included for both *Pioneering Spirit* and *Iron Lady*.
For the base case, the off-diagonal terms of the inertia matrix of *Iron Lady* are not included. For *Pioneering Spirit* however, the off-diagonal inertia terms are included.

6 Time domain modelling

6.1 Introduction to modelling the time domain

In the dynamic evaluation of the side-to-side mooring system, the second order wave drift forces are known to have a significant contribution to the environmental force. As these second order wave drift loads are non-linear, modelling in the time domain is inevitable.
These second order wave drift loads are captured in the Quadratic Transfer Function matrix, varying with frequency and incoming wave direction. Entries of this matrix are defined per unit wave amplitude.
The disadvantage of time domain modelling, compared to frequency domain modelling, is its complexity and computation time.

Time domain modelling requires input from the diffraction analysis output.
In the time domain model the mooring system has been added next to the multi-body configuration considered in the frequency domain, including the interaction between both floating bodies.

The hydrodynamic force can be described in terms of added mass and damping, respectively related to acceleration and velocity. In addition, load term, describing the external forces that are exerted on the bodies. These hydrodynamic forces are time-varying.
Similar to solving the motions in the frequency domain, the equations of motions specified for the time domain can be used to determine the motions at every time step. Equation 6.1 gives the static contribution at every time step and equation 6.2 represents the time varying dynamic force.
The hydrostatic force can be described by a restoring term, related to displacement, $x(t)$. Given by

$$F_{stat}(t) = C\, x(t) \tag{6.1}$$

$$F_{dyn}(t) = A(t) \cdot \ddot{x}(t) + \int_{-\infty}^{t} B(t-\tau) \cdot \dot{x}(\tau) \cdot d\tau \tag{6.2}$$

The equation of motion in the time domain derived by Cummins' consist of this static and dynamic part, as represented below.

$$[M + A] \cdot \ddot{x}(t) + \int_{0}^{\infty} B(\tau) \cdot \dot{x}(t-\tau) \cdot d\tau + C \cdot x(t) = F_{ext}(t) \tag{6.3}$$

With

- M the solid mass or mass moment of inertia matrix.
- A the hydrodynamic added mass matrix.
- $B(t-\tau)$ the damping matrix.
- C the stiffness matrix.
- $F_{ext}(t)$ the time-varying external forces applied specified per DoF.

- x(t), $\dot{x}(t)$ and $\ddot{x}(t)$ respectively the translational, velocity and acceleration at time t. Similar for all other DoF.

The damping matrix contains the so called retardation functions used to determine the damping term for cases with non-linearities. These retardation function are extensively explained in the literature report, [2].
The external forces are stored in the vector, for example mooring line forces or incoming wave and diffraction forces [3, 32].
The system matrices will have dimensions NxN with N being the total number of DoF in the system. In case of two coupled floating bodies, N will be equal to 12. These frequency dependent system matrices are determined in the frequency domain.

This chapter starts with the time domain model preparation, that is required to be able to build the time domain model in the dynamic software package 'Orcaflex'. Following with the modelling procedure to create the required results, the forces in the mooring system ad the corresponding maximum allowable sea state.
To confirm that the results from the time domain do make sense and can be used to draw conclusions from, the model is validated and verified.
Finally the limitations of the time domain model are discussed, followed by concise conclusion and reflection.
Figure 6.1 represents the part of the total thesis approach, as shown in Figure 3.1, that will be answered in this chapter.

6.2 Time domain modelling procedure

The time domain modelling starts with importing data from the radiation and diffraction calculation output and defining the environmental input. After that, the mooring system concepts are build and modelled. From post processing the time series output of the time domain model to do the statistic calculation gives the three hours maximum force, assuming the maximum mooring system force to be Rayleigh distributed. This corresponds with steps 3 and 7-13 of the stepwise approach as explained in section 3.1.

First, the base case model will be analysed followed by the mooring system improvement concepts. In case the performance of the mooring system improvement concepts does not exceed the base case, other improvement concepts are designed and build. Finally, when the performance is increased, various sea states are applied to find the limiting allowable sea state. For this sea state, the workability can be determined. Results regarding the three hours maximum mooring system and the workability will follow in chapter 8.
Only *Iron lady* will be subjected to wind waves and current forces while *Pioneering Spirit* is only subjected to first order motions, modelled as following the displacement RAOs that are received as output from the radiation and diffraction calculation.
This assumes ultimate DP capabilities of *Pioneering Spirit* which is expected to be realistic as *Pioneering Spirit* has DP capabilities to counteract 400 Tons of bottom tension, even while pipe transfer barges are moored alongside.

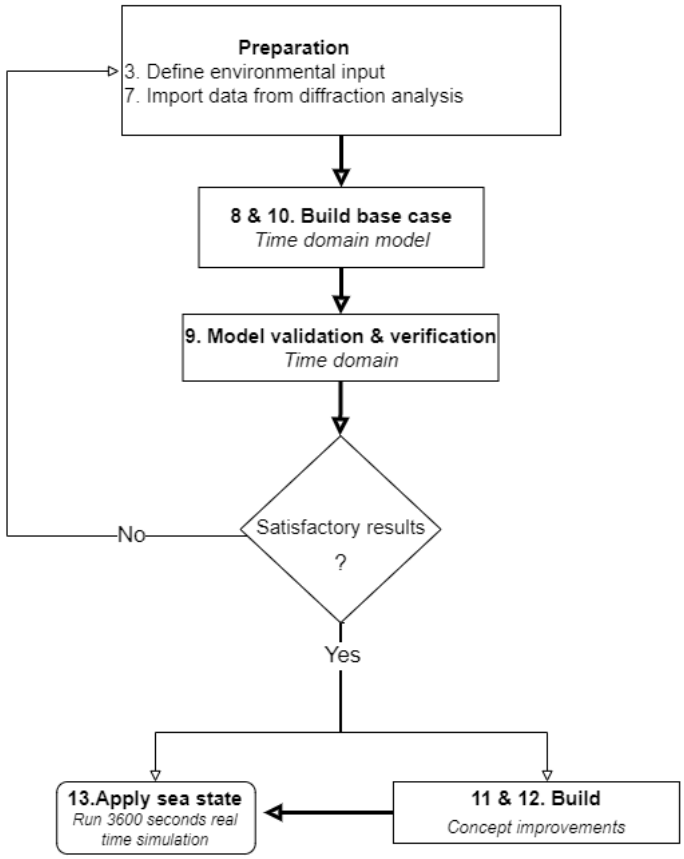

Figure 6.1: Time domain modelling procedure. The numbering corresponds with the stepwise thesis approach from section 3.1.

6.3 Time domain model preparation

This section describes the following:

- Input from diffraction analysis
- Environmental condition

Corresponding with step 3 and step 8 of the thesis approach, 3.1.

6.3.1 Input. Diffraction analysis results

6.3.1.1 Wave forces

The first order wave force consists of parts, the force due to the incoming and diffracted wave and the force due to the radiated wave.
The first order wave forces due to the incoming wave and the diffracted wave is included in the load RAO, this load RAO depends on frequency and incoming wave direction. Effects of the radiation force is captured in both the added mass and damping matrix. This is one way of hydrodynamic coupling between bodies in close proximity.

Second order wave forces are captured in the QTF that is imported from the diffraction analysis into the time domain model. The QTF varies with frequency and incoming wave direction. The QTF includes all contributions to the second order wave drift forces respectively the mean, sum frequencies and the

low frequency slow wave drift contributions.
The additional wave drift damping is added in the time domain model by modifying the QTF. The contribution of the additional wave drift damping depends on the wave encountering velocity the vessel, this is included in the Aranha's scaling factor as can be read in the literature report, chapter 4.

6.3.1.2 Floating object motions

The first order motions are included in the motion RAOs, respectively displacement, velocity and acceleration. These motion RAOs will be used for *Iron Lady* in the time domain validation step, section E.0.2.2. Furthermore, *Pioneering Spirit* will be modelled as following the RAOs, meaning that it will only follow its first order motions.

The motion RAOs, are imported for different incoming wave directions ranging from [-180,180]° with a step size of 15°. Data is provided for frequencies ranging from 0.1 to 1.3 rad/s with a step size of 0.05 rad/s, explained in section 5.7.

6.3.2 Input. Environmental conditions

6.3.2.1 Waves

A wave spectrum can be described by significant wave height, Hs, and peak period, Tp, and the type of wave spectrum, for example Pierson-Moskowitz.
Significant wave height is defined as the average height of the highest one third of the waves in the wave train. The peak period is defined as the period of the wave corresponding with the maximum amount of energy in the wave.
To determine the maximum allowable sea state for the different concepts, two spectra with different peak periods will be applied. The first spectrum with a Tp of 8 seconds, the second spectrum with a Tp of 12 seconds. The maximum allowable sea state will be found by varying the significant wave height.
Figure 6.2a represents a Pierson-Moskowitz wave spectrum with Hs = 2.5m and Tp 8 and 12 seconds.
Figure 6.2b represents the sea surface elevation over time at an undisturbed location far away from the floating structure.

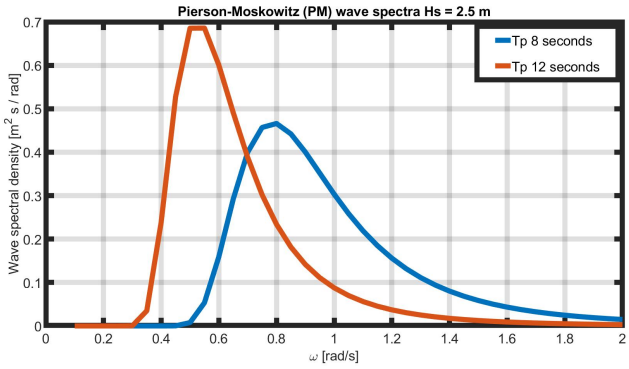

(a) Pierson Moskowitz wave spectra, for 2.5m significant wave height and a peak period of 8 (red) and 12 (blue) seconds.

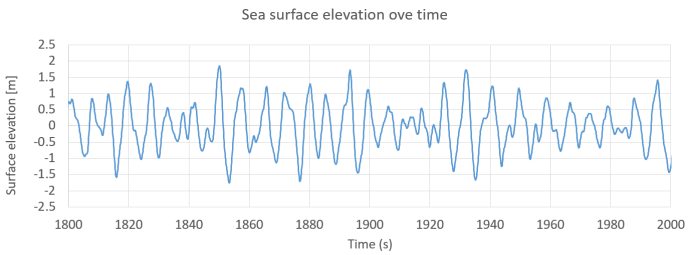

(b) Sea surface elevation at an undisturbed location, for a Pierson-Moskowitz spectrum with Hs = 2.5m and Tp = 8s.

Figure 6.2: Wave data. Wave spectra (left) and sea surface elevation time series (right).

In this research, the floating structures will be exposed to a uni-directional wave spectrum. This is expected to be conservative because in reality not all wave energy is concentrated in a single wave direction.

Applying a wave spectrum in Orcaflex results in a wave train with waves varying in height and period, within the set limits of the wave spectrum. The wave phase associated with each wave component is determined using a random number generator, the seed. If the seed is not varied and the wave train specifications, Hs and Tp, are kept constant, the exact same wave is applied each simulation.

In addition to the significant wave height and peak period, the type of wave spectrum determines the shape of the wave spectrum. Common known wave spectra are the Pierson-Moskowitz spectrum and a JONSWAP spectrum. Where in this research a Pierson-Moskowitz spectrum is applied, more details on why can be found in Appendix F, section F.1.2.1.

6.3.2.2 Wind and current

Metocean data is available for the reference location, based on 37 years of hindcast data, providing realistic input for wind and current load.
The reference locations are known to be in a tidal area, therefore the current velocity can be very well be estimated. The reference location is located in a fetch limited sea, which means that the sea can be described as wind sea and the wave height has strong relation with the wind speed. However, for simplicity both wind and current are assumed to be constant over time and independent of elevation above the free surface and sea bed respectively. The resulting wind and current force that is exerted on the structure will therefore also be constant over time. The magnitude of the wind and current speed is based on the metocean data available for the reference location.
To be able to calculate the wind and current force, the subjected area, drag coefficient and the relative velocity relative to the floating structure have to be known. The drag coefficient and area vary with incoming wave direction, these are computed in Appendix F.1.2 and plotted in Figure F.2.
To come up with conservative results, no current and wind shielding from *Pioneering Spirit* is taken into account.

Regarding current, the velocity considered is equal to 0.9 m/s, corresponding with 99 % workability which means that, annually, 99 % of the time the current velocity does not exceed 0.9 m/s. Further input data and the corresponding loads can be found in F.1.2.2 and E.0.1.3.
Regarding wind, the velocity is considered to be constant and equal to 12.86 m/s, corresponding with 25 knots and a workability of 92.5 % at the reference location. Further input data and the corresponding loads can be found in F.1.2.3 and E.0.1.3.

Table 6.1 displays the load contributions of wind, waves and current. Additionally the connection force and mean total force is given. To be in equilibrium, the total mean load should be zero. The relation between wave forces and the peak period can be learned from the results in Table I.1. In general, wave loads are smaller for swell waves. However, first order motions are larger.

Table 6.1: Magnitude of various contributions to the mean and max force in surge and sway direction. For environmental conditions from 135°. Wind 25 knots, current 0.9 m/s, waves Hs = 2.5 and Tp = 8s.

	Fx [kN]		Fy [kN]	
	Max	Mean	Max	Mean
Wind	-1.87E+02	-1.88E+02	1.91E+02	1.89E+02
Current	-6.89E+01	-7.04E+01	2.65E+02	2.39E+02
First order waves	1.09E+03	-7.86E-02	3.49E+03	-3.03E-01
2nd order wave drift	5.31E-02	-6.10E+00	6.42E+02	7.94E+01
Added mass and damping	5.73E+02	3.41E-01	3.45E+03	4.58E-01
Hydrostatic stiffness	3.00E+00	-1.54E-01	5.79E+00	-5.98E-02
Connection force	6.59E+02	2.64E+02	-1.10E+03	-5.07E+02
Total load	8.38E+02	-3.38E-02	1.84E+03	2.87E-01

6.4 Time domain model build

After gathering all the required input, the time domain model can be build. Building the model includes the body shapes, the fenders and the mooring lines.

6.4.1 Body shape

The body shapes of *Pioneering Spirit* and *Iron Lady* are drawn in Orcaflex for visibility purposes only. Figure 6.3a shows a representation of both bodies and their orientation.
The same holds for the wind turbine components that are drawn in Figure 6.3b, these structures have zero weight and inertia. The main purpose for drawing these parts is to give an impression how the loading condition for 8 wind turbines might look like.

(a) Topview of body shapes representing *Pioneering Spirit* (grey) and *Iiron Lady* (red), drawn in Orcaflex.

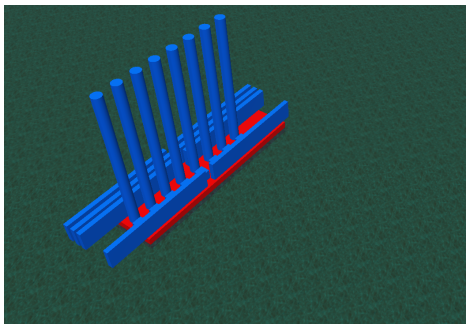

(b) Impression of example barge loading, isometric view. Showing turbines, blade racks and nacelle's as simplified structures.

Figure 6.3: Body shapes, drawn in Orcaflex.

6.4.2 Fenders

The main purpose of a fender is to prevent both vessels for colliding and to provide a reaction force upon the transverse vessel spacing being lower than the initial fender width.
Fenders float between the floating bodies, resulting in a compression force upon deformation. The main force component is in sway direction with a small surge and heave component due to friction between the fender and the hull.

Initially the fenders were modelled according to the example given by Orcaflex, [33], modelling the fenders as contact points, providing a connection upon contact only. However, this lead to instability in the numerical model. Therefore, a simplified fender modelling method is thought of and implemented. Modelling the fenders as links having a stiffness curve such that the fenders stay attached at all times but only providing a restoring term upon actual fender compression. The fenders are modelled as a link, representing a spring and damper system.
The stiffness properties are found from the fender brochure, [18]. The stiffness curve has to be adjusted such that it can only take compressive forces, no tension. Therefore, the end that is fixed to *Iron Lady* is located on *Pioneering Spirit* side, while the end that is fixed to *Pioneering Spirit* is located on *IL*. This means when the gap width between the vessels reduces, the spring will be elongated, resulting in a compressive force. This rather complex explanation words is explained in more detail in Appendix F, more specifically in Figure F.1.

Besides stiffness, the fenders consist of a small damping term to account for the expected energy dissipation in the system, for example due to deformation.
For this research the fender types that are available on *Pioneering Spirit* are modelled, unfortunately

research to fender damping for these, or fenders in general, is limited in literature. Therefore the damping curve should be defined appropriately, including a sensitivity to monitor the influence of fender damping on the results, mooring line loads and relative motions.
The method and outcome of this sensitivity analysis on fender damping is explained in section E.0.4.1. A damping factor of 2.5 % is found to be realistic. The damping factor is defined as percentage of the fender SWL at the largest expected fender velocity. The final fender damping curve is represented in Figure E.9.
To make sure the fenders provide only a reaction force in transverse direction and a small contribution in surge and heave direction to account for friction, the initial length of the fenders is elongated. Which means that upon relative motion the reaction force will be almost uni-directional. This requires the fender stiffness curve, as represented in Figure 4.4 to be corrected with its initial length accordingly. The initial fender length is realised by attaching the link more to the center of *Pioneering Spirit*, as can be seen in Figure 6.4. In this Figure *Pioneering Spirit* is drawn in three grey blocks, port side, center and starboard side.

In general, a symmetric mooring system minimizes dynamic loads in the mooring system because yaw moments can be well compensated. To optimize symmetry, the fenders are equally spaced over the overlap of *Pioneering Spirit* and *Iron Lady* in longitudinal direction.

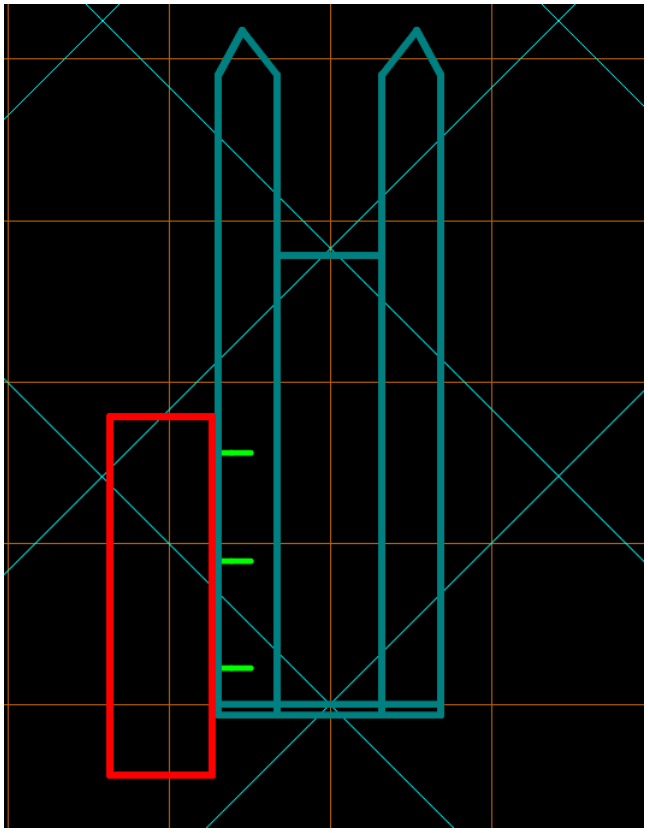

Figure 6.4: Top view. Three fenders (green) connected to *Iron Lady* (red) and *Pioneering Spirit* (grey). Connection point inside *Pioneering Spirit* to assure force is applied uni-directional.

6.4.3 Mooring lines

Mooring lines are modelled as line elements, consisting of several line sections, the section length can be optimized for computation time and accuracy. Each section is modelled as a lumped mass, [34]. The section length is set to a typical value of 5m, such that for an average line length of 90m, the number of

sections is around 18. The section length is most important to well describe the catenary shape of the mooring line therefore an section length of 5 % is expected to be satisfactory.
Performing simulations for 0.5m section length lead to an increase of mooring line load in the order of 5 % but also the computation time of increased with 300 %. Therefore, the 5 m value will be used in this research. However, it is recommended for future research to perform an in depth sensitivity analysis to optimize the section length with computation time and results.

The line elements are attached to *Iron Lady* on one side and to *Pioneering Spirit* at the other side. The axial stiffness can be defined and is set constant for all mooring lines. Besides stiffness, a damping term can be added, section E.0.4.2 represents the results from a sensitivity analysis on the mooring line damping term.
One mooring system design requirement is that at least 50 kN pre-tension should be applied to each mooring line, as stated in chapter 4. Pre-tension can be applied by means of the 'line wizard' tool in Orcaflex. This way each line length and fender compression is adjusted to reach the appropriate pre-tension.

No maximum mooring line load can be defined in the Orcaflex model. Therefore, line load results should be checked and not exceed the safe working load, as defined by the classification company, given in Table C.1.

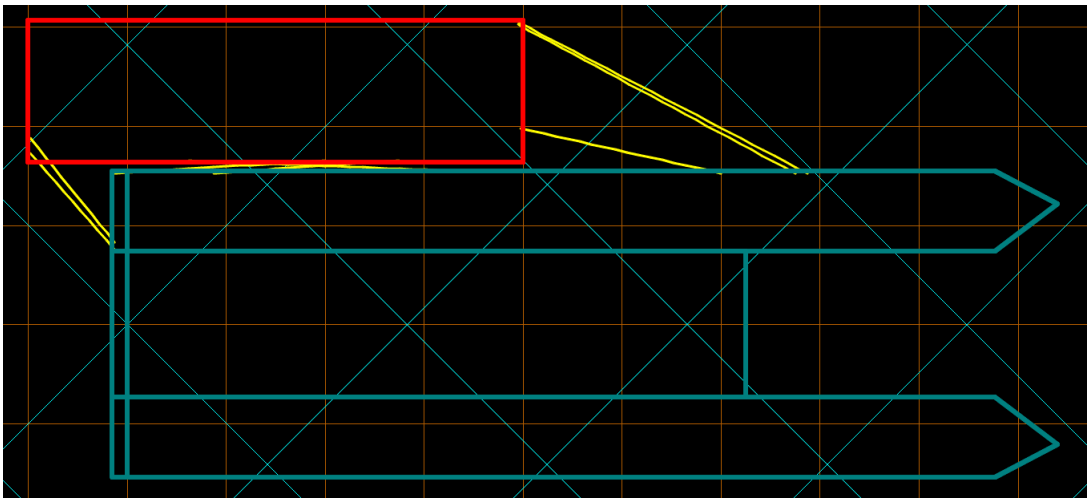

Figure 6.5: *Top view. Iron Lady* (red) and *Pioneering Spirit* (grey) including Mooring lines (yellow), modelled in Orcaflex. Spring lines are partly overlapped with the body drawings.

In the numerical models, mooring lines are attached at the locations of the fairleads on *PS*. Whereas in reality the mooring line leads all the way to the winch. This method neglects friction and stress concentrations between the line and the fairlead, however this is assumed to be more relevant for considering wear of the mooring line.

The mooring lines are modelled in several sections with different properties. This makes it possible to change the stretcher length and thereby the total stiffness of the mooring line. Changing the stiffness of the mooring line does not affect the mean mooring line load, but only the maximum loads and the offset of the moored structure.
This can be seen in the results, shown in section E.0.3.2, where results are given for a mooring system with lines consisting of 0 and 20 % of stretcher length. It can be concluded that the mooring line loads can be optimised by adjusting the stretcher length.

6.5 Time domain model validation and verification

Time domain simulations are performed in the dynamic analysis software 'Orcaflex'. There are many details behind results from this numerical software to solve this rather complex problem. Therefore, a proper model validation and verification is required to make sure the results are valid.
The following five validation steps will be described individually:

- Verification with analytical results.
- Comparing static solution from Orcaflex with the outcome of the quasi-static model.
- Validation of assuming relative motions and mooring loads to be Rayleigh distributed.
- Hydrodynamic effects that need to be considered.
- Time step convergence.

6.5.1 Verification with analytical results

First order wave loads and mean second order wave drift forces are analytically computed and compared with the output from Orcaflex, this can be read in the appendix E sections E.0.1.1 and E.0.1.2.
Similarly, the required input data and the methodology to compute the wind and current loads is described in section E.0.1.3. Only the results from the analytical and numerical current and wind load computation are shown below to convince the reader that these are acceptable.

Table 6.2: Comparing current force found from analytical solution and the orcaflex model for a 0.9 m/s current speed coming from 135°. The yaw moment is calculated around the vessel center of buoyancy.

Method	Fx [kN]	Fy [kN]	Mz [MNm]
Orcaflex	-71	238	7.75
Analytical method	-70	235	8.30

It can be seen that results are in the same order of magnitude. Therefore, the methodology Orcaflex applies can be considered as acceptable.
Similar situation occurs for the wind load for which the results are shown below.

Table 6.3: Comparing wind force, found from analytical solution and the Orcaflex model for 25 knots wind speed coming from 135°.

Method	Fx [kN]	Fy [kN]	Mz [MNm]
Orcaflex	-189	189	0
Analytical method	-180	180	0

6.5.2 Comparing static results from quasi-static and the time domain model

To start with a simplified model, excluding dynamics, prior to the diffraction analysis and time domain modelling, a quasi-static model is used to build and analyse the mooring system. To validate the Orcaflex model, the same mooring systems with the same properties, are build in the quasi-static model and in Orcaflex.The input is explained in detail in section E.0.3.1.
First, the pre-tension for both models is compared in Figure 6.6a because it will affect the magnitude of the load when applying environmental conditions. Second, Figure 6.6b represents the static solution from both the quasi-static and the orcaflex model. Besides, the mean load from running the dynamic simulation of the orcaflex model is plotted.
The quasi-static model computes the offset and static mooring loads upon applying the environmental conditions. Regarding wave loads only the mean wave drift force is included. Same is computed in the static simulation of Orcaflex.

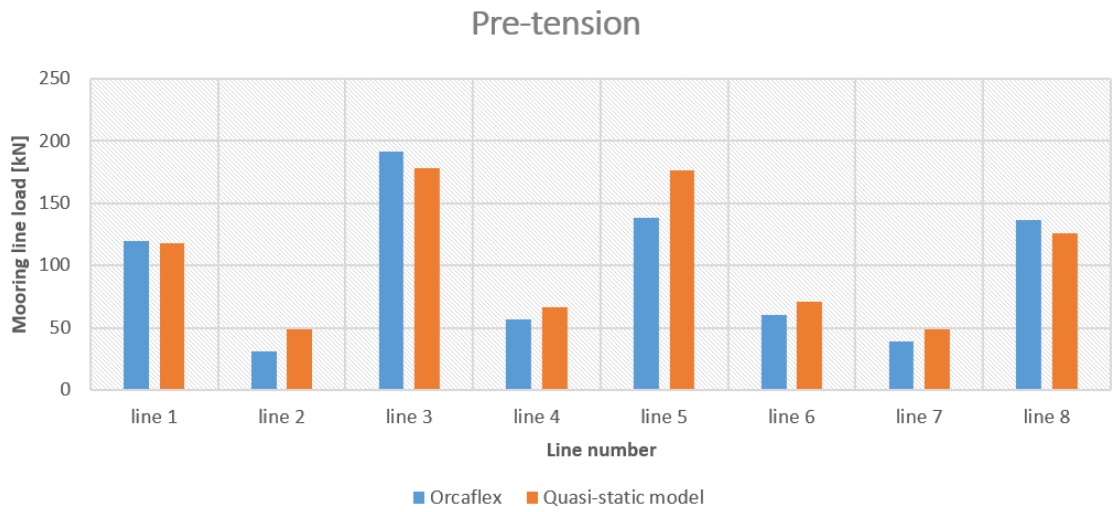

(a) static solution to find the pre-tension

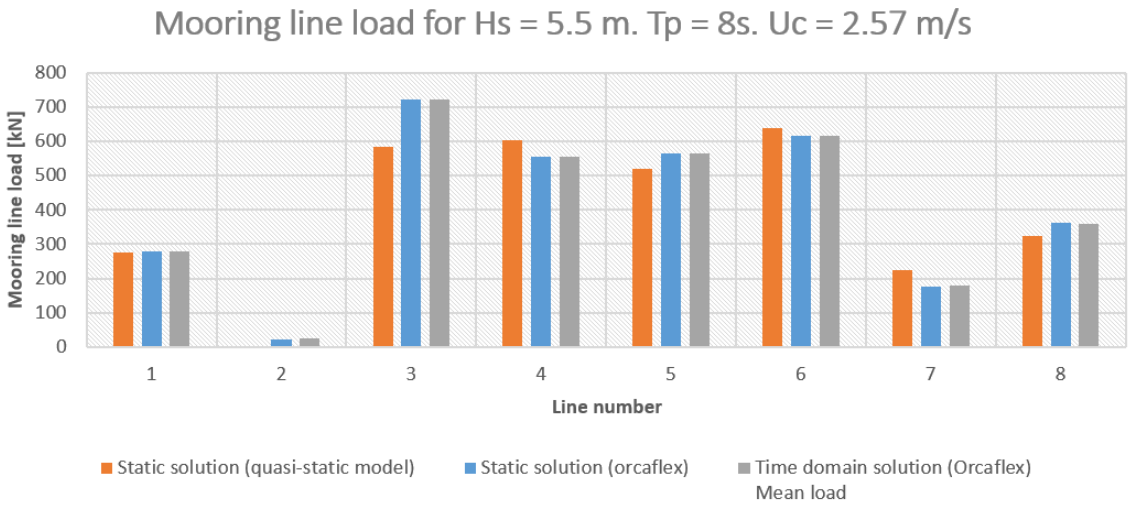

(b) Static solution for the loaded case.

Figure 6.6: Comparing results from the quasi-static solution and the static time domain solution. For the input given in Table E.4.

From these Figure 6.6a it can be learned that for both models the pre-tension matches which means that the mooring loads can be compared. Figure 6.6b shows that results from the three cases are close which confirms that the Orcaflex model provides acceptable results since the quasi-static tool is validated based on many years of Allseas experience.

Results slightly deviate due to small differences in input, e.g. in the quasi-static model, *Pioneering Spirit* is modelled as a quayside fixed to the seabed while in the Orcaflex model it is modelled with finite draft. Besides, the quasi-static model incorporates the QTF of *Iron Lady* as a single body, while the Orcaflex model uses the output of the multi-body diffraction analysis.

6.5.3 Rayleigh distribution in results

Time domain simulations are time consuming. To reduce the real time simulation length required to find results, the three hours maximum is found based on a shorter simulation time by applying statistical methods. This methodology requires maxima of the specific variable to follow a probability distribution, e.g Weibull distribution.
Common applied are Weibull and Rayleigh distribution. For the case of mooring line loads, results from both methods are represented in Figure 6.7 as well as the maximum value that occurs in three hours simulation time.

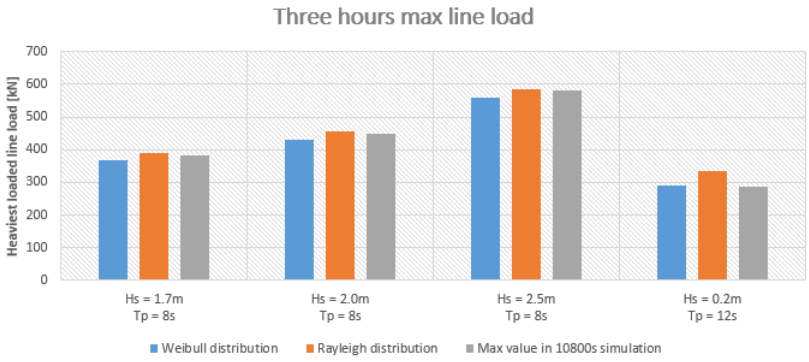

Figure 6.7: Three hours maximum mooring line force based on Weibull and Rayleigh distribution and the maximum value found in 10800s real time simulation.

It can be seen that results for both Rayleigh and Weibull distribution are close (within 5 %) to the maximum value occurring in three hour simulation time. Assuming results to be Rayleigh distributed provides highest loads and therefore most conservative results.
Therefore, mooring loads and relative vessel motions are assumed to be Rayleigh distributed in this research. Equations related to this method are explained in section 4.7. This validation step justifies whether it is valid to compute the three hours maximum assuming Rayleigh distribution.

Assuming maximum relative motions and mooring line loads to be Rayleigh distributed allows to determine the three hours maximum based on a shorter simulation length and statistical data. Whenever the floating structure, modelled in the time domain, is subjected to a wave spectrum, Orcaflex produces random wave trains that are send towards the structure.
Both the wave origin and the wave seed can be manually modified. The user-defined seed determines the combination of phases of the individual wave components in the wave train. Whenever the wave origin location and the seed is kept constant, the wave components will have the exact same phase for every simulation.
In case also the peak period is kept constant, the exact same wave train will be applied, let it be with different wave height, depending on the defined significant wave height. This means that the wave extremes are equally distributed for different trains, following the Rayleigh distribution. Figure 6.8 shows a time series of the wave elevation at an undisturbed location. In all cases the seed and wave origin location is kept constant. Run 1 and 2 represents the results for giving two times the same input, run 3 represents the case when the same seed and wave origin is applied but only the wave height is changed. It can be seen that at all cases the exact same wave train is applied, let it be with varying wave height, this proofs the consistency of Orcaflex. These results are relevant as in this research various wave trains will be applied with having the same seed, wave origin and peak period but different significant wave height in order to find the limiting sea state.

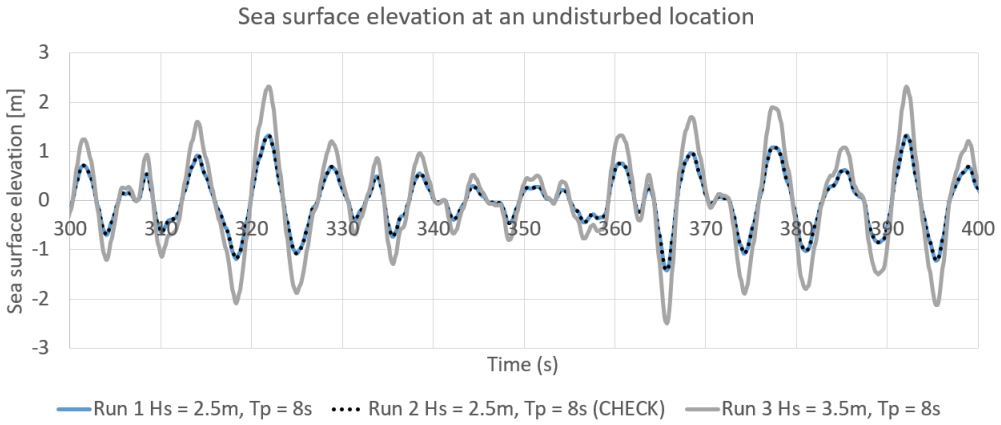

Figure 6.8: Undisturbed sea surface elevation for constant seed. Comparing three arbitrary runs.

To see how well the relative motions and the mooring line forces are estimated by assuming them to be Rayleigh distributed, the three hours maximum relative motions and the three hours maximum mooring line load is determined for different seeds, by applying the methodology as explained in section 4.7. In other words, the three hours maximum, based on Rayleigh distribution, is computed for different wave trains with equal statistic properties. Figure 6.9 provides the results for relative motion and mooring line force.

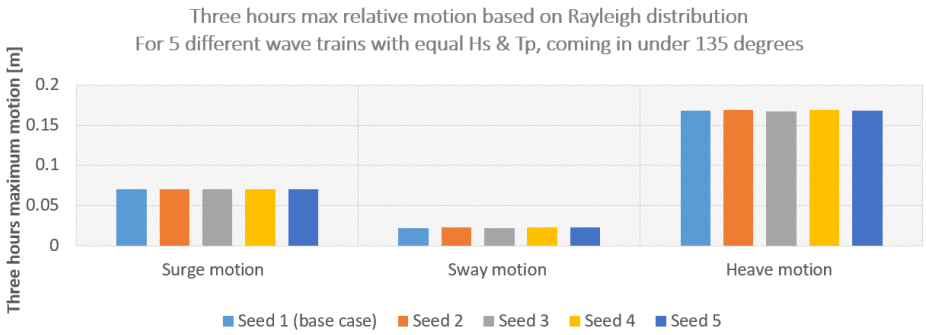

(a) Three hours maximum relative motion

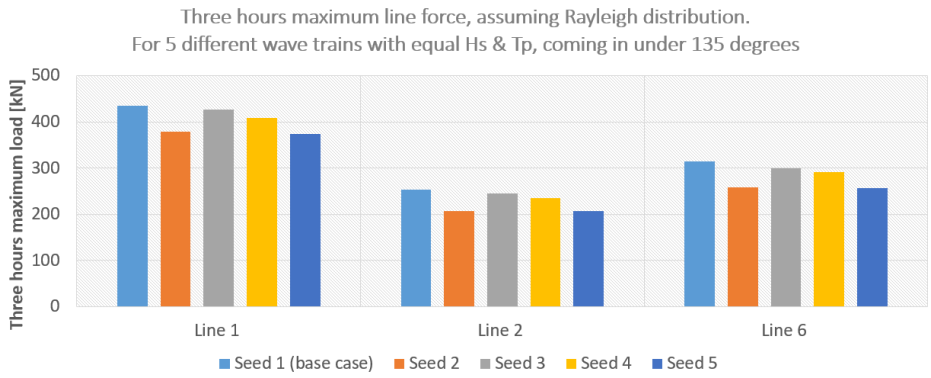

(b) Three hours maximum mooring line force

Figure 6.9: Three hours maximum relative motions and mooring line forces, assuming these to be Rayleigh distributed. Results for five different wave trains (seeds), with equal statistical properties (Hs and Tp).

The five wave trains, referred to as seeds in Figure 6.9, do have equal statistic properties (Hs and Tp). Therefore by comparing the maximum relative motions and maximum mooring line forces for these different wave train answers the question whether these variables follow a Rayleigh distribution. Because applying different wave trains result in different vessel motions over time, this affects how the waves encounter the vessel, with what relative motion and phase.
Figure 6.9 shows the results from computing the three hours maximum relative surge, sway and heave motion assuming these to be Rayleigh distributed. These simulations are done for waves coming from an angle of 135°, the maximum mooring line force is given for line 1,2 and 6. These lines are chosen arbitrarily.

From figure 6.9a it can be learned that relative motions can be assumed to follow a Rayleigh distribution, the discrepancy is in the order of 2 %. Looking at Figure 6.9b, it can be seen that assuming the maximum mooring line load to be Rayleigh distributed results in an discrepancy of 18 % at maximum.
The three hours maximum mooring line forces are important for comparing the workability of various mooring system concepts. Another method to compare the workability of various mooring system concepts would be to compare the maximum amplitude of the mooring line force for a certain real time simulation length. Figure 6.10 captures the results from running 3600 seconds real time simulation for the 5 different seeds and compute for each seed the maximum amplitude. The maximum amplitude can be found from the maximum and minimum value that occurs in the simulation, $(max - min)/2$.

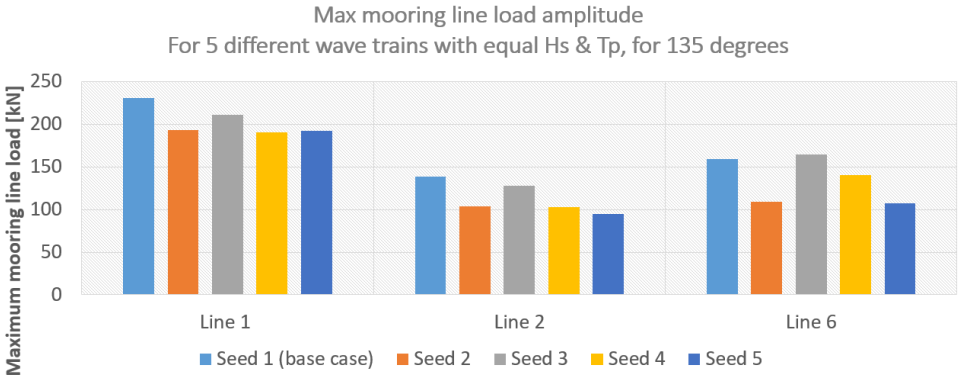

Figure 6.10: Maximum mooring line force amplitude, calculated by $(max - min)/2$, based on 3600 seconds simulation. Results for five different wave trains (seeds), with equal properties.

From figure 6.10 it can be seen that also these results vary with the seed. Comparing Figure 6.9b and Figure 6.10 shows that both methods are not perfect.
Since comparing three hour maximum loads is common used in industry, for this research the mooring line force is taken to be Rayleigh distributed. The question arises, what should be the real time simulation length to find sufficient accurate results. To determine the required simulation time, a convergence test is performed.

The approach is to run the model for 360, 1800, 3600 and 10800 seconds and compute the 3 hours maximum mooring line force. Results of these simulations are captured in the block diagram as shown in Figure 6.11.

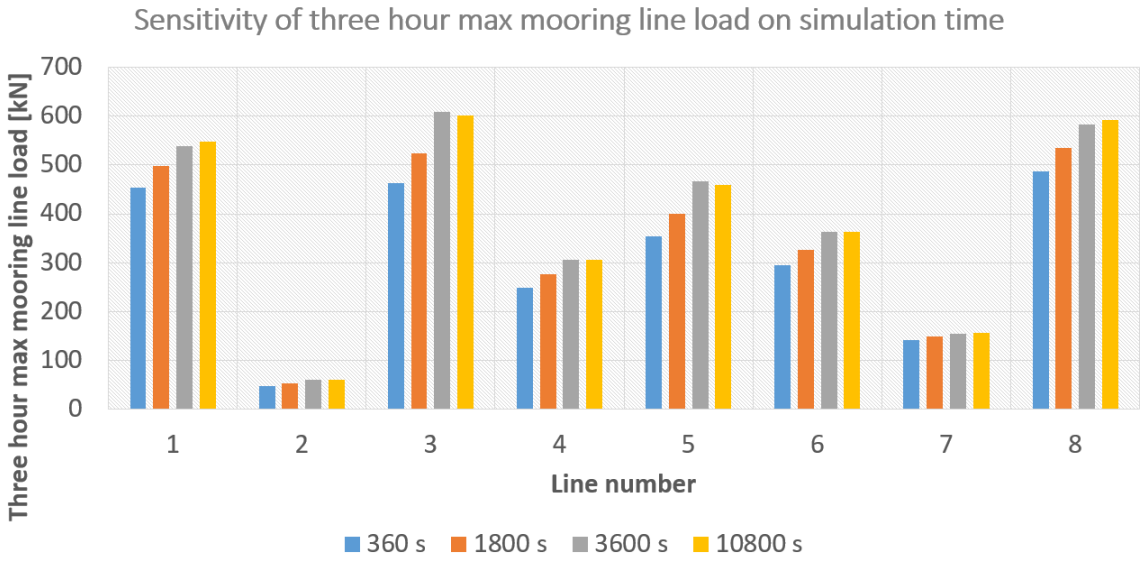

Figure 6.11: Three hours maximum mooring line force based on different real time simulation lengths.

From these results it can be seen that the three hours maximum mooring line force varies with real time simulation length. This is because of a certain simulation time is required to capture all the effects due to low frequency wave forces and non-linearity of the mooring system.
It can be seen that for 3600 seconds the result converges. Therefore, a real time simulation length of 3600 seconds will be applied in all cases throughout this research to compute the three hours maxima of the various mooring systems. For this real time simulation length also the three hours maxima data is converged for the motions.

Concluding. The maximum relative vessel motions can be assumed to be Rayleigh distributed.
Analysing the maximum mooring line force for different wave seeds with equal statistical properties shows that an inaccuracy of maximum 18 % is incorporated. This inaccuracy could be reduced by running each simulation with multiple wave seeds and pick the most conservative value. However, this is time consuming. Therefore, in this research each mooring system will be checked when using a wave train with the same seed, working with this 18 % inaccuracy and corresponding inaccuracy for workability in the order of 5 %.
The mooring system concepts will be compared based on a one hour real time simulation length.

6.5.4 Time step convergence

In the time domain model, the EoM is solved for each time step. The time step is by default set to 0.1 m. There is an optimum step size for computation time and accuracy.
How the time step affects the results is analysed by performing sensitivity analysis. Figure E.7 in Appendix E includes respectively the time series of the relative sway motion and the heaviest loaded line.

When finding the limiting sea state to determine the workability, the three hours maximum motion and forces are extracted. Table 6.4 includes the three hours maximum relative sway position and three hours maximum mooring load in the heaviest loaded mooring line and the corresponding CPU time required to run the model. It can be seen that the time step applied in this research, the base case, for both the relative motions and three hours maximum forces are converged for this time step. Therefore, the default time step of $\delta t = 0.1s$ is applied in this research.

Table 6.4: Sensitivity analysis of time step on relative sway motion and line load.

Time step, dt [s]				
0.005	0.01	0.05	0.1	1.0
Three hours max line force [kN]				
457.6	457.6	457.6	457.6	429.6
Three hours max relative sway position [m]				
62.88	62.88	62.88	62.88	62.84
Simulation CPU time [s]				
158580	69600	4140	975	541

6.5.5 Hydrodynamic effects

Orcaflex provides the option to include many different (non-) linear effects, these effects are shown in Figure 6.12. The contribution of these hydrodynamic effects to the vessel motions and mooring loads should be well understood in order to determine which effects have to be taken into account in the mooring analysis. A description of these hydrodynamic effects is represented in table 6.5 further down this chapter.

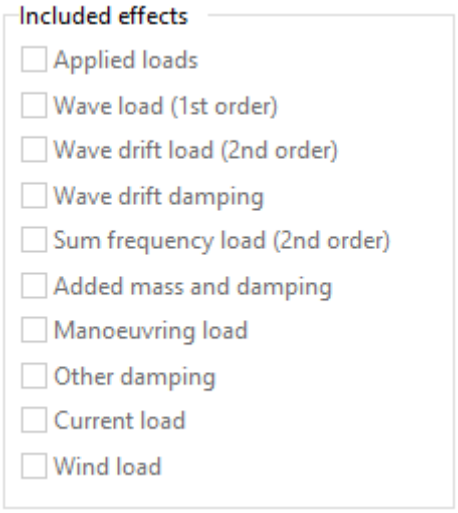

Figure 6.12: List of hydrodynamic effects that can be included in Orcaflex

To understand the influence of each effect, they are added one by one which means that the last sensitivity case includes all effects from Figure 6.12 that are relevant for this thesis.
This sensitivity analysis is performed for sea state, Tp = 8s and Hs = 2.5m sea state.
For this sensitivity analysis, the base case mooring arrangement, as shown in Figure E.6, is used.
Results will be given for 6 different sensitivity cases, named A to F, the meaning of these cases is elaborated in Table 6.5

Table 6.5: Sensitivity cases in analyzing the hydrodynamic effects

Case	Effect	Explanation
A	First order wave load	Loads as included in the load RAOs (Froude krilov forces + diffraction forces)
	Added mass and damping	Added mass and damping matrices (Radiation forces included)
B	Wave drift loads	Lower triangle of the QTF matrix. Includes mean and difference frequencies.
C	Wave drift damping	Encountering effect of the wave. Low frequency motion of the vessel relative to the current.
D	Sum frequency load	Upper triangle of the QTF matrix. Only sum frequencies included
E	Loads due to current	Relative fluid velocity around the structure causing force in surge and sway and a moment in yaw direction.
F	Loads due to wind	Relative velocity of air around the structure causing forces in surge and sway direction only. No yaw moment is taken into account.

The approach for analyzing the sensitivity of the hydrodynamic effects on the three hours maximum mooring line load can be seen in Figure 6.13. For each case additional effects are added.

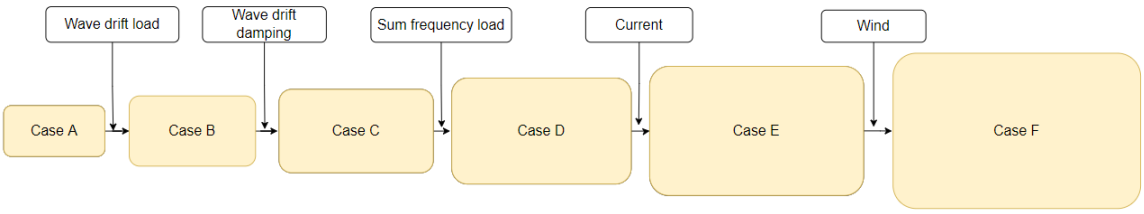

Figure 6.13: Overview of the different sensitivity cases and the hydrodynamic effects that are added.

Figure 6.14 shows the contribution of the hydrodynamic effects on the relative sway motion and the mooring line tension in a time series. Only Case A to D because wind and current loads result in offset and a static load only.

More details on these hydrodynamic loads and where they come from are explained in the literature report [2] and the Orcaflex manual, [35].

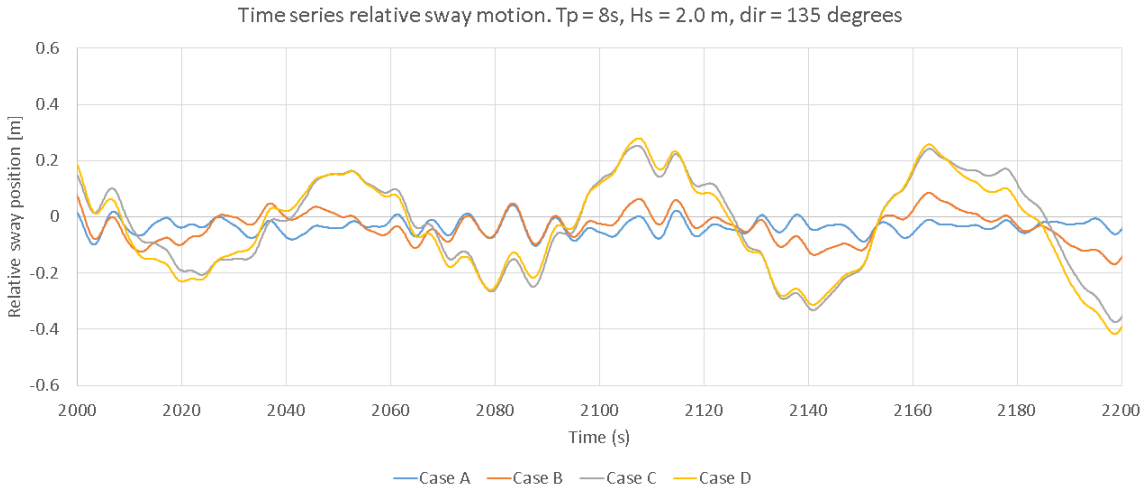

(a) Effect of hydrodynamic effects on relative sway motion

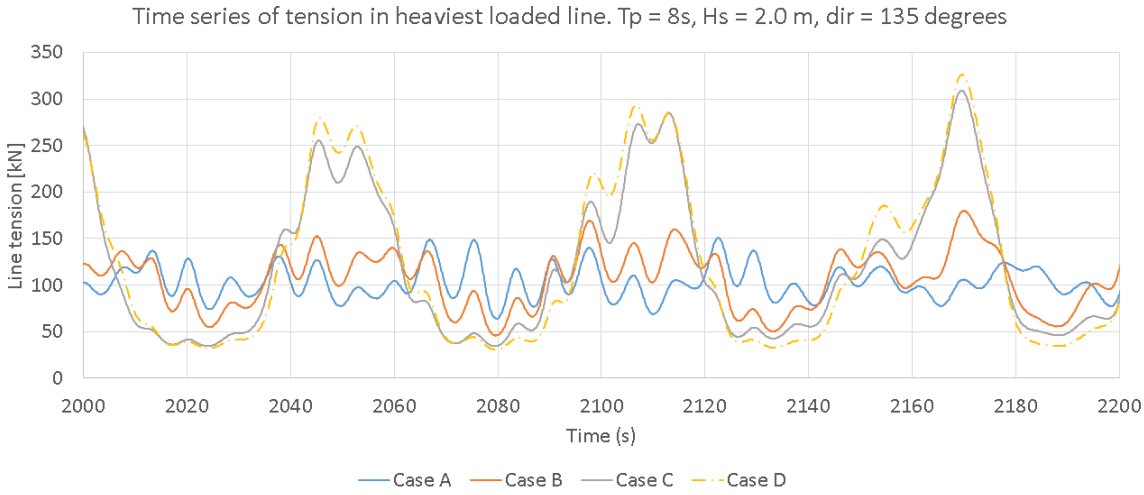

(b) Effect of hydrodynamic effects on mooring line tension.

Figure 6.14: Time series showing the effect of hydrodynamic effects on the relative sway motion and mooring line tension. For t = [2000 2200]s.

Figure 6.15 represents the results from this sensitivity analysis in the form of the maximum force occurring in a three hour sea state when analyzing the heaviest loaded mooring line.

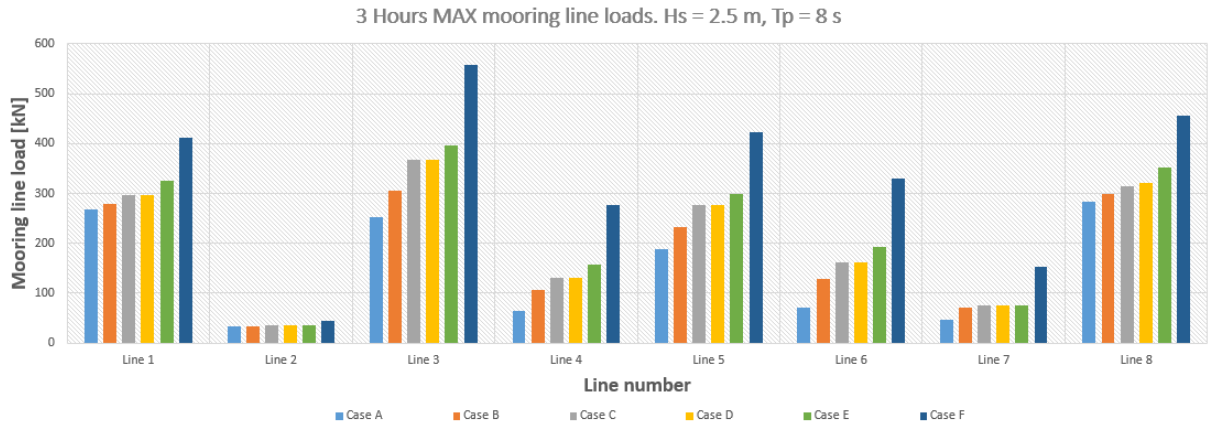

Figure 6.15: Results from sensitivity analysis, varying the hydrodynamic effects that are applied as explained in Table 6.5. 3 Hours max mooring line loads for Hs = 2.5 m and Tp = 8 s.

It can be learned that case A and B have a relatively small contribution to the vessel motions and mooring loads. Case C, the wave drift damping, has a large contribution. While Case D again only has a minor contribution to the vessel motions and mooring loads.
The contribution of the wave drift damping term requires more in depth research as it seems counter intuitive that increasing the vessel damping and including the effect of current on waves that are aligned. A. Ghadirian *et al.* confirm in their research on wave-current interaction that following currents causes reduction of the wave loads, [36].
When 0.0 m/s instead of 0.9 m/s current is incorporated, the wave drift damping reduces the mooring line load.
Regarding the sum-frequency loads, these have a negligible contribution to the mooring line load, since this is a mooring system with rather low stiffness. Therefore these will be left out of this research, because including the sum-frequency load heavily increases the computation time because the entire QTF needs to be considered instead of only the mean and lower diagonal.

It would be interesting to perform the same sensitivity analysis for different sea states because these hydrodynamic effects are frequency dependent, this is considered as subject to further research.

6.6 Time domain model outcome

From the time domain model results, the maximum force in the mooring system that occurs in a three hour sea state can be extracted. This force should be within 5 % of the SWL of the mooring system. If not, the sea state should be adjusted until the limiting sea state is found. For this sea state, the workability of the mooring system can be computed. This corresponds with step 13, in the thesis approach, section 3.1.

The maximum force in the mooring lines can be split up in the static and dynamic load.

$$F_{max} = F_{static} + F_{max,dyn} \tag{6.4}$$

The static part includes pre-tension in the mooring lines and the constant loads that are applied, e.g. mean wave drift forces and constant wind and current loads.
The dynamic or transient part includes the time varying part of the load. In order to determine the max load of the dynamic part, the 3 hour max dynamic amplitude is determined from applying the following relations to the time history data.

6.6.1 Static solution

The static solution only includes the mean loads exerted on the structure. Main contributions are pre-tension, wind and current loads and the mean second order wave drift force.

6.6.2 Dynamic solution

For the dynamic solution, the equations of motion is solved for each time step. In case the vessel motion is pre-defined, as will be the case for *Pioneering Spirit*, the vessel motions at each time step will be determined by the displacement RAOs that are imported from the diffraction analysis.
Solving the problem with use of the hydrodynamic matrices, requires added mass and damping matrices with a sufficient frequency range. The added mass and damping matrices do not depend on incoming wave direction.
For frequencies outside the range of the input data, a comparable interpolation and extrapolation method as for the motion RAOs, as explained in section 6.3.1.2, is used for the added mass and damping terms.

From the added mass and damping values at the highest frequency imported, together with the impulse response function, as shown in equation 6.5, enables to calculate the added mass at infinite frequency with use of equation 6.6, known as the high frequency limit. With Tc the cutoff time in seconds, f the frequency in Hz, A and B respectively added mass and damping.

$$\mathrm{IRF}(\tau) = c(\tau) \int_{f=0}^{\infty} 4\boldsymbol{B}(f) \cos(2\pi f t) \mathrm{d}f \tag{6.5}$$

$$\boldsymbol{A}_i(\infty) = \boldsymbol{A}\left(f_i\right) + \frac{1}{2\pi f_i} \int_{s=0}^{T_c} \mathrm{IRF}(s) \sin\left(2\pi f_i s\right) \mathrm{d}s \tag{6.6}$$

By default Orcaflex uses a cutoff tolerance of 2.0 % as a percentage error relative to the largest damping term given, corresponding with $Tc = 3073$s. From this input, Orcaflex calculates the cutoff time that gives this level of approximation of the damping term. The approximation error on the added mass will be similar. In this research this default setting is applied as well as a very low, 0.1 %, cutoff tolerance which had no significant affect on the results.

OrcaFlex will then automatically calculate the cutoff time that gives this level of approximation of the damping levels; the approximation error on the added mass will be similar.

6.6.2.1 Integration scheme

For the time domain solution, Orcaflex can apply two different integration schemes, explicit or implicit. For the explicit scheme Orcaflex uses a semi-implicit Euler with a constant time step. Since the modelled mooring lines are rather stiff, the numerical model gets easily unstable and therefore a small time step is required to have a sufficient small error.
For the implicit integration scheme, the solution at time t+1 depends on both the solution t and t+1. As a consequence, a number of iterations are required to solve for the next time step.
In general the implicit method provides better stability and larger time steps could be used, leading to an total shorter computation time. The time step can either be set constant or variable. In case of variable time step, the step size depends on the number of iterations taken for previous time steps. Unfortunately, a variable time step cannot be applied when having frequency dependent added mass and damping matrices as is the case in this research. Furthermore, a variable time step can introduce high frequency noise into the system, [37].
By default the time step is set to be constant and equal to 0.1 seconds, as discussed in section 6.5.4.
For this research, default settings are used for the solving method, implicit integration with constant time step of 0.1 seconds.
When starting the dynamic simulation, all initial positions and orientations are known from the static solution. All forces and moments are computed for that specific time step. Substituting these forces in the equations of motion gives the new positions and orientations. This is repeated for every time step.

6.6.2.2 Numerical stability

In order for the dynamic solution to converge, numerical stability is required. Numerical damping is added to the dynamic solution in the Orcaflex model to remove the artificial, non-physical high frequency responses that are associated with discretisation (e.g. in the lines). This damping leads to more stable convergence and hence allows for longer time steps and shorter simulation time. When using implicit integration, Orcaflex uses a built-in value of 0.4 [24]. This means that at each time step 40 % of the energy in these non-physical high frequency modes is dissipated, [38].

6.7 Time domain conclusion and reflection

The time domain model started with importing results from the diffraction analysis. After the design wind, current and waves are defined, it is explained how the model is build in the dynamic software, Orcaflex. To confirm the reader of the quality of the time domain model and the conclusions that will be drawn, a detailed model validation and verification is performed with satisfactory results and quantifying the limitations.
The main disadvantage of the time domain model is the calculation effort and the rather cumbersome to post-process the data.
The next step in the report is describing concepts on how the mooring system can be improved to ultimately increase the workability of the mooring system. Including how these systems are modelled in the time domain.

7 New mooring system design

As a result of the previous chapters, a validated an verified time domain is available to evaluating new mooring system concepts.
Four different concepts will be presented in this chapter varying from minor adjustments to the base case system to implementing current state-of-the-art mooring systems.
A fifth concept is done research to but not incorporated in the time domain model due to limited information available in literature, this 'ShoreTension' system is described in Appendix, H section H.3.
Each concept description is build out of the following components: general description, explaining the advantage and purpose with respect to the base case, how the system can be modelled in the time domain and a reference to the broader scope and practicality of the concept.

These concepts originate from the literature research, discussions with Allseas' personnel on board and in the office, discussions with external companies e.g. Cavotec MoorMaster and from experience and sensitivity analyses with the quasi-static model as described in Appendix C. Besides, practice and building of mooring system concepts in the time domain model provided understanding in what would work and what not, these 'practice concepts' are not relevant for the report and therefore not described.
Results of the concepts that are described in this chapter, together with the base case, will be represented in the subsequent chapter.
This chapter explains step 11 and 12 of the thesis approach, as described in chapter 3.1.

7.1 Challenging barge position

In chapters 2 and 4 it is stated that extending the barge from *Pioneering Spirit* is required to be able to fully unload the barge. Therefore, the barge is less shielded from *Pioneering Spirit* when considering 45, 90 and 135 ° waves. This section points out what the effect of barge extension is on the environmental loads acting on the barge, by means of a sensitivity analysis. Two cases are analysed, the base case where the barge is extending 40m from *Pioneering Spirit*, represented in Figure 2.5b, and the case where the barge stern is aligned with the stern of *Pioneering Spirit*.
Figure 7.1 represents the first order relative surge, sway and yaw motion for the two cases.

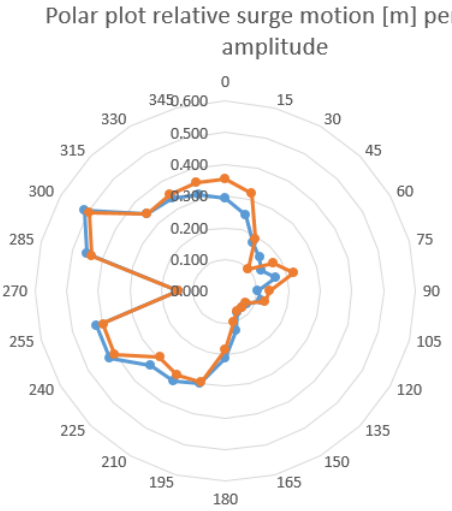

(a) Polar plot relative surge motion

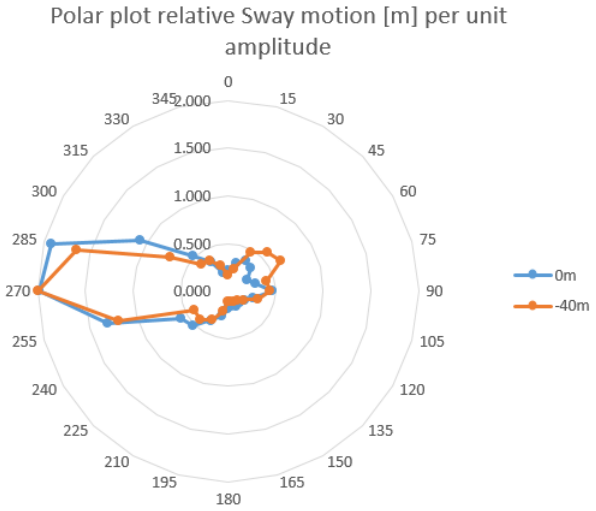

(b) Polar plot relative sway motion

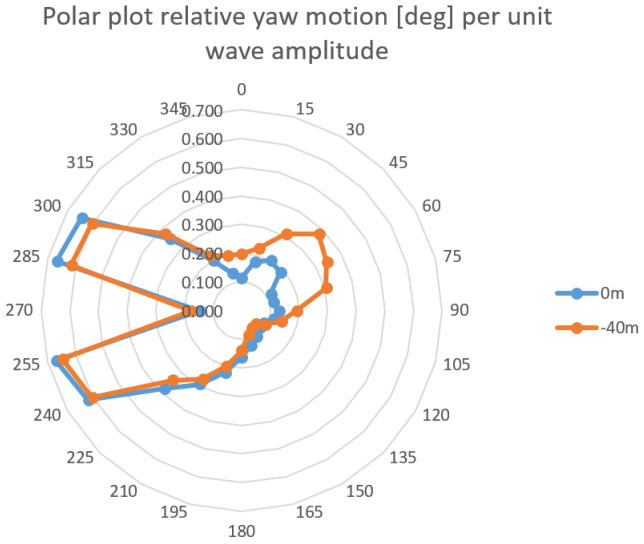

(c) Polar plot relative yaw motion.

Figure 7.1: First order relative surge, sway and yaw motions for two vessel orientations. '-40m' refers to the 40m barge extension in this research, '0m' means the barge and *Pioneering Spirit* stern are aligned. The location for the relative motion is point 'A' in Figure 2.5b. Hs = 2.5m and Tp = 8s.

The difference in relative motions between the two cases in Figure 7.1 represents the effect of shielding on the barge motion. It can be learned that for 135 ° incoming wave direction there is only a minor difference in relative first order motions. This corresponds with what we see in Figure 5.16, the wave amplitude is evenly reduced for both barge locations.
Also for 90 ° waves, relative motions for both '-40m' and '0m' are comparable, probably due to the excessive roll motion of *Pioneering Spirit* resulting in radiating waves causing relative motions of the barge.
For 45 ° waves however, there is a large difference in relative first order motions for the two cases in Figures 7.1. This is due to the fact that for '-40m', the waves are enclosed in the corner between *Pioneering Spirit* stern and the barge, as can be seen in Figure D.4, resulting in high relative motions.

Besides understanding the relation between barge extension and relative first order motions, it is in-

teresting to check how barge extension affects the wave forces acting on the barge and the resulting mooring loads.
To analyse these loads in the time domain model, the 'ship extender' mooring system, as described in section 7.5, is used because this system allows to have the exact same mooring arrangement for both 0 and -40 m barge extension by shifting the mooring line connection points 40m in positive x-direction. This assures a valid mooring load comparison because the heaviest loaded line has the exact same orientation.

Analysing the first order wave forces and the mooring loads show similar sensitivity on barge extension as the relative first order motions.
Figure 7.2 shows time series of the first order wave loads and the heaviest loaded mooring line for 135 ° waves. It can be seen that both wave and mooring loads are comparable for both barge extensions.
Considering 90 ° waves also shows that first order wave loads and mooring loads are comparable for both barge extensions.

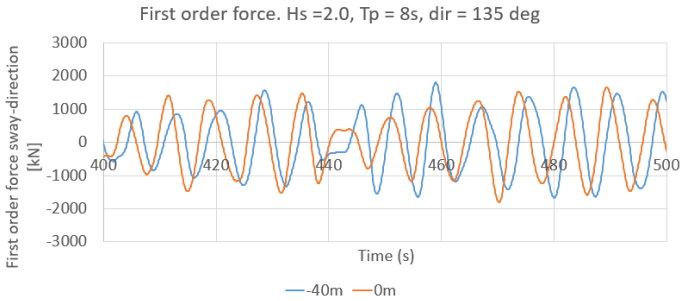

(a) First order wave forces acting on the barge. With three hours maxima for [-40m,0m] respectively [2727,2510] kN.

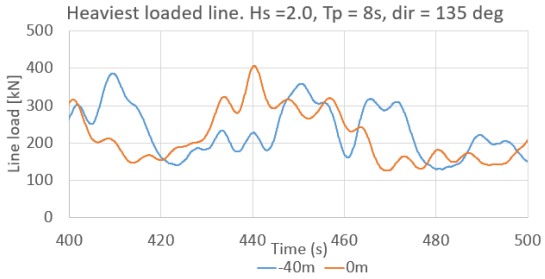

(b) Heaviest loaded mooring line load. With three hours maxima for [-40m,0m] respectively [415,432] kN.

Figure 7.2: Time series of the relative sway motion (left) and heaviest loaded line load (right) when for 135 ° waves. Hs = 2.0m, Tp = 8s, Wind and current are excluded. The exact same mooring configuration is used for both barge orientations.

For 135 and 90 ° incoming waves, the first order forces and mooring loads are comparable for both barge extensions. Therefore, it can be concluded that for these wave directions, not necessarily the wave loads acting on the barge are challenging for '-40m'. However, connecting a mooring system to the 40m extended barge is a challenge because no lines oriented in perfect sway direction and negative surge direction can be added to the barge stern, as can be seen in Figure 2.5b.

For 45 ° however, the first order wave and mooring forces are much larger for '-40m' than for the '0m' case. As can be seen in Figure 7.3. Similar ratio between the two barge extensions is found for the second order wave drift force, these results are not included in the report.
This difference in forces is related to the amount of shielding. Furthermore, Figure 7.3b shows that this sea state is not realistic for 45° because the line load exceeds the SWL and lines become slack because of the excessive relative vessel motions.

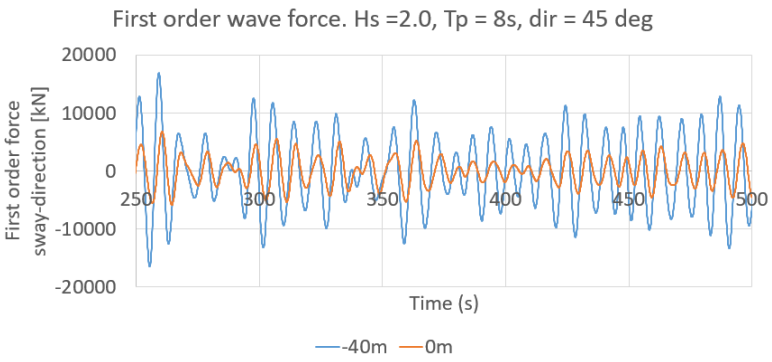

(a) First order wave forces acting on the barge. With three hours maxima for [-40m,0m] respectively [1.92E4,7.54E3] kN.

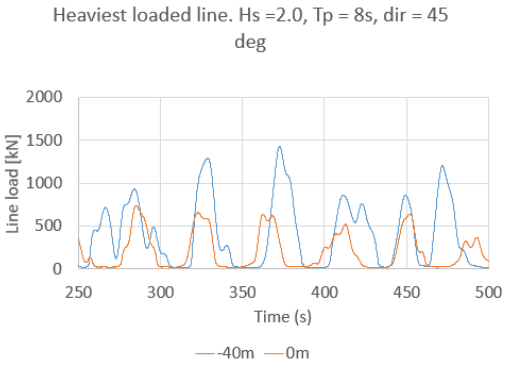

(b) Heaviest loaded mooring line load. With three hours maxima for [-40m,0m] respectively [1373,920] kN.

Figure 7.3: Time series of the relative sway motion (left) and heaviest loaded line load (right) when for 45 ° waves. Hs = 2.0m, Tp = 8s, Wind and current excluded. The exact same mooring configuration is used for both barge orientations.

7.2 Philosophy of improvement

For Allseas' offshore wind turbine installation concept, the barge has to be secured alongside *Pioneering Spirit* for multiple days and the workability is expected to be limited by the mooring system, emphasizing the urge for high workability of this mooring system. Looking ahead in the results, as will be represented in chapter 8, the annual workability for the base case mooring system is 67 and 16 % for the reference locations where respectively wind and swell seas dominate. This emphasizes the need for improvement.
The workability depends on two main criteria: the SWL should not be exceeded and relative motions should be within the pre-defined limitations. These criteria are strongly related via the mooring system properties. Therefore, the first philosophy of improvement is on optimizing the system properties, stiffness, damping and capacity.
For example, reducing the system stiffness increases the amplitude of the low frequency relative motions while it reduces the mooring load amplitude, explained in the subsequent paragraph. The system stiffness is defined as stiffness of all mooring system components combined.
In reality, the damping properties of a conventional mooring system, including mooring lines and fenders, cannot be easily adjusted and therefore the main focus in this section is on stiffness.
To allow for a higher sea state without exceeding the SWL, the capacity of the mooring system can be increased, for example by increasing the number of mooring lines to share loads or implementing higher capacity mooring lines. However, the mooring system should be practical, a large number of mooring lines is difficult to handle, increases risk of clashes and requires many connection points. Furthermore, the highest loaded line determines the workability, most often with many mooring lines the line orientations are less optimal.
Increasing the SWL of a single mooring line is disregarded as it is limited to the local structural capacity. The circular dependence of system properties and system response (motions and loads) denotes the complexity of increasing the workability by improving the mooring system.

To understand the sensitivity of relative motions on the mooring system properties, more specifically on stiffness, Figure 7.4 compares three time series of the relative sway motion when the base case mooring system is implemented with three different stiffnesses. Comparing the case where no stretcher line is involved but only steel wire with a high constant axial stiffness, with the case adding a 20m stretcher line to the steel wire in each mooring line. Because of that, the total system stiffness changes. Figure 7.4a shows its effect on the first order motions and Figure 7.4b its effect on low frequency motions.

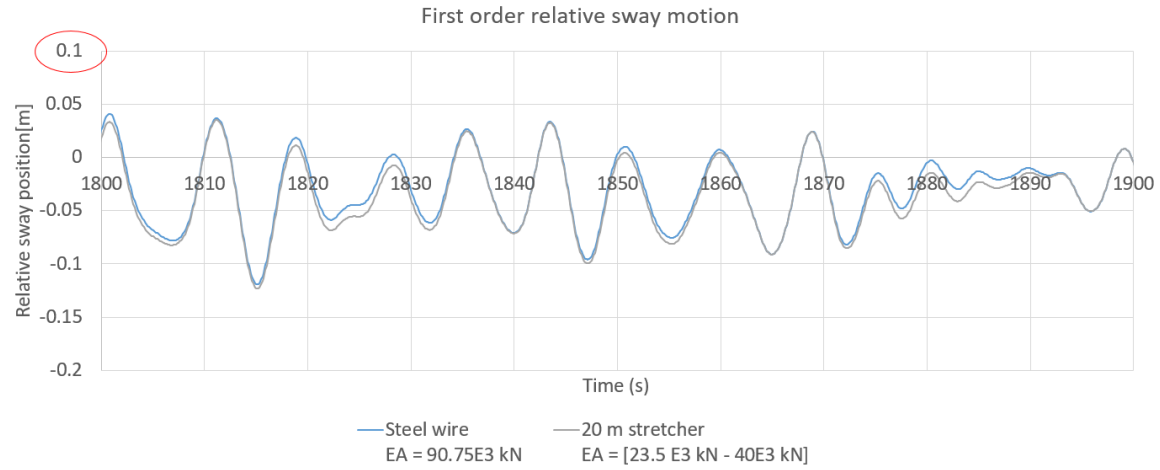

(a) Including first order load effects. For t = [1800,1900]s. Three hours maximum values for [Steel wire, 20m stretcher] = [0.07,0.07]m

(b) Including second order load effects. For t = [1500,2500]s. Three hours maximum values for [Steel wire, 20m stretcher] = [0.43,0.55]m

Figure 7.4: Sensitivity of system properties (line stiffness) on first order (upper) and low frequency (lower) relative sway position. For the base case mooring system. Hs = 2.0 m, Tp = 8s for 135 ° waves.

No static loads (wind and current) are included in the above results, otherwise a clear difference in offset would be visible for both system stiffnesses.
From Figure 7.4 it can be learned that the first order motions are not necessarily affected by the mooring system stiffness, while the low frequency motions are.
In general, first order motions have zero mean because of linearity. The first order motions in Figure 7.4a present non-zero mean because only a limited time range is shown.
Low frequency motions will include a small offset due to the mean second order wave drift force. However, this offset cannot be recognized in Figure 7.4b.

First order motions depend on the hydrodynamic system matrices. Since this research includes vessels with large mass and inertia and therefore the natural period of the floating body including mooring system is large compared to the wave period.
On the contrary, the low frequency motions originate from the slow varying second order wave drift

force and the interaction between different mooring system components. Because the natural period is in the same range, these motions are affected by the mooring system properties. Figure 7.4b shows the effect of mooring system stiffness on the low frequency relative sway motions.

Figure 7.5 represents the effect of mooring system stiffness on both the relative sway motions and the mooring line load of the heaviest loaded line, with wind and current applied co-linear with the waves. Three curves are included, two curves with constant axial stiffness of 75 E3 kN and 37.3 E3 kN, the third curve with a constant stretcher length of 20m.

Increasing the axial stiffness means larger system stiffness since the line length is constant for both cases. For the third curve, each mooring line has a constant stretcher length of 20m. Therefore the axial stiffness differs depending on the total mooring line length in the range of 23.5 E3 to 40E3 kN. Why especially these three stiffnesses are shown will be thoroughly explained in the discussion, section 9.3.4.

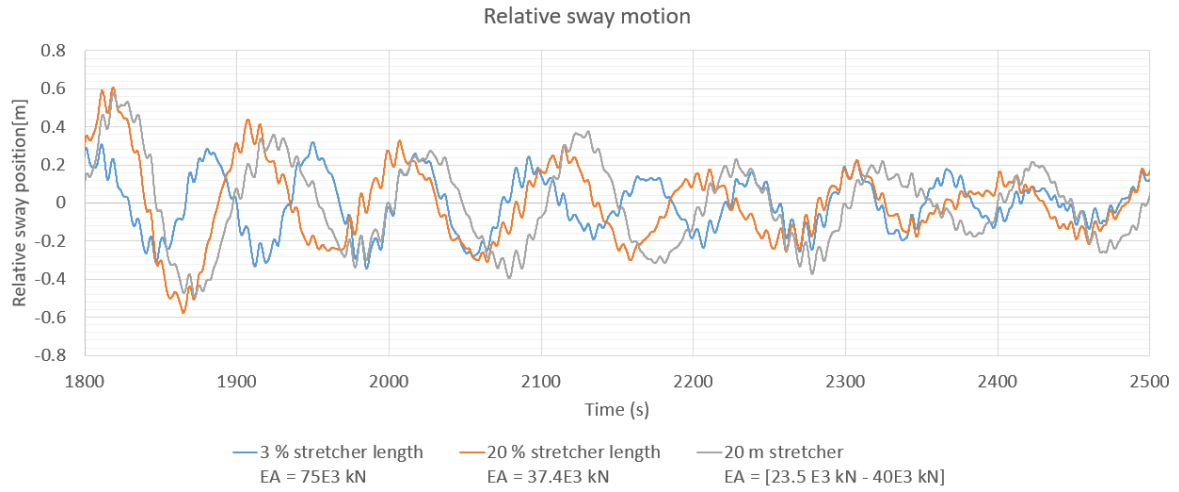

(a) Relative sway motion. Excluding the offset, as given in Table 9.1. For 20m stretcher line, the axial stiffness differs per mooring line in the allocated range.

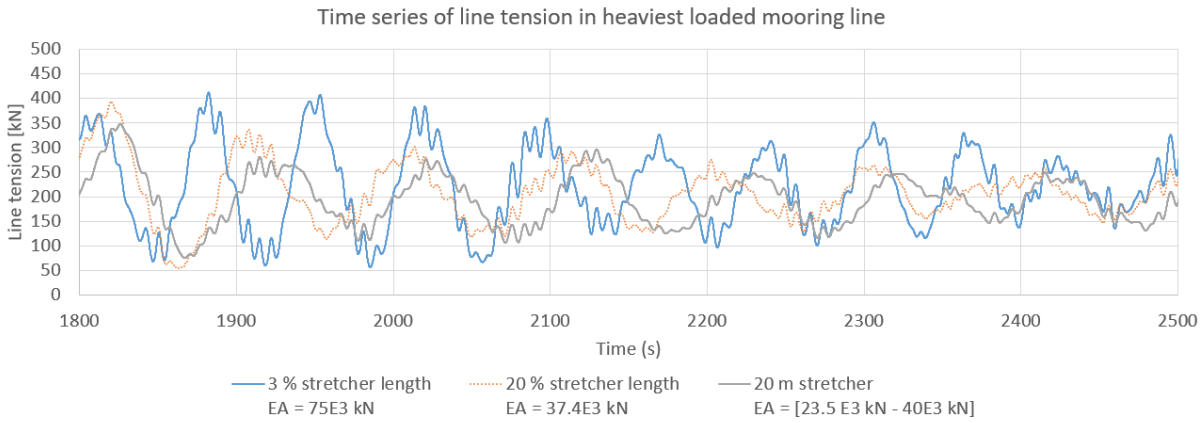

(b) Line load of heaviest loaded line in this mooring arrangement. This line is oriented in surge direction. Initial line length of 75m. For 20m stretcher line, the axial stiffness differs per mooring line in the allocated range.

Figure 7.5: Time series showing the effect of the stretcher length on the relative sway motion (upper) and load in the heaviest loaded line (lower). For the base case mooring system subjected to Hs = 2.0m and Tp = 8s for 135 ° waves with wind and current aligned.

Table 7.1: Statistical data corresponding with above Figures 7.5a and 7.5b.

		Heaviest loaded mooring line force [kN]	Relative sway position [m]
Three hours max	3 % stretcher length EA = 75E3 kN	457.60	0.88
	20 m stretcher EA = [23.5 E3 kN - 40E3 kN]	334.16	1.46
	20 % stretcher length EA = 37.4E3 kN	363.67	1.31
Mean	3 % stretcher length EA = 75E3 kN	221.82	0.47
	20 m stretcher EA = [23.5 E3 kN - 40E3 kN]	196.19	0.90
	20 % stretcher length EA = 37.4E3 kN	207.63	0.79

From Figure 7.5a it can be seen that the high stiffness mooring system results lower amplitude for the low frequency relative sway motions. Because the load increases more rapidly due to line elongation caused by relative motions. These loads in the mooring system can be seen in Figure 7.5b where the stiff mooring system shows larger amplitude of the dynamic loads in the mooring system. The mean load in the mooring system is equal for all cases. Because the mean load should equal the mean environmental forces that are applied, which are independent of the mooring system properties.
Overall, from Figure 7.5 it can be learned that the low frequency relative vessel motions can be controlled by the mooring system stiffness. Increasing stiffness leads to higher dynamic loads in the mooring system.

Besides optimizing the system properties itself, another philosophy of improvement is to improve the efficiency of the the mooring system properties. Where efficiency is defined as most optimal usage.
In that perspective, in the first concept 'new line orientation' the lowest loaded mooring line in the base case mooring system is reoriented in order to make sure the load is more evenly spread over the mooring lines.
For the second concept 'Fairleads at hull side', the mooring line connection points are relocated to reduce the vertical force component in the mooring line to increase the capacity to take loads in horizontal direction.
In general, a mooring system is preferred to be symmetric in the horizontal plane as this enables to correct for dynamic loads in the various mooring system components (lines). However, realising a symmetric mooring system is challenging for the vessel orientation in this research. The third concept 'Ship extender' describes how a more symmetric mooring system can be realised.
Due to the mooring line orientation, they often consist of a x, y and z force component. Because of that, motion in surge direction also leads to a force component in sway direction resulting in unwanted motions. The 'MoorMaster' concept implements a state of the art mooring system providing forces in perfect x and perfect y direction independently, besides it has the ability to freely follow motions in z-direction. With that, using the available force capacity more efficient and reducing low frequency relative vessel motions.

7.3 New line arrangement

The level of improvement that can be made with respect to the base case depends on how well the base case mooring system performs and whether results are acceptable. When analysing the base case, line 2 represented in Figure 4.8, did not take much load for 45,90 and 135° incoming direction. Therefore, the purpose of this line arrangement is to adjust the line arrangement such that all lines are evenly loaded,

optimized for 135°. In addition, the purpose of this line arrangement is to increase the capacity in sway direction.
Finally, this new line arrangement concept gives reference for the base case, what the quality of the base case is and whether results are reasonable. The line arrangement is represented in Figure 7.6.

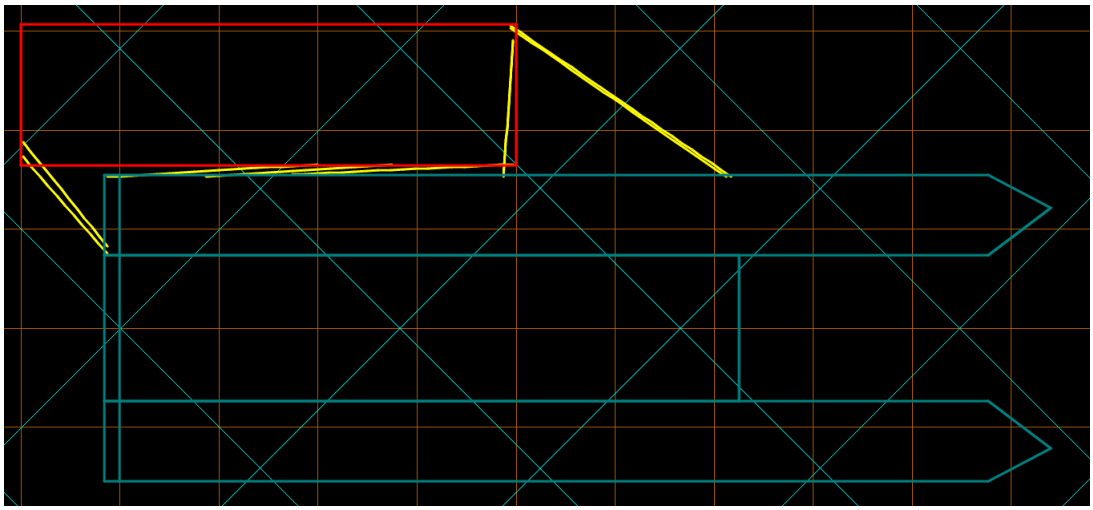

Figure 7.6: Top view of new line arrangement

Similar modelling approach is applied as for the base case, fenders are modelled as a link with spring and damper properties and mooring lines with constant axial stiffness. These Mooring operate at a SWL of 453 kN. Only the line arrangement differs. From Figure 7.6 it can be seen that the line at *Iron Lady* bow is relatively short and partly reaches over the deck. Short and thus relatively stiff lines can lead to excessive loads and a mooring line reaching over the deck affects the deck space available and reduces safety. The reason for still choosing the orientation of this line is the fixed location of the connection point at *Pioneering Spirit*.
The system properties of this concept will be comparable to the base case with a slight reduced stiffness in surge direction and increase in sway direction. Since this mooring system consist of eight lines, the total installed load capacity is eight times the SWL, approximately 3600 kN.
Whether the line orientation of this concept really is improved will be confirmed by the results and discussed in chapter 9.

7.4 Fairleads at hull side

A challenge expected in the base case mooring system is the steep mooring lines due to the large difference in freeboard between *Iron Lady* and *Pioneering Spirit*. These steep mooring lines limit the force that can be exerted on the barge in horizontal direction.
Placing the fairleads along the hull side enables a more horizontal mooring line arrangement. Which is expected to increase the workability. Two concepts will be presented, one inspired by an aircraft carried which will be explained in Appendix H. The second method includes welding fairleads along *Pioneering Spirit* hull, as represented in Figure7.7.

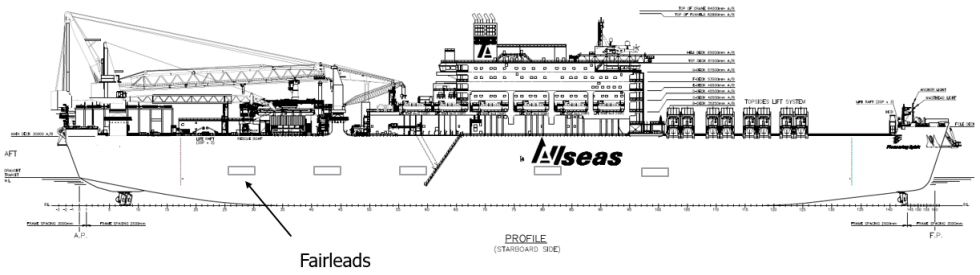

Figure 7.7: *Pioneering Spirit* side view, representing the location of fairleads (grey blocks) at the hull side.

The major challenge with these faileads at the hull side is the increased drag when these fairleads are submerged due to deep draft, however, sailing usually happens at a shallow draft. Additionally, these fairleads could limit the available space for fenders when mooring to a quay or mooring a barge alongside.
The system properties are comparable to the base case mooring system, except for a slightly increased stiffness and capacity in surge and sway direction because the vertical component is removed..
Regarding modelling this improved concept, mooring lines can simply be connected at a lower elevation at the hull.

7.5 Ship extender

Restricting the barge stern in sway and yaw direction is known to be challenging with the base case mooring system. This restriction however, is essential to restrict the barge yaw motion and sway motion especially for environmental loading direction of 90°.
To connect mooring lines at the barge stern in perfect sway direction, the easiest way would be to attach a mooring line to *Pioneering Spirit* starboard side. However, this would clash with the wind turbine foundation and JLS beam, for reference see Figure 2.2.
To solve this problem, mooring lines could be attached to a strong point extending from *Pioneering Spirit* port side stern referred to as 'ship extender'.

The purpose of a ship extender is to better be able to restrict sway and yaw motion for bow quartering and for beam loading. This way, the optimum heading is to have environmental loads from 135 ° but if heading control cannot be assured at all times, sufficient capacity to restrict beam waves is preferable. Either to have a non-zero workability and to reduce the risk when environmental loads come from 90°. The length of the ship extender that is implemented in this thesis has a length of 50 m and is intended to be attached to the hull by means of a hinge type of connection. Three fairleads will be located at the tip of the ship extender. Mooring lines will reach from winches at *Pioneering Spirit* stern through the fairleads at the ship extender towards the bollards on the barge. Further conceptual design of this ship extender will not be considered. Figure 7.9 represents the in place and an example of not in place orientation of the ship extender. The ship extender can either rotate in the horizontal plane or in the vertical plane.

The same type and number of mooring lines as for the base case will be used. Which means a SWL of 453 kN and a total capcity of 3600 kN. With respect to the base case, the ship extender increases the mooring system stiffness mainly in sway direction and reducing in surge direction.

In terms of modelling, the mooring lines are attached to *Pioneering Spirit* 50 m extended from the stern, as can be seen in Figure 7.8. As a consequence of connecting mooring lines to the ship extender, the mooring arrangement slightly changes.

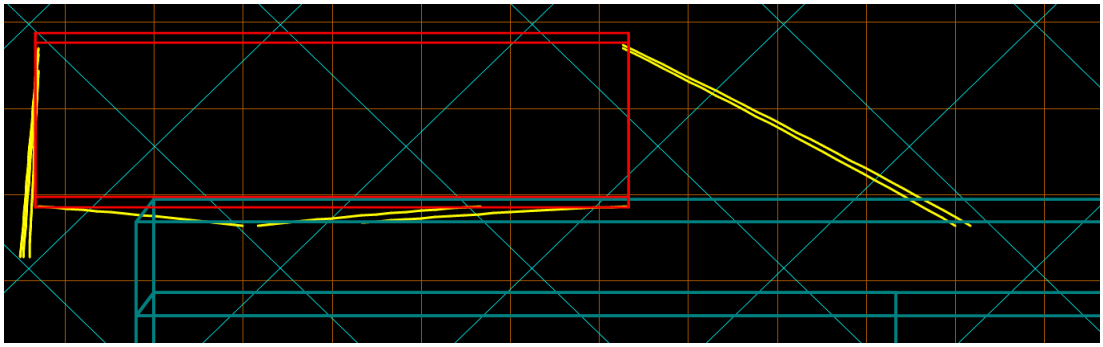

Figure 7.8: Top view of the ship extender. With mooring lines drawn in yellow. The barge in red and *Pioneering Spirit* in grey.

Challenges that come with the ship extender concept are mainly on the practical side. Starting with installing the ship extender and operating with a steel construction extended from *Pioneering Spirit* adds on risks. Furthermore, the large bending moment of the ship extender around point 'A', in Figure 7.9. Additionally, depending on the winch location on *Pioneering Spirit* stern, the mooring line will go with a small radius curvature through the fairlead at the ship extender which might lead to wear.

(a) Ship extender operational.

(b) Ship extender in storage conditions, example orientation.

Figure 7.9: Ship extender represented in red. In place (left), not in place (right). The dashed line a mooring line, the grey blocks the JLS beams and point A the hinge connection.

7.6 Cavotec MoorMaster ® system

Similar to all mooring systems, the purpose of the Cavotec MoorMaster ® system is to restrict vessel motions. The Cavotec MoorMaster system is later referred to as 'MoorMaster system'.
The challenge in the conventional mooring system is when mooring lines are elongated, they exert a force in both surge and sway direction. Additionally, lines can only apply tension while the fenders only provide a force upon compression. Both reasons leading to dynamic motions of the barge. The advantage of the MoorMaster system is that it can exert forces in perfect surge and perfect sway direction and both tension and compression at the same location at the barge.
The MoorMaster system consists of a rigid part, that is usually connected to a quayside, and hydraulic cylinders operating a vacuum pad. These hydraulic cylinder haves stiffness and damping properties and can be extended with a certain stroke. This rigid part, hydraulic cylinder and vacuum pad is defined as a single MoorMaster device. Multiple MoorMaster devices can be installed on a quayside or a vessel. Figure 7.10 represents a single MoorMaster device.
The MoorMaster system is able to follow vessel motions in all 6 DoF while restricting only surge and sway motions. In case multiple MoorMaster devices are installed, the vessel yaw motion can be restricted as well because.

If number of MoorMaster devices are installed, the vessel can move/translate against the quayside by disconnecting the vacuum pads one by one and reconnecting at another location alongside the hull. This operation is referred to as 'stepping'.
The MoorMaster system is usually applied for mooring to a quayside, for example in a container terminal. However, I see potential in implementing the MoorMaster system in a side-to-side mooring operation because of the advantages mentioned above. This lead to implementing the MoorMaster system in the side-to-side mooring operation is one of the concepts for improving the mooring system.

Figure 7.10: Cavotec MoorMaster system Close up. *source: Brochure MoorMaster* [8]

The advantages of the MoorMaster system are listed:

- The system properties are software based. Which results that the system properties can fine-tuned for each operation. For example if environmental loads from 90 ° are expected, the number of MoorMaster devices restricted sway motions can be increased.
- The MoorMaster can take both compressive and tensile forces. This enables to follow and control vessel motions in both directions.
- The MoorMaster system can apply both compressive and tensile forces in perfect surge and sway direction at the same location. Where for conventional mooring systems the mooring lines are oriented in both surge and sway direction and tensile and compressive forces are applied at different locations on the vessel leading to more dynamic loads.
- Forces in the MoorMaster system are constantly measured. Giving insight in the loading capacity.
- The MoorMaster systems can connect within 30 seconds. This can reduce the lead time when installing the mooring system[8].
- The MoorMaster system reduces human interface which increases safety but also make sure the mooring system is installed properly. As on board vessel knowledge and time is most often limited.
- Due to the 'stepping' function, the barge can easily be translated along the barge hull.
- The installed capacity can 'simply' be increased by increasing the number of devices because loads are relatively well divided.

In terms of maintenance on the MoorMaster system, some regular maintenance has to be executed. This can be done with crew from the company that uses the MoorMaster system.
After some years a minor overhaul is required. This will be done at location where the MoorMaster system is installed, this operation needs to be executed by Cavotec personnel.
Eventually a major overhaul needs to take place, for this operation the MoorMaster system has to be disassembled and brought back to the fabrication hall for refurbishment, [39].

The MoorMaster system is proven technology as it is implemented at multiple quaysides around the globe. Therefore, it is assumed that the MoorMaster system suffices the class requirements as defined by classification companies, e.g. DNV.

Next to the MoorMaster system, another state-of-the art mooring system, the 'DockLock' system, which has a comparable working mechanism. The difference with the MoorMaster system is in the connection method. DockLock uses electromagnetic pads where the MoorMaster system uses vacuum pads. Currently the MoorMaster system is further developed than the DockLock system. As the method how to model these system will be similar, only the MoorMaster system will be considered in this thesis.

7.6.1 System properties

The stroke of the MoorMaster system is defined as the region between minimum and maximum position that can be reached by the vacuum pad. For example, the stroke in sway direction is 1.6 m. Which means that the vacuum pad can reach from -0.8 m till 0.8 m, in sway direction. With 0.0 m being the equilibrium position.
In reality, no reaction force can be applied when the stroke is exceeded. Because no contact is possible upon exceeding the stroke.

Table 7.2: MoorMaster system properties. *These values correspond with a MoorMaster system consisting of two vacuum pads. *Source: MoorMaster Brochure [8]*

Variable	Symbol & unit	Value
Stroke, surge	S_x [m]	[-0.2,0.2]
Stroke, sway	S_y [m]	[-0.8,0.8]
Max reaction force surge*	$F_{max,x}$[kN]	200
Max reaction force sway*	$F_{max,y}$ [kN]	400

The reaction forces given in Table 7.2 can be guaranteed whenever the vacuum pad is within the stroke limits.
The maximum reaction force corresponds with the SWL of the MoorMaster system. If the SWL is exceeded, the system will resist vessel motion with the maximum reaction force until the end of its range of motion when it will safely disconnect.
The reaction force in surge direction comes from the friction force between the hull and the vacuum pad. The friction coefficient is 0.5, the maximum reaction force in surge direction corresponds with $F_{friction,x} = \mu \cdot F_y$ with μ the friction coefficient and F_y the reaction force from the vacuum pad. Resulting in $F_{x,max} = 200$ kN.
The capacity of a single MoorMaster device is 400 kN when taken loads in perfect sway direction and 200 kN for perfect surge direction. The capacity for combined loads in surge and sway direction is somewhere in between these values. This makes Modelling the MoorMaster system challenging as it has contributions in both surge and sway directions with each a contribution from stiffness and damping, resulting in four load contributions which together may not exceed the SWL of the MoorMaster device. How this challenge is solved will be explained in section 7.6.3.

Spring and damping values
The MoorMaster system properties can be adjusted via software. Since no typical stiffness and damping properties could be given by the Cavotec MoorMaster company, the spring and damping values have to be defined.

The stiffness and damping properties for these MoorMaster devices is assumed to be linear within its stroke and saturate upon exceeding the maximum extension or velocity limit. This saturation is build in to make sure the model is stable but should not be reached when finding the limiting sea state, since in reality the reaction force will go to zero when exceeding the stroke limit.
Defining the stiffness and damping coefficients is based on the maximum reaction force the MoorMaster system can take. These parameters are defined by the Cavotec MoorMaster company, in their brochure [8] and represented in Table 7.2.

In this research, one combination of stiffness and damping terms is modelled for the MoorMaster devices. These damping and stiffness curves are represented in Figure 7.11 and 7.12.
The maximum reaction force reached at its maximum allowable extension is 100 % of the capacity of the MoorMaster system. At the maximum velocity in the MoorMaster system, 40 % of the capacity is reached.
Since no limits on relative velocity are provided by Cavotec MoorMaster, the maximum velocity is based on the expected maximum first order relative velocity between *Iron Lady* and *Pioneering Spirit*, equal to 0.1 m/s.

Because the maximum reaction force and stroke is different for surge and sway direction, both surge and sway direction have different stiffness and damping curves for the two different cases as described above. These curves are represented in the Figures 7.11 and 7.12.

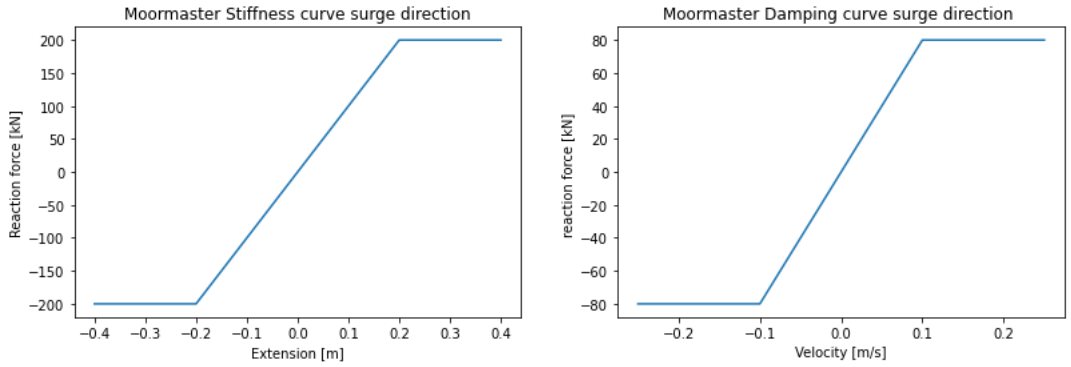

(a) Stiffness curve

(b) Damping curve

Figure 7.11: MoorMaster stiffness (left) and damping (right) curves for restricting surge motions.

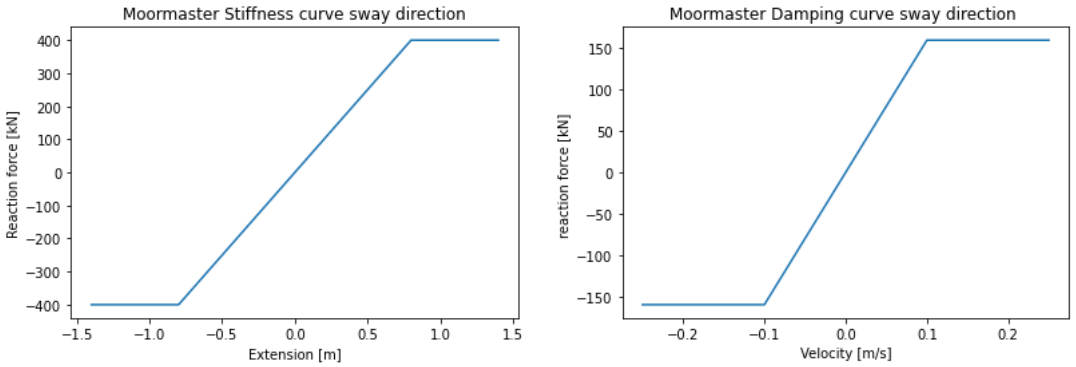

(a) Stiffness curve

(b) Damping curve

Figure 7.12: MoorMaster stiffness (left) and damping (right) curve for restricting **sway** motions.

Considering the stiffness curve, Figure 7.11a, shows a linear stiffness within the stroke of the MoorMaster system, equal to 0.4 m in surge direction. In reality the MoorMaster system automatically disconnects when the stroke is exceeded. After that, it can automatically reconnect at another location on the hull, this phenomena is called 'stepping'. Stepping is not possible within one wave period and is therefore excluded from the numerical model.
Regarding the damping curve, the maximum relative velocity of 0.1 m/s is used as limit, according to the MoorMaster company this relative velocity limit is realistic [39]. The reaction force due to damping saturates upon exceeding the relative velocity.
Regarding the stiffness curve in sway direction, in reality when the stroke in sway direction is exceeded, the MoorMaster system disconnects. Upon disconnection the barge is not connected to *Pioneering Spirit*, which is not allowed to occur. Similar as to surge, the reaction force saturates when the stroke is exceeded.
When finding the limiting sea state for the MoorMaster system concept, it should be confirmed that both the stroke and the Safe Working Load is not exceeded.

7.6.2 Minimum number of MoorMaster devices

To implement the MoorMaster system in the mooring configuration, the number of MoorMaster devices that is required needs to be estimated. This can be done by considering the static and dynamic environmental forces that are acting on the barge.
Considering the static load acting on the barge, the maximum mooring line force for the base case mooring system corresponds with 50 % of the SWL in the heaviest loaded mooring line. The other 50 % of the SWL comes from the dynamic load contributions, as can be seen from the data in table E.5. Using these results, the number of MoorMaster systems that is required will be based on the static environmental force acting on the barge and assuming this will also contribute to 50 % of the SWL in the MoorMaster system.

The environmental static and dynamic force acting on the barge in surge and sway direction depends on the incoming wave direction. These loads are summarized in Table 7.3 and come from 6.3, 6.2 and I.1.
The static load is given for 45, 90 and 135°. The number of MoorMaster systems is based on environmental loads coming in under 135°. However, the workability will be determined also for 45 and 90°.

Table 7.3: The first order loads have zero mean. Hs = 2.5 m and Tp = 8s is applied to determine the mean second order wave drift load.

Mean Load contribution			
Incoming direction [deg]	Wind [kN]	Current [kN]	second order wave force [kN]
Surge direction			
45	188.0	71.8	132.9
90	1.4	0.5	29.0
135	-188.0	-71.0	-6.0
Sway direction			
45	188.0	241.4	617.9
90	266.7	470.6	290.3
135	188.0	238.0	79.4

Considering the mean load for 135° and the maximum reaction force of a MoorMaster device is 200 kN in surge and 400 kN in sway direction. Taking into account that 50 % comes from the static load and 50 % from the dynamic loads means that at least 3 MoorMaster devices need to be placed in surge and 3 in sway direction.

7.6.3 Modelling

The MoorMaster system will be modelled like the fenders, as explained in section 6.4.2. The MoorMaster system is modelled as a link with spring and damper properties. Each end of the link is attached to one vessel. Figure F.1, shows how the connection to the different vessels is made. The link is given an initial length of 40 m to make sure the reaction force is applied exactly in surge direction, or exactly in sway direction.
The stiffness and damping curves that are defined in the section above are imported in the time domain model.

The Moormaster device is either aligned in x-direction to restrict the surge motion, or aligned in y-direction to restrict the sway motion, Represented in Figure 7.14. The MoorMaster system is modelled as being able to take both compressive and tensile forces.

7.6.4 MoorMaster design implementation

In this research, the MoorMaster system is implemented in the side-to-side mooring system. In order to do so, the MoorMaster devices are located on port side of Iron Lady.
The MoorMaster devices are located at three different locations on the barge, respectively stern, center and bow. At each location two MoorMaster devices are located, one for restricting surge and one for sway direction. This results in the arrangement as represented in Figure 7.13, at each red and yellow arrow a spring and damper is placed. How this MoorMaster implementation is modelled in Orcaflex is shown in Figure 7.14.

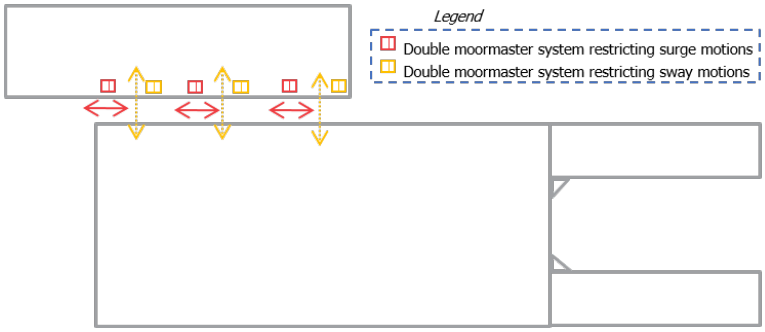

Figure 7.13: Cavotec MoorMaster implementation in a side-to-side mooring operation. The arrows represent a spring and damper, red refers to restricting surge motion and yellow refers to restricting sway motion.

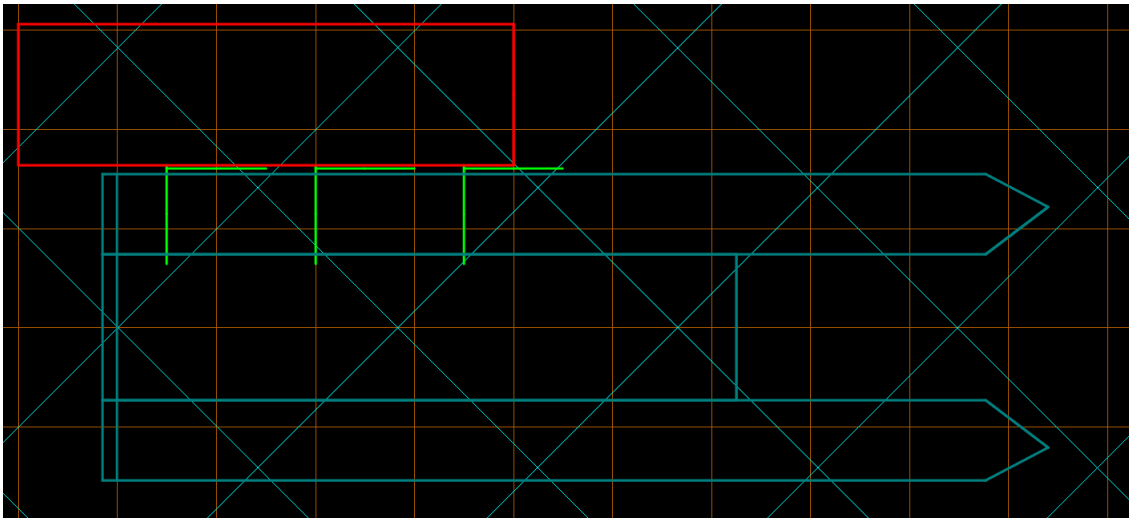

Figure 7.14: MoorMaster implementation in a side-to-side mooring operation. The red body representing *Iron Lady*, the grey body representing *Pioneering Spirit*. The yellow line representing the MoorMaster system in surge and sway direction.

7.6.4.1 Expected challenges

The challenges that come when implementing the MoorMaster system concept are listed:

- Before installing the MoorMaster system, in general a strong business case is required because the system is rather expensive. Details on the financial feasibility is considered outside the scope of this thesis [39].
- Additional mooring lines might be required for redundancy. In case of power loss, the vacuum pads will stay attached for a period of time but not be able to reconnect.
- Relative vessel motions should stay within the limited stroke. next to that, the hull surface should be applicable to attach vacuum pads, smooth, undisturbed and flat surface is required. Exceeding the limits could lead to reduction or even total loss of the reaction force.
- The MoorMaster system will be rigidly connected to one barge. In case multiple barges will be used to transport wind turbine components, each barge requires MoorMaster systems to be installed.

7.6.5 Sensitivity analysis MoorMaster system properties

The MoorMaster system properties, stiffness and damping, affect the MoorMaster system performance. For the current MoorMaster modelling method as described in section 7.6.1, only one combination of stiffness and damping is included.
To understand the effect of stiffness and damping on the relative sway motions and mooring loads, a sensitivity analysis is described in this section. Results from this analysis can be used to further optimize the MoorMaster system properties.

The stiffness is varied by modelling three stiffness curves as represented in Figure 7.15. The maximum capacity is kept constant at 400 kN. Figure 7.16a and 7.16 respectively represent the relative sway motion and the force in the heaviest loaded MoorMaster system. The corresponding statistical data is represented in Table 7.4.

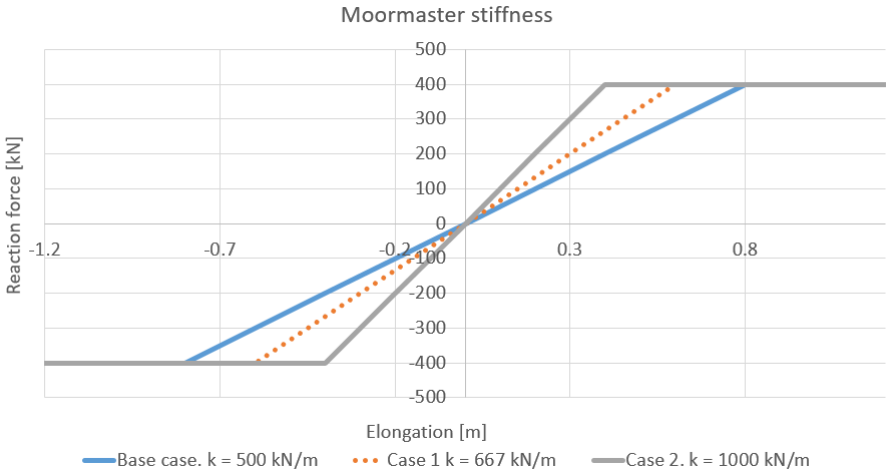

Figure 7.15: Stiffness curves, with saturation at [base case, case 1, case 2] = |[0.8,0.6,0.4]|m

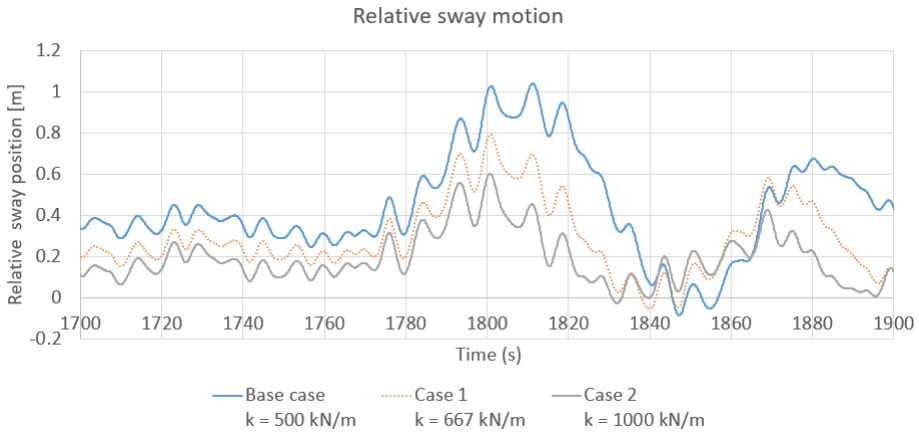

(a) Relative sway motion at location 'A', shown in Figure 2.5b.

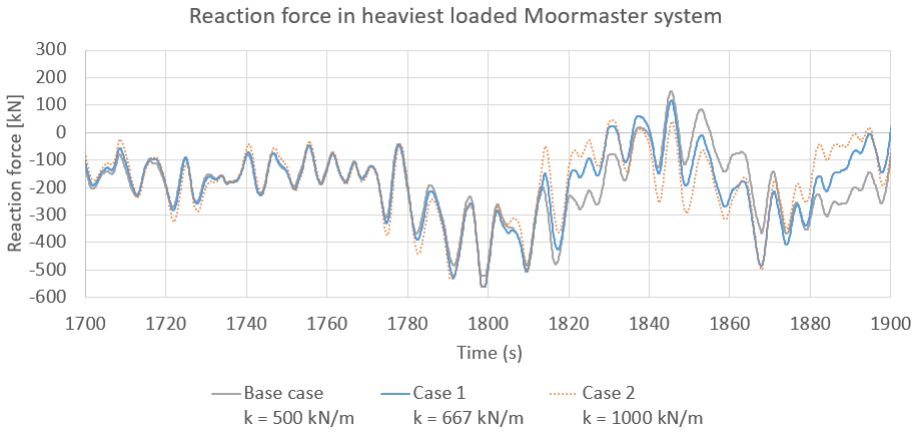

(b) Heaviest loaded MoorMaster system load.

Figure 7.16: Input and results from the MoorMaster stiffness sensitivity analysis. Environmental loads are co-linear from 135 °, with wind, current and waves respectively 25 knots, 0.9 m/s and Hs = 3.2 Tp = 8s.

Table 7.4: Statistical data corresponding with results in Figure 7.16. Including the relative difference w.r.t. the base case

	Base case k = 450 kN/m	Case 1 k = 600 kN/m	Case 2 k = 900 kN/m
Three hours max relative y motion [m]	0.90	0.69 (-23%)	0.53 (-41%)
Mean relative y-motion [m]	0.38	0.25 (-34 %)	0.17 (-55 %)
Three hours max y MoorMaster load [kN]	-489	-531 (-9%)	-574 (-17%)
Mean force [kN]	-167	-167 (0%)	-167 (0%)

Considering the relative motions, Figure 7.16a and Table 7.4, it can be seen that the MoorMaster stiffness affects the offset and the amplitude of the second order motion.
Regarding the mooring loads, shown in Figure 7.16b and Table 7.4, higher stiffness increases the dynamic load in the mooring system. Mean loads are constant and independent of stiffness, which is correct because the mean environmental load is constant for all cases.
This means that similar results are obtained as for changing the stiffness in the base case mooring system, as described in section 7.2. In other words, when the relative motions limit is not yet reached, it is

preferable to reduce the stiffness of the MoorMaster system in order to minimize mooring loads.

Similar approach is applied to understand the affect of damping in the MoorMaster system. The max reaction force due to damping is kept constant at 160 kN.

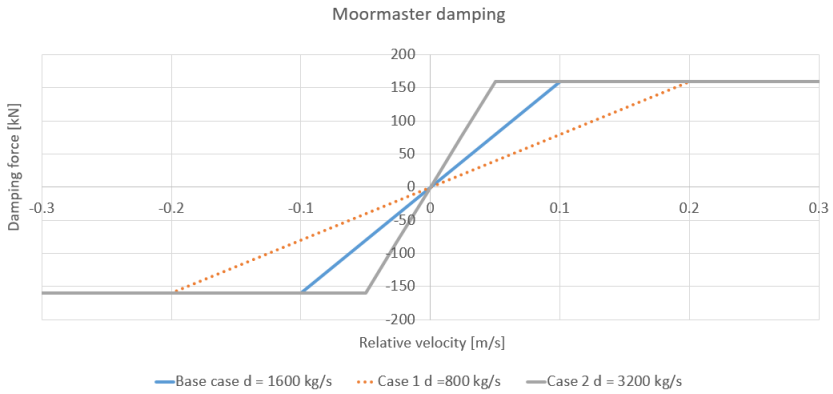

Figure 7.17: Damping curves, with saturation at [base case, case 1, case 2] = |[0.1,0.2,0.05]|m/s

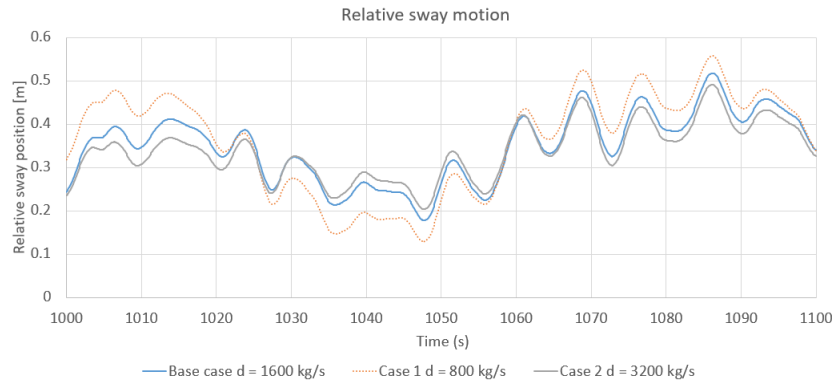

(a) Relative sway motion at location 'A', shown in Figure 2.5b.

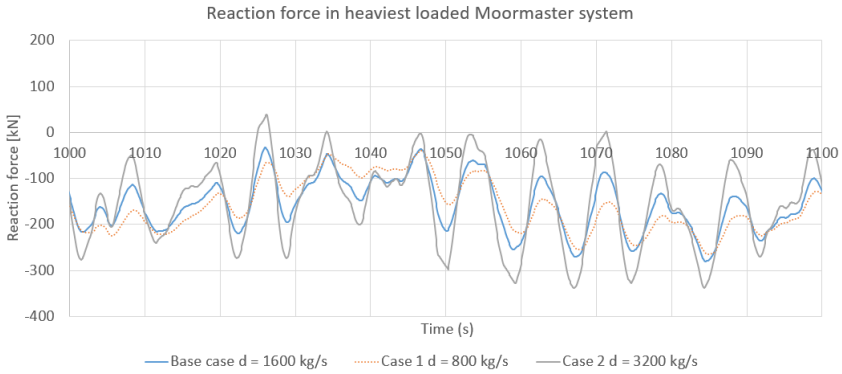

(b) Reaction force in the Heaviest loaded MoorMaster device.

Figure 7.18: Input and results from the MoorMaster damping sensitivity analysis. Environmental loads are co-linear from 135 °, with wind, current and waves respectively 25 knots, 0.9 m/s and Hs = 3.2 Tp = 8s.

Table 7.5: Statistical data corresponding with results in Figure 7.18.

	Case 1 d = 800 kg/s	**Base case** d = 1600 kg/s	Case 2 d = 3200 kg/s
Three hours max relative y motion [m]	1.03 (14%)	0.90	0.82 (-9%)
Mean relative y-motion [m]	0.38 (0%)	0.38	0.37 (-3%)
Three hours max y- Moormaster load [kN]	-476 (-3%)	-489	-583 (-20%)
Mean force [kN]	-167 (0%)	-167	-167 (0%)

Figure 7.18a and Table 7.5 show that large damping reduces the amplitude of the second order relative sway motion.
Regarding the mooring loads, Figure 7.18b and Table 7.5, show that large damping increases the dynamic load in the mooring system. Similar as for the stiffness sensitivity analysis, the mean loads are constant which is correct.
In case the relative motion limit is not yet reached, it is preferable to keep the damping in the system low in order to reduce mooring loads.

Concluding. Above results show that the MoorMaster system properties can be further optimized because there is a trade of between motion limits and mooring forces. The optimum MoorMaster system properties can be found by tweaking stiffness and damping parameters in order to make sure both motions and mooring loads reach the limit.

8
Workability study

The objective of this thesis is to improve the mooring system of a barge moored alongside *Pioneering Spirit* in offshore conditions. Each mooring system concept should satisfy the design requirements, as stated in section 4.3, the main design requirement is that the Safe Working Load and relative motion limit should not be exceeded. The main design criteria is optimizing the workability of the mooring system.
Results will be provided for co-linear wind, waves and current load. Wind and current speed are constant and time and constant over the vertical, respectively 25 knots and 0.9 m/s. Regarding waves, a Pierson-Moskowitz spectrum with peakedness factor of 1.0 and peak periods of Tp = 8s and 12s with a varying significant wave height are applied to determine the workability.

This chapter provides in the first section the relative vessel motions for stern-quartering, beam and bow-quartering waves to give insight in whether the design requirement is met.
The second section provides results showing how heavily the mooring system is loaded when applying only constant wind and current loads.
Finally, an example calculation of computing the workability from time series data is provided as well as high level results on the performance of each mooring system concept for the free mentioned environmental loading directions.

This section includes the results from step 13 and 14 of the stepwise approach. The results are found by following the flow diagram as represented in Figure 8.1. In the thesis approach this goes hand in hand with step 11 and 12, developing and building the improved concept as described in the previous chapter.

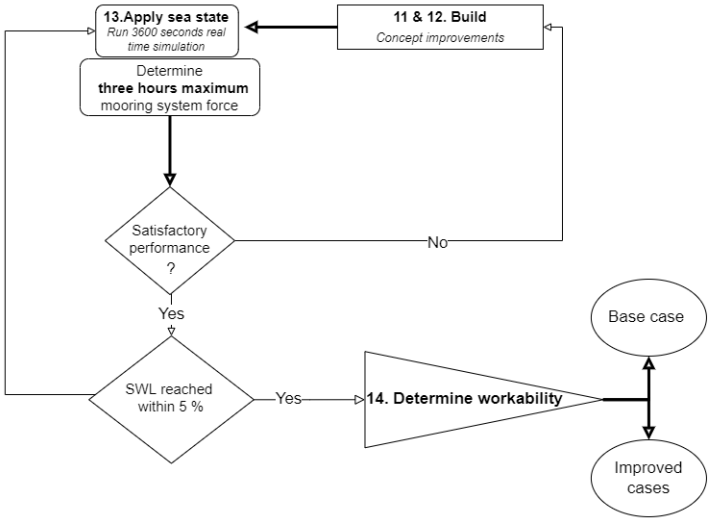

Figure 8.1: Approach to find the workability results, as part of the total thesis approach.

8.1 Performance mooring system concepts

Figure 8.2 shows the relative sway motion and the heaviest loaded line load for all mooring concepts that consist of mooring lines.
Figure 8.2a shows that low frequency relative sway motions are lower when implementing the 'new line orientation' because reorientation of the lines increases the capacity and stiffness in sway direction. Other concepts show comparable relative sway motion.
Figure 8.2b shows similar behavior in all line loads except for the 'new line orientation' where the governing line becomes almost slack and has high peak loads. This is because the governing line is relatively short and therefore stiff. On top of that, this line is attached far from the center of the barge and thus faces large motions due to yaw.
Overall, no clear conclusions on mooring system performance can be drawn from these Figures therefore it is recommended to focus on the statistical results as will be represented in section 8.5.2.

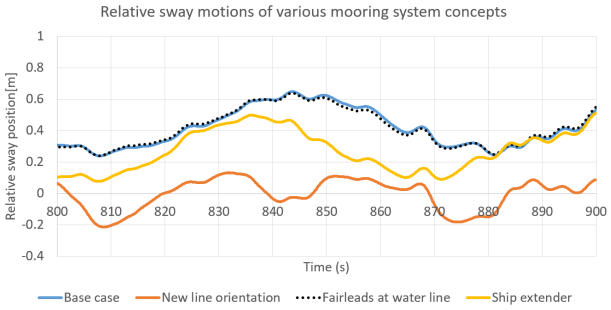

(a) Relative sway motion.

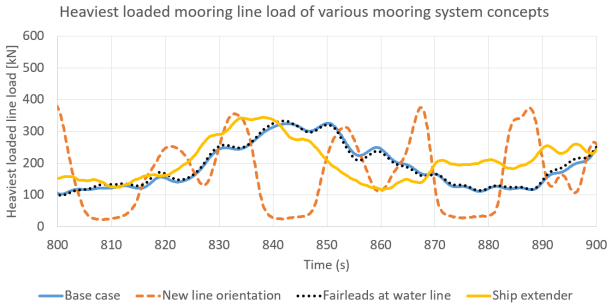

(b) Heaviest loaded mooring line load.

Figure 8.2: Relative surge and sway motions, at location 'A', shown in Figure 2.5b, when implementing the base case and various mooring system concepts. Environmental loads are co-linear from 135°, with wind, current and waves respectively 25 knots, 0.9 m/s and Hs = 2.0 Tp = 8s.

8.2 Performance Base case versus MoorMaster mooring system

This section compares the performance of the base case and the MoorMaster mooring system by comparing the relative motions and the corresponding connection forces acting on the barge, e.g.loads from fenders and mooring lines.

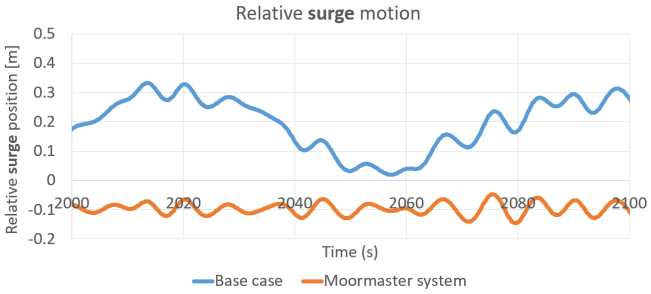

(a) Relative surge motion.
Three hour max [Base case, MoorMaster] = [-0.41,0.17]m. Mean = [-0.19,0.10]m

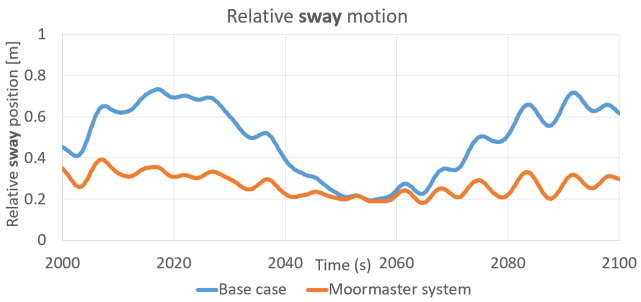

(b) Relative sway motion.
Three hour max [Base case, MoorMaster] = [0.89,0.51]m. Mean = [0.47,0.28]m

Figure 8.3: Relative surge and sway motions, at location 'A', shown in Figure 2.5b, when implementing the base case and the MoorMaster mooring system. Environmental loads are co-linear from 135°, with wind, current and waves respectively 25 knots, 0.9 m/s and Hs = 2.0 Tp = 8s.

- Figure 8.3a shows:
  - Different sign in offset. Because the line orientation of the base case causes large forces in surge direction due to the offset in sway direction. Resulting in an overall positive offset for the base case mooring system while the mean forces are directed in the negative surge direction.
  - The amplitude of the low frequency motion is heavily reduced, or even removed, by the MoorMaster system. While the first order motions have similar amplitude for both mooring systems.
- Figure 8.3b shows:
  - Similar results occur for sway motion as for surge motion. Overall, the relative motions are small for these environmental conditions. For example looking at the sway motion of the base case, moving 0.55m in 30 seconds should not be a problem.
  - Considering the mean position indicates that the MoorMaster system has higher stiffness. However, in this case the offset in surge motion is also affecting the offset in sway motion.

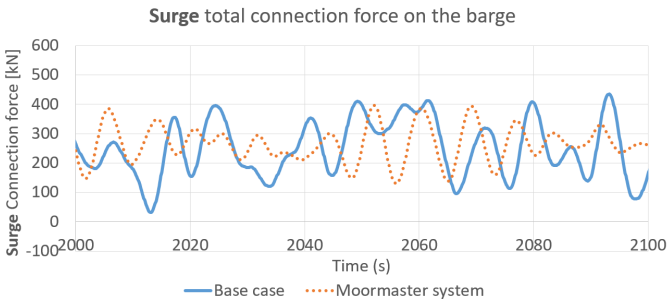

(a) Surge. Three hour max [Base case, MoorMaster] = [544,486] kN. Mean = [262,263] kN

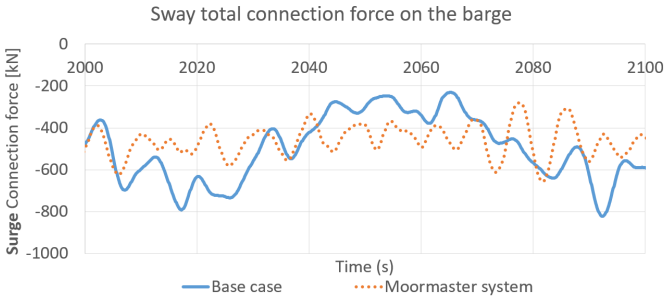

(b) Sway. Three hour max [Base case, MoorMaster] = [-900,-769]kN. Mean = [-479,-477] kN

Figure 8.4: Connection forces at the barge, when implementing the base case and the MoorMaster mooring system. Environmental loads are co-linear from 135 °, with wind, current and waves respectively 25 knots, 0.9 m/s and Hs = 2.0 Tp = 8s.

- Figure 8.4a shows:

  - The MoorMaster system has lower variation in the amplitude of the connection force. Confirmed by the lower three hours maximum value for the MoorMaster connection force. The mean force is equal for both systems, making the results trustworthy because the mean environmental loads are independent from the mooring system performance.

- Figure 8.4b shows:
  - Rather high amplitude for the low frequency connection forces in sway direction. Confirmed by the difference in three hours maximum values. Again the mean force corresponds in both systems.
  - The forces exerted on the barge by the MoorMaster system are less extreme while the motions are even more reduced. Keeping forces and motions low is preferable for a mooring system.

From the motions and forces as shown above, it can be concluded that the MoorMaster system shows promising results compared to the base case mooring system because both relative motions and connection forces are reduced. This relation can be understood when looking at Figure 8.5.

In Figure 8.5a, the surge displacement is plotted against the reaction force in sway direction. For the MoorMaster system these are uncorrelated. This means that surge motion does not result in a reaction force in sway direction. The MoorMaster surge motion circling around -0.1m corresponds with the offset in surge direction. Circling around -500 kN is the reaction force due to the offset in sway direction For the base case mooring system however, surge displacement and sway reaction force are correlated. Increasing relative surge motion results increases the reaction force in negative sway direction.
This curve learns that the MoorMaster system uses its force capacity more efficient by correcting motions in surge direction with forces in perfect surge direction.

Analysing Figure 8.5b in the same way learns that: The force in the Moormaster due to offset in surge direction is approximately 300 kN. Moreover, motion in sway direction does not result in a reaction force in surge direction.
For the base case system however, the correlation learns that motion in sway direction results in a negative reaction force in surge direction. The calculated correlation values can be found in the Figure captions.

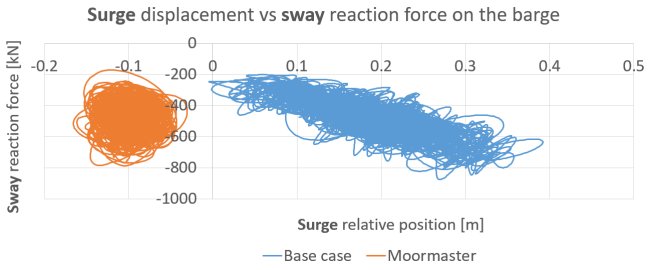

(a) Correlation Surge displacement vs sway reaction force. [Base case, MoorMaster] = [-0.77,0.01]

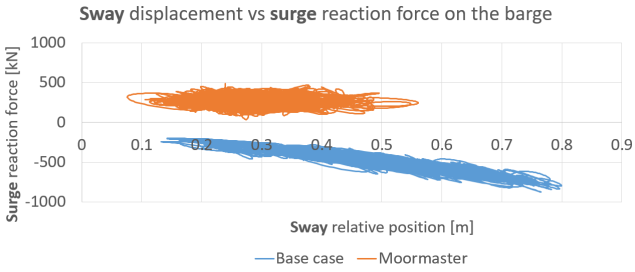

(b) Correlation sway displacement vs surge reaction force. [Base case, MoorMaster] = [-0.30, -0.002]

Figure 8.5: Correlation between relative surge motion and sway connection force and vice versa. Environmental loads are co-linear from 135 °, with wind, current and waves respectively 25 knots, 0.9 m/s and Hs = 2.0 Tp = 8s.

Concluding. The MoorMaster system is very well suitable for operations with strict motion limits. Furthermore, the MoorMaster uses its installed capacity much more efficient because of the ability to apply forces in perfect surge or sway direction. In other words surge displacement - sway reaction force, and vice-versa, have a very low correlation. This ultimately increases the allowable sea state that causes the SWL and motion limits to be reached and therefore increases the workability.

8.3 Relative motions

The relative surge, sway and heave motion at point 'A' in Figure 2.5b are computed for each concept for three incoming wave directions. The relative motion is expressed as the three hours maximum, including the offset and the motion amplitude. Before considering a mooring system concept as improved, the relative motion should be in the order of the base case mooring system. Results are captured in Tables 8.2 and 8.3. The contribution from offset to the three hours maximum position, for Tp is 8 seconds is shown,in Table 8.1. The offset for Tp is 12 seconds is in the same order of magnitude because the constant wind and current load have the largest contribution to the offset, compared to the mean second order wave drift forces. Therefore the offset for Tp is 12 seconds is not presented. From the offset results it can be seen that for each concept the offset is comparable or lower than for the base case, satisfying the design requirement on offset.

Table 8.1: **Offset** in surge and sway direction. Corresponding with the maximum workable sea state for Tp = 8 seconds. Environmental loads are co-linear from 135°

Case	Surge [m]	Sway [m]
Base case	0.19	0.47
Improved orientation mooring lines	0.13	0.04
Fairleads at hull side	0.18	0.46
Ship extender	0.03	0.30
MoorMaster system	0.10	0.34

Table 8.2: **Three hours maximum** relative position for **Tp = 8s** and the corresponding maximum workable sea state. Environmental loads are co-linear from 135°.

Case	Surge [m]	Sway [m]	Heave [m]
Base case	0.40	0.89	0.15
New orientation mooring lines	0.50	0.38	0.16
Fairleads at hull side	0.40	0.83	0.13
Ship extender	0.33	0.74	0.17
MoorMaster system	0.20	0.70	0.20

Table 8.3: **Three hours maximum** relative position for **Tp = 12s** and the corresponding maximum workable sea state. Environmental loads are co-linear from 135°

Case	Surge [m]	Sway [m]	Heave [m]
Base case	0.32	0.56	0.04
New orientation mooring lines	0.28	0.09	0.01
Fairleads at hull side	0.26	0.55	0.01
Ship extender	0.34	0.67	0.13
MoorMaster system	0.21	0.42	0.23

Regarding results in Table 8.3, for the base case, new line orientation and the fairleads at hull side concept, the SWL was already almost reached upon applying wind and current loads. Therefore, these results seem not to match with the limiting relative motions for Tp = 8s. Concise description of what we learn from Tables 8.2 and 8.3 is listed below, one line for each concept.

- **Base case**. Very well restricting surge motions, because lines oriented for 135° loading resulting in high stiffness. Low heave due to the limited allowable wave height, as heave is mainly determined by incoming wave height.
- **New line orientation**. In this arrangement lines are more orientated in sway direction compared to the base case. Therefore, more stiffness in sway direction resulting in lower excitations in sway but higher in surge direction.
- **Fairleads at hull side**. Comparable motions compared to the base case, as expected.
- **Ship extender**. More excessive surge motions compared to the base case, sway motions however are in the same order.
- **MoorMaster system**. Sufficient performance, compared to the base case. Surge motions are higher but allowable. Stroke of the MoorMaster system is not exceeded in all directions.

8.4 Wind and current contribution

Table 8.4 provides the three hours maximum load of the heaviest loaded component in the mooring system, expressed as percentage of the SWL. This gives insight how much of the mooring system capacity is used to take the static load.

Table 8.4: Heaviest loaded mooring component upon wind and current load, expressed in percentage of the Safe Working Load. For incoming direction 135, 90 and 45°.

Force in Heaviest loaded component [%]	Incoming direction [°]		
Case	135	90	45
Base case	43	100	82
New orientation mooring lines	36	59	47
Ship extender	46	55	51
Fairleads at hull side	41	100	82
MoorMaster system	43	100+	100+

Concise description of what we learn from Table 8.4, for each concept, is listed below.

- **Base case**. For 135° only 43 % of the SWL is caused by wind and current load. For 90° waves, 100% of the SWL is reached and no additional wave load can be taken, resulting in 0% workability for beam waves.
- **New line orientation**. Regarding static loads, this concept is able to take higher wind and current loads compared to the base case.
- **Fairleads at hull side**. Showing comparable results as for the base case.
- **Ship extender**. Capable for all incoming directions, around 50 % of the SWL caused by wind and current load.
- **MoorMaster system**. Already 43 % of the SWL is reached by wind and current applying wind and current loads from 135°. For wind and current from 90 and 45°, the SWL is already exceeded which means that no waves can be taken in combination with this wind and current load. Because for 90 and 45 ° the SWL is exceeded, the exact force cannot be determined and no static solution is available.
  The reader could presume that for 135 and 45 ° the static load should be the same. However, the MoorMaster devices are not evenly distributed over the barge length due to the barge extension, Therefore the MoorMaster devices are loaded differently.

8.5 Workability

This section provides an example how the workability is computed. After that, the workability results for the 5 different mooring concepts is stored in Tables, 8.6,8.7 and 8.8 for 135, 90 and 45° respectively.

8.5.1 Detailed case workability calculation

For one case, the workability calculation is explained step by step. Including the following results:

- Workability for both reference locations. Southern North Sea characterized as wind sea, Saint-Nazaire as more of a swell sea. The workability is expressed as annual percentage of time that the operational limits are not exceeded.
- Three forces are given as percentage of the SWL.
  - Three hours maximum of the maximum loaded component in the mooring system, occurring at the limiting sea state. This value should reach 100 % with a 5 % margin.
  - Mean value of the maximum loaded component in the mooring system. To see the contribution of static and dynamic load to the maximum load.
  - The standard deviation of three hours maximum force of all system components. This represents the variation of load that each mooring system component takes. For a well performing mooring system, the load should be evenly divided over all components, resulting in a low standard deviation.

Results from the diffraction analysis, are imported in the time domain model. Mooring system concepts are modelled in the time domain model, applying environmental conditions and running the model provides time history data on relative motions and mooring loads from which the mooring system workability can be computed.
First, the workability of the base case system in wind seas for T_p is 8 seconds, will be calculated as an example calculation.
The methodology to compute the three hours maximum mooring load and relative motions and from that the workability, as explained and justified in section 4.7, will be applied.
The three main discussion points to this method are:

- Significant wave height for the limiting sea state is rounded to the nearest decimal. However, the step size for significant wave height in the wave probability scatter diagram is 0.5m. Linear interpolation is applied to find probabilities with a step size of 0.1m significant wave height.
- A simplification in the number of sea states that need to be analysed is applied by checking only two peak periods.
- Three hours maxima of the relative vessel motion and the mooring load are found from the time series. This assumes these variables to follow a Rayleigh distribution which assumes a linear relation between wave amplitude and mooring line force.

The approach from the example calculation will be applied to compute the data represented in Tables 8.6, 8.7 and 8.8. Figure 8.6 presents the time series of the mooring line load when applying both wind and current forces, as defined in section 6.3.2.2, and two different sea states. The time series of the heaviest loaded line is shown and analysed since this line determines the limiting sea state.

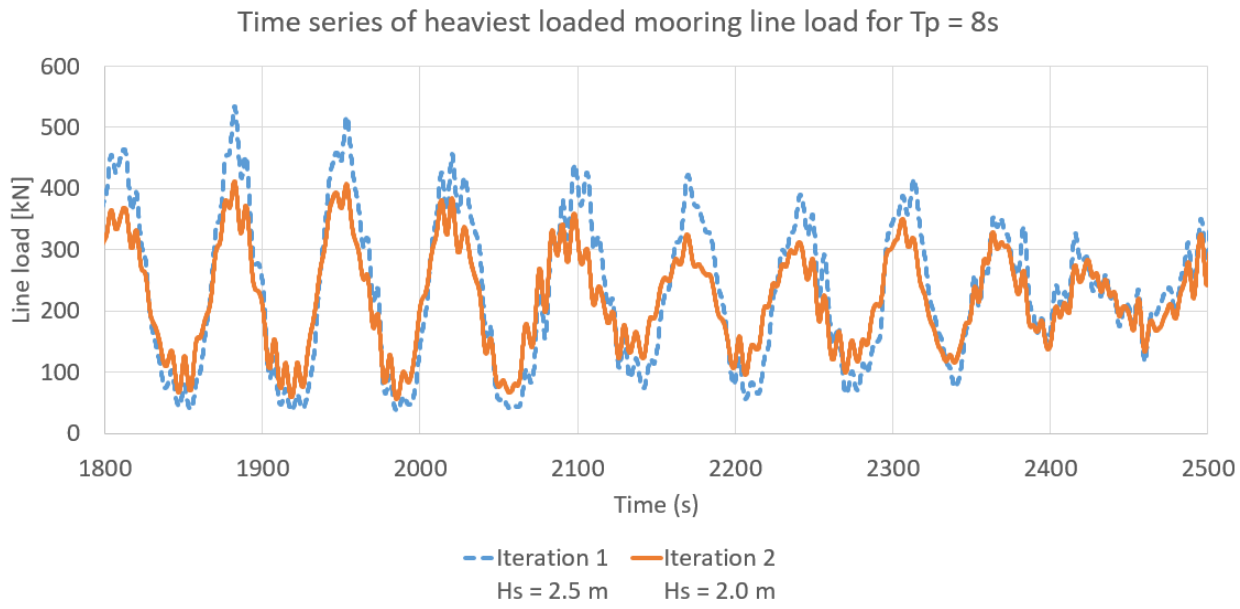

Figure 8.6: Snapshot of a 3600 seconds time series of heaviest loaded mooring line, for two sea states.

Table 8.5: The input, intermediate results and output data corresponding with the iterations to find the limiting sea state of the base case mooring system. The heaviest loaded mooring line is considered while determining limiting sea state. With SWL = 453 kN.

Variable	Symbol & unit	Tp = 8 seconds Iteration 1	Tp = 8 seconds **Iteration 2**	Tp = 12 seconds Iteration 1	Tp = 12 seconds **Iteration 2**
		Input			
Significant wave height	Hs [m]	2.5	**2.0**	0.5	**0.2**
		Results			
Mean	μ [kN]	236	**222**	158	**158**
Standard deviation	σ [kN]	104	**70**	174	**89**
		Output			
Three hours max	F_max [% of SWL]	131	**102**	171	**105**
SWL within range?	[-]	No!	**Yes**	No!	**Yes**

From these limiting sea states, [Tp = 8s, Hs = 2.0m] and [Tp = 12 s, Hs =0.2m], the workability can be computed. By means of applying equations 4.13 and 4.12 to the wave probability scatter diagram as represented in Figure 4.10. Equation 8.1 includes the computation of the annual probability, P in %, of having a sea state equal or lower than Hs of 2.0 m and Tp is 8 seconds. Equation 8.3 shows how the total

annual workability, W in %, is computed based on the limiting sea state for two peak periods.

$$\begin{aligned} P_{Hs=2.0,Tp=[0-8]s} =& P_{Hs=[0-0.5],Tp=[0-8]s} + P_{Hs=[0.5-1.0],Tp=[0-8]s} P_{Hs=[1.0-1.5],Tp=[0-8]s} + P_{Hs=[1.5-2.0],Tp=[0-8]s} \\ =& \sum (0.15 + 2.55 + 2.77 + 2.17 + 1.11 + 0.88 + 0.72) + \\ & \sum (0.36 + 6.39 + 8.15 + 4.87 + 3.35 + 2.35) + \\ & \sum (0.24 + 4.6 + 8.88 + 3.11 + 2.17) \\ & \sum (0.18 + 3.88 + 5.22 + 1.43) = 65.5\% \end{aligned} \tag{8.1}$$

$$\begin{aligned} P_{Hs=0.2,Tp=[8-12]s} &= 0.2 \cdot \frac{P_{Hs=0.5,Tp=[8-12]s} - P_{Hs=0.0,Tp=[8-12]s}}{0.5} \\ &= 0.2 \cdot \frac{\sum (1.08 + 0.89 + 0.72 + 0.46) - 0.0}{0.5} = 1.3\% \end{aligned} \tag{8.2}$$

$$W_{base\ case} = P_{Hs=2.0,Tp=8s} + P_{Hs=0.2,Tp=12s} = 67.0\% \tag{8.3}$$

8.5.2 High level results from the workability study

The methodology as described in the previous section is applied to all mooring systems, for three environmental loading directions, 45,90 and 135 °. Results are captured in the following three Tables.

Table 8.6: Results for bow quartering, 135 °, waves, wind and current.

Mooring system	Workability [%]		Force in mooring system [%]		
	Southern North Sea	Saint Naizare	Maximum	Mean of the max loaded component	Standard deviation of the components
Base case	**67**	**16**	**101**	**49**	**30**
New orientation mooring lines	69	16	105	39	36
Fairleads at hull side	62	15	100	48	27
Ship extender	74	23	102	50	17
MoorMaster system	**82**	**40**	**101**	**45**	**8**

Table 8.7: Results for beam, 90 °, waves, wind and current.

Mooring system	Workability [%]		Force in mooring system [%]		
	Southern North Sea	Saint Naizare	Maximum	Mean of the max loaded component	Standard deviation of the components
Base case	0	0	100	100	32
New orientation mooring lines	10	2	102	59	35
Fairleads at hull side	0	0	100	100	30
Ship extender	36	10	104	58	28
MoorMaster system	0	0	100+	100+	/

Table 8.8: Results for stern quartering, 45 °, waves, wind and current.

Mooring system	Workability [%]		Force in mooring system [%]		
	Southern North Sea	Saint Naizare	Maximum	Mean of the max loaded component	Standard deviation of the components
Base case	8	1	104	84	40
New orientation mooring lines	10	2	104	48	35
Fairleads at hull side	6	1	99	84	38
Ship extender	17	5	94	53	29
MoorMaster system	0	0	100+	100+	/

Most important learnings from the results are listed below. In general, the MoorMaster shows promising workability increase for 135° especially for a sea state governed with swell waves.
Each concept is loaded within 5 % of the SWL at the limiting sea state. Except for the MoorMaster concept where the SWL is already exceeded without sea state.

- **Base case**. For 135° waves the base case system performs reasonably well, 67 %, workability for wind seas. The base case performs less in seas with a large contribution of swell. The standard deviation of mooring system components lies around 30 % which means that the load is reasonably well divided over mooring system components. For 90 and 45° waves this system has zero workability.
- **New line orientation**. For 135° waves this system has comparable workability as for the base case. With a slight workability increase for beam waves.
- **Fairleads at the hull side.** Similar results as for the base case system.
- **Ship extender**. Regarding 135° slight increase of workability, low standard deviation so load is well divided over mooring system components. Large increase of workability for 90 and 45°. For 45° low contribution from static loads, 28 %.
- **MoorMaster system**. Regarding 135° high workability, especially for swell seas. Besides the standard deviation in mooring components loads is low, meaning that loads are well divided over mooring system components. 90 and 45° zero workability and high standard deviation.

9 Discussion and recommendations

This chapter discusses the results as presented in chapter 8 and recommends topics for follow up research, this is part of step 15 of the stepwise approach as explained in section 3.1. Four sections are presented. Approach refers to the content of this report up until chapter 4. Modelling decisions discusses chapter 5 to 7. Thesis results discusses chapter 8. Finally, the results of each mooring system concept are concisely discussed.

9.1 Approach

This section discusses the approach of the research statement. More specifically, the design requirements as stated in chapter 4, the base case mooring system and the longitudinal barge extension. Finally, a recommendation on the financial aspect.

9.1.1 Mooring system design requirements

A pre-tension of 50 kN per mooring line is defined as requirement. In the numerical model, pre-tension is applied while environmental loads are excluded. In reality, environmental conditions cannot be excluded therefore the crew applies pre-tension based on their experience and the actual environmental conditions.

When defining the mooring system design requirements, motion limits of the barge load (wind turbines) is disregarded. These limits can be translated to motion limits of the barge and included as design requirements in future research.

For a mooring system to comply with the design code, a redundancy check is required. Mooring system redundancy is defined as the ability to keep position upon failure of one equipment component, for example a line breakage.
This redundancy is recommended as subject for the next step in improving the mooring system design. A standby tug could be incorporated for redundancy or to increase the overall workability.

9.1.2 Environmental loading direction

In this research, results are found for three incoming environmental loading directions that are realistic for barge mooring because of shielding. Moreover, wind, wave and current contributions are aligned.
It is recommended to analyse also head waves, 180 °. This way the optimum shielding is considered with bow-quartering waves with a varying angle of 45 °, analysing angles [90,135,180]°.

Pioneering Spirit sailing at slow speed while *Iron Lady* being moored alongside is part of the mooring procedure scope. However, yet only the case of zero forward speed is examined. It is recommended to compute the mooring system workability at slow speed. Starting simple by applying an additional current component, more detailed by applying forward speed to the vessels.

9.1.3 Base case mooring system

Winches located at *Pioneering Spirit* stern that are included in the base case mooring system, do not yet exist. However, there are plans for these to be installed.
Line 1 and 8 of the mooring system are attached to the winches at *Pioneering Spirit* stern as represented in Figure 4.8. These mooring lines increase the risk of clashing with the JLS beams and the pre-installed wind turbine foundation. Well understood when looking at Figure 2.2.

9.1.4 Longitudinal barge extension

In the defined vessel orientation, the barge stern is extended 40m from *Pioneering Spirit* stern to increase the barge area reachable by the crane used for unloading. Other solutions to optimize the barge unloading could be looked into and might be promising, for example a skidding system or rotating the barge half way the operation.
Nevertheless, this vessel orientation is interesting because of its challenging vessel motion and possible application to other projects. For example, when lifting a topside with the 5000 Tons crane for which this mooring operation is required as well.

9.1.5 Loading conditions

To determine the loading conditions, the combined VCG is calculated based on transporting 8 disassembled wind turbine components. Due to incorporating incorrect tower mass, the VCG is found to be located at 13.2 above the keel line while a value of 12.1 m is considered in the hydrodynamic model. This results in a slight reduction of the roll and pitch restoring terms as well as roll and pitch mass moment of inertia. Leading to a change of the roll restoring term,C_{44}, of 4%. The pitch restoring terms C_{55}, of 0.25%. The roll mass moment of inertia, I_{xx}, increases with 8.5 % and negligible difference for pitch.
The VCG affects mainly the roll motion and with that the forces in the mooring system. However, the same loading condition is used for all mooring system concepts and therefore not affect the results of this research.

9.1.6 Financial aspect

The results show that for some of the mooring system concepts the workability increases. To assure feasibility, not only the performance but also the costs should be considered. Large expenses can originate from required vessel modifications, investment and maintenance. This topic is interesting subject for future research.

9.1.7 MoorMaster system properties

The stiffness and damping properties of the MoorMaster system are not available in literature. To understand the relation between the performance of the MoorMaster system and the stiffness/damping properties, a sensitivity analysis is performed, described in section 7.6.5.
Before performing the workability study, the MoorMaster system properties have been checked to be realistic by engineers of the Cavotec MoorMaster company. The sensitivity analysis has been performed after the workability study is performed. Which means that the knowledge from the sensitivity analysis is not incorporated in the system properties that are applied while determining the workability. This means that conservative results are found for the MoorMaster system because the system properties can be further optimized. Directions to determine what are the optimal system properties are given in section 7.6.5. Its relation to workability is left for future research.

9.2 Modelling decisions

Modelling decisions made in chapter 5 to 7 are discussed in this section. Starting with the mooring line and fenders followed by the motion response of *Pioneering Spirit*. Finally, a recommendation on analysing the hydrodynamic data.

9.2.1 Mooring lines and fenders

Wear and tear of the mooring system equipment is disregarded. Regarding the fenders, damping factors are estimated and validated with a sensitivity analysis. The damping factor heavily affects the mooring system force, therefore more detailed research in the correct fender damping factor is recommended.

9.2.2 Motion response of Pioneering Spirit

In the time domain model, *Pioneering Spirit* is modelled to follow the motion RAOs. Meaning that only first order wave forces are considered as external force. Wind, waves and second order wave drift forces are excluded from *Pioneering Spirit*.
First order motions have zero mean, this modelling decision assumes to have sufficient DP capability to compensate for the mean environmental loads which is realistic for these environmental conditions. This is based on Allseas experience and on the DP system installed on *Pioneering Spirit*.
For *Iron Lady* however, wind waves and current forces are taken into account. Regarding current and wind, no shielding from *Pioneering Spirit* is included while it has a deeper draft than *Iron Lady* and only a part of the wind turbine towers exceed *Pioneering Spirits'* height above the waterline.
Contributions of second order sum frequency loads are excluded from the simulations, based on a sensitivity analysis and and the increased computation time. It is recommended to analytically derive which hydrodynamic effects need to be included and which can be disregarded.

9.2.3 Hydrodynamic data

Mainly the hydrodynamic data of *Iron Lady* is analysed, e.g. in the validation steps regarding numerical challenges. It would be interesting to also analyse the hydrodynamic data of *Pioneering Spirit* in more detail and perform the validation tests. Because the data of *Pioneering Spirit* has a considerable contribution to the mooring loads especially for swell areas.

Regarding the environmental load effects that are incorporated in the time domain model, the effect of current on the wave drift damping requires future research because in the time domain model, increased current leads to increased load contribution from the wave-drift damping force.

9.2.4 VLID damping factor

In this research, the damping factor applied to the VLID to account for the numerical gap resonance effect is based on both experimental data and Allseas experience, [26]. Furthermore sensitivity in the RAOs is analysed.
To better understand how this damping factor is affecting the results of this research, the mooring loads can be determined for the various VLID damping factors. This can for example be done by implementing the outcome of the diffraction analyses in the time domain model and computing the corresponding mooring load for a specific sea state.

9.3 Thesis results

This section concisely discusses the workability results and the assumption made to find these results.

9.3.1 Workability

Workability results depends on the wind, current and wave data for the reference location. To simplify the problem, the wind and current speed is set to be constant, corresponding corresponding with 92.5 % and 99% respectively. As a result of the high wind and current load, very limited workability in terms of sea state can be found for stern-quartering and beam waves.
It is recommended to scale wind speed with the sea state because these are related when considering a fetch limited reference location, as is the case in this research. This would result in more realistic results for the workability.
The current however should kept constant corresponding with 99% workability as mainly tidal current is present at the reference location.
Workability regarding waves is determined by analysing two different peak periods with varying significant wave height, as explained in section 4.7. Accuracy of the workability can be increased by analysing wave conditions for more than two peak periods. Especially for peak periods around the natural vessel frequencies as it will lead to excessive motions.

9.3.2 Dynamic load for swell and wind seas

Vessel motions consist of first order motions and low frequency motions. The amplitude of first order motions can be found in the RAOs that are received from the diffraction analysis or computed from the hydrodynamic matrices when excited by first order wave forces. For low frequency waves, the surge, sway and yaw the first order motions are much larger than for higher frequency waves. Besides, the peak period nearing the natural period in a certain DoF also heavily increases the vessel motions.
Figure 9.1 shows the sway motion of both *Iron Lady* and *Pioneering Spirit* for the same wave height but a Tp of 8 and 12 seconds of which the latter results in higher motions.
The dynamic mooring loads are induced by these first order forces/motions as well as the second order forces. Figure 9.2a shows that the second order forces are smaller for Tp = 12 seconds than for Tp = 8 seconds. The mooring loads, as represented in Figure 9.2b are much larger for Tp = 12 seconds. However in this Figure, it must be noted that for Tp = 12 seconds the line becomes slack which also can lead to higher mooring loads, slack lines can be prohibited by increasing pre-tension.
Wind seas generally have a lower peak period, in the range of Tp = 8s while swell seas more in the range of Tp = 12s.
Therefore it can be concluded that swell waves lead to more excessive first order motions resulting in excessive mooring loads and therefore lower workability compared to wind sea areas.

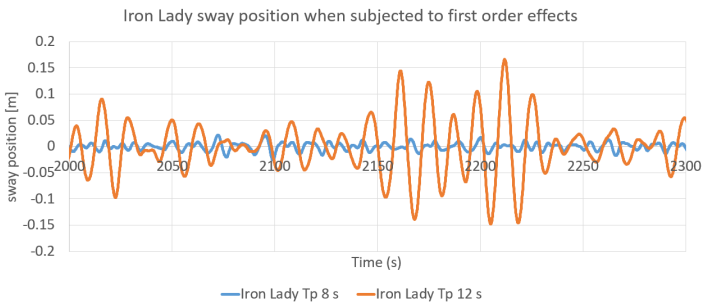

(a) Time series sway motion *Iron Lady*. Subjected to both first and second order forces.

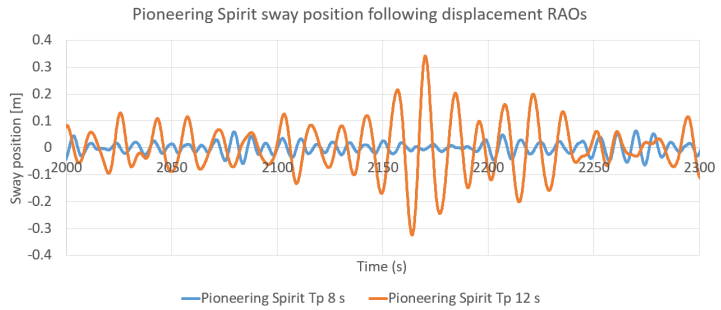

(b) Time series sway motion *Pioneering Spirit* when Subjected to first order forces.

Figure 9.1: Sway motion of *Iron Lady* and *Pioneering Spirit* for a Tp of 8 and 12 seconds and Hs = 1.7m.

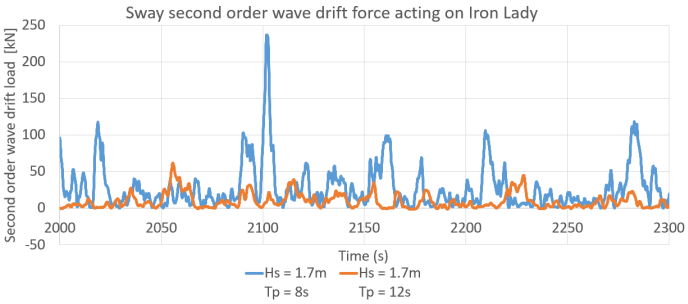

(a) Time series of second order wave drift load acting on *Iron Lady* for a Tp of 8 and 12 seconds

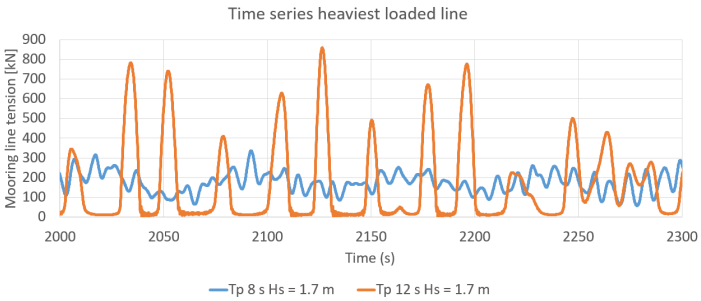

(b) Max loaded mooring line for a Tp of 8 and 12 seconds and Hs = 1.7m.

Figure 9.2: Second order wave drift force (left) and mooring loads (right) for Tp = 8 and 12 seconds.

9.3.3 Rayleigh distribution

Maximum Relative vessel motions and mooring line loads are assumed to be Rayleigh distributed. Validation and verification points out that relative motions can be assumed to be Rayleigh distributed. The maximum force in the mooring system brings in an inaccuracy up to 18 %, as pointed out in section 6.5.3. Nevertheless, maximum mooring line loads are assumed to be Rayleigh distributed because of its advantage of limited required computation time. To reduce the inaccuracy, the same seed (same wave train) is applied for every simulation.
It is strongly recommended to apply multiple wave trains, with equal statistic parameters, extract the maximum mooring load that occurs and use the extreme value.

Assuming the maximum mooring line load to be Rayleigh distributed allows to use equation 4.11 to compute the three hours maximum value. The number of cycles occurring in a three hour sea state, N, is related to T_z, the average period of the cycles that the mooring line crosses the mean load. Overall, mainly the low frequency force variation leads to crossing the mean load. Therefore, the number of cycles is found to be underestimated.
Depending on the contribution of the low frequency varying force, N was found to range between 500 and 1000 for the mooring systems consisting of mooring lines. While N was found to be in the range of 900 to 1100 for the MoorMaster system.
Considering equation 4.11, this leads to a 5 % difference of the value under the square root that will be multiplied with the standard deviation. Again depending on the force variation, the standard deviation, this lead to a maximum difference of 3.5 % in the maximum mooring line load which will have only a minor effect on the workability.
Large N results in a large force and is therefore more conservative. Therefore, the workability results of the MoorMaster system are conservative w.r.t. to the base case mooring system.

9.3.4 Stretcher length

The objective in this research was to assume each mooring line length to consist of 20 % stretcher and 80 % steel wire, implemented as a constant axial stiffness. The value for the axial stiffness is computed as the weighted average with respect to the ratio of steel wire and stretcher. This is incorrect and different from computing the overall axial stiffness considering the two line sections as serial springs. The correct method of computing the combined axial stiffness is explained in section 4.2.1.1
Due to this error, the axial stiffness implemented in this research corresponds with 3 % stretcher length, which means a relatively stiff mooring line.
To understand the effect of this error on the results, the time series of the relative sway motion and the line load in the heaviest loaded line is represented in Figure 7.5. Table 9.1 represents its effect on the workability and the relative sway motion. Three options are compared:

- 3 % stretcher length, **applied** to compute the results of this research.
- 20 % stretcher length, **initially intended to apply** in this research. This stretcher length ratio is realistic to be applied in industry.
- 20 m stretcher length in each mooring line. Therefore each mooring line has a different axial stiffness. This would be a **more realistic** input as the stretcher lines, available on board, have a fixed length.

Table 9.1: Effect of stretcher length on workability and relative sway position results for 135 ° environmental loading. The allowable three hour relative sway position amplitude is 1.0m above the offset. **The offset is excluded in the Three hour maximum relative position**.

	3% stretcher length	20 % stretcher length	20 m stretcher length
Workability Southern North Sea [%]	66.8	82.6	87.0
Workability Saint Naizare [%]	16.5	45.7	55.0
Results specifically for Tp = 8s			
3hr max force [% of SWL]	101	102	102
3hr max relative sway position [% of allowable]	42	81	101
Offset [m]	0.47	0.84	0.99

From Figure 7.5a it can be seen that shorter stretchers result in higher stiffness which reduces the amplitude of the second order motion in sway direction, as discussed in section 7.2.
From Figure 7.5b it can be seen that higher stiffness results in higher amplitude in the line tension, while the mean load is independent from the line stiffness.
From Table 9.1 it can be learned that for 20 % and 20 m stretcher lengths the workability increases w.r.t. 3 % stretcher length. This is because a softer mooring system results in lower amplitude in the mooring loads and therefore higher sea state can be applied before reaching the SWL, see Figure 7.5b. However, with the softer mooring system the sway offset and relative motions increase. Therefore as long as the motions are within limitations, a softer mooring line is preferred to have optimum workability.
Table 9.1 shows that the mooring system stiffness heavily affects the workability for swell areas. This is related to the fact that for swell waves the first order motions are more excessive as can be seen in the vessel RAOs, for *Iron Lady* shown in Figures 5.5. Because first order motions cannot be restricted by the mooring system, it is preferred to have a soft mooring system when subjected to high first order motions to limit mooring line loads due to first order motions.

This knowledge heavily affects the outcome of this research. To make a valid comparison between different mooring system concepts when considering the SWL limit, the relative motion at the limiting sea state should be in the same order for all sea states. It is found that for a lower system stiffness the motions increase while mooring loads reduce.
For the comparison of different mooring systems in this research, the relative motions at the limiting sea state were in the same range which makes it a fair comparison. It can be learned that in case a strict motion limit is given, the MoorMaster system provides best workability results. However, if the motion

limit is less strict, it is suggested to reduce the stiffness of the base case mooring system and analyse the performance of a softer MoorMaster system.

9.4 Concept-wise discussion on results

This section concisely discusses the relative motion, static force and the workability results of each mooring system concept.

- **Base case**. Reasonable results are found for the workability of the base case mooring system in wind seas. For swell seas however, the workability is rather low. This is mainly caused by the stiff mooring system and excessive first order motions for longer waves.
  Line 2, shown in Figure Figure 4.8, takes only a small load for all considered loading directions. Consequently this line can be reoriented to take more load, as done in the 'new line orientation' concept.
- **New line arrangement**. This concept shows similar results to the base case. Only a slight increase in workability is recognized for this mooring system, mainly in beam waves because one of the lines is more oriented in sway direction compared to the base case. Increased workability for beam seas reduces the severity of the risk that the optimal heading cannot be kept at all times. Where the optimal heading is 135°, providing maximum shielding.
- **Ship extender**. The ship extender shows promising results for beam waves. Because mooring lines at the barge stern are more oriented in sway direction. This increases operational resilience because the vessel heading won't be always perfectly at 135° but can shift to 90 °.
  In terms of practicality, the ship extender seems challenging with a structure extending 50m from *Pioneering Spirit* stern but it is possible. However, the increased risk of collision with an installed wind turbine (foundation) is expected to increase. For example due to an unforeseen yaw motion. The mooring procedure is slightly more complex because of the risk of a tug colliding with the ship extender, installing the mooring system is not expected to be affected.
- **Fairleads at hull side**. Placing fairleads along the hull shows comparable behavior and results as for the base case, which means no improvement here. Furthermore, the system becomes more complex and less practical.
  Initially, it was expected to have steep mooring lines because of the large difference in freeboard between *Pioneering Spirit* and *Iron Lady*. However, in this research there is only 6m difference due to the loading conditions. Next to that, fairly long mooring lines are incorporated, resulting in an angle of 4° with the horizontal at maximum. Therefore the mooring line force contribution due to the vertical component is rather low. So long lines solve the problem of difference in freeboard. However, this concept could work if rather short lines are incorporated.
- **MoorMaster system**. With its high workability in combination with rather low relative motions, the MoorMaster concept shows promising results. Only for 135° since for the other directions contributions from wind and current are excessive. In the workability study only one combination of stiffness and damping curve is analysed. Therefore, it is expected that the performance of the MoorMaster system can be further optimized by adjusting stiffness and damping properties.
  These promising results originate from the fact that this system can provide forces in perfect surge and sway direction and both in tension and compression at the same location on the vessel. This reduces the dynamic loads in the system.
  The reason why the system is working for 135° and not for 45° is because of asymmetry in MoorMaster devices on the barge. To make the MoorMaster concept work for 90° and 45° additional MoorMaster devices could be installed or system properties can be optimized for the specific loading direction.
  Due to lack of information from MoorMaster, no limits on relative velocity are known for the MoorMaster system. According to the MoorMaster company, the relative velocities incorporated in this model are acceptable.
  It would be interesting to model the MoorMaster system in combination with stiff fenders, this allows to use larger stroke to follow the vessel sway motion and might increase the workability in

case larger relative motions are allowed. In that case, the MoorMaster compressive stroke should equal the maximum expected fender compression to prevent for collision of the barge with the MoorMaster system
Additionally, it would be interesting to investigate the relation between installed capacity (number of MoorMaster devices) and the workability of the system.

It is recommended to further investigate combinations of various mooring system concepts. For example, combining the MoorMaster system with additional mooring lines. This improves the mooring procedure as the MoorMaster system can connect quick, safe and easy. The mooring lines can be added for redundancy and to increase the workability of the mooring system. Additionally, this system is expected to come with lower costs.

This research learned that first order motions cannot be restricted while low frequency motions can. It would be interesting to do future research into possibilities to designing a mooring system that can follow first order motions and restricts only the low frequency motions. The MoorMaster system would be a good starting point as its properties are software based, for example by implementing a low-pass filter that can detect and restrict certain motion frequencies.

10 Conclusion

Continuous development in the wind turbine industry leads to increasing size of wind turbines. Allseas investigates the possibility to enter the offshore wind turbine installation industry with the large sized multi-purpose vessel, *Pioneering Spirit*.
For Allseas' preliminary wind turbine installation design, wind turbines are assembled offshore, requiring wind turbine components to be brought from shore to *Pioneering Spirit* by means of a cargo barge. This requires a proper mooring procedure of which the mooring system is an essential part. The mooring system secures the barge alongside *Pioneering Spirit* where it has to stay for multiple days. In the pre-defined vessel orientation the barge stern is extended 40m in longitudinal direction from *Pioneering Spirit* stern, in order to increase the barge area reachable by the unloading crane to optimize barge unloading.

This lead to the main research question of this thesis how the mooring system to secure a barge alongside *Pioneering Spirit* can be improved, including evaluation of the dynamic loads. To answer this question, four sub questions arise. Starting with defining how the mooring system is involved in the mooring procedure and what design considerations hold? What methodology should be applied to build and validate a multi-body hydrodynamic model in the time domain, including a mooring system? One concept for improvement implements the state-of-the-art Cavotec MoorMaster system. A method should come up with to model this concept in the time domain model to describe reality as close as possible. Finally, a methodology is required to evaluate and compare various mooring system concepts to judge the performance of the mooring system concepts.

Question 1. The mooring system is part of the mooring procedure with the purpose to secure the barge alongside. The main design requirement is that the Safe Working Load and motion limits are not exceeded. On top of that, the goal is to maximize workability.
Considering 135 ° waves, extending the barge 40m from *Pioneering Spirit* stern does not increase wave loads on the barge compared to aligning the vessel sterns. However, the mooring system design for this barge position is challenging. More specifically, to restrict sway motions of the barge stern.

Question 2. Diffraction analysis is required to determine hydrodynamic data that describes the multi-body model and to provide first and second order forces. The software used in this research, Ansys Aqwa, applies potential flow theory to perform the diffraction analysis. Therefore, the outcome needs to be validated for the numerical effect of gap resonance and irregular frequencies. It is found that these numerical effects do not affect results in this research. Other required validation steps are mesh size convergence, the additional roll damping term to account for viscous damping.
Outcome from the diffraction analysis is imported in the time domain model, which enables to capture non-linearities such as wind, current and a non-linear mooring system. Most important time domain model validation steps are: comparing with results from the quasi-static analysis, time step convergence, analysing which hydrodynamic effects need to be taken into account and understanding the inaccuracy by computing the three hours maximum based on a shorter real time simulation length. Time domain modelling is performed in the dynamic software Orcaflex.

Question 3. One concept for improvement includes a MoorMaster system, consisting of devices that are rigidly connected to the barge, having a hydraulic cylinder with vacuum pads that connect to the vessel hull in 30 seconds. The MoorMaster system applied in this research consists of six MoorMaster devices in total, three orientated in surge and three in sway direction. The main advantages are that each device can exert both tensile and compressive forces at the same location. Furthermore, forces can be applied in perfect surge or sway direction and therefore reduce dynamic behavior in motions and loads.
The MoorMaster devices are modelled as links with stiffness and damping properties. Constant stiffness and damping is applied within the system limitations, outside the limitations stiffness and damping curves saturate. A sensitivity analysis on stiffness and damping properties is performed, learning that a trade off should be made between relative motions and mooring loads, regulated by system stiffness and damping.

Question 4. New mooring system concepts are compared to the base case mooring system. From the time series data, the three hours maximum relative motions and mooring loads are computed, this allows to find the limiting sea state. The workability corresponding with the limiting sea state and location specific metocean data, is used to compare the mooring system concepts. Two reference locations are defined, a wind sea area and swell sea area.
Besides waves, 25 knots wind and 0.9 m/s current is applied. These velocities correspond with workabilities of 99 % and 92.5% respectively, corresponding with the Southern North sea location. Wind and current speed is assumed to be constant over time and independent of elevation. All environmental conditions are applied co-linear and the main focus is on bow-quartering direction where *Pioneering Spirit* provides most wave shielding to the barge.
Via the mooring system, the low frequency motions can be restricted while the first order motions cannot. Therefore, swell wave conditions that lead to high first order motions are found to be challenging.

Two main philosophies of improvements discovered in this research are: optimizing mooring system properties of capacity, stiffness and damping, and optimizing the efficiency of using the mooring component capacity.
Leading to four concepts:

- 'New line orientation' where the orientation of mooring line is optimized to evenly divide mooring loads over all lines.
- The 'Ship extender' concept allows to restrict the barge stern in sway direction by creating a mooring line connection point that extends from *Pioneering Spirit*.
- The 'Fairleads at hull side' concept reduces the vertical force component in the mooring lines.
- The 'MoorMaster system' concept is a state-of-the-art system where system properties can be adjusted via software.

Results on relative motions show that the mooring systems analysed in this research are too stiff since the relative motions are far below the motion limit. This leads to low/conservative results on workability.
Results from evaluating the base case mooring system shows reasonable performance for the wind sea location and bad performance for swell areas, respectively a workability of 67 % and 16 %.
For each mooring concept the static load contributes about 45 % of the Safe Working Load and 55 % from dynamic load. Relative motions strongly depend on mooring system stiffness properties, the stiffnesses incorporated in the workability study leads to comparable relative motion for each mooring system concept. The relative motion limits are not exceeded.

Referring to the main research question, the mooring system can be improved where most promising results are found when implementing the MoorMaster system. The workability study shows that with incorporating the MoorMaster system, the workability for both reference locations can be increased by 15 and 24 % for wind and swell areas respectively. On top of that, the part in the mooring procedure of bringing the barge alongside is heavily improved. Furthermore, MoorMaster system properties are software based and therefore can be optimized for a specific environmental loading direction. Additionally, the capacity of this concept can be increased by increasing the number of MoorMaster devices.

Recommended further research is captured in three main points:

- **MoorMaster concept.** Delve deeper in the exact working principle of the MoorMaster system by further discussion with the Cavotec MoorMaster company and preferably compare numerical results with experimental data. Second, it would be interesting to extend the sensitivity analysis on MoorMaster system properties, e.g. how does the maximum reaction force due to damping relate to the three hours maximum load.
  An interesting addition to the MoorMaster system would be to combine fenders with the MoorMaster devices such that its main capacity can be used to apply tensile forces instead of compressive forces.
  To increase redundancy of the MoorMaster system, the combination with MoorMaster devices and Mooring lines could be analysed.
  Additionally, the relation between workability and number of MoorMaster devices should be checked in case of a feasibility study.
  The financial aspect of the MoorMaster system should be checked, to see whether it is a feasible solution.
- **Head waves.** Analyse the mooring system performance when the multi-body system is subjected to head waves. This way the performance is analysed for the most optimal wave direction 135° with a direction shift of 45° to 90 and 180 °
- The next step in the mooring analysis of these concepts would be to perform a redundancy check in order to comply with classification rules.

References

[1] *Kabinet wil windenergie op zee verdubbelen | NOS*. URL: https://nos.nl/artikel/2421669-kabinet-wil-windenergie-op-zee-verdubbelen.

[2] A. Sinke. *Mooring design , related to Pioneering Spirit Master of Science Thesis Literature research Mooring design , related to Pioneering Spirit Dynamic analysis and improvement of a mooring system to increase operability*. Tech. rep. Delft: Delft University of Technology, 2022, p. 100.

[3] J M J Journée and W W Massie. *Offshore hydromechanics first edition, TU Delft*. Tech. rep. 2001.

[4] Mingsheng Chen et al. "Effects of gap resonance on the hydrodynamics and dynamics of a multi-module floating system with narrow gaps". In: *Journal of Marine Science and Engineering* 9.11 (Nov. 2021). ISSN: 20771312. DOI: 10.3390/jmse9111256.

[5] Yujie Liu and Jeffrey M. Falzaranoa. "Irregular frequency effects in the calculations of the drift forces". In: *Ocean Systems Engineering* 9.1 (Mar. 2019), pp. 97–109. ISSN: 2093677X. DOI: 10.12989/ose.2019.9.1.097.

[6] Majid A Bhinder et al. "Modelling mooring line non-linearities (material and geometric effects) for a wave energy converter using AQWA, SIMA and Orcaflex". In: *Proceedings of the 11th European Wave and Tidal Energy Conference* October (2015), pp. 1–10.

[7] Oil Companies International Marine Forum. *Mooring equipment guidelines : (MEG3)*. Witherby Seamanship International, 2008, p. 278. ISBN: 9781905331321.

[8] Moormaster Company. *MoorMaster ® Mooring system*. Sept. 2021.

[9] S.Sonethavy and V.Cazenave. *WOS-T&I_RFE-026_Haliade-X_WIV Requirements for Installation Rev.02*. Tech. rep. General electric company, 2020.

[10] *MoorMaster™ NxG Automated Vacuum Mooring. A New Generation*. URL: https://www.moormaster.com/.

[11] *Offshore mooring design basics*. URL: https://www.mermaid-consultants.com/offshore-mooring-basics.html.

[12] *Hollandse Kust (zuid) Wind Farm Zone Wind Farm Sites I & II Project and Site*. Tech. rep. Utrecht: Netherlands Enterprise Agency, Oct. 2017.

[13] *Hindcast ²*. URL: https://app.metoceanview.com/hindcast-squared/#/.

[14] Robert H Stewart. "Physical oceanography". In: *Deep Sea Research Part B. Oceanographic Literature Review* 34.8 (1987), pp. 629–645. ISSN: 01980254. DOI: 10.1016/0198-0254(87)95466-5.

[15] Tessa Gordelier et al. "Investigating polymer fibre optics for condition monitoring of synthetic mooring lines". In: *Journal of Marine Science and Engineering* 8.2 (2020). ISSN: 20771312. DOI: 10.3390/jmse8020103.

[16] Hugh Sercliff Michael Ashby and David Cebon. *Materials engineering, science, processing and design*. 3rd ed. Cambridge, UK: Elsevier, 2014, p. 637. ISBN: 978-0-08-097773-7. DOI: https://doi.org/10.1016/S1369-7021(10)70042-0.

[17] Steven Wardeneier. *Lankhorst Ropes, the master of innovation in ropes*. 2012.

[18] Trelleborg Marine Systems. *Safe berthing and mooring*. 1.2. Trelleborg, Sweden: Harrison Sigala, 2008.

[19] Sang Min Park et al. "Effect of pneumatic rubber fenders on the prevention of structural damage during collisions between a ship-shaped offshore installation and a shuttle tanker working side-by-side". In: *Ships and Offshore Structures* 0.0 (2022), pp. 1–13. ISSN: 17445302. DOI: 10.1080/17445302.2022.2085898. URL: https://doi.org/10.1080/17445302.2022.2085898.

[20] American Bureau of Shipping. *Position Mooring Systems*. Tech. rep. 2020. URL: www.eagle.org.

[21] internal Allseas. *Mooring rope equipement available Pioneering Spirit*. Tech. rep. 2014. URL: http://www.daekwang.net.

[22] "General guidelines for marine projects". In: *DNVGL-ST-N001* (2015).

[23] R Feenstra. *R. Feenstra*. Tech. rep. 2018.

[24] *Dynamic analysis: Time domain solution*. URL: https://www.orcina.com/webhelp/OrcaFlex/Content/html/Dynamicanalysis,Timedomainsolution.htm.

[25] Myung-IL Roh. *Free Surface Effect*. Tech. rep. Seoul: Department of Naval Architecture and Ocean Engineering Seoul National University, 2016.

[26] Hooshang Radfar. *Investigating the first order motions of the cargo barge inside the slot of Pieter Schelte*. Tech. rep. 2015.

[27] Lingzhi Xiong et al. "Motion responses of a moored barge in shallow water". In: *Ocean Engineering* 97 (Mar. 2015), pp. 207–217. ISSN: 00298018. DOI: 10.1016/j.oceaneng.2015.01.018.

[28] MARIN. "Pieter Schelte Model Tests". In: ().

[29] Xin Xu et al. "Time-domain simulation for coupled motions of three barges moored side-by-side in floatover operation". In: *China Ocean Engineering* 29.2 (Apr. 2015), pp. 155–168. ISSN: 08905487. DOI: 10.1007/s13344-015-0012-4.

[30] ANSYS Aqwa-Line Manual. "Aqwa™-line manual". In: April (2009).

[31] Imanol Touzon et al. "Frequency domain modelling of a coupled system of floating structure and mooring Lines: An application to a wave energy converter". In: *Ocean Engineering* 220 (2021). ISSN: 00298018. DOI: 10.1016/j.oceaneng.2020.108498.

[32] Symposium On, S U P Treqry, and W.E. Cummins. "The impulse response function and ship motions". In: January (1962).

[33] Orcina. *C09 Fenders*. Tech. rep., pp. 1–2.

[34] Kai-Tung Ma et al. *Mooring System Engineering for Offshore Structures*. 1st ed. 2019. ISBN: 9780128185520.

[35] *Vessel theory: Wave drift and sum frequency loads*. URL: https://www.orcina.com/webhelp/OrcaFlex/Content/html/Vesseltheory,Wavedriftandsumfrequencyloads.htm.

[36] Amin Ghadirian et al. "Wave-current interaction effects on waves and their loads on a vertical cylinder". In: *Coastal Engineering* 165 (Apr. 2021). ISSN: 03783839. DOI: 10.1016/j.coastaleng.2020.103832.

[37] *General data: Implicit integration*. URL: https://www.orcina.com/webhelp/OrcaFlex/Content/html/Generaldata,Implicitintegration.htm.

[38] J.Chung and G.M.Hulbert. *A Time Integration Algorithm for Structural Dynamics With Improved Numerical Dissipation: The Generalized-alpha Method*. Tech. rep. Michigan: The university of Michigan, 1993. URL: http://asmedigitalcollection.asme.org/appliedmechanics/article-pdf/60/2/371/5463014/371_1.pdf?casa_token=_MBHvT5a9nAAAAAA:S1UBJi-qWY-KydKMY1EkzPcWT1a91-Z3tGLMqCDj-olKHhv5QsitG-uGO_10nVkOI_-4kxg.

[39] John Groen and Nicklas Vedin. *Meeting with Cavotec Moormaster*. July 2022.

[40] DNV GL- CP-205. *DNV-RP-C205: Environmental Conditions and Environmental Loads - Recommended Practice*. Tech. rep. April. 2014. URL: www.dnvgl.com..

[41] J.N.Newman. *Marine Hydrodynamics*. 40th anniv. London: MIT press, 2017. ISBN: 9780262534826.

[42] *Pneumatic Rubber Fender Triangle - Tenwolde*. URL: https://tenwolde.com/sales-rental/fenders/pneumatic-rubber-fenders/pneumatic-rubber-fender-triangle/.

[43] W E Zwart. *Delft Offshore and Dredging Engineering Analysis of Ship Motions in Shallow Water Development of a numerical tool for fluid-structure interaction in shallow water*. Tech. rep.

[44] O.M. Faltinsen. *Sea loads on ships and offshore structures*. First. Cambridge, UK: University of Cambridge, 1993, p. 166. ISBN: 0521458706.

[45] DNV GL As. *CLASS GUIDELINE Wave loads*. Tech. rep. 2018. URL: http://www.dnvgl.com,.

[46] *Beaufort Wind Scale*. URL: https://www.wpc.ncep.noaa.gov/html/beaufort.shtml.

[47] *Safer mooring; efficient and sustainable operations*. Tech. rep.

[48] A C M Vreeburg. *ShoreTension as cargo handling system: controlling the relative horizontal motions between the HTV and the cargo during offshore loading and discharge*. Tech. rep.

A Literature

A.1 Chapter Reviews from the literature report

This section includes a brief review and summary of every chapter, these chapter reviews are copied from the literature report. Upon interest the reader can decide which chapter to dive further into. The literature report can be send as an additional report to this Master Thesis report.

A.1.1 Review chapter 2 - Hydrodynamics

Waves are generated by multiple sources, mainly due to wind and the motion of floating bodies in close proximity. Waves can mathematically be described as a sinusoidal function with an amplitude, frequency and phase.
Force and motion RAOs describe the first order wave force and motion as function of incoming wave amplitude. Wave spectral density describes the wave energy per wave frequency for an irregular wave pattern, a JONSWAP wave spectrum can be applied for the North Sea.

First order motions have zero mean by itself, while the low frequency motions, induced by second order wave drift forces, have non-zero mean. Combining first order and second order motions results in an first order motion around the low frequency second order motion.
The buoyancy forces causes a hydrostatic force in heave, roll and pitch motion.
Ship stability depends mainly on relation between the location of the CoG and the Center of Buoyancy. Partly filled ballast tanks reduce the ship stability.
Hydrodynamic first order forces has three contributions. First, the force due to the incoming wave, also known as Froude-Krilov force. Second, a diffraction force accounting for the fact that the incoming wave is disturbed by the floating body. Third, waves that are generated due to motion of the body, called radiating waves. These radiation effects are captured in the added mass and damping matrices.
Wave forces can be computed by describing the incoming wave as a wave potential, rewrite the wave potential to a pressure distribution by applying the Bernoulli equation. The forces and moments can be found from integrating the pressure distribution over the surface area. These wave potentials can be found from radiation and diffraction software based on potential theory.

Similarly second order wave drift forces can be determined. Wave drift forces can be written as a function of the wave amplitude squared, referred to as Quadratic Transfer Function (QTF). The Near Field and Far Field method are common known methods to compute the QTF. The Near Field approach solves the QTF by setting a small domain and applying boundary conditions around the circumference of the structure. This method takes more computational effort but also more accurate results compared to the Far Field method. The Far Field approach takes a large domain with boundary conditions far away from the structure. This simplifies the problem since the integration boundaries are less comprehensive. For a multi-body system the Near Field approach is required to compute QTFs for IL and *Pioneering Spirit* separately.

The mean second order wave drift force is located on the diagonal entries of the QTF. Difference and

frequencies are stored in the off-diagonal entries of the QTF. QTFs are computed for different frequencies, degrees of freedom and incoming wave direction. The QTF consists of five contributions.

A.1.2 Review chapter 3 - Numerical modelling

Three different modelling domains are commonly used to analyse a mooring system, respectively a quasi-static, frequency and time domain model. In the quasi-static model only the static problem is solved whereas in the frequency and time domain model the dynamic problem is solved. The solving method that is required depends on the type of mooring system and the operating conditions. These requirements are defined by classification companies, for example DNV.
Quasi-static analysis solves the static problem and disregards all dynamic effects. Safety factors for the mooring line forces are required in case a quasi-static analysis to account for the dynamic effect.
In the diffraction analysis, the body motions are computed by solving the equations of motion for varying the frequency and incoming wave direction. The equation of motion includes the mass and stiffness matrix, together with the frequency dependent added mass, damping matrix and forcing term determine. Only linear relations can be captured in frequency domain. Since non-linear loads have to be taken into account for modelling a mooring system, time domain modelling is required.

For this thesis, the radiation diffraction solver, Ansys Aqwa, is used to determine the hydrodynamic parameters of the multi-body system. The solving method is based on potential theory which includes three main assumptions, the flow is assumed to be non-viscous, irrotational and incompressible.
Potential theory applies a number of boundary conditions in order to be able to determine the fluid potential around the structure, for each frequency. First, assuming the flow to be continuous and incompressible leads to the fact that the Laplace equation should be satisfied. Second, no leakage will occur at the seabed. Third, at the water surface the pressure will be atmospheric. Fourth, the normal component of the particle velocity at the free surface is equal to the free surface fluid velocity. Fifth, infinitely far away from the structure, the radiation potential will be zero. The same boundary conditions holds for the second order effect, only in a more comprehensive way.
The floating body is divided into a number of panels, called a mesh. From this fluid potential, the source strength at every panel is computed for different frequencies and incoming wave directions. From this source strength, the pressure distribution over the floating body can be determined which enables to calculate the first order wave forces. From these first order wave forces, the first order motions can be computed via the equations of motion.

Performing the diffraction analysis for a multi-body system is known to be subjected to the numerical challenges of gap resonance and irregular frequencies. The gap resonance effect occurs due to the fact that viscosity is neglected in the radiation and diffraction software, leading to unrealistic wave heights in the gap between the bodies. Several methods exists to correct for the gap resonance effect, in this thesis a damping lid will be added. This damping lid accounts for viscosity by adding an additional boundary condition to the free water surface.
Irregular frequencies are caused while determining the source strength at a panel. This method includes computing the determinant of a matrix. For some frequencies, the determinant happens to be zero, leading to unrealistic source strengths. This results in unrealistic spikes in the hydrodynamic matrices and also the RAOs. Similar as for the gap resonance effect, also for irregular frequencies several methods can be applied to remove these. Most commonly an internal damping lid, comparable to the damping lid for the gap resonance effect, is applied.

The time domain model solves the equations of motion as a function of time. This requires comprehensive steps to be taken to transform hydrodynamic data, that is found from the diffraction analysis, into the time domain modelling. This way the diffraction analysis and time domain models are connected.
The dynamic software package Orcaflex will be used to create the time domain model.

A.1.3 Review chapter 4 - Multi-body dynamics

The equation of motion that is solved in the domain consist of the constant mass and stiffness matrix, a time dependent added mass and damping matrix and a time dependent forcing vector. The equation of motion is solved at every time step.
Exciting a body at its natural frequency causes excessive motions. At this resonance frequency, mainly the amount of damping in the system determines the maximum excitation. The damping can be defined as percentage of the critical damping of a system. Taking damping into account leads to a small deviation of the natural frequency.

Added mass is defined as the virtual mass added to the system when moving through a fluid. Added mass takes into account that water particles surrounding the floating body have to be accelerated when moving through a fluid.
Damping extracts mechanical energy from the system when being in motion. There are multiple sources of damping which can be subdivided in potential and viscous damping. Potential damping has its main contribution from wave radiation. Viscous damping is added manually because the radiation diffraction solver is based on potential theory and so neglects viscosity. Only viscous roll damping is added for slender structures, damping in other DoF can be neglected.

Many different (hydro)dynamic effects exist, with each its own contribution to the vessel motion and its contribution to the complexity and computation time of the system. A limited number of these effects are included in the quasi-static model. Data required to compute some of the hydrodynamic effects, e.g. first order wave forces, is computed in the diffraction analysis. Most of the hydrodynamic effects, described in this thesis, are included in the time domain model. Effects that are considered outside the scope of this thesis are excluded from the numerical models.

Radiation and diffraction terms are captured in the hydrodynamic, added mass and damping, matrices. Wave forces consist of first order and second order wave drift forces. For the second order wave drift forces the full QTF can be taken into account where the diagonal terms describe the mean forces, the lower triangle off-diagonal terms describe the low frequency wave drift forces and the upper triangle terms describe the sum frequency terms. Additionally wave drift damping can be included by modifying the QTF. This modification is based on the ratio between the frequency corresponding with the specific entry and the peak frequency of the incoming wave spectrum.
Current and wind forces depend on the subjected area, drag coefficients and velocity relative to the structure. The current drag coefficient depends on the under water vessel shape. The wind drag coefficient depends on the above water shape of the vessel, including the deck loading.

The interaction effect of the mooring line can either be included in the total system matrices or added as additional forcing terms as separate matrices.
Water depth is heavily affecting added mass and damping matrices in case of shallow water conditions.

A.1.4 Review chapter 5 - Mooring

The conventional way of mooring, including mooring lines and fenders, has been applied for a long time and still works today. However, this method is known to be time consuming and can lead to unsafe situations. Therefore innovative concepts are entering the market or already on the market.
Cavotec Moormaster, later referred to as 'Moormaster', is one of those, having developed a system which restricts vessel motions by connecting a large vacuum pad. This vacuum pad is fixed to a hydraulic arm, with variable stiffness and damping properties that can be adjusted via software. The Moormaster system is usually fixed to the quayside. However, there is potential in applying this Moormaster system in side-to-side mooring configurations in offshore conditions.
Next to the Moormaster system, using vacuum pads, Cavotec also developed a system with the same working principle but instead of vacuum pads using electromagnetic pads. This system is known as the Cavotec Dock Lock system.

Another state-of-the-art mooring system is the Shore-Tension system. This system consists of a hydraulic cylinder that is attached to one end of the mooring lines, while the other end is attached to a fixed point, for example a mooring winch with a brake applied. This hydraulic cylinder has variable stiffness. Because of that, the Shore-Tension system can keep constant tension at the mooring line. The purpose of this system is that it can heavily reduce vessel motions.

For the conventional mooring system, mooring line material properties together with the fender properties determine the mooring system properties, stiffness and damping. Usually, mooring lines consist of two sections, one longer section which is stored on the winch, additionally a smaller section, the so-called stretcher, can be added to create the best mooring line properties. The main purpose of adding the stretcher line is to adjust the line stiffness and to create a weak link. This weak link is preferred as it is easier and cheaper to replace the stretcher line instead of replacing the whole mooring line that is stored on the winch.
Snap loads in the mooring system have to be prohibited by applying proper pre-tension.
Fenders in the mooring system prevent for collision between separate floating bodies. This is done by providing a reaction force upon compression.

Anchoring can be a good way for barge mooring in relatively shallow waters. Criteria for determining the optimum anchoring method are: soil conditions, water depth, required anchoring time and costs.
Towing operations should preferably be executed by tugs or Anchor Handling Tug Supply vessels. The most important requirement for a tug is the maximum bollard pull that can be delivered to the towed structure. Several towing arrangements exists, the towing arrangement is designed based on the available tugs, bollard pull, the precision that is required for the operation and the environmental conditions that are expected to occur.

A.1.5 Review chapter 6 - Multi Criteria Analysis

The Multiple Criteria Analysis is a structured way to determine which concept is most suitable based on the criteria that is defined, the criteria ranking and the concept ranking. The multiple criteria analysis can be applied to decide which mooring procedure improvement is best.
The set of criteria can originate from different scopes, a scope is for example safety. These criteria can be ranked by performing an Analytical Hierarchy Process which gives each criteria its own weight.

A.1.6 Review chapter 7 - Workability

Workability is defined as the annual percentage of time that an operation can be performed within the operational limits.
To determine the workability, a reference location has to be defined consisting of sufficient metocean hind cast data.

Irregular waves are assumed to be Gaussian distributed provided that the water surface has zero mean and a narrow banded frequency range. If that is satisfied, the extreme wave elevation can be assumed Rayleigh distributed. This enables to compute the expected three hours maximum single amplitude motion from the zeroth spectral moment, which can be computed from the spectral density. The three hours maximum single amplitude is defined as the maximum amplitude that passes by in a three hour lasting sea state.
The same approach can be applied to determine the three hours maximum mooring line loads in the time domain simulation. The only difference between computing the three hours maximum in the frequency domain and in the time domain is that for the time domain, the zeroth spectral moment is computed from the standard deviation of the time history data, while in the frequency domain the zeroth spectral moment is directly calculated from the spectral density.

To calculate the workability, first the maximum allowable sea state is determined. The maximum allowable sea state corresponds with the sea state at which the, three hours maximum forces in the

mooring system are close to the safe working load. Based on the maximum allowable sea state and the wave scatter diagram for the reference location, the workability can be found.

A.2 Reflection on literature report

After the introduction, the second chapter starts with basic theory. Hydrostatics, hydrodynamics and linear wave theory is applied in this thesis. This basic theory forms the basis for the rather complicated hydrodynamic (interaction) effects.
First order wave forces are described by amplitude, frequency and phase. These waves have zero mean. The first order wave force has three contributions that are important in this thesis, incoming wave force, radiation and diffraction force.
Besides first order, second order wave drift forces are important for a side-to-side offshore mooring system. These second order wave drift force are captured in the Quadratic Transfer Function (QTF). The mean second order wave drift force is on the diagonal entries of the QTF matrix. The QTF matrix is determined in the radiation and diffraction software and depends on frequency and incoming wave direction. The QTF is included in this thesis and determined based on the near field approach.
A frequency domain model only includes linear effects. Since non-linearities need to be incorporated when evaluating the dynamic loads in the mooring system, time domain modelling is required.

The third chapter discusses the numerical modelling. Numerical modelling is used to dynamically evaluate the mooring system concepts, based on the maximum mooring line force that occurs in a three hour sea state.
The modelling phase will start with a quasi-static analysis to simply start understanding the system.
The radiation and diffraction solver Ansys Aqwa, that is based on potential flow theory, is used to perform the diffraction analysis. The output, which consists of load and displacement RAOs and hydrodynamic matrices, will be imported in the time domain model. The time domain modelling is performed in the dynamic analysis software, Orcaflex. Orcaflex is able to solve the hydrodynamic problem while including non-linear effects.
Offshore bodies floating in close proximity are prone to numerical challenges, including the gap resonance effect and irregular frequencies. These challenges can be helped with applying a damping LID, which adds a boundary conditions to the fluid flow.
Both challenges occurred in the numerical models build in this thesis. Its effect will be analysed in the final report.

The fourth chapter is about the dynamic interaction of floating structures in close proximity. Mooring system forces depend on the mooring system properties and the relative body motions. The body motions are described by their equations of motion. Consisting of system matrices, among which the frequency dependent hydrodynamic matrices, added mass and damping. These hydrodynamic matrices are determined with the diffraction analysis.
The first order radiation effects lead to interaction of both vessels that are in close proximity. These radiation effects are included in the added mass matrix.
Damping consist of potential and viscous damping. Due to the large size structures in this thesis, potential damping has the largest contribution and viscous damping can be neglected.
The second order wave drift force and second order wave drift damping, the first order loads and the constant wind and current loads and also the water depth are considered important effects for considering the forces in the mooring system.
Chapter 5 goes into detail about the mooring system. The purpose of a mooring system is to restrict relative vessel motions. For the conventional way of mooring, including mooring lines and fenders, material properties are key in determining the mooring system properties. Current state of the art mooring systems are used as source for mooring system improvement ideas.
Snap loads are not considered as these are assumed to be prohibited by applying correct pre-tension in the system, following guidelines from classification companies.

Chapter 6 provides a method how to compare several mooring procedure concepts. The MCA can be applied to compare mooring procedure concepts. The first step is define the important scopes, for example safety. Second step is to determine the criteria for each scope. Criteria is defined 'would like' to be satisfied. Whereas the mooring procedure requirements have to be satisfied. The set of criteria can be ranked with applying the Analytical Hierarchy process, giving each criteria its own weight. In the end each concepts can be scored for all the criteria.
Throughout this thesis, the focus shifted from improving both the mooring system and procedure towards mainly improving the mooring system. Therefore, in the final thesis report, only minor attention is paid to the MCA.

Chapter 7 explains how the mooring system concepts can be compared. Using workability. Workability is defined as the annual percentage of time that an operation can be performed within the operational limits. The workability can be computed from the limiting sea state and the metocean data at the reference location. At the limiting sea state, the mooring system SWL is reached. The maximum mooring line force is determined for a three hour sea state. The metocean data includes wave scatter diagrams ad wind and current data.

B
Mooring procedure

The scope of the mooring procedure ranges from a barge leaving the harbour up to barge disconnecting from *Pioneering Spirit* after it is successfully unloaded.
This procedure heavily depends on the experience and know-how of the crew involved.

This chapter addresses the full scope of improving the mooring procedure, as represented in Figure B.1. Starting with the purpose of the mooring procedure and describing the equipment that is involved. After that, the design requirements and criteria can be determined.
The base case mooring procedure will be explained, followed by a risk assessment and explanation of the Multiple Criteria analysis.
Then a single mooring procedure concept will be provided as suggestion for improvement. Finally, the base case and the improved concept will be scored.

The purpose of this chapter is mainly providing food for thought and going through the method to improve a mooring procedure.
The main focus of this thesis is on improving the mooring **system** as described in the main report. However, the mooring system is strongly related to the mooring procedure scope and therefore cannot be left out.

B.1 Stepwise approach

The stepwise approach to improve the mooring procedure includes:

1. Define requirements for the offshore mooring procedure of a cargo barge, related to transport of wind turbine components.
2. Define the base case mooring procedure.
3. Perform a risk assessment for the mooring procedure.
4. Come up with concepts for improving the mooring procedure.
5. Perform a Multiple Criteria Analysis (MCA) for the mooring procedure concepts.
6. Conclude and discuss whether the mooring procedure is improved, based on the MCA.

This stepwise approach shows the method that is applied to improve the mooring procedure. Improving the mooring procedure is analysed at a higher level, as the focus of this thesis is on improving the mooring system.

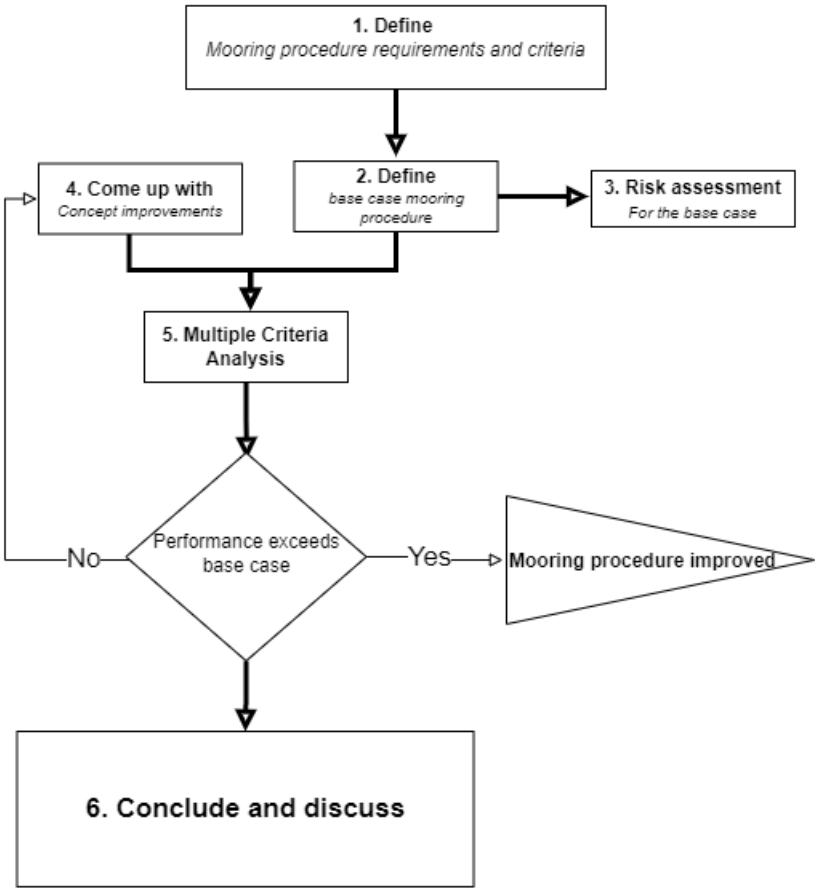

Figure B.1: Flow diagram showing the thesis approach to improve the mooring procedure.

B.2 Purpose of the mooring procedure

To assure a continuous wind turbine installation operation. The process of transporting wind turbine components should be continuous. This can be realised with a well designed mooring procedure.
The main purpose of the mooring procedure is to safely transport wind turbine components from shore to *Pioneering Spirit* which is located at an offshore location. The mooring procedure cycle closes when the barge is brought back after it is fully unloaded. The mooring procedure is explained step by step in section B.6.

B.3 Equipment involved

The design requirements mostly depend on the equipment that is involved in the operation. Like the weak link principle, the most limiting equipment determines the mooring procedure design requirements. The equipment involved is described in chapter 2.

B.4 Design requirements

This section represents the most important design requirements defined for the mooring procedure. Design requirements start with following the design codes as defined by the classification company, for

example DNV. The requirements related to offshore operations are based on long term experience and are well described in the DNV design code DNV-ST-N001, [22].
There is a narrow gap between design requirements and design criteria. Requirements must to be satisfied for each mooring procedure concept. While criteria can be seen as 'would like to have' specifications. For example, the mooring procedure should enable that the barge can be fully unloaded, which is a requirement. The criteria, related to this, is optimizing efficiency of the barge unloading operation. The mooring procedure criteria will be discussed in the coming section.

1. Health, safety and environment must satisfy classification requirements at all times, with health of personnel as highest priority.
2. The mooring procedure has to enable that all wind turbine components are unloaded from the cargo barge.
3. To assure a continuous operation, the mooring procedure should be applicable to multiple barge sizes.
4. Barge loading requirements.

B.4.1 Health, Safety and Environment

Health, safety and environment (HSE) is a very comprehensive requirement with many interfaces and therefore requires to be further defined.
It is considered outside the scope of this thesis to discuss the entire HSE scope in detail. There will only be touched upon the most important HSE aspects related to a mooring procedure.
Safety of personnel, health, has priority at all times. As humans are involved in the mooring procedure, human errors cannot be disregarded, which means that injuries might happen. Fatalities however, should be prohibited at all costs. Fortunately there is always a HSE officer and Marine Warranty Surveyor involved in any offshore operation who are responsible for safe operation.
Safety includes bringing wind turbine components intact from shore to the offshore located wind turbine installation vessel. This scope includes for example redundancy of the towing operation. But also that correct planning while considering the weather forecast.
Environmental impact needs to be satisfy regulations in accordance with DNV, [22], environmental impact should be minimized and/or compensated for. This scope includes for example the treatment of ballast water, taking ballast water in at location A requires ballast water treatment before it can be discharged at location B to prevent for disturbing the local environment.

To emphasize on the fact that the safety requirement is very comprehensive, consider contingencies that exist in reality. Example contingency cases are: failure in mechanical or electrical systems, e.g. a mooring winch, DP capability reduction, leakage or flooding, structural failure, pollution, human errors, Man overboard and many more.
Several methods exist to secure safe operation while accounting for these contingencies. For example regarding structural integrity, the Load Resistance Factor Design method can be applied. For this method, load safety factors can be incorporated to account for uncertainties.
More on HSE will follow in the concise risk assessment in section B.7.

B.4.2 Unloading

The main purpose of the mooring procedure is to bring wind turbine components from shore to the installation vessel that is located offshore. This adds the requirement that the barge, bringing these wind turbine components, needs to be able to be fully unloaded.

One cargo barge is expected to be able to bring approximately 8 disassembled wind turbines. Considering the weights and sizes of tower, nacelle and blades learns that the towers and nacelle's should be lifted within the relatively small radius of the 5000 tons crane. The blades however, can be lifted with a large crane radius due to the low weight and height.
The rather straightforward design requirement of barge unloading becomes challenging when considering the crane location on the installation vessel, represented by the blue 'x' in Figure B.2.

Figure B.2 shows the orientation of the vessels and the location of the 5000 and 600 ton cranes at *Pioneering Spirit*, including their large and small reach.
The total area that can be reached in the orientation as shown in Figure B.2, is estimated with use of a Monte Carlo simulation. The Monte Carlo simulation generates a random number, uniform distributed, number for x and y in the range of the barge boundaries. This location is checked to fall within or outside the defined circles.

In case of using *Iron Lady* as a cargo barge, aligning the stern of both the barge and *Pioneering Spirit* results in 48 % of the barge area reachable with the small crane radius of the 5000 tons crane.
This limits the requirement of fully unloading the cargo barge.
Several solutions can increase the reachable barge area. One of them is to extend the barge from *Pioneering Spirit* stern, in longitudinal direction. Another option is to design a skidding system on the barge to shift the wind turbine components over the barge. Also rotating the barge 180° around the z- axis during the operation could be an option.
Within Allseas, it is defined to include the first option in the scope of this thesis, meaning that the barge will extend for 40 m from *Pioneering Spirit* stern.
This results in that approximately 65 % of the barge area can be covered for components that require a small crane radius and 80% for parts that suffice with a large crane radius. This estimation is based on 10E6 Monte-Carlo iterations.
The exact figures of barge area that can be reached in this configuration and the component weight and size that are considered cannot be shared as this data is confidential.
Figure B.2 represents the vessel orientation with *Iron Lady* extending from *Pioneering Spirit* stern.

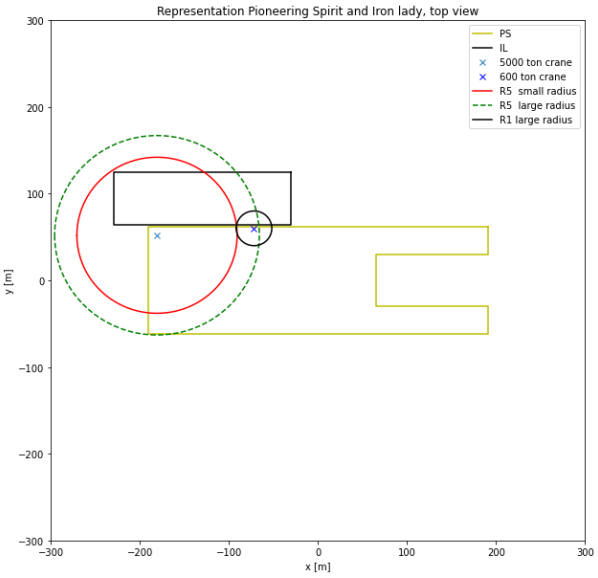

Figure B.2: Vessel orientation showing the area on the barge that can be reached in case of the barge being 40 m extended from *Pioneering Spirit* stern. Large crane radius corresponding with lifting small, low weight parts. Small crane radius vice versa.

B.4.3 Continuous operation

To have a continuous operation, the mooring procedure should be applicable to multiple barge sizes because it will not always be a similar sized barge that brings the wind turbine components.
For example the towing operation should be made applicable but also the capacity of the equipment that is involved, for example the anchor lines.
For this thesis however, only *Iron Lady* will be considered.

B.4.4 Barge loading requirements

Wind turbine towers have to stay upright at all times, this has to do with electronics inside the tower. This requirement constraints especially the barge transport, crane handling an installation phase.
Besides the motions, position, velocity and acceleration, for the wind turbine components are limited. These limits are not included within the scope of this thesis.

B.5 Design criteria

The most important design criteria is financially related, a very intricate criteria as it touches many interfaces. The criteria can be defined as: the costs related to the mooring procedure should be optimized. Some interfaces are listed below of which the most important ones will be discussed.

1. Minimize the number of (standby) tugs required.
2. Minimize complexity of the mooring procedure, strive to simple operations.
3. Reduce lead time and operation time.
4. High robustness against heavy environmental conditions, increase workability.
5. High resilience in case of emergencies.
6. Assure continuity for the wind turbine installation process.
7. Minimize environmental impact.
8. Minimize risks in the mooring procedure.

Minimizing the use of tugs does not necessarily reduce the total operation costs, as the use of tugs could increase the workability of installing the mooring system and reduce lead time which, this could lead to increased profits. Besides, increasing the number of tugs could improve the workability of the mooring system which means that the barge can stay alongside during more extreme sea states. Furthermore, a minimum number of tugs has to be involved to assure safe operation.

The mooring procedure can easily become complex, for example when multiple different companies are involved or many different equipment components with low reliability.
It is important that in case of emergencies, the mooring procedure can be adjusted to the emergency and satisfy the HSE requirement at all times.
Continuity of the wind turbine process contributes to the overall workability. This requires for example that at all times wind turbine components should be available.
The environmental impact on an offshore operation should preferably come down to zero. As this statement is rather theoretical, the environmental impact has to be minimized and if possible compensated.
From the risk assessment, the risks will be expressed in probability, severity, precautions and mitigation's, as will come in section B.7. The risk that the mooring procedure brings should considered when designing and evaluating mooring procedure concepts.

B.6 Base case mooring procedure

The mooring procedure can be simplified in four different steps. Respectively; transit, approach, mooring and finally unmooring after the barge is fully unloaded.
A schematic overview is shown in Figure B.3. The improved mooring procedure will be explained in detail in section B.9.

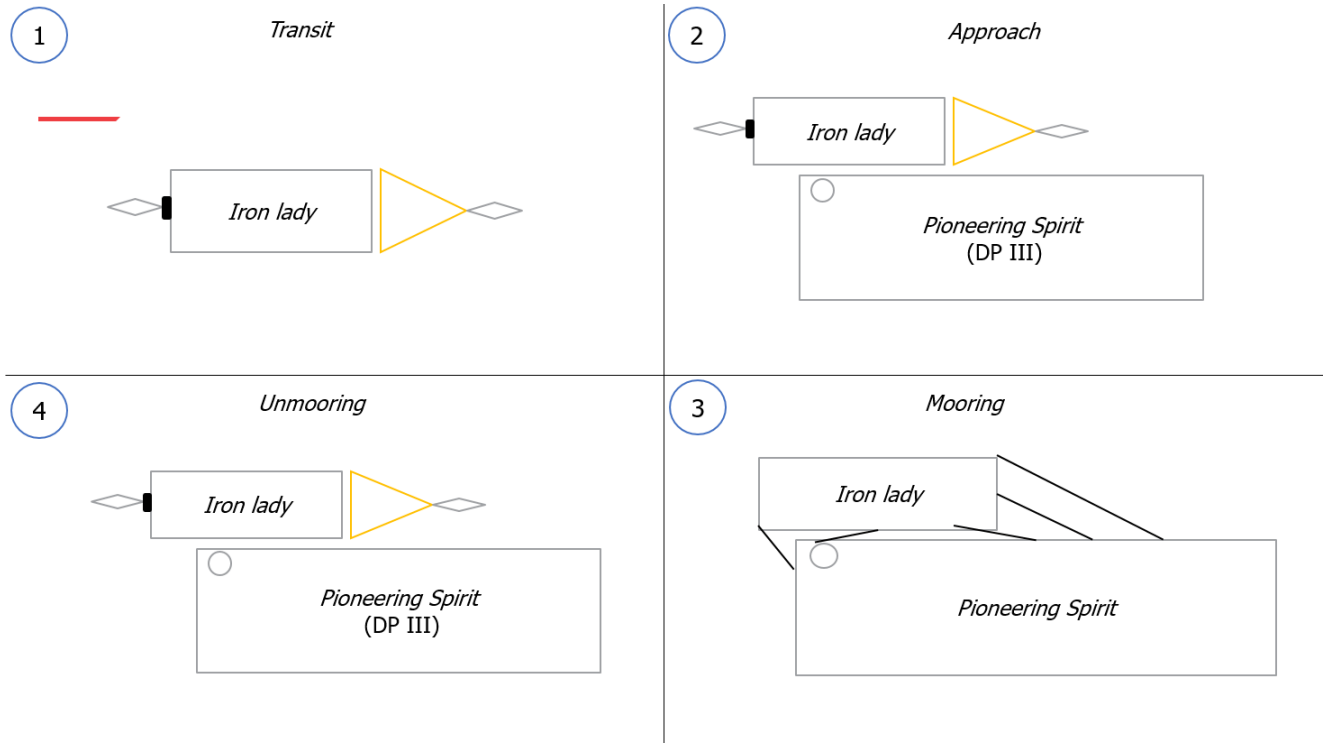

Figure B.3: Simplified mooring procedure represented in three steps

B.6.1 Heading control

To reduce forces in the mooring system during the wind turbine installation procedure, full heading control would be preferred to maximize shielding of the barge from *Pioneering Spirit*. Optimum shielding results in optimum workability of the mooring system.
The orientation in how the wind turbine is installed onto the foundation is fixed. However, the required heading of *Pioneering Spirit* can be set by the orientation of how the wind turbine tower is connected to the wind turbine assembling equipment.
Assuming that assembling the wind turbine will take 24-48 hours, and giving the fact that the weather forecast is reliable 24-48 hours in advance. It can be said that optimum heading can be assured throughout the operation.

B.6.2 Step 1 - Transit

Transit is defined as the transport from shore to the installation vessel that is located offshore. Three tugs will be required to bring the barge from the fabrication yard towards the wind farm where *Pioneering Spirit* will already be located.

B.6.3 Step 2 - approach

Usually three to four tugs are used to bring the barge alongside. The number of tugs required depends on the environmental conditions, the cargo requirements and the redundancy and precision that is required. For the base case, the barge approaches *Pioneering Spirit* inside the wind field, this requires high redundancy. This redundancy can be considered as a precaution for the risk that the barge cannot be held in place.
During the process of bringing the barge alongside, one or two tug(s) will be pushing and one or two tug(s) will be pulling. The pulling tug(s) is in control of the relative heading between the barge and *Pioneering Spirit*.

Assuming *Pioneering Spirit* to have fixed position, either by operating on DP III or being on anchorage. *Pioneering Spirit* is orientated such that it provides optimal shielding to the cargo barge.
The approach step in the mooring procedure is challenging because two floating bodies are in close proximity but not yet connected. This increases the probability of collision between *Pioneering Spirit* and the cargo barge.

B.6.4 Step 3 - Mooring

Whenever the barge and *Pioneering Spirit* are in close proximity both vessels can be connected. Installing the mooring arrangement consist of multiple steps, explained below.

1. Crew on the cargo barge brings 'messenger line' onto *Pioneering Spirit*.
2. Crew on *Pioneering Spirit* attaches mooring line to the messenger line.
3. Crew on the barge pulls in messenger line and attaches the mooring line onto the bollard. Optionally, the mooring line goes through a fairlead at *Pioneering Spirit* and/or at the barge.
4. The winches on *Pioneering Spirit* are used to apply pre-tension to mooring lines whenever all mooring lines are installed.

After the mooring system is correctly installed, the wind turbine installation operation can start with unloading the wind turbine components.
The 5000 Tons crane connects to wind turbine components on the cargo barge. After that, the components are directly placed into the wind turbine assembling equipment, which means that the crane has to connect only once to the wind turbine components. The wind turbine assembling equipment is still in concept phase and cannot be explained here.
After assembling the wind turbine will be installed onto the pre-installed foundation in one go. The orientation of the wind turbine tower relative to the pre-installed foundation is pre-predefined and fixed. This has to do with properly connecting the electrical components.

One cargo barge is expected to bring eight disassembled wind turbines, assembling and installation of one wind turbine is expected to take 24 hours. As a result, the cargo barge is expected to be alongside *Pioneering Spirit* for at least eight days in case of disregarding contingencies.

B.6.5 Step 4 - unmooring

After fully unloading, the barge can be disconnected in the same but reverse way as step 2 - approach.

B.7 Risk assessment

The purpose of the risk assessment is to identify the risks that should be considered when developing a mooring procedure.
A concise risk assessment is performed for the mooring procedure in general, not related to a specific mooring procedure concept.
Risk can be defined as probability times severity (Risk = Probability x Severity). Where probability is the chance for the situation to occur and severity describes the impact of the consequences. Probability will be a value between 0 and 100 %, severity can be ranked for example between 0 and 10. Where 10 means that the consequences of the risks are disastrous and 0 means that the consequences are not a problem at all.
Precautions can be taken to reduce the risk, this can be done by reducing the probability and/or the severity. Additionally, mitigation's can be applied with the same purpose. Mitigation's are actions to reduce the severity of the risk.
As an example, imagine an oil spill around an offshore structure. Doing a daily maintenance round along all the valves and pipe connections can be a precaution while installing a floating oil barrier can be seen as mitigation.

The Risk assessment starts with identifying the most important risks, after that possible precautions and mitigation's are suggested.
When comparing various mooring procedure concepts, for each concepts a risk assessment should be performed, or the risks should be considered as criteria in the Multiple Criteria Analysis, more on this to come in section B.8.

B.7.1 Risks

Six risk that are considered as important are identified and listed below.

1. Unwanted disconnection from tug during transit.
2. Excessive sea state occurring during transit.
3. Collision between two vessels during barge approach and mooring system installation.
4. Reduction of DP capability of *Pioneering Spirit* during barge approach.
5. Unwanted motion of wind turbine components (barge loading) with respect to the barge.
6. In case of anchorage, unwanted loss of anchorage capacity.

B.7.2 Precautions and mitigation's

Possible precautions and mitigation's are given for the risks as described above. Number 1 of the precautions and mitigation's corresponds with risk 1 in the list above. First the precautions:

1. Thorough inspection of the tug-barge connection system before leaving the quay side.
2. Thorough weather window analysis, based on multiple data sources, before leaving sheltered conditions. Make sure limits will not be exceeded based on the forecast and monitoring of measurements in the field and on board.
3. Multiple pre-installed fenders around *Pioneering Spirit* hull.
4. Perform DP trials before barge connection.
5. Inspection before leaving sheltered areas.Install additional girders on the barge as strong points that can take the impact when wind turbine parts might start moving.
6. Having a second pre-installed anchor in close proximity.

Possible mitigation's to the risks as defined above are:

1. In case of line failure. Having a new set of lines available on the tug. Besides, an additional messenger lines can be pre-installed to make sure a new line can always be attached to the barge.
2. For longer transits, safe harbours can be found along the route.
3. *Pioneering Spirit* has a large draft range. If possible the draft can be reduced to make sure any damage will be above the waterline. Additionally hull reinforcement could be applied but this will not be feasible.
4. Make sure the barge is on the shielded side of *Pioneering Spirit* which is on the correct heading to provide shielding. Install a sufficient fender capacity, so *Pioneering Spirit* will push the barge via the fenders.
5. Move the barge in optimal heading with the use of tugs, while waiting for better weather. If weather conditions allow, repair sea fastening of the turbine parts to the deck, possibly with the help of a crane vessel.
6. Apply a large safety factor for the anchor capacity.

When performing a detailed risk analysis, the list of risks should be analysed and scored in terms of probability, severity, pre-cautions and mitigation's.

B.8 Multiple Criteria Analysis

The multiple Criteria Analysis is applied to quantify the level of improvement of mooring procedure concepts compared to the base case mooring procedure. MCA consist of three steps respectively: determine scopes and criteria, rank criteria and lastly scoring different concepts for the criteria. Please refer to the 'Multiple Criteria Analysis' appendix in the literature report Appendix for detailed information on the MCA method, [2].

B.8.1 Criteria

The criteria that will be used to score the different mooring procedure concepts corresponds with the design criteria that are explained in section B.5.

B.8.2 Analytical Hierarchy Process

Before being able to score each mooring concept based on the list of criteria, the different criteria has to be ranked in terms of importance. All criteria will be compared and receive a weight, the criteria considered as most important receives the heaviest weight.
Figure B.4 represent the method how the different criteria are ranked. each entry represent the ratio of importance between the criteria that is on the row and the criteria that is on the column. For example, entry (2,1) represent a 1. Which means that criteria 2 is as important as criteria 1. Entry (3,1) represents 1/9 which means that criteria 3 is 9 times less important as criteria 1. Entry (5,1) represent 5. Which means that criteria 5 is 5 times as important as criteria 1.

Analytical Hierarchy Process		Column Criteria							Weightings
		Criteria 1	Criteria 2	Criteria 3	Criteria 4	Criteria 5	Criteria 6	Criteria 7	
Row Criteria	Criteria 1	1	1	9	1	1/5	1	5	16%
	Criteria 2	1	1	9	1/5	1/5	1/5	1	9%
	Criteria 3	1/9	1/9	1	1/5	1/5	1/5	1	3%
	Criteria 4	1	5	5	1	1	1	5	20%
	Criteria 5	5	5	5	1	1	9	1	29%
	Criteria 6	1	5	5	1	1/9	1	1/5	12%
	Criteria 7	1/5	1	1	1/5	1	5	1	11%

Figure B.4: Analytical Hierarchy Process results matrix. For ranking the criteria based on their importance

B.8.3 Score

After the criteria are scored, the final step of the MCA is scoring each mooring procedure concept for the different criteria.
The scoring of the concept is given in the range from [-2,2] with step size 1, where 0 means that the mooring procedure is not improved with respect to the base case. 1 means that the mooring procedure is slightly improved, 2 means heavily improved and vice versa.

The weight of the criteria together with the scoring determines which mooring procedure concept is improved most compared to be base case.
This scoring method helps to quantify the score of the different mooring procedure concepts.
It should be taken into account that there is overlap between the design requirements, criteria and the risk assessment. As many criteria and risks boils down to safety which is included in the requirements

already.
The scoring for the mooring procedure concepts and the base case will be described in section B.10.

B.9 Improved mooring procedure concept 1

The main focus of this mooring procedure concept is to reduce the number of tugs that is required to bring the barge alongside *Pioneering Spirit*. Furthermore, to strengthen the reliability of the continuous process. This will be done with implementing an offshore anchoring system.

This mooring procedure concept will be explained in 4 steps, similar to the base case system. The procedure is represented in Figure B.5.

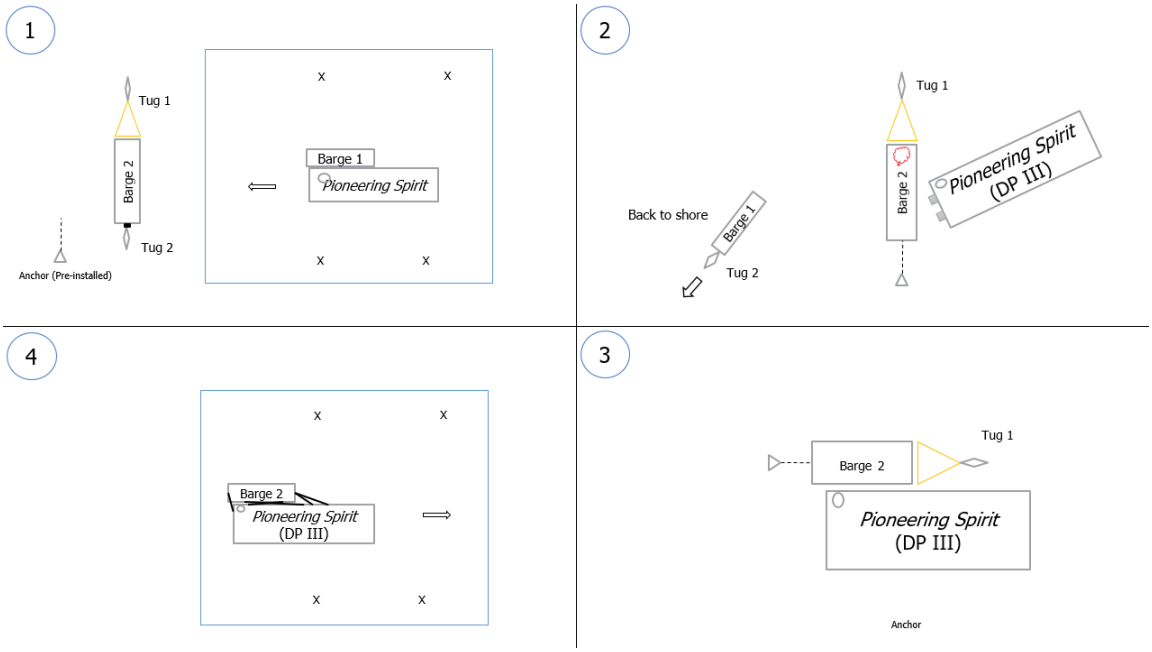

Figure B.5: Top view. Mooring procedure improvement, concept 1

B.9.1 Step 1 - Approach and anchorage

Barge 2, loaded with wind turbine parts, is brought from shore towards the wind field with use of two tugs, referred to as tug 1 and tug 2. Outside the wind field, tug 2 connects barge 2 to a pre-installed anchor, while the tug 1 stays connected to barge 2.
At the same time, *Pioneering Spirit* sails out of the wind field towards barge 2.

B.9.2 Step 2 - Back to shore and barge unloading

In this step, all vessels are outside the wind field. Barge 1 will be disconnected from *Pioneering Spirit* an brought back to shore with use of tug 2.
Barge 2 is still connected to the pre-installed anchorage and tug 1 in still connected to barge 2 and controlling its heading.
Pioneering Spirit approaches barge 2 while its heading and location is controlled by the DP III system. In this configuration the wind turbine components that cannot be unloaded when the barge is moored alongside are unloaded, referred to as the red area in step 2 of Figure B.5.

B.9.3 Step 3 - Barge connection

After the critical parts are unloaded from barge 2, *Pioneering Spirit* aligns its heading with barge 2. While the barge heading is still controlled by tug 1 and the heading and location of *Pioneering Spirit* is still controlled with the DP III system.
When barge 2 and *Pioneering Spirit* are aligned, the barge can be secured to *Pioneering Spirit*.
After all lines are installed, the anchor can be released and the mooring lines can be tensioned. Upon releasing the anchor, the 1 will disconnect from barge 2.

B.9.4 Step 4 - Sail into the wind field

In the final step, *Pioneering Spirit* sails back into the wind field with the loaded barge moored alongside. The challenging part of in this mooring procedure is the disconnection of the empty barge in step 2. The empty barge has to be disconnected from *Pioneering Spirit* while only 1 tug is attached to the barge. Even when the barge has sufficient bollard pull capacity to overcome the environmental load, there is lack of redundancy. Preferably, a third barge will be involved as the mooring operation only has to be performed once every eight days.
The upside is that at least one tug less is required in the mooring procedure. In case of limiting sea state in the weather forecast, an additional tug could be included on standby.
Additionally, due to the connection outside the wind field the required redundancy is reduce. Next to that, due to the anchorage that is included, the mooring procedure is more reliable as *Pioneering Spirit* does not have to wait for the barge. This is important because *Pioneering Spirit* is known to be an expensive vessel with a high hourly rate.
Concluding. This concept provides a good alternative to conventional mooring with making use of anchorage, because of the anchorage, the number of tugs that is required can be reduced from four to three or two and the overall reliability is expected to increase. The use of a pre-installed anchor is believed to lead to overall cost saving.

B.10 Results mooring procedure improvement

Figure B.6 shows the scoring Table for the criteria as explained in section B.5. Concept 1 is compared to the base case. In case of improvement, the score will be positive. In case concept 1 scores less than the base case, the score is negative.

Holt Matrix			Base case	Concept 1
Minimize the number of (standby) tugs required.	Criteria 1	6%	0	2
Minimize complexity of the mooring procedure, strive to simple operations.	Criteria 2	3%	0	-1
Reduce lead time and operation time.	Criteria 3	8%	0	1
High robustness against heavy environmental conditions	Criteria 4	9%	0	-1
High resilience in case of emergencies.	Criteria 5	21%	0	0
Assure continuity for the Wind Turbine Installation process.	Criteria 6	15%	0	1
Minimize environmental impact	Criteria 7	8%	0	0
Minimize risks in the mooring procedure.	Criteria 8	30%	0	-1
	Weighted net effect		0	-1

Holt Matrix Scoring	
Comparison Relative to Baseline	
Much Better Than	2
Better Than	1
Same As	0
Worse Than	-1
Much Worse Than	-2

Figure B.6: Template for MCA results

The explanation for the scoring is listed below for each criteria.

1. The required number of tugs is reduced from 4 to 3. Therefore, score 2.
2. Including anchorage and the limited number of tugs makes concept 1 more complex. Score -1.
3. Due to the anchorage the lead time will be slightly reduced. Score 1.

4. Due to the reduced number of tugs. The robustness will reduce. Score -1.
5. During operation, less tugs will be available. However, an anchorage system can be used in case of emergency. Overall score 0.
6. Due to the anchorage offshore, it is easier to bring the barge well in time and make sure *Pioneering Spirit* can continue operation. Score 1.
7. Less tugs are required and the operation time is expected to be reduced which reduces the fuel consumption. However, an anchorage system has to be installed which might disturb marine life at the seabed. Score 0.
8. Due to the reduction of tugs. The probability for most of the risks is expected to increase. Score -1.

Concluding. the base case and concept one have comparable score. More specifically, the base case has a slightly higher overall score. Therefore, concept 1 does not provide an improved mooring procedure.

C
Static modelling

C.1 Introduction into the quasi-static model

The modelling phase in this master thesis started with a quasi-static analysis, to start understanding the system behaviour in a simplified way. Due to limited accuracy, no conclusions may be drawn based on quasi-static modelling for an offshore mooring between two vessels, according to DNV.
To perform this quasi-static analysis an in-house python tool developed at Allseas is used. This performs an iterative process to find the equilibrium position and mooring line loads for the environmental conditions that are applied.
The input, results and limitations will be discussed throughout this section.

Input for the quasi-static analysis starts with an excel interface where the mooring configuration can be designed. This excel file can be uploaded in the python tool where environmental conditions can be applied and from that the mooring line loads are computed.
Results, including pre-tension and mooring line loads for each wind direction and peak period, are given as output.
This path is represented in the flow diagram in Figure C.1.

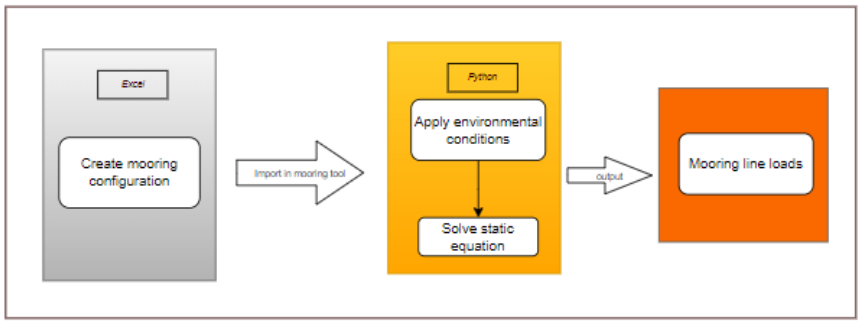

Figure C.1: Flow diagram showing the quasi-static modelling procedure

The static problem can be solved by the following function.

$$\sum F_{mooring,sys} = \sum F_{env} \tag{C.1}$$

With $F_{mooring,sys}$ the resultant force of the mooring system, including lines and fenders. This resultant for and moment is calculated for three degrees of freedom, surge, sway and yaw.
The force contribution of a single mooring line or fender can be found by $F = ku$, with k the line or fender stiffness in N/m and u the elongation in m.
F_{env} is the total environmental force vector, also for three degrees of freedom. The quasi-static python tool stops iterating whenever equation C.1 is satisfied. At the final iteration, the equilibrium position is known.

C.1.1 Input, mooring configuration

While designing the mooring configuration, the following parameters can be defined:

- Barge position, the longitudinal extension from the stern of *PS*.
- Number of lines and their orientation
- Mooring line material properties
- Stretcher length to adjust the total line stiffness
- Fender type and their location
- Area subjected to wind and current forces
- Wind and current coefficients

C.1.2 Input, environmental loading conditions

In the end, environmental conditions, together with pre-tension, determine the magnitude of the loads in the mooring system. Environmental loading includes wind, current and wave loading.
Regarding the wind load, a wind spectrum can be applied, for which the 'Froya' wind spectrum is used. For current, the velocity is assumed to be constant over the entire water depth. Since the shape of Iron Lady is rectangular the projected area to current is calculated as Length x Draft and Width x Draft for the transverse and longitudinal subjected area respectively. The area subjected to wind load is modelled as a rectangular with an area of 7100 m^2 subjected to wind in sway direction and 4250 m^2 subjected to wind in surge direction. How drag coefficients for current and wind are determined will be elaborated in sections 6.3.2.1 and 6.3.2.2.
For the wave load a JONSWAP spectrum is applied with the significant wave height, Hs as input. The maximum wave load is checked for a range of peak periods, in order to be conservative, this is based upon class requirements as stated by DNV,[40]. Which states that wave spectra with peak periods in the range of $\sqrt{13H_s} < T_p < \sqrt{30H_s}$ have to be analyzed.
To account for the wave drift forces, the Quadratic Transfer Function (QTF) is received from Ansys Aqwa and imported in the python tool.

C.1.3 Initial conditions

Before the iteration starts, the mooring lines should have a certain pre-tension. The pre-tension boundaries can be given as input. The amount of pretension can be adjusted by changing the initial spacing between both vessels, which influences the initial compression force, delivered by the fender.
Considering the hydrodynamic effects, as shown in table 6.5. The hydrodynamic effects included in the quasi-static analysis are briefly explained.

C.1.4 Shielding

When starting the quasi-static modelling there was not yet an Ansys Aqwa model containing both *Pioneering Spirit* and *IL*. Therefore an 'Ansys Aqwa based' approximation of shielding was applied, this approximation uses wave data around *Pioneering Spirit* single body model. *Pioneering Spirit* has been modelled as a single body in Ansys Aqwa, from which shielding data is obtained for the grid size as shown in Figure C.3a. For each location the wave amplification factor is determined. This ratio is simply the ratio between the undisturbed incoming wave components and the disturbed wave components. Plotting the amplification factor with respect to incoming wave frequency is referred to as 'Sea State RAO'. Both incoming and shielded wave spectrum are shown in Figure C.2.

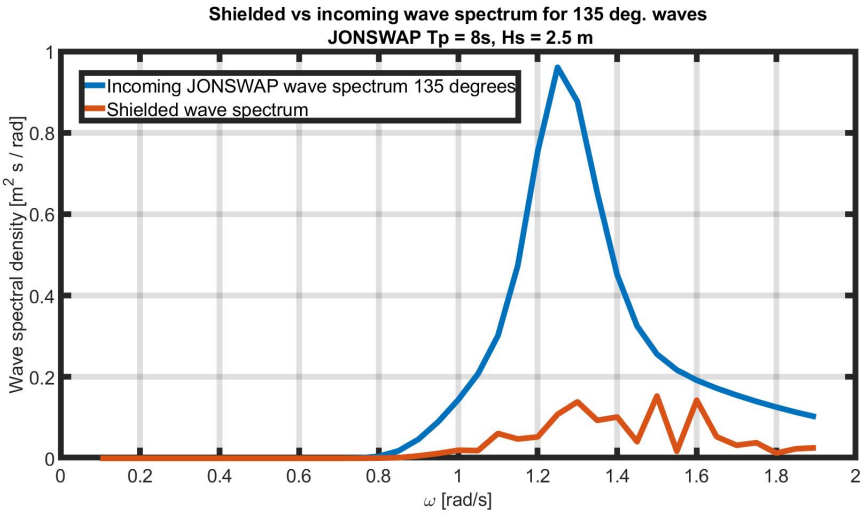

Figure C.2: Comparison between incoming wave spectrum, JONSWAP with Tp = 8s and Hs = 2.5, peakedness factor 3.3, and the shielded wave spectrum behind *Pioneering Spirit* when waves coming in under an angle of 135 degrees. The location for the shielded spectrum is at the center of the barge.

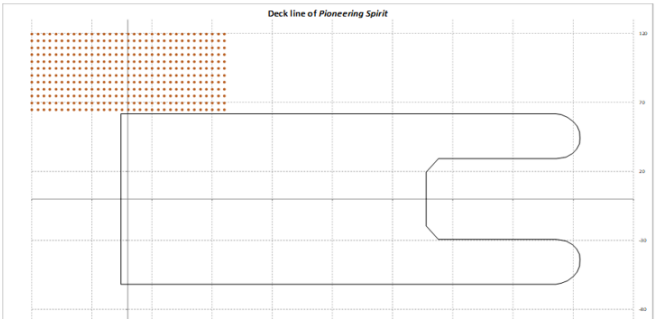

(a) Representation *Pioneering Spirit* and grid size for which Sea State RAO data is available

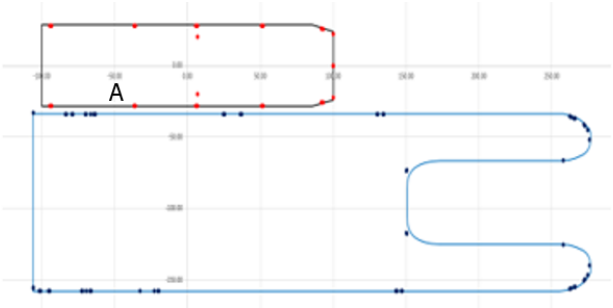

(b) Vessel orientation *Pioneering Spirit* and *Iron lady* in case of zero barge extension in longitudinal direction. Point A is not relevant for now.

Figure C.3: Clarification quasi-static analysis input data

Three incoming environmental loading directions are considered respectively 45, 90 and 135 degrees. For these directions *Pioneering Spirit* will provide shielding to *Iron Lady*, therefore these orientations are most likely to be applied. The main focus is on 135 degrees loading direction since this provides the best shielding, also in the case of barge extending from *Pioneering Spirit* stern. The orientation of the vessels and directions is shown in Figure C.3b. Radiation and diffraction effects together lead to wave shielding. Therefore these three effects are included at once in the quasi-static modelling.

C.1.5 Sensitivity analysis

In order to familiarize with the mooring system behavior, a sensitivity analysis is performed with use of the in-house python tool. Initially, shielding is included via the method as described in section C.1.4 resulting in a shielding factor of [0.76, 0.37, 0.38] for [45,90,135] degrees environmental loading condition respectively, the configuration is shown in Figure C.3b.

The systematic approach consist of the following sensitivity cases

- **Wave direction & wave height**. Three base-case scenario's are defined with incoming wave direction of 45, 90 and 135 degrees. The shielding factor with the corresponding direction results in different wave heights.
- **Wind speed**. The wind speed is changed from 12 to 16 m/s.
- **Current**. The current is changed from 1 to 1.5 knots.
- **Number of lines**. The number of lines is changed with the mooring configuration. From 4 lines to configurations with 6 and 8 lines respectively.
- **Stretcher length**. The mooring line stiffness is changed with adjusting the stretcher length while keeping the total mooring line length constant. In other words the mooring system stiffness is changed.
- **Allowable excursion**. The allowable excursion is defined as the excursion at which the iteration will be stopped. The allowable excursion is set such that it will never stop the iteration. Otherwise no correct equilibrium point can be found, as described in section 5.1 of the literature report, [2].
- **Fender type**. Three different fenders are implemented in the mooring tool, each fender has a corresponding (non-linear) stiffness curve.
- **Environmental loading direction**. To see whether it is conservative to assume that all environmental forces are aligned, a direction shift between wind and current direction with respect to incoming wave direction is applied.

C.1.6 Quasi-static model check

Before drawing conclusions from the results it is important to perform model checks to see whether the results make sense. Furthermore it is important to understand the limitations of the model, as will be explained in the next paragraph.
Important limitations of the quasi-static analysis are listed below.

C.1.7 Quasi-static modelling Limitations

- No dynamics are taken into account, only mean loads.
- Wind shielding is neglected.
- Stretchers, made out of synthetic fibres, are assumed to have linear stiffness. So, viscoelastic properties are neglected.
- The allowable excursion is set to be unlimited, which in theory assumes that mooring lines can elongate till infinity with constant stiffness.

C.1.8 Results

Figure C.4 represents all results from the sensitivity analysis. Where the maximum line tension represents the sensitivity of various variables. This data is processed and results are summarized is the list below.

	Result Code	(Shielded) significant wave height	incoming Wave direction	Mooring line tension [% of SWL] L1	L2	L3	L4	Max	Equilibrium position Surge	Sway	Yaw
		Hs_s [m]	alpha [°]	[%]	[%]	[%]	[%]	[%]	[m]	[m]	[deg]
base case	Run1	1.9	45	111	79	0	91	111	0.11	0.94	0.57
	Run 2,2	0.925	90	146	55	0	173	173	0.38	2.95	0.42
	Run3	0.95	135	61	1	32	100	100	0.09	0.56	-0.28

Legend	
Base case	
wind	
Number of lines	
Stretcher length	
Fender type	
Wave height	
Change wrt base case	x
Allowable excurion exceeded	2.00

	Result Code	Spacing barge and PS	(Shielded) significant wave height	incoming Wave direction	Wind speed	Current speed	Number of lines	Total line length [m] L5	L6	L7	L8	Stretcher length [m] L1	L2	L3	L4	L5	L6	L7	L8	Fender type	e tension [Max	Equilibrium position Surge	Sway	Yaw
		[m]	Hs_s [m]	alpha [°]	u [m/s]	v [knots]	[-]	[m]	[m]	[m]	[m]	[m]	[m]	[m]	[m]	[m]	[m]	[m]	[m]	[-]	[%]	[m]	[m]	[deg]
	Run3	5.19	0.95	135	12	1	4	0	0	0	0	20	20	20	20	0	0	0	0	Other fender	100	0.09	0.56	-0.28
	Run6	5.19	0.95	135	16	1	4	0	0	0	0	20	20	20	20	0	0	0	0	Other fender	166	0.25	2.22	-0.97
	Run9	5.19	0.95	135	12	1.5	4	0	0	0	0	20	20	20	20	0	0	0	0	Other fender	115	0.13	0.65	-0.29
V1	Run12	5.17	0.95	135	12	1	6	72	86	0	0	20	20	20	20	20	20	0	0	Other fender	74	0.02	0.05	-0.21
V2	Run15	5.17	0.95	135	12	1	6	50	58	0	0	20	20	20	20	20	20	0	0	Other fender	94	0.08	0.13	-0.18
V1	Run18	5.17	0.95	135	12	1	8	74	79	50	58	20	20	20	20	20	20	20	20	Other fender	47	0.02	0.05	-0.16
V2	Run21	5.17	0.95	135	12	1	8	58	59	50	58	20	20	20	20	20	20	20	20	Other fender	57	0.03	0.06	-0.14
	Run 57	5.19	0.95	135	12	1	4	0	0	0	0	51	57	64	51	0	0	0	0	Other fender	100	0.17	1.11	-0.57
	Run33	3.06	0.95	135	12	1	4	0	0	0	0	20	20	20	20	0	0	0	0	PS0	101	0.09	0.50	-0.28
	Run36	3.18	0.95	135	12	1	4	0	0	0	0	20	20	20	20	0	0	0	0	PB0	101	0.09	0.55	-0.28
	Run39	5.19	1.52	135	12	1	4	0	0	0	0	20	20	20	20	0	0	0	0	Other fender	114	0.22	1.34	-0.58
	Run42	5.19	0.38	135	12	1	4	0	0	0	0	20	20	20	20	0	0	0	0	Other fender	92	0.08	0.49	-0.28

Figure C.4: Results quasi-static sensitivity analysis compared to base case scenario. Showing the maximum mooring line tension for different sensitivity cases. Legend located in the right top.

Results from the sensitivity analysis will listed without further explanation, since they are assumed to be straight forward.

- For the specific barge loading the mooring system is very sensitive to wind loading.
- $F = ku$ works since the equilibrium position doubles when the stiffness of all mooring lines is factored by $\frac{1}{2}$.
- Increasing number of mooring lines increases the total system stiffness, so reduces the equilibrium offset, also individual line load reduces.
- It is conservative to assume that all environmental loads are aligned.
- Keep the mooring system as symmetrical as possible is preferred to keep mooring line loads low.
- Mooring line stiffness should be based on the expected line elongation, which can be known from loading direction and connection point at the barge. E.g. line connected close to the center of rotation will experience minor elongation.

This quasi-static analysis has limited accuracy. Nevertheless, for some mooring configurations it is sufficient to perform a quasi-static analysis only, however larger safety factors have to be applied to account for these inaccuracies. The required safety factor for offshore mooring systems can be found from DNV, and are stated in the table below. The inventory of mooring lines that is available on *Pioneering Spirit* is pre-defined the stiffness of these mooring lines can be adjusted by changing the stretcher length. The average SWL can be found by knowing the MBL of the available mooring lines and the safety factor corresponding to the modelling method.

Table C.1: Safety factors for offshore moorings, given by DNV, [22]. Average SWL values are based on MBL of the winches on *Pioneering Spirit* equal of 77 Ton. The value in bold is used as SWL in this thesis.

Analysis condition	Analysis method	Design Safety Factor [-]	Average SWL [Ton]
Intact	Quasi-static	2	38.6
Intact	Dynamic	1.67	**46.2**
Redundancy check	Quasi-static	1.43	54
Redundancy check	Dynamic	1.25	62

D

Validation and verification of the diffraction analysis and frequency domain modelling

Section 5.5 discusses the verification and validation steps that have been performed to validate and verify the results from the diffraction analysis and from the frequency domain model, to make sure correct input will be used for the time domain model. This section provides some additional information as well as some extra validation steps. The content of this chapter is listed below.

- Analytical estimation of the natural frequencies. Including computing moments of inertia, hydrostatic stiffness, added mass and damping and finally the natural frequencies.
- Additonal information on gap resonance effect and the VLID.
- Additonal information on the sea state RAOs
- A list of extra checks to perform before importing results from the diffraction analysis in the time domain model.
- Results from the single and multi-body sensitivity analysis on the diffraction analysis and frequency domain model.

D.0.1 Verification with analytical results

D.0.1.1 Analytical estimation of the natural frequencies

Each DoF has its natural frequency, defined as the lowest frequency at which resonance occurs in the system. At this resonance frequency, excessive motions can occur. Because the purpose of the mooring system is to restrict relative vessel motions, these natural frequencies are important in the mooring system analysis.

The undamped natural frequencies for both translation and rotation can be estimated with the following formulas.

$$\begin{aligned} \omega^2_{n,translation} &= \frac{C}{m + a(\omega)} \\ \omega^2_{n,rotation} &= \frac{C}{I + a(\omega)} \end{aligned} \tag{D.1}$$

With C the stiffness term for the specific DoF, m mass, I the mass moment of inertia and $a(\omega)$ the frequency dependent added mass term. In this section, all these variables will discussed one by one. Closing of with showing the occurrence of resonance frequencies in the RAOs.

The mass of the barge, in other words displacement, is pre-set to 6 m according to the sailing requirements. The inertia terms are calculated from the VCG location and the barge shape.

D.0.1.1.1 Moment of inertia To determine the mass moment of inertia, first the mass radii of gyration are determined. As an example, the equation to calculate the transverse radius of gyration is represented. These can be determined with equation D.2.

$$k_{xx} = 0.289 \cdot B \cdot \left(1.0 + \left(\frac{2 \cdot \overline{KG}}{B}\right)^2\right) \tag{D.2}$$

With B the body breadth and KG the height of the CoG above the keel line.
For a rectangular barge shaped structure equations D.3 can be used to find the range of all three radii of gyration, with L the length of the barge. These rules of thumb are learned from *J.M.J. Journée and W.W. Massie*, [3].

$$\begin{aligned} k_{xx} &\approx 0.30 \cdot B \text{ to } 0.40 \cdot B \\ k_{yy} &\approx 0.22 \cdot L \text{ to } 0.28 \cdot L \\ k_{zz} &\approx 0.22 \cdot L \text{ to } 0.28 \cdot L \end{aligned} \tag{D.3}$$

From these radii of gyration, the mass moments of inertia can be computed with.

$$\begin{aligned} I_{xx} &= {k_{xx}}^2 \cdot \rho\nabla \\ I_{yy} &= {k_{yy}}^2 \cdot \rho\nabla \\ I_{zz} &= {k_{zz}}^2 \cdot \rho\nabla \end{aligned} \tag{D.4}$$

Regarding the mass moments of inertia, the required input for the diffraction analysis (Ansys Aqwa) is the mass together with the location of the CoG and the barge dimensions and water density. To verify the moment of inertia that is computed in Ansys Aqwa, first the transverse moment of inertia is calculated by using equation D.2, the output is checked whether it fits within the boundaries of equation D.3. After that, the radius of gyration, together with the density and displacement, is substituted into equation D.4.

Additionally, the area moments of inertia are calculated from the geometry in Ansys Aqwa. To verify these results, it can be assumed that *Iron Lady* is a box shaped barge as its block coefficient is almost equal to 1. With this assumption, its transversal area moment of inertia can be estimated with

$$I_{area,x} = \frac{1}{12} \cdot L \cdot B^3 \tag{D.5}$$

With L the length of the barge and B the breadth both in m. Both The mass and area moments of inertia from Ansys Aqwa are found to correspond with the computed results. The assures the reader that the correct units are applied.

D.0.1.1.2 Hydrostatic stiffness The hydrostatic stiffness can be analytically computed based on the barge waterplane area, A_{wl}, and the metacentric height, GM. The waterplane area depends on the draft and can be found from a stability booklet describing the hydrostatic properties of a vessel for variable draft, GM depends on the loading conditions.

$$\begin{aligned} \text{heave} &: c_{zz} = \rho g A_{WL} \\ \text{roll} &: c_{\phi\phi} = \rho g \nabla \cdot \overline{GM} \\ \text{pitch} &: c_{\theta\theta} = \rho g \nabla \cdot \overline{GM}_L \end{aligned} \tag{D.6}$$

With ∇ the water displacement and $G\bar{M}$ the transverse metacentric height and $G\bar{M}_L$ the longitudinal metacentric height. The method to compute the metacentric heights is only included in the literature report.
The restoring force depends heavily on the loading condition, both the location of the center of gravity

and the location of the CoB. The loading condition for the transport of wind turbine parts is based on the required draft of Iron Lady for transport. The method to determine the location of the CoG is included in section, 5.3. The CoG is assumed to be right above the CoB, which means zero heel and zero trim for the equilibrium position.

Table D.1: Results from computation hydrostatic stiffness of Iron Lady . With $A_{wl} = 1.1E4\ m^2$ at a draft of T = 6 m.

Variable	Symbol & unit	Analytical solution	Aqwa result
Input			
Vertical center of gravity	KG [m]	12.1	12.1
Vertical center of buoyancy	KB [m]	3.00	3.00
Results			
Roll second area moment of inertia	$I_{area,x}$ [m^4]	3.08E+06	2.96E+06
Pitch second area moment of inertia	$I_{area,y}$ [m^4]	3.81E+07	3.50E+07
Transverse metacentric height above center of buoyancy	BM_T [m]	47.8	45.8
Longitudinal metacentric height above center of buoyanc	BM_L [m]	5.92E+02	5.41E+02
Transverse metacentric height above CoG	GM_T [m]	38.7	36.7
Longitudinal metacentric height above CoG	GM_L [m]	5.83E+02	5.32E+02
Final results			
Restoring term Heave	C33 [kN/m]	1.11E+05	1.11E+05
Restoring term roll	C44 [kNm/rad]	2.59E+07	2.26E+07
Restoring term pitch	C55 [kNm/rad]	3.90E+08	3.47E+08

As can be seen from table D.1, the results from the analytical solution and Aqwa slightly deviate. This is according to expectations due to the fact that in the analytical method the the second area moment of inertia is computed using equation D.5. This assumes the barge to be perfectly rectangular shaped. Whereas Aqwa uses the actual shape of the barge, which has a block coefficient of, $c_b = 0.97$. Resulting in a difference of approximately 10% for the roll and pitch stiffness, coming from the difference in second area moment of inertia. As the detailed vessel shape models are imported in Ansys Aqwa, the results from Ansys Aqwa are believed to be accurate, with the analytical calculation it can be confirmed that results are in the correct range, 10 % difference is acceptable because multiplying the LOA and breadth with the block coefficient reduces the error to less than 1.5 %

D.0.1.1.3 Added mass Having verified the mass moments of inertia and stiffness brings to the following missing parameter, added mass, required to determine the natural frequency.
Added mass is the virtual mass added to the system because surrounding fluid has to set in motion when moving a through the fluid, [41].
The frequency dependent added mass is computed from the fluid potential in the diffraction potential software, Ansys Aqwa. Following equation

$$a_{kj} = -\Re e\left[\rho \iint_{S_0} \phi_j n_k \cdot dS_0\right] \tag{D.7}$$

With ϕ_j the radiation potential. To verify the added mass as determined in Ansys Aqwa, the heave added mass for a square 2D shape with rib length 2B can be estimated following the method as described by J.N. Newman in his book, "Marine Hydrodynamics", [41].

$$A_{33} = 4.754\rho(\frac{B}{2})^2 A_{66} \quad = 0.725\rho(\frac{B}{2})^4 \tag{D.8}$$

With A_{33} and A_{66} the added mass per unit length, ρ the water density and B the breadth of the body. For the yaw moment, the draft is assumed to be half the rib length. For this simplification it is assumed that the barge is squared in the y-z plane. While in reality it is a rectangular shaped barge. This method only gives the low frequency added mass while the added mass is frequency dependent. Therefore the low frequency added mass will not give realistic results for the natural frequency.
Results of the low frequency added mass from solving equation D.8 and the output of the radiation diffraction software are listed in table D.2.

Table D.2: Added mass verification. The ratio represents the difference between the analytical and numerical added mass term.

Variable & unit	Analytical method (A)	Ansys aqwa (N)	Ratio A/N
A33 [Ton]	7.92E+05	1.17E+06	1.48
A66 [$Tonm^2$]	9.81E+07	6.53E+07	0.67

From table D.2 it can be seen that the values do have the same order of magnitude. Differences are expected to be caused by the fact that equation D.8 is not suitable for a rectangular barge shape.

D.0.1.1.4 Damping As the required input for the undamped natural frequency are gathered, the damped natural frequency, in rad/s, can be estimated by solving

$$\omega_1 = \omega_n \sqrt{1 - \zeta^2} \tag{D.9}$$

$$\begin{aligned} b_{c,z} &= \sqrt{2(m + a_{zz})k_{zz}} \\ b_{c,\phi} &= \sqrt{2(I_{xx} + a_{\phi\phi})k_{\phi\phi}} \end{aligned} \tag{D.10}$$

With ζ the damping ratio, depending on the critical damping, b_c in kg/s. Where equation D.10 shows the critical damping for translation, more specifically heave, and rotation, roll in this case respectively. $\zeta = b/b_c$ with b the damping term in kg/s.

Similar as for the added mass, the frequency dependent damping term is determined from the fluid potential, captured in the equation below.

$$b_{kj} = -\Im m \left[\rho\omega \iint_{S_0} \phi_j n_k \cdot dS_0 \right] \tag{D.11}$$

As the damping coefficients go to zero for low frequencies, the low frequency damping coefficient cannot be estimated with use of analytical relations. Therefore, the damping term is not verified in this thesis.

D.0.1.1.5 Natural frequency in RAOs Finally, all data necessary to analytically determine the natural frequency is available. However, for the added mass only the low frequency values are available and no damping terms can analytically be determined which means that the natural frequency can only be estimated. The purpose of this estimation is to see whether the results from Ansys Aqwa come close to the analytical values. The natural frequencies and periods from Ansys Aqwa are captured in Table F.5. According to the theory described in this section, at the resonance frequencies, peaks should be visible in the RAOs because they describe the frequency dependent vessel motions for each DoF. In section 5.5.1 Figure 5.5 represents the RAOs *Iron Lady*, the RAO shapes are briefly discussed. RAOs for *Pioneering Spirit* cannot be shown because of confidentiality.

D.0.1.2 Gap resonance and damping lid (VLID)

Effect of damping lid on the hydrodynamic data regarding *Iron Lady* roll motions.

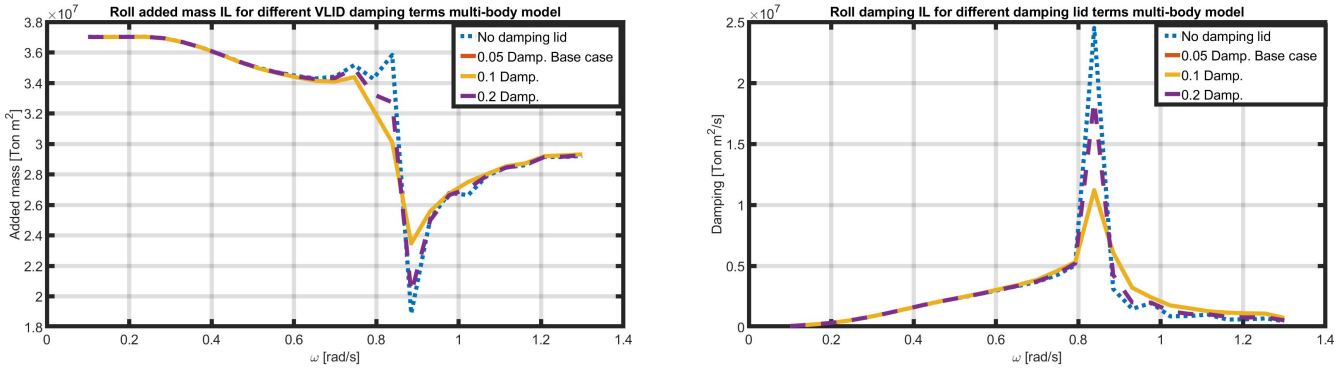

(a) Roll added mass (b) Roll damping

Figure D.1: Roll added mass (left) and damping (right) of Iron Lady at the CoG, for various VLID damping factors

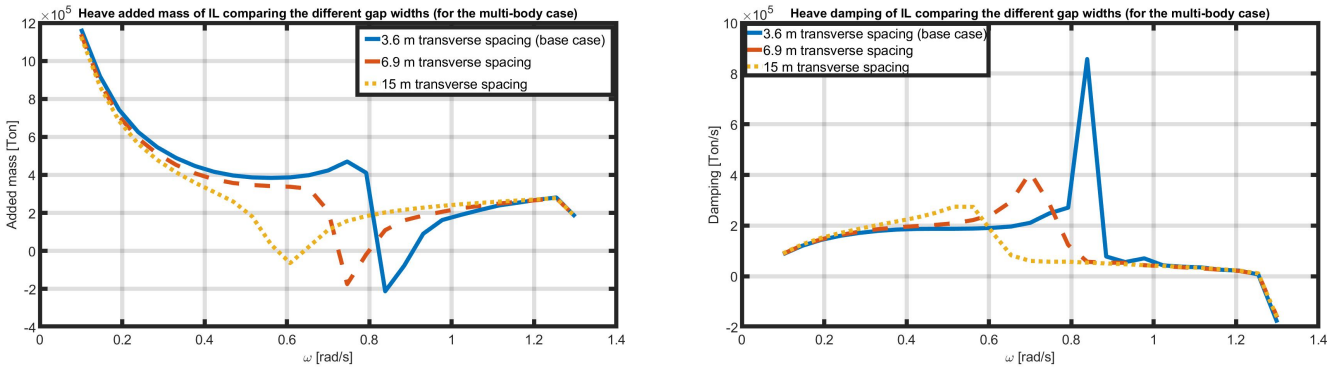

(a) Heave added mass (b) Heave damping

Figure D.2: Heave added mass (left) and damping (right) of Iron Lady at the CoG, as part of the multi-body model, comparing for different transverse spacing's, in other words 'gap widths', respectively 3.6, 6.9 and 15 m.

Figure D.2 confirms the hypothesis that the remarkable peak in the added mass and damping curves being a result of the gap resonance effect. The transverse spacing of 3.6m is not chosen arbitrarily but comes from the width of the fenders fixed to Iron Lady, see Figure D.3a, together with a single Yokohama 3.3x6.6 P80 fender, as used in this research.
The figure of 6.9m transverse spacing comes from installing a triangular shaped fender, consisting of three Yokohama fenders, which doubles the transverse spacing. The 15m vessel spacing is chosen arbitrarily to see the effect of gap resonance for a large gap width.

Figure D.2b shows that the vessel interaction reduces with increasing transverse spacing, according to expectations. The reduction of interference is known from the peak height reduction. The slight increase of damping for the lower frequencies is unknown, as a slight reduction in damping would be expected because of the increased spacing between the vessels.
Figure D.2a shows a shift in the peaks towards a lower frequency, corresponding with the damping

results. Furthermore it can be seen that for a larger transverse spacing the added mass slightly reduces for the lower frequencies which makes sense, as the gap is larger there is less 'sticking' effect of water in the gap.

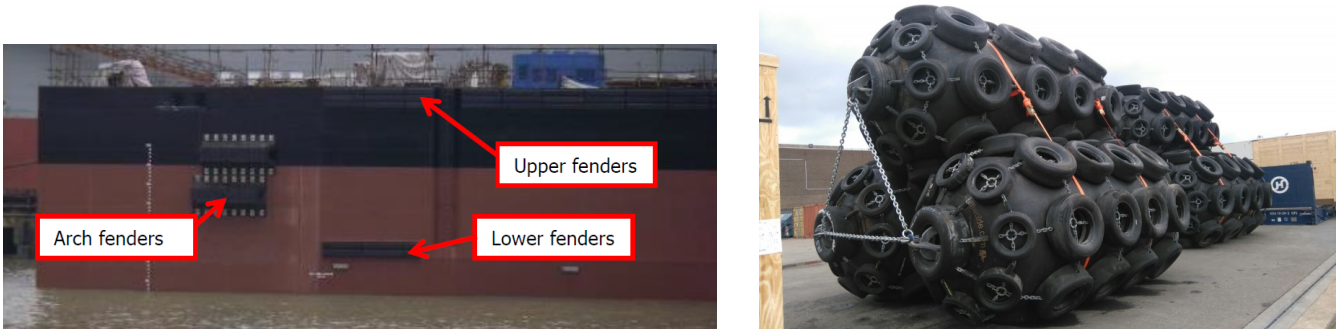

(a) Fenders fixed t Iron Lady with a thickness of 0.3 m

(b) Three Yokohama fenders oriented as triangle to double vessel spacing.
Downloaded from the Tenwolde website, Courtesy of Tenwolde, [42]

Figure D.3: Fenders installed on *Iron Lady* (left) and triangle of three Yokohama fenders (right)

VLID damping factor. Researchers derived an empirical formula to estimate the required damping factor for the VLID, [26]. This formula only takes viscous effects due to friction into account, e.g. wave breaking is not considered in this relation.

$$\epsilon = 2\frac{\sqrt{\nu}\omega^{5/2}T}{gd} \tag{D.12}$$

With ν the kinematic viscosity, ω the gap resonance frequency, T the body draft, d the gap width. Substituting results form table 5.2 and 5.3, for a transverse spacing of 3.6 m. Results in a very small damping factor of $2.2E-4$.
Since the result from this method seems to be unrealistically low, therefore this result is not applied in this thesis. In order to apply this method, more detailed research would be required.

D.0.2 Sea state RAOs

Figure D.4, represent the shielding behind *Pioneering Spirit* for high and low frequencies in case waves coming from 45 degrees. Considering the wave elevation that can be read from the color scale, for high frequencies waves come together in the corner in between the stern of *Pioneering Spirit* and *Iron Lady*. This is expected to be related to waves that are reflecting from *Pioneering Spirit* stern. This wave reflection contributes to excessive wave elevations at the gap.

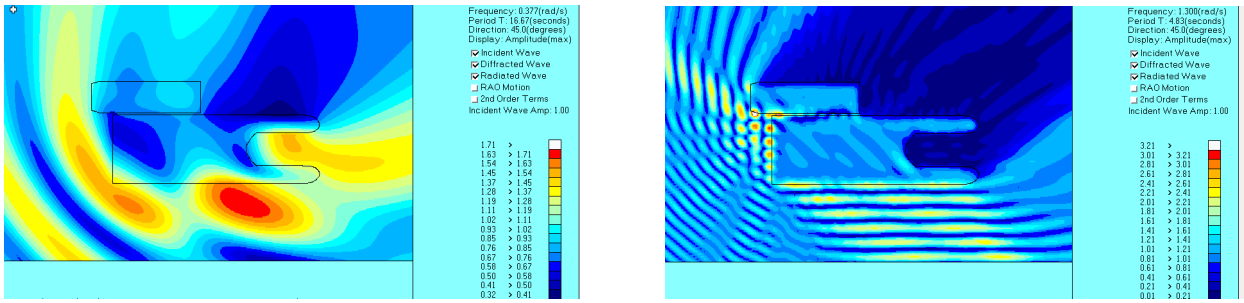

(a) Low frequency (0.38 rad/s).

(b) High frequency (1.30 rad/s).

Figure D.4: Visualization of wave amplitude shielding from *Pioneering Spirit* for wave directions 45°, at low frequency (left) and high frequency (right).

D.0.3 Additional checks

[noitemsep,topsep=0pt] There are some simple checks that need to be performed to make sure Aqwa provides the correct output. These tests are inevitable since this data will be used as input for Orcaflex to perform the time domain modelling. The most important simple checks are listed below.

- Weight of the structure and displaced volume, these should correspond.
- Added mass and damping matrices should be symmetric.
- CoG and CoB should satisfy expectations from intuition and analytical calculations.
- Comparing the motions in the CoG of the floating body with the motions at a certain node away from the CoG. The latter motions should be larger and make sense.
- Aqwa GS visualization software should be used to check the orientation of the floating bodies.

The above checks are performed for the multi-body model, giving satisfactory results.

D.0.4 Sensitivity analyses

The purpose of a sensitivity analysis is to understand how various variables are affecting the results, by performing various simulation while varying only one variable at a time.
For the single body sensitivity analysis the results are defined as the motions at the CoG, more specifically the maximum position that is reached in a three hour sea state. The results are computed for waves coming from 135° for both single and multi-body sensitivity analysis.
For the multi-body sensitivity analysis the results are defined as the relative motions between both bodies, at a fixed location at port Side stern of the cargo barge. More specifically, the relative motion between the crane tip at *Pioneering Spirit* and the deck of *Iron Lady* are used for reference.
Since motions in the frequency domain are first order and therefore have zero mean, no mooring system is included in frequency domain sensitivity analysis.

D.0.4.1 Single-body sensitivity analysis

To simplify the problem and to properly understand the influence of each variable. First a single-body sensitivity analysis is performed. Analysing the cargo barge only.

D.0.4.1.1 Sensitivity cases The following sensitivity cases are considered for the single body sensitivity analysis.

- Water depth

- Additional viscous damping factor
- Location of Vertical Center of Gravity
- Including Off-diagonal inertia terms

D.0.4.1.2 Single body sensitivity results The results of the sensitivity analysis are concisely represented in Table D.3. Initially, only diagonal terms of the mass moment of inertia matrix are included. Therefore, in the third row, results are given for the case the off-diagonal mass moment of inertia terms are included.

Table D.3: Results from sensitivity analysis, comparing relative vessel motions. The distinction is made between 0, 1 and 2 with 0 meaning not sensitive at all. 1 meaning medium sensitive and 2 meaning heavily sensitive. For waves coming from 135°.

DoF	Surge	Sway	Heave	Roll	Pitch	Yaw
Water depth	0	0	1	1	0	1
Off-diagonal inertia terms	0	0	0	2	0	0
Vertical Center of Gravity	0	0	0	2	0	0
Additional viscous roll damping	0	0	0	1	0	0

It can be seen that the water depth is affecting the heave and roll and yaw motions. Research showed that added mass and damping terms increase with lower water depth because water particles are more restricted to follow the vessel motions.
Furthermore, the VCG heavily affects the roll motion which makes sense because it affects the mass moment of inertia term. It would be expected that also the pitch motion would be slightly affected.
Obviously the additional viscous damping affects the roll motion only.

D.0.4.2 Multi-body sensitivity analysis

For the multi-body sensitivity analysis both *Pioneering Spirit* and *Iron Lady* are included in the orientation as shown in Figure 2.5, point A in this figure shows the location at which the relative motions are determined.

D.0.4.2.1 Multi-body sensitivity cases The following sensitivity cases are considered for the multi-body sensitivity analysis.

- **Transverse spacing between *Pioneering Spirit* and *IL***. The spacing between the vessels is mainly determined by the size of the fenders. Vessel motions, due to radiation and diffraction, but especially the numerical error of gap resonance is sensitive to the spacing between vessels.
- **VCG**. The VCG is included in the Metacentric height (GM) which is important factor in ship stability. The transverse GM together with the heel angle determines the righting arm to correct for the roll motion. Similar approach holds for the longitudinal case and pitch motion. Since $GM_{transverse} << GM_{longtidunal}$ the roll motion is more sensitive to a shift of the VCG.
- **Viscous roll damping**. Since viscosity is neglected in potential flow software, an additional roll damping term is added to correct for this limitation. Especially the roll motion is influenced by this damping term.
- **Damping factor surface lid (VLID)**. To correct for the numerical error of gap resonance, a surface lid is applied in between the floating bodies to suppress the wave elevation in the gap. The added damping factor should correct for the numerical error but should not disturb the vessel motions.
- **Water depth.** Based on literature, changing the water depth is expected to influence vessel motions heavily, [43].
- **Barge longitudinal extension**. For the WTI project it might be necessary to let the barge extend from *Pioneering Spirit* stern to comply with unloading requirements. This might influence the relative vessel motions, for example due to change in shielding.

D.0.4.2.2 Multi-body body sensitivity results The results for the multi-body sensitivity analysis are shown in Table D.4. It can be seen that the longitudinal length the barge extends from *Pioneering Spirit* stern, heavily affects the relative motions which makes sense because the shielding is reduced.

Table D.4: Results from sensitivity analysis, comparing relative vessel motions. The distinction is made between 0, 1 and 2 with 0 meaning not sensitive at all. 1 meaning medium sensitive and 2 meaning heavily sensitive. For waves coming from 135°

DoF	Surge	Sway	Heave	Roll	Pitch	Yaw
Damping lid factor	0	0	0	0	0	0
Transverse vessel spacing	1	1	1	0	1	1
Barge longitudinal reposition (extending *Pioneering Spirit*)	1	2	1	2	1	2
Water depth	1	1	2	2	1	0

Figure D.5 gives the ratio between the relative vessel motions for fixed location A, as defined in Figure 2.5. This ratio gives insight how the relative vessel motion changes for the various sensitivity cases. The ratio is determined according to the following relation. As a side note, for the cases with ratio's far from 1.0 also the absolute difference should be checked to see the sensitivity.

$$ratio = \frac{\text{Relative vessel motion, sensitivity case}}{\text{Relative vessel motion, base case}} \tag{D.13}$$

Findings from the sensitivity analysis for both the *Iron Lady* as single body and the multi-body model, in frequency domain, are given below.

			ratio compared to base case. >1 larger than base case					
	VLID Damping factor	Internal lid	Surge motion at CoG	Sway motion at CoG	Heave motion at CoG	Roll motion at CoG	Pitch motion at CoG	Yaw motion at CoG
	[-]	yes/no	[-]	[-]	[-]	[-]	[-]	[-]
Base case	0.05	no	NvA	NvA	NvA	NvA	NvA	NvA
Internal lid	0.05	yes	1.0	1.0	1.0	1.0	1.0	1.0
lid damping factor	0.1	no	1.0	1.0	1.0	1.0	1.0	1.0
	0.2	no	1.0	1.0	1.0	1.0	1.0	1.1
	0	no	1.0	1.0	1.0	1.0	1.0	1.0

Figure D.5: Results from sensitivity analysis in frequency domain. Comparing relative vessel motions for the base case with the internal LID and Damping LID.

The sensitivity analysis for the VLID and the ILID show agreement with the earlier conclusion that the floating bodies included in this thesis are not affected by the numerical affects of gap resonance and irregular frequencies. Because including an ILID or varying the VLID damping factor does not affect the maximum relative first order motions that occur in a three hour sea state.

E

Time domain model validation and verification

Section 6.5 represented the steps that are taken to validate and verify the time domain model. This chapter will provide additional information to these steps or describe validation steps that are relevant but not required in the main text.
To build up confidence in the numerical model, simulations are simplified in the following steps.

1. Step 1. Iron lady single body model. Including only first order effects.
2. Step 2. Pioneering Spirit and Iron Lady multi-body model excluding mooring lines. Considering only first order effects.
3. Step 3. Pioneering Spirit and Iron Lady multi-body model, including mooring lines. Considering both first and second order effects

Step 1 is explained in section E.0.2.1, Step 2 will be discussed in section E.0.2.2, step 3 will be discussed in section 6.5.5.

E.0.1 Verification with analytical results

Basic analytical relations will be applied to check whether the magnitude of the hydrodynamic forces is in the correct range.

E.0.1.1 Verification of the first order wave force

The first order wave consists of three parts. Incoming wave force, also known as Froude-Krilov force, the diffracted wave force due to disturbance of the wave field and the force due to wave radiation. The wave radiation force results are captured in the added mass and damping matrices The Froude-Krilov and diffraction force will be analytically estimated in this section.
Analysing the simplified case for the barge as a single body, moored with a single mooring line and considering beam waves only. For this computation, the barge will be subjected to a linear wave with a set wave height and period.

Froude-Krilov force
The undisturbed wave amplitude can be described by the following relation. Applying the incoming wave direction, $\mu = 90°$ for beam waves.

$$\zeta(x,t) = \zeta_a \cos(kx\cos\mu + ky\sin\mu - \omega t) = \zeta_a \cos(ky - \omega t) \tag{E.1}$$

The corresponding wave potential is:

$$\Phi_0(x,z,t) = \frac{\zeta_a g}{\omega} e^{kz^*} \sin(kx\cos\mu + ky\sin\mu - \omega t) = \frac{\zeta_a g}{\omega} e^{kz^*} \sin(ky - \omega t) \tag{E.2}$$

From the velocity potential, the pressure in the fluid can be found from applying the Bernoulli equation:

$$p_0 = -\rho \frac{\partial \Phi_0}{\partial t} = \rho \zeta_a g e^{kz^*} \cos(ky - \omega t) \tag{E.3}$$

The force vector can be determined from the pressure distribution over the hull.

$$\bar{F} = -\int_{S_n} p \cdot \bar{n} dS \tag{E.4}$$

With $\bar{n}$ the direction of the forcing vector. Since this simplified case is only checked for beam waves, n_2 simplifies to $n = (0, 1, 0)$ for sway direction.

Substituting the values gives the Froude-Krilov force in sway direction for the case of beam waves.

$$F_{w,2} = -\int_{z_1}^{z_2}\int_{x_1}^{x_2} \zeta_a \rho g e^{kz^*} \cos(kx + \omega t) \cdot n_2 dx dz^* \tag{E.5}$$

When only interested in the maximum contribution, $\cos(kx + \omega t)$ can be assumed to be equal to 1.

$$\begin{aligned} F_w &= -(x_2 - x_1)\int_{z_1}^{z_2} \zeta_a \rho g e^{kz^*} \cos(kx + \omega t) \cdot n_2 dz^* \\ &= -(x_2 - x_1)\,\zeta_a \rho g n_2 \cos(kx + \omega t)\frac{1}{k}\left[e^{kz^*}\right]_{z_1}^{z_2} \\ &= -(x_2 - x_1)\,\zeta_a \rho g n_2 \cos(kx + \omega t)\frac{1}{k}\left(e^{kz_2} - e^{kz_1}\right) \end{aligned} \tag{E.6}$$

In the above equation, z^* refers to the z coordinate with respect to the mean water surface. Considering the transverse surface of *Iron Lady* with a length of 200 m and a draft of 6 m, $x = [0, 200]$ m and $z = [0, 6]$ m respectively.

Assuming linear airy waves, the wave number, k, can be computed via the dispersion relation.

$$k = \frac{\omega^2}{g} \tag{E.7}$$

With ω the exciting frequency in rad/s.
The next step is computing the force contribution due to the disturbed wave field.

Diffraction force
For computing the diffraction force, full wave reflection on the body is assumed, meaning that the body is modelled as a vertical wall. This results that the diffraction force equals the Froude-Krilov force. Therefore the total first order firce would be equal to two times this Froude-Krilov Force. This assumption is only valid for deep water conditions and very short wave periods, such that the energy is concentrated at the surface.
Table E.1 shows the results of the first order wave force contribution calculated in Orcaflex, Aqwa and analytically with the equations as described above.

Table E.1: Verification first order wave load for beam and stern waves. Waves with 8 seconds period and 1.25 m amplitude. The water depth is 30 m and body draft 6 m.

Method	Variable & Unit	Beam waves	Stern waves
Orcaflex result	**Total** first order force [kN]	2.33E+04	5.45E+03
Ansys Aqwa	Froude krilov contribution [kN]	2.41E+04	3.71E+03
	Diffraction contribution [kN]	1.43E+04	5.86E+03
	Total first order force [kN]	2.39E+04	5.34E+03
Analytical result	Froude krilov contribution [kN]	1.83E+04	5.22E+03
	Diffraction contribution [kN]	1.83E+04	5.22E+03
	Total first order force [kN]	3.66E+04	1.04E+04

It can be seen that results from Orcaflex and Ansys Aqwa do match, which makes sense because the first order wave loads are imported from Ansys Aqwa into Orcaflex.
The analytical result are in the same order of magnitude. However, results do not match exactly. The assumption of full wave reflection is probably not valid for these wave and water depth conditions. This hypothesis is based on the fact that the total first order wave load as calculated in the radiation diffraction software, Ansys Aqwa, is close to the analytically calculated Froude-Krilov force.

E.0.1.2 Verification of the second order wave force

The second order wave drift force consist of a constant and a dynamic part. Only the mean part will be calculated, including the corresponding offset while moored to a soft mooring line.

Mean second order wave drift force
The mean second order wave drift force can be computed by considering the vessel to be a vertical wall. This method assumes all waves are reflected by the structure and that waves are relatively small with respect to the vessel draught and that the wave energy is concentrated at the sea surface.
The mean second order wave drift force per unit length can be estimated with the following equation [44].

$$\bar{F} = \frac{-1}{16} \cdot \rho g \cdot H_s \tag{E.8}$$

Considering the case for a significant wave height of 2.5 m and the barge length to be 200 m. The mean second order wave drift force is in the order of 760 kN both from the analytical and Orcaflex solution.
From the mean force the offset of the system can be calculated by solving dividing the mean force with the total mooring system stiffness in the specified direction.

E.0.1.3 Verification of current and wind forces

In this section the wind and current force exerted on *Iron Lady* are estimated with analytical formulas. After that, these analytical results are compared with the output of Orcaflex.

Current force
To ensure that the current force calculated in Orcaflex is realistic, the order of magnitude is compared to the results of applying common known relations. Only the forces in the x-y plane are important since these have mainly to be taken by the mooring system.

$$
\begin{aligned}
F_c, x &= \frac{1}{2} \cdot \rho_w \cdot A \cdot C_d \cdot V_c^2 \cdot \cos\beta \cdot |\cos\beta| \\
F_c, y &= \frac{1}{2} \cdot \rho_w \cdot A \cdot C_d \cdot V_c^2 \cdot \sin\beta \cdot |\sin\beta| \\
M_z &= \frac{1}{2} \cdot \rho_w \cdot A \cdot x \cdot C_d \cdot V_c^2 \cdot \sin\beta \cdot |\sin\beta| + \frac{1}{2} \cdot V_c^2 \cdot (A_{22} - A_{11}) \cdot \sin 2\beta
\end{aligned} \tag{E.9}
$$

The analytical method applies 2D strip theory and calculates the force and moment contribution for all strips. For detailed information, the reader is referred to chapter 4 the literature report, [2].

Table 6.2 gives the results from computing the current force both in Orcaflex and the analytical method, applying equations E.9. Input data for the current calculation is included in table E.2.

Table E.2: Input for the current load calculation.

Variable	Symbol	Unit	Value
Max drag coefficient [Surge, Sway, Yaw]	$[Cd_x, Cd_y, Cd_{yaw}]$	[-]	[1,1,0.08]
Subjected Area	$[A_x, A_y, A_{yaw}]$	$[m^2]$	[3.41E2, 1.16E3, 2.40E5]
Current velocity	V_c	$[m/s]$	0.9
Incoming wave direction	β	[°]	135
Added mass coefficients	$[A_22, A_11]$	[Ton]	[6.63E3, 3.00E4]
LCG of the lateral exposed area	x	[m]	4.6
Water density	ρ_w	$[Ton/m^3]$	1.025

Considering the side view of *Iron Lady*, it can be seen that the barge has not a perfect rectangular shape but is curved at the bow. Therefore the center of pressure is not exactly at the center of the barge, which causes a yaw moment represented by 'x' in table E.2.
For the yaw moment, the drag coefficient is unknown. Therefore a default value from Orcaflex is applied.
As the drag coefficients change with incoming direction, the wind and current drag coefficients are represented in Figure F.2.

Wind force
The order of magnitude of wind force computed in Orcaflex is verified by performing a simple analytical calculation, using comparable relations for the force in surge and sway direction as given in equation E.9. Symmetric loading is assumed and therefore it is assumed that no yaw motion will be induced due to wind forces.
Table E.3 shows the input that is used for computing the force due to wind. Table 6.3 shows the wind force that is computed in Orcaflex and the results from applying the simple formulations as described above.

Table E.3: Input for wind calculation.

Variable	Symbol	Unit	Value
Velocity	v_w	[m/s]	12.86
Air density	ρ_{air}	$[kg/m^3[$	1.225
Kinematic viscosity air	μ_a	$[m^/s\ ]$	1.48E-5
Drag coefficient [Surge, Sway, Yaw]	$[Cd_x, Cd_y, Cd_{yaw}]$	[-]	[0.2,0.2,0]
Incoming wind direction	β	[°]	135
Turbine tower height	H	[m]	140
Tower diameter	D	[m]	10

Similar as for current, the drag coefficients are direction dependent, this curve is shown in Figure F.2. These drag coefficients depends on the Reynolds number of the flow around the structure. From this

Reynolds number and taking the shape of the structure into account, enables to compute the drag coefficients according DNV guidelines, [40].

E.0.2 Compare with frequency domain results

For this model check, results for the first order motions in time domain are compared with the first order motions in the frequency domain. In order start simple and build up complexity, first the barge as a single body is analysed. After that the relative motions between the barge and *Pioneering Spirit* will be analysed.

E.0.2.1 Single body first order motions

Simulations in the frequency domain only include linear first order motions. Whereas simulation in time domain usually includes non-linear higher order motions.
To check whether results from the frequency domain model and the time domain model do correspond, only first order effects are included in the time domain modelling.
Figure E.1 represents the results for comparing the first order positions from the frequency domain and the time domain model. The first block represents the result from the frequency domain analysis. The second block includes the result from the time domain analysis for the case the vessels follow the displacement RAOs. These displacement RAOs are given as output from the frequency domain and imported in the time domain software. The third block shows the relative position that is calculated in the time domain, based on the hydrodynamic matrices that are computed in the frequency domain software and imported in the time domain software.
The reason for adding this second step is to slowly build up complexity. While analysing the results we are interested in, the forces in the mooring system, Orcaflex will calculate the motions based on the hydrodynamic matrices.

The positions represented in Figure E.1 represent the three hours maximum that is computed based on the assumption that the motions are Rayleigh distributed. Whether this assumption is correct is discussed in section 6.5.3.
The yaw rotational motion is excluded from this validation step because the yaw motion is constrained in the time domain simulation.

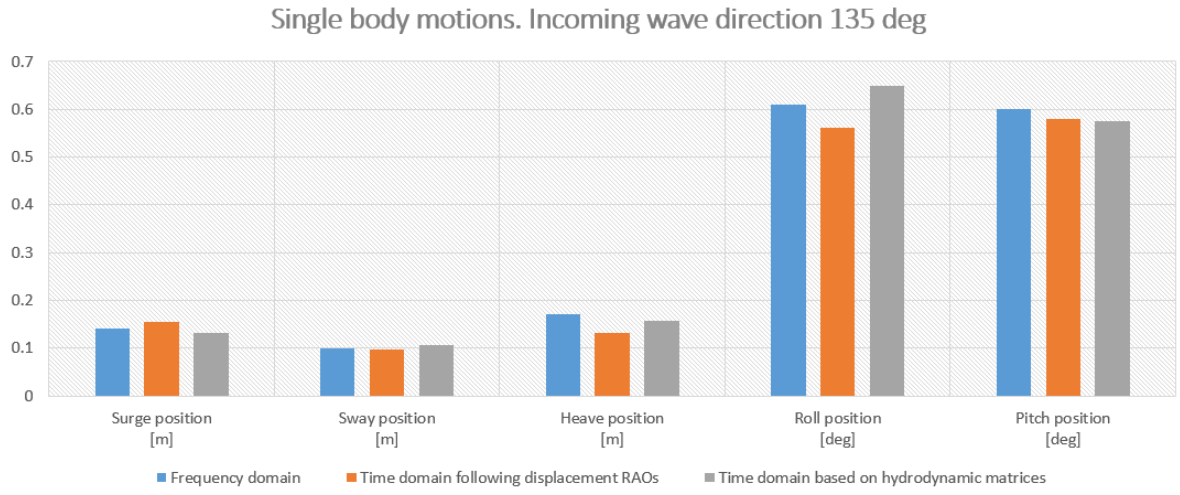

Figure E.1: Three hour maximum surge, sway, heave, roll and pitch position at the CoG, for waves coming from 135°, Hs = 2.5m, Tp = 8s. Comparing results from frequency domain with time domain solutions. For *Iron Lady* as a single body.

As can be seen form Figure E.1, for all DoF the results do match pretty well. For 45 and 90° however, the calculated roll motions deviates for the three different methods.

E.0.2.2 Relative positions and velocities

The same approach as for single body case is applied for this multi-body case. The difference is that for this multi-body case the relative motions are compared instead of the motions of a single body.
Relative motions are calculated in Orcaflex by including a 'motion sensor' which is a comparable structure as the fenders that are shown in Figure 6.4. These 'links' have a negligible stiffness and tension. One end of this link is attached to *Pioneering Spirit* while the other end of this link is attached to *Iron Lady*, with a certain initial length. The length and velocity of this link is calculated at each time step which enables to read the maximum extension and velocity.
A picture of these x, y and z motion sensors is represented below.

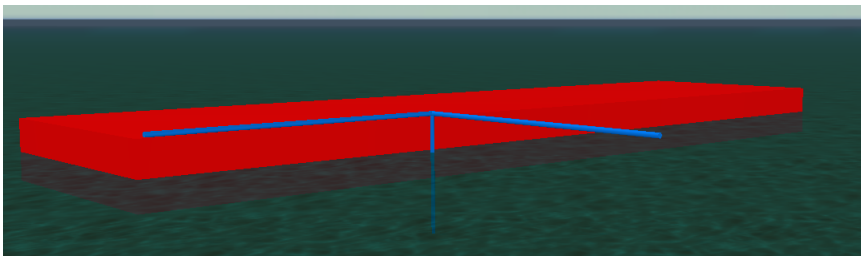

Figure E.2: Relative motion sensor, represented in blue. For surge, sway and heave direction. Operating as measurement tape.

Since only first order, zero mean, effects are included, *Pioneering Spirit* and *Iron Lady* are not connected by a mooring system in this validation step. However, it turned out that the yaw moment did not have a zero mean. Therefore the yaw motion is restricted with a small rotational stiffness of 1.0 kN/deg to remove the mean yaw moment.
Figure E.3 shows the relative surge, sway and heave positions and velocities for waves coming from an angle of 135°. It would be interesting to also compare the results for waves coming from 45, 90 and 180° to see the effect of shielding.

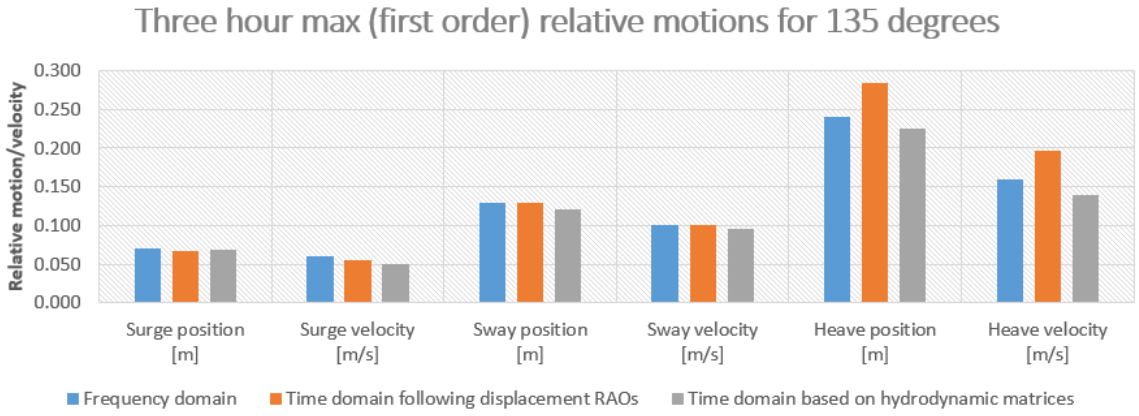

Figure E.3: Three hours maximum relative motion and velocity, at location 'A' in Figure 2.5b, For waves coming from 135°.

Figure E.3 shows that results from the frequency domain and time domain model correspond reasonably well. However, there are some differences, especially the difference between the time domain solution

based on the displacement RAOs and the time domain solution based on the hydrodynamic matrices is interesting. These results are combined by plotting the time history data, as shown in Figure E.4.

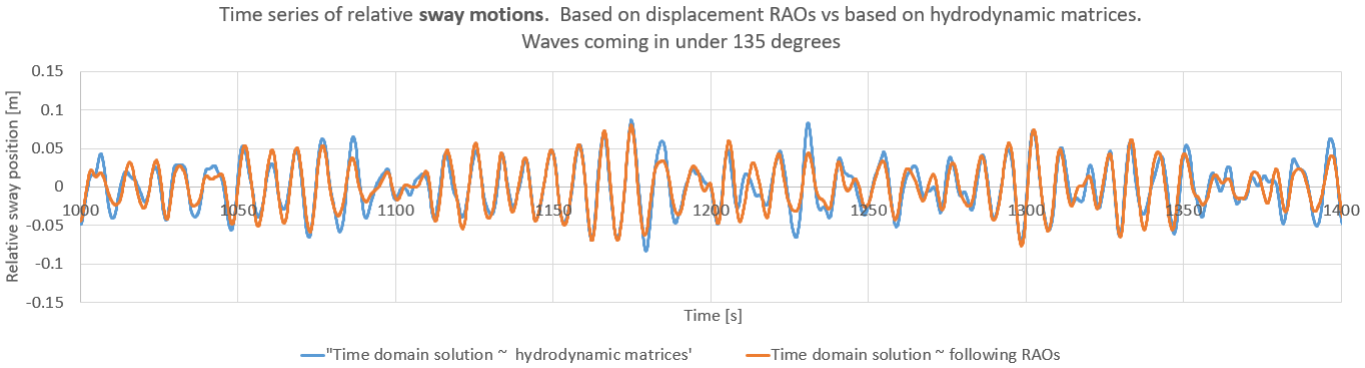

Figure E.4: Time series of relative sway motions, measured with motion sensor, presenting results for two solving methods. For waves coming from 135°.

Figure E.4 represents the time series of relative sway motion between 1000 and 1800 seconds real time simulation.
Also from the time history results it can be seen that the relative sway positions based on displacement RAOs and based on the hydrodynamic matrices do correspond reasonably well.

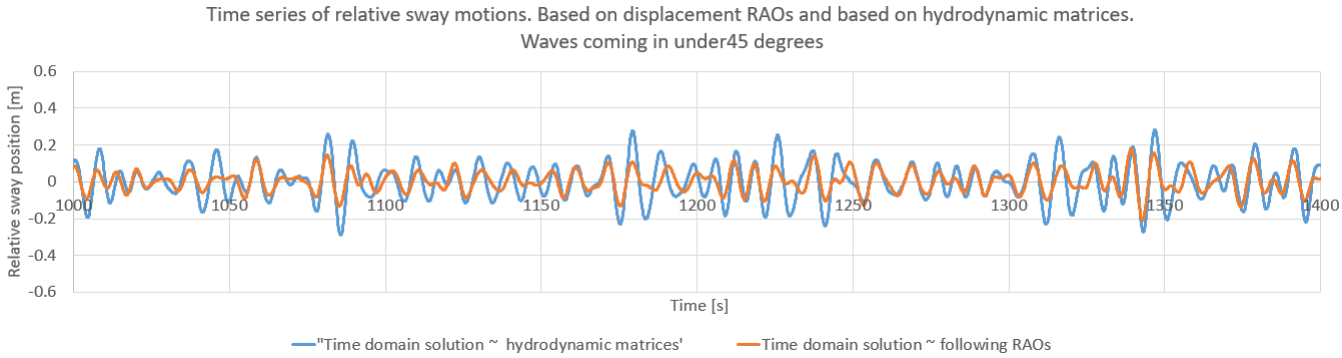

Figure E.5: Time series of relative sway motions, measured with motion sensor, presenting results for two solving methods. For waves coming from 45 degrees.

Similar results are shown for waves coming from 45 °, represented in Figure E.5. It can be seen that for 45 ° the results do deviate more. However, the Orcaflex models that are used to compare the solution based on hydrodynamic matrices and displacement RAOs are checked by the Orcaflex Help Desk, Orcina. Their conclusion was that these results do converge well and the error can be explained by three main statements, as listed below.

- **Constraint.** Similar as for analysing the single body motions, a constraint is required to correct for the non-zero first order wave force. The translational and rotational stiffness is set to be a low value of 1 kN/m and 1 kNm/deg in order to minimize its effect on the motion. However, the effect of the constraint on the relative sway motions cannot be neglected.
- **Solving method.** Computing the relative motions based on the RAOs and based on the hydrodynamic matrices is a totally different solving method. Therefore, difference in these results is more than usual. However, it is good to understand that there are difference in order to consider the accuracy of the maximum forces in the mooring system that will depend on the maximum first order motions.

- **Inaccuracy in reading the hydrodynamic matrices.** As described in section 6.6.2, the frequency domain simulations are run for a limited number of wave directions and frequencies. In between these frequencies, the hydrodynamic coefficients need to be estimated in Orcaflex and Ansys Aqwa. The interpolation and extrapolation method this software applies can contribute to differences in the results. More on this in section 6.6.2

E.0.3 Sanity checks

Modelling goes hand in hand by performing sanity checks, simple checks to confirm results do make sense.

E.0.3.1 Comparing static time domain results with quasi-static results

First the pre-tension in the quasi-static and in the time domain simulation is compared to understand what contribution of pre-tension is to the total load, represented in Figure 6.6a. After that, environmental conditions of current and waves is applied, the values can be found in table E.4, drag force due to wind loading is neglected in this case. The mooring configurations from the quasi-static and time domain model are shown in Figure E.6. The mooring configurations are exactly the same, also the line numbering.

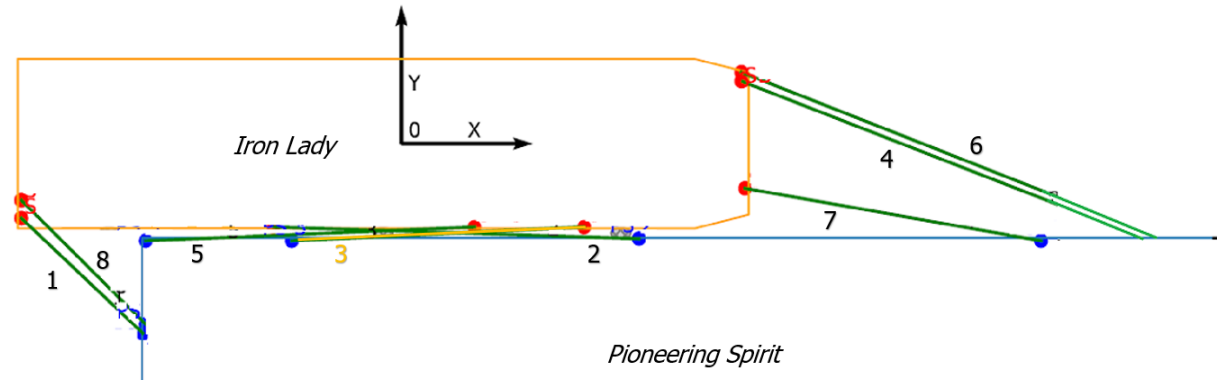

(a) Mooring configuration quasi-static analysis

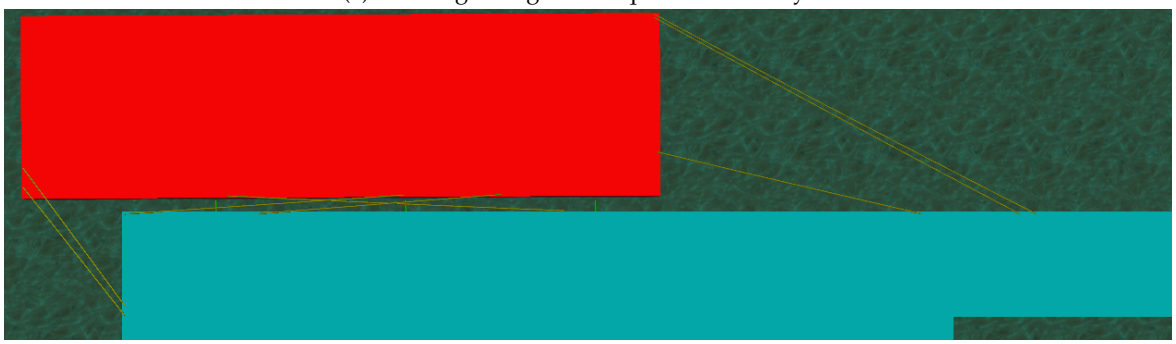

(b) Mooring configuration time domain analysis

Figure E.6: Mooring configurations used for comparing Quasi-static and Time Domain results

Input required to be able to compare results from both modelling methods are shown in table E.4. Both models use same fender stiffness, represented in Figure 4.4. Drag coefficients as defined in table E.2 are applied.

Table E.4: Input for comparing quasi-static analysis and Time Domain analysis.

Variable	Symbol & unit	Value
Axial mooring line stiffness	k_{line} [kN]	6.00E+04
Significant wave height	H_s [m]	5.5
Peak period	Tp [s]	8
Incoming direction, waves and current	β [°]	135
Current speed	u_c [m/s]	2.57
Wind speed	u_w [m/s]	0
Number of mooring lines	N [-]	8

Excessive values are applied for Hs and u_c to be able to see large difference compared to the pre-tension. Figure 6.6b represents the mooring line force from the static solutions.

E.0.3.2 Line stiffness versus mean and maximum mooring line load.

The mooring line consist of steel wire and stretcher. To simplify modelling the mooring line it is modelled as made out of one material. Before doing so, the combined axial stiffness needs to be computed. The equation to do so is derived below.
The mooring line can be considered as two serial springs, taking the same force with different elongation. f_{wire} and f_{str} the ratio's of wire and stretcher respectively, f_{tot} = 1.0. T the mooring line tension in kN, EA the axial stiffness and u elongation in m.
Starting the derivation with stating that the force is equal in both springs in case of serial springs

$$T = k_{wire} \cdot u_{wire} = k_{str} \cdot u_{str} \tag{E.10}$$

The combined stiffness for serial springs can be computed from the individual springs.

$$\begin{aligned} \frac{1}{k_{tot}} &= \frac{1}{k_{wire}} + \frac{1}{k_{str}} \\ \frac{f_{tot}}{EA_{tot}} &= \frac{f_{wire}}{EA_{wire}} + \frac{f_{str}}{EA_{str}} \\ EA_{tot} &= \frac{f_{tot}}{(\frac{f_{wire}}{EA_{wire}} + \frac{f_{str}}{EA_{str}})} \end{aligned} \tag{E.11}$$

Substituting the axial stiffness for the steel wire and the polypropylene stretchers of respectively $90.75E3$ kN and $11.08E3$ kN gives the combined axial stiffness.
Due to incorrect methodology of computing the total axial stiffness, a value of The total axial mooring line stiffness applied in the numerical model is equal to $EA_{tot} = 75E3kN$. This corresponds with 3 % stretcher and 97 % steel wire length. Initially a value of 20 % stretcher length was used, a more realistic value. However, due to incorrect methodology applied to compute the combined axial stiffness, the axial stiffness corresponds with 3% stretcher length.

Changing the stretcher length should not affect the mean loads in the mooring system since the load that is applied is equal in both cases. Table E.5 shows three hours max and mean values for different stretcher lengths.

Table E.5: 3 hours maximum and mean values for varying stretcher length in the base case mooring system. For 135° incoming environmental load.

	Line 1	Line 2	Line 3	Line 4	Line 5	Line 6	Line 7	Line 8
Axial stiffness of 90.75E3 kN								
3 hr Max	459	60	478	237	356	284	139	494
Mean	146	42	170	114	130	131	81	163
Axial stiffness of 75E3 kN								
3 hr Max	333	67	366	230	318	253	129	363
Mean	146	38	154	118	133	129	71	161

Table E.5 shows results for this sanity check and confirms that changing the stretcher length, resulting in lower axial stiffness, does not affect the mean load but only the maximum mooring line load.

E.0.3.3 Time step convergence

Figure E.7 shows respectively the time series of the relative sway motion and the heaviest loaded line, in the range of [2000,2500] seconds. This range is chosen to make sure the model is in 'equilibrium' and no simulation start errors are involved.
It can be seen that for these time steps the time series converge. Therefore, the default time step of $\delta t = 0.1s$ is applied in this research.

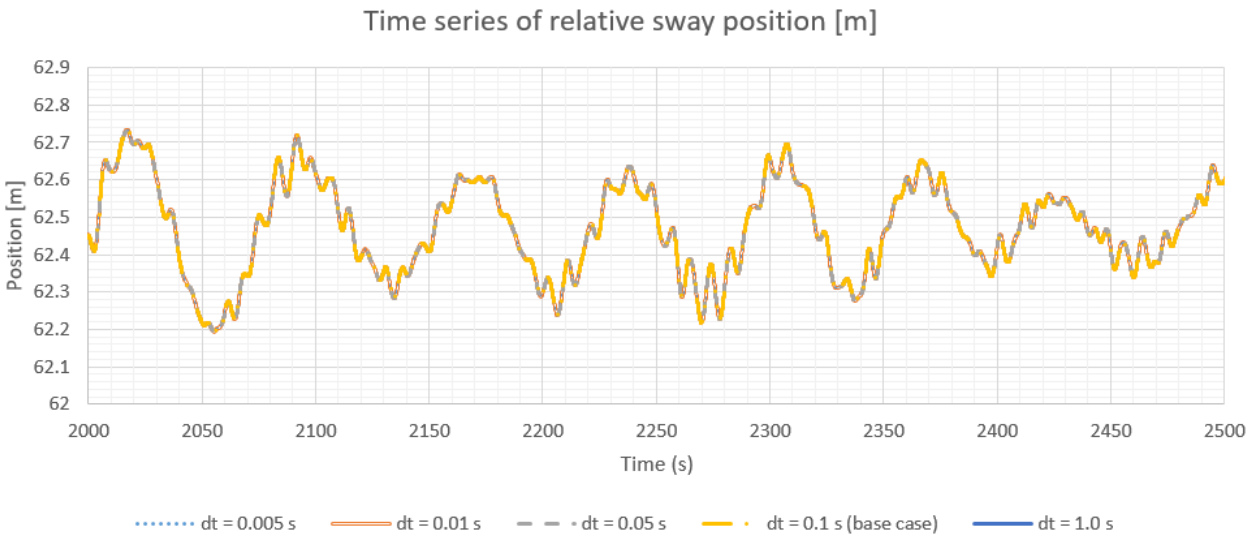

(a) Relative sway motion

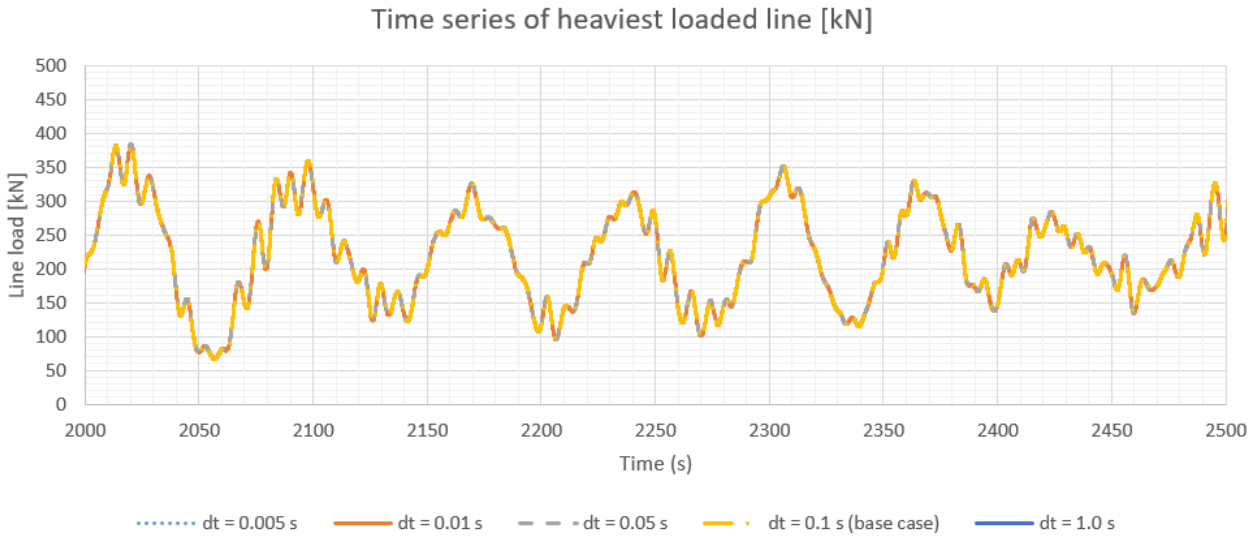

(b) Heaviest loaded line load

Figure E.7: Time series of relative sway position (upper) and line load (lower) for various step sizes. For 135 ° waves and Tp = 8s and Hs = 2.5m.

E.0.3.4 Additional checks

A list of possible sanity checks is given below. Results from these checks are not included in the report because they are irrelevant. Results did make sense therefore, the modelling proceeded.

- Motions outside the CoG should exceed the motions at the CoG. As this result is obvious, no results are included in the report.
- Reducing the line stiffness, by increasing the stretcher length, how does it influence the mean, minimum and maximum loads in the mooring system.
- The three hour maximum wave height at an undisturbed location should correspond with $H_{max} = 1.86 \cdot H_s$ following the Rayleigh distribution.

E.0.4 Sensitivity analysis

Similar as for the frequency domain validation, a sensitivity analysis will be performed to understand the effect of various variables. First a sensitivity analysis for the fender and mooring line damping that will be applied in the time domain model. After that, comparing the mooring line forces when computing the second order wave drift forces with including the Newman approximation and the full QTF.

E.0.4.1 Fender damping

In the time domain model, fenders are modelled as a spring and a damper. Spring characteristics of the fenders that are available on *Pioneering Spirit* can be found from the fender specification sheet, [18]. For damping however, no data is available.
In reality, fenders are expected to have some damping, for example due to deformation. To understand the effect of the damping term that will be added, as sensitivity analysis has to be performed. The effect will be analysed by comparing the three hour maximum mooring line loads for the different fender damping factors.

The damping factor is defined as percentage of the maximum reaction force at maximum velocity of the fender. In equation form:

$$b_{fender} = \frac{F_{damp}}{F_{reaction,max}} \tag{E.12}$$

With b_{fender} the fender damping coefficient, F_{damp} the maximum reaction force contribution due to damping and $F_{reaction,max}$ the fender reaction force at maximum compression, as given in the specification sheet. Figure E.8 shows the three hours maximum mooring line load for the base case mooring system for several fender damping coefficients. It can be seen that the mooring line loads are sensitive to the fender damping coefficient.

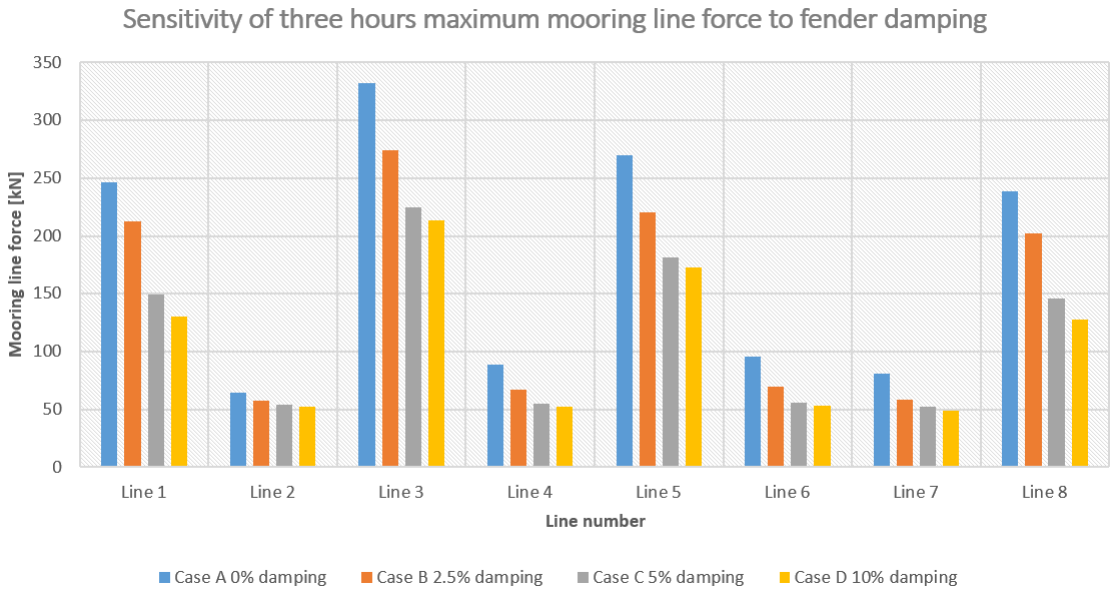

Figure E.8: Effect of fender damping to three hours maximum mooring line load. For environmental loading from 135 °.

Concluding. Based on the investigation to effects of pneumatic fenders on the prevention of ship collision by Park *et al.* [19], investigating comparable pneumatic fenders as used in this research. Park *et al.*

found that the contribution of damping to the total reaction force increases with penetration while for low penetration the damping is in the order of a few percent.
Because the environmental loading directions as analysed in this research lead to minor fender compression, a fender damping factor of 2.5 % will be applied, defined as the maximum force contribution due to damping corresponds with 2.5 % of the maximum reaction force in case of full compression. Due to lack of research, the damping curve is assumed to be linear shaped and saturates upon reaching maximum velocity, the damping curve is shown in Figure E.9.
It is expected that fenders with this specific damping coefficient can be manufactured by the supplier company, Trelleborg and therefore lead to realistic results.

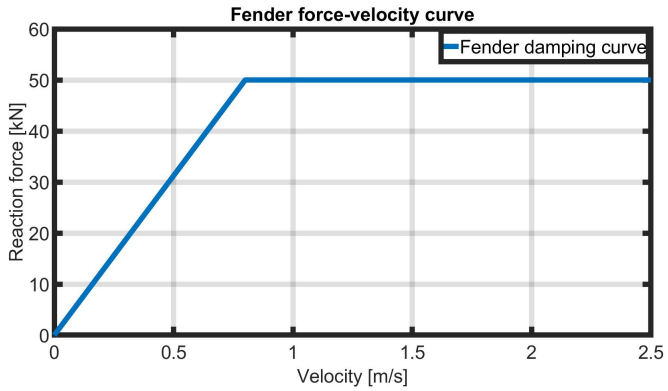

Figure E.9: Fender damping curve presenting reaction force in kN with corresponding velocity in m/s

E.0.4.2 Mooring line damping

Similar as for the fenders, mooring line specifications are known for lines that are available on *Pioneering Spirit*. For mooring line damping, the damping coefficient can be defined as percentage of critical damping. Figure E.10 represents the sensitivity of the three hours maximum mooring line load on the mooring line damping coefficient.

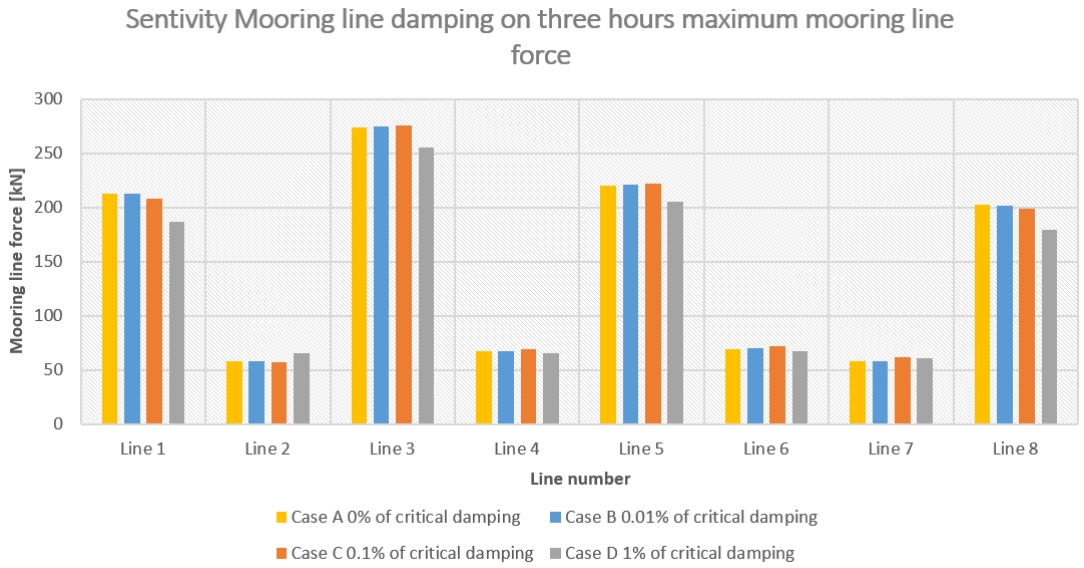

Figure E.10: Effect of mooring line damping to three hours maximum mooring line load.

Concluding. The three hours maximum mooring line load is not sensitive to the damping factor. Ultimately a damping factor of 0.0 % of the critical damping is arbitrarily chosen and applied in all cases, corresponding with Case A in Figure E.10.

E.0.4.3 Newman approximation versus full QTF

Regarding the second order wave drift forces, two methods are available to determine the second order wave drift force from the QTF that is imported from the frequency domain. The Newman approximation and the full QTF.

Newman came up with a method to estimate off-diagonal entries of the QTF from the diagonal entries. This simplifies the QTF and with that, reducing the computation time of the second order wave drift forces by a lot. In terms of accuracy, it is written that the Newman approximation method is less accurate than using full QTF values. Especially for shallow water conditions.
In order to see the difference in results between both methods, the results are compared in Figure E.11

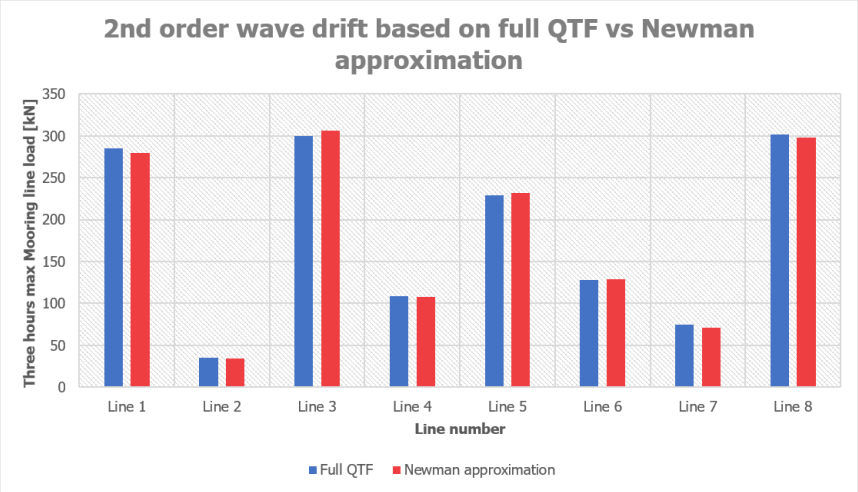

Figure E.11: Comparison of mooring line loads for two methods of applying second order wave drift loads to the system.

Considering the fact that when using the full QTF method, the computation time is approximately 5 times as long, compared to using the Newman approximation. Additionally, comparing these methods only show a minor difference. Therefore, the Newman approximation will be applied in this thesis.

After satisfactory results have been found from the time domain model validation and verification. The next step is finding the results from the time domain simulation that we are looking for, chapter 8.

F
Model parameters

F.1 Time domain modelling

Figure F.1 shows how the fender as a spring damper system is modelled. When PS moves towards IL, the spring is elongated and therefore will result in a force counteracting the motion of PS, i.e. result in a compressive force.

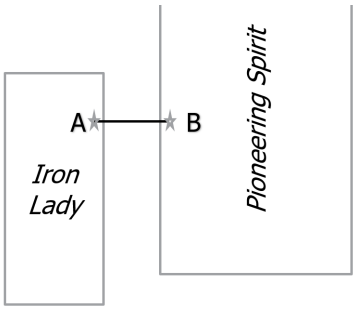

Figure F.1: Fender modelling. Point A is attached to *PS*, point B is attached to IL.

F.1.1 Vessel specifications

F.1.1.1 Iron Lady

Massive amounts of data from the diffraction analysis is imported in the time domain model. Obviously, not all data can be represented here. However, some snapshots of data are given to show insight of the order of magnitude but also to proof the model to be correct. For example, the added mass and damping matrix should be symmetric, as explained in the literature report, [2]. Therefore, Orcaflex only accepts symmetric added mass and damping matrices as input.
The center of gravity is located at (95.5,0,12.1) - *(x,y,z)* from the origin, defined at the stern of Iron

Lady in the transverse center of the barge at the keel line. The CoB of is located at (95.9, 0,3.0) in the same order as the center of gravity and from the same origin. These values make sense, the CoB being approximate half the draft as the barge is rectangular shaped. Moreover, the x and y location almost perfectly correspond, meaning that the initial trim and heel are close to zero. The displaced volume of *Iron Lady* corresponding with a draft of 6 m, ∇ is 64.6E3 m^3
The following tables represent inertia, added mass, damping and stiffness data.
The dimensions for the added mass matrix are M for the diagonals of the first 3 rows and columns and ML for all the off-diagonal terms, the last 3 rows and columns have dimension ML^2 with M referring to mass in unit Ton and L for length in m. Iron Lady displacement at a draft of 6m is approximately $M_{IronLady} = 6.6E + 04$ Ton. A_{ij} denotes the added mass in i^th direction due to acceleration in the j^th direction.

Table F.1: Mass moments of inertia for *Pioneering Spirit* and *Iron Lady*. With unit $Tonm^2$

	Ixx	Ixy	Ixz	Iyy	Iyz	Izz
Pioneering Spirit	8.99E+08	-1.27E+07	-5.10E+07	4.78E+09	1.75E+07	5.48E+09
Iron Lady	2.49E+07	0	0	1.66E+08	0	1.66E+08

Table F.2: Added mass matrix of Iron Lady for a period of 9.61 s. At a draft of 6m. With units as defined above

	Surge	Sway	Heave	Roll	Pitch	Yaw
Surge	3.7E+03	-1.5E+03	-5.2E+03	3.1E+04	3.3E+05	-5.8E+04
Sway	-1.5E+03	4.7E+04	7.7E+04	-5.4E+05	-1.3E+06	5.9E+05
Heave	-5.2E+03	7.7E+04	4.0E+05	-1.5E+06	-3.3E+06	1.4E+06
Roll	3.1E+04	-5.4E+05	-1.5E+06	3.8E+07	2.6E+07	-9.3E+06
Pitch	3.3E+05	-1.3E+06	-3.3E+06	2.6E+07	7.4E+08	-8.6E+07
Yaw	-5.8E+04	5.9E+05	1.4E+06	-9.3E+06	-8.6E+07	9.2E+07

The dimensions for the damping matrix are $\frac{FT}{L}$ for the diagonal of the first 3 rows and columns. $\frac{FT}{rad}$ For all the off-diagonal entries and $\frac{FLT}{rad}$ for the diagonal entries of the last 3 rows and columns. With F referring to force in unit Newton, L to length in m and T to time in seconds.

Table F.3: Damping matrix of Iron Lady for a period of 9.61 s. At a draft of 6 m. With units as defined above

	Surge	Sway	Heave	Roll	Pitch	Yaw
Surge	1.9E+03	-7.7E+02	-3.4E+03	2.0E+04	6.1E+05	-5.4E+04
Sway	-7.7E+02	8.1E+03	1.2E+04	-1.7E+05	-1.8E+05	-9.2E+04
Heave	-3.4E+03	1.2E+04	2.0E+05	-2.6E+05	-1.9E+06	9.9E+04
Roll	2.0E+04	-1.7E+05	-2.6E+05	3.7E+06	5.0E+06	1.2E+06
Pitch	6.1E+05	-1.8E+05	-1.9E+06	5.0E+06	3.3E+08	-5.9E+06
Yaw	-5.4E+04	-9.2E+04	9.9E+04	1.2E+06	-5.9E+06	2.0E+07

Table F.4: Hydrostatic stiffness matrix of Iron lady at a draft of 6 m. Wit dimension F/L for translations and FL/rad for rotations.

	Heave	Roll	Pitch
Heave	1.11E+05	-2.84E-01	-3.26E+05
Roll	-2.84E-01	2.39E+07	-1.49E+01
Pitch	-3.26E+05	-1.49E+01	3.47E+08

As can be seen, the stiffness matrix is symmetric confirms the model to be correct at this point.

F.1.1.1.1 Natural frequencies Natural frequencies of *Pioneering Spirit* are listed in the table below. These natural frequencies are calculated in the frequency domain, in Ansys Aqwa. Since the added mass is a function of frequency, the added mass and the frequency should be iterated untill the added mass corresponding with the natural frequency is used to compute the natural frequency.

Table F.5: Natural frequencies and periods. Extracted from the frequency domain analysis. Surge, Sway and Yaw are not restricted

Variable	Symbol and unit	Surge	Sway	Heave	Roll	Pitch	Yaw
Pioneering Spirit natural frequency	ω_n [rad/s]	N/A	N/A	0.28	0.43	0.2	N/A
Pioneering Spirit natural period	T_n [s]	N/A	N/A	22.4	14.6	31.4	N/A
Iron Lady natural frequency	ω_n [rad/s]	N/A	N/A	0.47	0.64	0.44	N/A
Iron Lady natural period	T_n [s]	N/A	N/A	13.4	9.8	14.3	N/A

F.1.1.2 Pioneering Spirit

Unfortunately no details on the hydrodynamic data of *Pioneering Spirit* can be shown because of confidentiality. However, it is checked that added mass, damping and stiffness matrices are symmetric. The total displacement is in the order of 10 times the displacement of *Iron Lady* which is acceptable since *Pioneering Spirit* is at a draft of 17m.
Also for *Pioneering Spirit* the CoG and CoB differ only in height which means the initial heel and trim are approximately zero.

F.1.2 Environmental loads

The environmental conditions that are applied in the Orcaflex model are explained below. Second order wave drift forces, wind and current are considered not to act on *Pioneering Spirit* since the capacity of the DP system is assumed to be ideal. Only wind, waves and currents are acting on Iron Lady. However, *Pioneering Spirit* is set to follow the displacement RAOs that are given as input from the diffraction analysis.

F.1.2.1 Waves

Section 6.3.2.1 states that to describe a wave train several wave spectra shapes exist. Two of them being a Pierson-Moskowitz and a JONSWAP spectrum. Why the first type is applied will be explained in this section.

Assuming that the wind blew steadily over a large area for a long period of time, the waves will come in equilibrium with the wind, known as a fully developed sea. The Pierson-Moskowitz wave spectrum describes the wave spectral density per frequency for such a fully developed sea. This Pierson-Moskowitz spectrum can be transformed to a wave spectrum that is applicable to a not fully developed sea. Wind blowing over a limited fetch length can lead to a not fully developed sea.

A fully developed sea means that waves are dissipated from each other due to difference in phase velocity.
For deep water conditions, the wave phase velocity can be described by the dispersion relation. The wave phase velocity is a function of the wave number and therefore related to the wave frequency.

$$v_p = \sqrt{\frac{g}{k}} \tag{F.1}$$

With v_p the wave phase velocity in m/s, k the wave number with unit [1/m]. Low frequency waves have a lower wave number and therefore a higher phase velocity. Due to the difference in wave velocity, waves disperse which means that the total energy in a wave spectrum will be more spread out over the entire frequency range. Whereas for a fetch limited wave spectrum, the energy will more converge to a single wave frequency. Resulting in a higher and narrower peak at one specific period, the peak period. For more detailed information, the reader is referred to the literature report belonging to this thesis, chapter 2 [2].

For North Sea regions a JONSWAP spectrum is best applicable, due to the limited fetch length. Both a Pierson-Moskowitz and a JONSWAP wave spectrum can be described by the same analytical relation, as represented in equation F.2, the only difference is the peakedness factor. The peakedness factor that transforms a Pierson-Moskowitz spectrum to a JONSWAP spectrum is 3.3. Applying a peakedness factor of 1.0 results in a standard Pierson-Moskowitz spectrum.

$$S_\zeta(\omega) = \frac{320 \cdot H_{1/3}^2}{T_p^4} \cdot \omega^{-5} \cdot \exp\left\{\frac{-1950}{T_p^4} \cdot \omega^{-4}\right\} \cdot \gamma^A \tag{F.2}$$

With

- $\gamma = 1$ (peakedness factor for Pierson-Moskowitz)
- $A = \exp\left\{-\left(\frac{\frac{\omega}{\omega_p}-1}{\sigma\sqrt{2}}\right)^2\right\}$
- $\omega_p = \frac{2\pi}{T_p}$ (circular frequency at spectral peak)
- $\sigma =$ a step function of ω : if $\omega < \omega_p$ then: $\sigma = 0.07$ if $\omega > \omega_p$ then: $\sigma = 0.09$

The parameters for the wave spectra, as listed above have been defined according to the class requirements as stated by DNV, [45].

The force in a mooring system depends on the relative vessel motions. The vessel motions depend on the incoming wave spectrum and the vessel RAOs.
To achieve conservative results for the maximum mooring system force, the incoming wave spectrum should be conservative since the RAO is computed in the diffraction analysis and imported in the time domain.
Interesting combinations for receiving conservative results is analysing a peak period close to the natural period of the floating structure. This means that the structure oscillates at its natural period with a lot of energy.

Therefore, it is conservative to apply a peakedness factor of 3.3. Corresponding with a JONSWAP wave spectrum with a narrow and high peak at the peak period. However, when the peak period of the JONSWAP wave spectrum is far from the natural period, it is more conservative to use a peakedness factor of 1.0.
In this research, the natural frequencies of *Iron Lady*, *Pioneering Spirit* and the mooring system connecting both bodies are not in the same range, see Table F.5. Therefore, it is assumed to be conservative to use a peakedness factor of 1.0, this value will be applied throughout this thesis.

Based on previous, without further investigation it is not possible to conclude that a peakedness factor of 3.3 is more conservative than a peakedness factor of 1.0.
In order to determine what wave spectrum is governing, a sensitivity analysis would be required, varying the peakedness factor. However, this is considered to be outside the scope of this thesis.

F.1.2.2 Current

To compute the load contribution from the current, note that *Iron Lady* is a standard rectangular shaped barge, therefore both lateral as longitudinal Cd values are 1.0, [40]. The area subjected to longitudinal and lateral current direction is respectively $A_{long} = DW$ and $A_{long} = DL$ with D the draft, W the width and L the length of the barge in m. Forces in longitudinal and transverse direction are taken into account. No additional yaw moment is applied in Orcaflex, the yaw moment is calculated in Orcaflex and consist of a contributions due to the cross flow and the Munk moment.
Additional relevant parameters will be provided in section E.0.1.3 where the force due to current is computed.

F.1.2.3 Wind

According to the Beaufort Wind Scale a wind speed of 25 knots corresponds with waves in the range of 4 m, depending on the fetch length [46]. Since a significant wave height of 2.5 m is set as design sea state, this wind speed and sea state corresponds and taking a higher wind speed into account would not make sense.
Regarding the area subjected to wind load, mainly the barge loading is subjected to wind forces as the freeboard of *Iron Lady* is only 7 m in height moreover it will be shielded from *Pioneering Spirit*. Regarding the barge loading, mainly the turbine towers are subjected to wind loads because of their large height and diameter, respectively 140 m and 10 m. Therefore only the wind load on eight turbines is taken into account, the wind load on the nacelle and turbine blades are neglected for simplicity.
To determine the Cd values, the turbine towers are assumed to be perfect circular shapes, with constant diameter over height. The design wind speed of 25 knots, together with the ambient kinematic viscosity of $\nu = 1.48E-5m/s^2$ gives the Reynolds number of the flow around the structure, by applying equation F.3.

$$Re = \frac{vD}{\nu} \tag{F.3}$$

With v the speed in m/s and D the diameter in m. Based on guidelines provided by DNV, the Cd value of these turbines related to wind, is found to be 0.2, [40]. As the tower is assumed to be a perfect cylinder, the shape factor is equal in both surge and sway direction. The subjected area, $A_{sway} = A_{surge} = D \cdot H$ with H the height of the tower. Due to symmetry no yaw moment is induced on a single turbine tower. Furthermore, for simplicity no yaw moment is taken into account for the total barge loading.

Three main variables have to be known in order to estimate wind and current force acting on the structure. First, drag coefficients, these are estimated following the guidelines from classification companies. Second, subjected area, these can be approximated knowing the structure and loading dimensions and corresponding draft. Third, the relative wind and current velocity.

Figure F.2 shows the drag coefficients that are applied for wind and current.

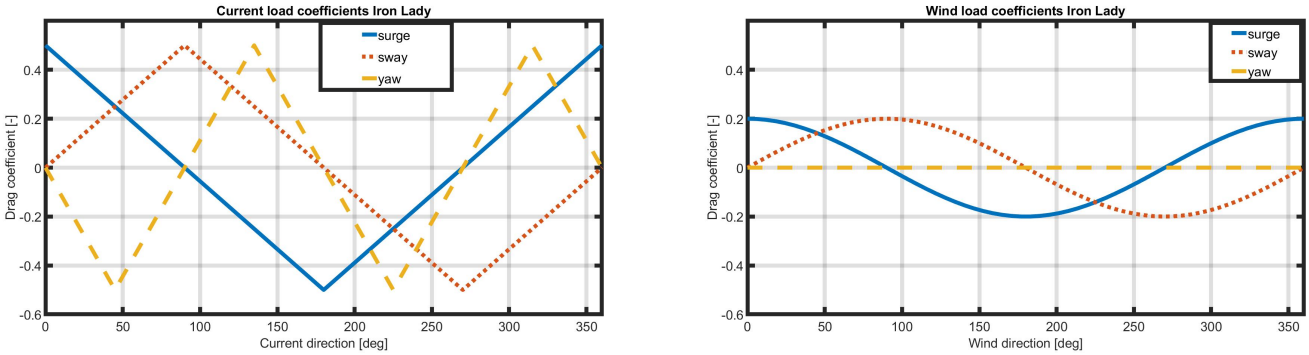

(a) Current drag coefficients for surge, sway and yaw

(b) Wind drag coefficients for surge, sway and yaw

Figure F.2: Drag coefficients applied for current (left) and wind loads (right).

G
Metocean data

ANNUAL WAVE SCATTER

Tp [s] -->		0	1	2	3	4	5	6	7	8	9	10	11	12	13	14	15	16	17	18	19		
Hs [m]		1	2	3	4	5	6	7	8	9	10	11	12	13	14	15	16	17	18	19	20	Total	Accum
0	0.5	-	0.00	0.43	0.06	0.07	0.09	0.21	0.70	1.20	1.60	1.11	0.46	0.56	0.20	0.26	0.09	0.19	0.01	0.05	0.01	7.3	7.3
0.5	1	-	-	0.13	1.14	0.86	1.35	1.46	2.34	4.37	5.93	6.39	3.04	4.22	1.46	1.39	0.41	0.70	0.11	0.25	0.05	35.6	42.9
1	1.5	-	-	-	0.06	0.32	0.94	1.29	1.41	1.55	2.27	3.71	2.90	4.23	2.09	1.58	0.63	0.69	0.11	0.24	0.06	24.1	67.0
1.5	2	-	-	-	-	0.01	0.23	0.68	0.93	1.04	1.07	1.35	1.01	2.52	1.63	1.54	0.64	0.58	0.12	0.24	0.05	13.6	80.6
2	2.5	-	-	-	-	-	0.01	0.22	0.46	0.60	0.74	0.76	0.60	1.16	0.97	1.05	0.52	0.36	0.09	0.10	0.03	7.6	88.3
2.5	3	-	-	-	-	-	-	0.02	0.16	0.30	0.44	0.55	0.42	0.62	0.60	0.73	0.44	0.38	0.09	0.12	0.02	4.9	93.2
3	3.5	-	-	-	-	-	-	-	0.02	0.11	0.27	0.36	0.33	0.37	0.27	0.47	0.25	0.34	0.08	0.08	0.01	3.0	96.1
3.5	4	-	-	-	-	-	-	-	0.00	0.02	0.11	0.18	0.17	0.27	0.14	0.21	0.17	0.21	0.08	0.07	0.01	1.7	97.8
4	4.5	-	-	-	-	-	-	-	-	0.00	0.02	0.08	0.10	0.19	0.09	0.12	0.09	0.13	0.05	0.08	0.02	1.0	98.8
4.5	5	-	-	-	-	-	-	-	-	-	0.00	0.02	0.05	0.10	0.07	0.08	0.04	0.04	0.02	0.05	0.01	0.5	99.2
5	5.5	-	-	-	-	-	-	-	-	-	-	0.00	0.02	0.04	0.04	0.05	0.02	0.02	0.02	0.03	0.01	0.2	99.5
5.5	6	-	-	-	-	-	-	-	-	-	-	-	0.01	0.02	0.03	0.03	0.01	0.01	0.01	0.01	0.00	0.1	99.6
6	6.5	-	-	-	-	-	-	-	-	-	-	-	-	0.00	0.01	0.02	0.00	0.00	0.00	0.00	-	0.0	99.6
6.5	7	-	-	-	-	-	-	-	-	-	-	-	-	0.00	0.00	0.01	0.01	0.00	0.00	0.00	-	0.0	99.7
7	7.5	-	-	-	-	-	-	-	-	-	-	-	-	0.00	0.00	0.01	0.00	0.00	0.00	0.00	-	0.0	99.7
7.5	8	-	-	-	-	-	-	-	-	-	-	-	-	-	-	0.00	-	-	0.00	0.00	-	0.0	99.7
8	8.5	-	-	-	-	-	-	-	-	-	-	-	-	-	-	-	-	-	-	-	-	0.0	99.7
8.5	9	-	-	-	-	-	-	-	-	-	-	-	-	-	-	-	-	-	-	-	-	0.0	99.7
9	9.5	-	-	-	-	-	-	-	-	-	-	-	-	-	-	-	-	-	-	-	-	0.0	99.7
9.5	10	-	-	-	-	-	-	-	-	-	-	-	-	-	-	-	-	-	-	-	-	0.0	99.7
10	10.5	-	-	-	-	-	-	-	-	-	-	-	-	-	-	-	-	-	-	-	-	0.0	99.7
10.5	11	-	-	-	-	-	-	-	-	-	-	-	-	-	-	-	-	-	-	-	-	0.0	99.7
11	11.5	-	-	-	-	-	-	-	-	-	-	-	-	-	-	-	-	-	-	-	-	0.0	99.7
11.5	12	-	-	-	-	-	-	-	-	-	-	-	-	-	-	-	-	-	-	-	-	0.0	99.7
Total		0.0	0.0	0.6	1.3	1.3	2.6	3.9	6.0	9.2	12.4	14.5	9.1	14.3	7.6	7.6	3.3	3.7	0.8	1.3	0.3		
Accum		0.0	0.0	0.6	1.8	3.1	5.7	9.6	15.6	24.8	37.2	51.7	60.8	75.1	82.8	90.3	93.6	97.3	98.1	99.4	99.7		

Figure G.1: Annual wave scatter diagram of the reference location in the Bay of Biscay.

H
Design process

H.1 Approach

This thesis started with a literature research including state-of-the-art mooring systems and how designing a mooring system usually is approached within Allseas. Designing a mooring system starts with stating requirements, among them the requirements as state in the design code, defined by DNV [22]. Next to design requirements, the design criteria should be defined to have a clear view on the purpose of the improvement. These requirements and criteria are discussed in chapter 4.
The next step is having brainstorm sessions, with Allseas' crew both on board the vessel and in the office. Besides, practice with building and analysing mooring concepts in the quasi-static and the time domain helped in finding concepts for improvement.
Ultimately, the main focus is on the modelling phase of mooring system improvements and less on the practical conceptual thinking this is part of future research.

One conceptual design will be discussed in this chapter, related to the concept 'fairleads along the hull'. This appendix is part of step 11 of the total thesis approach, as explained in section 3.1.

H.2 Fairleads at hull side

This section discusses the practical realisation of placing fairleads along the hull side. Two methods or concepts have come up. The first concept is inspired by an navy aircraft carrier, as represented in Figure H.1. The second concepts includes welding fairleads at various location along the hull.

Figure H.1: Aircraft carrier with mooring lines going inside the hull.
Courtesy:http://www.defenseimagery.mil/

Aircraft carrier For navy aircraft carriers, all mooring equipment is placed inside the vessel unlike ordinary vessels where the mooring equipment is located on the top deck. The main purpose for the aircraft carrier is to optimize available deck space.
Aircraft carriers are operating at almost constant draft, *Pioneering Spirit* however operates at a draft varying between 13 and 27 m. This makes placing fairleads along the hull challenging because the elevation of the output point along the hull should be variable.

Applying the mooring concept of an aircraft carrier to *Pioneering Spirit* results in a system consisting of a winch room that is located under deck, a mooring line guide, several output points along the hull and a messenger line winch on the deck. The winch control panel will be wireless, enabling the winch operator to walk outside and have a perfect overview of the mooring arrangement. The ship layout of this mooring system concept is represented in Figure H.2.

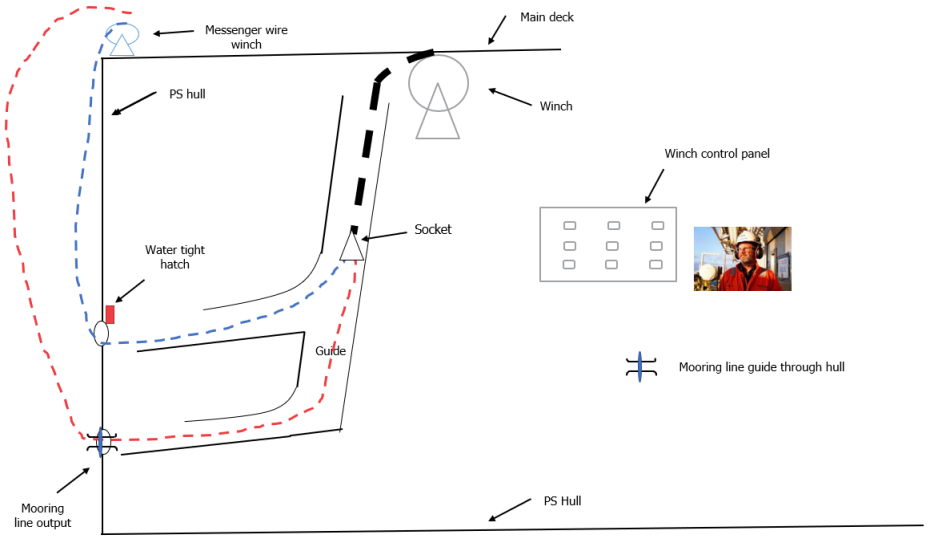

Figure H.2: Aircraft carrier inspired concept. The mooring line in black, the messenger line in blue and red. Small winch on deck used for the messenger line, large winch inside the vessel used for the mooring line. Wireless mooring winch control

The mooring line is stored on the winch, located in a winch room under deck. Two messenger lines are connected to the mooring line. Depending on the messenger line that is payed in, red or blue, the mooring line output can be chosen. An additional benefit would be that more deck space will be available.
Ultimately, this concept is rather theoretical and less practical with the main reasons being:

- Mooring line guide partly submerged and with that the mooring line and messenger line.
- Would work for new build vessels, not for adjusting an existing vessel.
- Mooring line guide will result in friction of the mooring line, leading to wear.
- Most of the time, the messenger line will be below the waterline, increasing drag forces.
- Challenging maintenance due to the complex mooring line guide.

The mooring line guide system is inspired by the tube through a vessel which usually guides the anchoring line.

H.3 (Additional)ShoreTension concept

The heaviest loaded line in a mooring system determines the workability of the according to the weakest link principle. This line load consist of a static and dynamic part, where the dynamic part determines the maximum load. The ShoreTension replaces the heaviest loaded lines with a line that keeps constant tension. That forces the other lines to take the dynamic load. This ShoreTension system is currently only applied in ports, however, due to its promising performance it is interesting to implement this system in a side-to-side mooring system.

The ShoreTension system consists of a hydraulic cylinder, a mooring line, winch and bollard. The mooring line at the winch of *Pioneering Spirit* is attached to the hydraulic cylinder which is connected and attached to the bollard on *Iron Lady*. This hydraulic cylinder has a stroke of several meters and variable stiffness, this enables to keep constant tension on the mooring line within the stroke of the hydraulic cylinder. If the tension in the mooring line exceeds a certain limit, the system pays out; providing slack in the line opposite happens when the line gets slack. Upon exceeding the stroke limit, the tension in the mooring line increases like an ordinary mooring line [48]. The stiffness parameters of the hydraulic cylinder can be pre-defined, if the tension level between the outgoing and in going motions differs, the system does work and dissipates energy from the system. Similar as for the base case, three Yokohama fenders are incorporated in the ShoreTension system. An example ShoreTension implementation is visualized in Figure H.3.

Figure H.3: ShoreTension (left hand) implemented at a harbor quay side.
source: ShoreTension brochure [47]

The main purpose of the ShoreTension system is that mooring lines are more evenly loaded and mooring line loads can be controlled within the stroke of the hydraulic cylinder, On top of that, ShoreTension claims to be able to reduce up to 90 % of the vessel motions compared to conventional mooring systems [47]. Additionally, because the heaviest loaded lines have constant tension, the risk of snap loads will be reduced. As for the MoorMaster system, with the ShoreTension system, human interfaces are reduces which increases the performance of the mooring system.

H.3.1 System properties

Where the conventional mooring line has relatively constant stiffness and variable tension, the shoretension has the exact opposite. The ShoreTension system has a SWL of 1500 kN. However, the mooring lines have a SWL of 453 kN and will therefore be governing. Eight lines will be installed and thus a load capacity of 3600 kN.

H.3.2 Modelling

The base case concept consists of eight mooring lines. For the ShoreTension concept, the four heaviest loaded lines are replaced by a constant tensioned line, represented as blue lines in Figure H.4. The environmental loads are assumed to be aligned and coming in under an angle of 135° while determinng which line is heaviest loaded.

It is not possible to replace all 8 lines with a ShoreTension system as the problem becomes static indefinite. The EoM should be solved for three DoF requiring three lines with variable load, to have a statically determined system.
Modelling the ShoreTension system consist of 4 steps:

- Apply the set environmental conditions to the base case model, run 3600 seconds real time simulation
- Determine the mean force of the heaviest loaded lines.
- Build the ShoreTension system by replacing the 4 heaviest loaded lines by the mean load, determined in the previous step.
- Apply the same set of environmental conditions and run 3600 seconds real time simulation.

The fenders are modelled as explained in section 6.4.2.

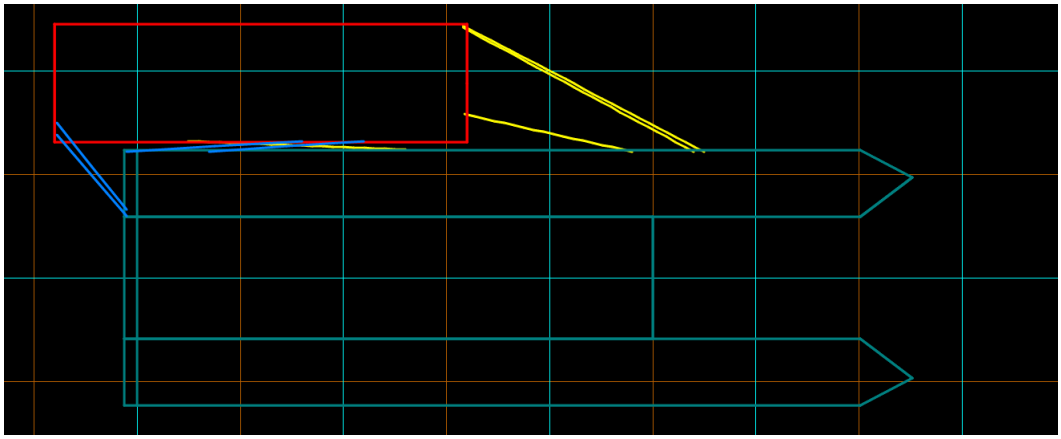

Figure H.4: Top view of the ShoreTension model. With mooring lines drawn in yellow. The barge in red, *Pioneering Spirit* in grey and the constant tension lines in blue.

H.3.3 Expected difficulties

Which mooring line is heaviest loaded depends mainly on the incoming environmental loading directions. For this thesis, wind, waves and current is assumed to be aligned. However, in reality that is not the case. Therefore it is hard to decide upfront which mooring line will be heaviest loaded and which mooring line should be connected to the ShoreTension system.
Unfortunately, the ShoreTension system could not provide detailed information on the exact working principle, the system properties and the modelling method. Therefore, modelling the ShoreTension system is still in progress and the results will be excluded from the report for now.

Results

I.1 Sensitivity analysis pre-tension

As described in section 4.3.6, the pre-tension applied on board cannot be read out properly and is applied by the crew based on experience. In crew perspective, the pre-tension is sufficient if no lines are slack. Pre-tension is applied to all lines at the same time, such that the mooring system is installed as designed.

To understand how this difference between the numerical model and reality affects the mooring loads and with that the results of this thesis, a sensitivity analysis is performed by varying the pre-tension of each mooring line in the numerical model. Pre-tension is the initial tension in the mooring lines.
Figure I.1, represents the line load of the heaviest loaded line for various pre-tensions. In this analysis, the base case mooring system is included. Wind, waves and current respectively 25 knots, Hs = 2.0m and Tp = 8s, 0.9 m/s all coming from 135 °.
Changing the pre-tension not only changes the offset and motions but also the mean mooring loads and how mooring loads are divided over the different mooring lines. However, for all pre-tensions analysed, the same line took the heaviest load.
It is found that changing the pre-tension from 50 to 200 kN did not affect the three hours maximum mooring load much. Therefore, it can be stated that pre-tension is not affecting the results of this research.

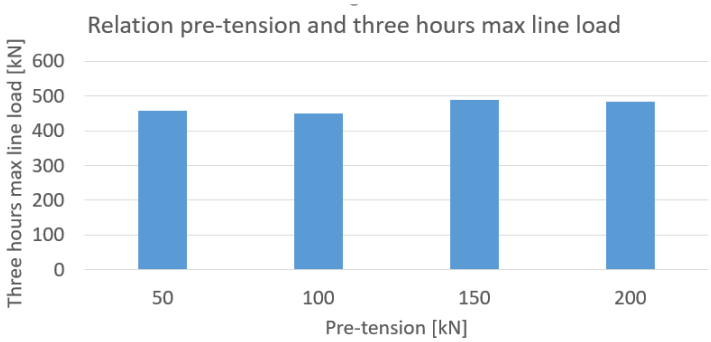

Figure I.1: Relation between pre-tension and the three hours maximum line load.

I.2 Load contributions

Table I.1: External load contributions in sway direction due to bow-quartering waves, for Hs = 2.0 m and Tp = 8 and 12 s. Current and wind load are constant, Given in Tables 6.3 and 6.2.

Contribution	Tp = 8 s		Tp = 12 s	
	Mean [kN]	Max [kN]	Mean [kN]	Max [kN]
First order waves	7.2E-02	2.8E+03	-1.4E+00	2.3E+03
2nd order wave drift	5.1E+01	4.1E+02	1.3E+01	9.6E+01
Added mass and damping	-9.2E-03	2.7E+03	1.1E+00	1.9E+03
Hydrostatic stiffness	-3.5E-02	3.8E+00	-2.2E-01	1.5E+01

The main difference between Tp = 8s and 12s is in the first order force and the added mass and damping terms, capturing the radiation forces. So in case of the lower peak period, the body moves with higher frequency and therefore increased added mass and damping, partly related to the radiation term.